UNIVERSITÀ DEGLI STUDI DELLA TUSCIA DI VITERBO

DIPARTIMENTO DI SCIENZE E TECNOLOGIE PER L'AGRICOLTURA, LE FORESTE, LA NATURA E L'ENERGIA

CORSO DI DOTTORATO DI RICERCA

BIOTECNOLOGIE VEGETALI - XXIV Ciclo

INNOVATIVE APPROACH TO PHARMACEUTICAL BIOTECHNOLOGY BASED ON LAYER-BY-LAYER TECHNIQUE

CHIM/06

Coordinatore: Prof. Stefania Masci

Tutor: Prof. Raffaele Saladino

Dottorando: Melissa Guazzaroni

Alla mia famiglia,

presente e futura

TABLE OF CONTENTS

ABSTRACT **I**

RIASSUNTO **III**

LIST OF PAPERS **V**

LIST OF TABLES **VII**

LIST OF FIGURES **IX**

LIST OF SCHEMES **XIII**

Chapter 1: Enzymes as powerful biocatalysts for green chemistry **1**

1.1 Biocatalysis **1**

1.1.1 Biocatalysis in organic solvent media 2

1.2 Enzyme immobilization **3**

1.2.1 Chemical methods 4

1.2.2 Physical method 5

1.2.3 Layer-by-layer method 6

1.3 Oxidative enzymes as biocatalysts **7**

1.4 Tyrosinases **9**

1.4.1 Structural properties of tyrosinases 10

1.4.2 Catalytic cycle 11

1.4.3 Substrate stereospecificity and tyrosinase inhibitors 13

1.4.4 Tyrosinases as biocatalysts 14

1.5 Laccases **16**

1.5.1 Structural properties of laccases 17

1.5.2 Catalytic cycle of laccases 18

1.5.3 Biotechnological application of laccases 19

References **21**

Chapter 2 Characterization of organic compounds: instruments at service of biotransformations **25**

2.1 Gas Chromatography-Mass Spectrometry (GC-MS) **25**

2.1.1 Applications of GC-MS 28

2.2 Nuclear Magnetic Resonance (NMR) 30

2.2.1 Two-dimensional nuclear magnetic resonance (2D-NMR) 34

2.3 Gel Permeation Chromatography (GPC) 38

2.3.1 Applications 40

References 42

Chapter 3 Immobilized tyrosinase for catechol synthesis: aqueous biotransformation 43

3.1 Introduction 43

3.2 Results and discussions 46

3.2.1 Optimization of tyrosinase immobilization 46

3.2.2 Effect of pH on tyrosinase activity 50

3.2.3 Storage and thermal stability 52

3.2.4 Kinetic assay 54

3.2.5 Recycle and reusability 55

3.2.6 Oxidation of phenols 56

3.3 Conclusions 63

3.4 Experimental Section 64

3.4.1 Tyrosinase immobilized on alumina spherical particles and coated with polyelectrolyte layers 64

3.4.2 Tyrosinase immobilization on Eupergit®C250L 65

3.4.3 Tyrosinase immobilization on Eupergit®C250L and coating with Layer-by-Layer method 65

3.4.4 Determination of protein concentration 66

3.4.5 Activity assay 66

3.4.6 Kinetic assay 66

3.4.7 Stability assay 66

3.4.8 Transmission Electron Microscopy (TEM) measurements 67

3.4.9 Scanning Electron Microscopy (SEM) measurements 67

3.4.10 Enzyme recycling 67

3.4.11 Phenols oxidation 68

3.4.12 Identification and characterization of oxidation products 68

References **73**

Chapter 4 Immobilized tyrosinase for catechol synthesis: biphasic organic/aqueous biotransformation **75**

4.1 Introduction **75**

4.2 Results and Discussions **77**

4.2.1 Tyrosinase extraction 77

4.2.2 Evaluation of the enzymatic activity and kinetic parameters of tyrosinase 79

4.2.3 Tyrosinase immobilization procedure 80

4.2.4 Optimization of water requirement for the oxidation in organic solvent 84

4.2.5 Oxidation of phenols 86

4.3 Conclusions **93**

4.4 Experimental Section **94**

4.4.1 Extraction of tyrosinase 95

4.4.2 Tyrosinase immobilization on Eupergit®C250L 96

4.4.3 Tyrosinase immobilization on Eupergit®C250L covered with Layer-by-Layer method 96

4.4.4 Determination of protein concentration 96

4.4.5 Activity assay 96

4.4.6 Optimization of water requirement 97

4.4.7 Kinetic assay 97

4.4.8 Scanning Electron Microscopy (SEM) measurements 97

4.4.9 Enzyme recycling 98

4.4.10 Phenols oxidation. General procedure 98

4.4.11 Identification and characterization of oxidative products 99

References **103**

Chapter 5 Tyrosinase in lignin oxidative functionalization **105**

5.1 Introduction **105**

5.2 Results and discussions **109**

5.2.1 Treatment of lignin by tyrosinase 109

5.2.2 ^{31}PNMR characterization of lignin 110

5.2.3 GPC analysis of lignin after tyrosinase treatment 111

5.2.4 GC-MS analysis of lignin after tyrosinase treatment 113

5.3 Conclusions **115**

5.4 Experimental Section **115**

5.4.1 Tyrosinase extraction 116

5.4.2 Lignin oxidation 116

5.4.3 Quantitative ^{31}PNMR 116

5.4.4 GPC analysis of lignin 117

5.4.5 GC-MS analysis 117

5.4.6 Tyrosinase immobilization 117

References **118**

Chapter 6 Immobilized laccase in chemical biotransformation: synthesis of aldehyde by laccase mediator system **119**

6.1 Introduction **119**

6.2 Results and discussions **121**

6.2.1 Laccase immobilization 121

6.2.2 Kinetic parameters of immobilized laccases 124

6.2.3 Effect of pH on laccase activity 124

6.2.4 Storage and thermal stability 126

6.2.5 Alcohol oxidations 127

6.3 Conclusions **133**

6.4 Experimental Section **134**

6.4.1 Laccase immobilization on Eupergit® C250L 134

6.4.2 Laccase immobilization on Eupergit® C250L covered with Layer-by-Layer method 135

6.4.3 Laccase immobilization on alumina particles covered with Layer-by-Layer method 135

6.4.4 Determination of protein concentration 136

6.4.5 Activity assay 136

6.4.6 Kinetic assay 136

6.4.7 Storage stability assay 136

6.4.8 Enzyme recycling 136

6.4.9 Alcohol oxidation 137

6.4.10 Identification and characterization of oxidative products 137

References **139**

APPENDIX **141**

ABSTRACT

In recent years, the use of enzymes as natural catalysts has received a great attention in the development of organic synthesis, especially in the frame of green chemistry. In fact, due to the high chemical and energy efficiency of enzymatic transformations, biocatalysis is one of the greenest technologies that works perfectly with the emerging trend of bio-based sustainable feedstock. Indeed, biocatalysts can prevent waste generation by performing catalytic processes with high chemo-, stereo- and regio- selectivity under very mild reaction conditions of temperature, pH, pressure and solvent, working predominantly in aqueous systems. These properties minimize the problems of undesired side reactions and make the processes environmentally friendly. In addition to the unquestionable advantages, there are some drawbacks that lead to a limitation of enzymes for industrial applications: the high cost of isolation and purification of enzymes; the instability of their structures once they are isolated from their natural environments; their sensitivity both to process conditions other than the optimal ones, normally narrow-ranged, and to trace levels of substances that can act as inhibitors. Also, unlike conventional heterogeneous chemical catalysts, most enzymes operate dissolved in water in homogeneous catalysis systems, which is why they contaminate the product and cannot be recovered in the active form from reaction mixtures for reuse. Several methods have been proposed to overcome these limitations, one of the most successful being enzyme immobilization. Immobilization is achieved by fixing enzymes to or within solid supports. By mimicking the natural mode of occurrence in living cells, where enzymes for the most cases are attached to cellular membranes, the systems stabilize the structure of enzymes, hence their activities. Thus, as compared to free enzymes in solution, immobilized enzymes are more robust and more resistant to environmental changes. More importantly, the heterogeneity of the immobilized enzyme systems allows easy recovery of enzyme and product, multiple reuses of enzymes, continuous operation of enzymatic processes, rapid termination of reactions and greater variety of bioreactor designs. Nevertheless, compared with the free enzyme, the immobilized enzyme has usually its activity lowered and the Michaelis-Menten constant increased. These alterations result from structural changes introduced to the enzyme by the applied immobilization procedure and from the creation of a microenvironment in which the enzyme works, different from the bulk solution. In spite of these disadvantages, the creation of a microenvironment may allow to the enzyme to remain active at different temperatures or pHs than would be predicted when immobilization do not occurs, increasing the application possibilities.

The present PhD project will be focused on the development and characterization of novel immobilization systems of oxidative enzymes based on the Layer-by-Layer (LbL) method, and on their application to pharmaceutical biotechnologies.

In particular, tyrosinase from *Agaricus bisporus* and laccase from *Trametes versicolor* were immobilized through two different procedures:

- Chemical immobilization, using the commercially available epoxy-resin Eupergit®C250L as support;
- Layer-by-Layer immobilization, based on the consecutive deposition of alternatively charged polyelectrolytes onto a surface to form microcapsules. The polyelectrolyte films have the ability to protect proteins from high-molecular-weight denaturing agents or bacteria and to allow regulation of the permeability towards small substrates, which can enter the multilayer and react with the catalytic site. Specifically, poly(sodium 4-styrenesulfonate) (PSS) was chosen as negative layer and poly(allylamine hydrochloride) (PAH) as positive one. The polyelectrolytes deposition took place on two different surfaces: one consisted of chemically immobilized enzymes on Eupergit®C250L and the other formed by enzymes supported on particles of aluminum oxide (Al_2O_3).

Novel heterogeneous biocatalysts were first characterized for their kinetic properties and assayed for their stability to changes in pH and temperature, and then they were used as catalysts for the synthesis of high added-value molecules. In detail, tyrosinase-based biocatalysts were applied for the synthesis of catechols that are molecules with significant pharmaceutical properties, including antioxidant and antitumoral activities. The synthesis of catechols was conducted both in aqueous than in biphasic medium, using dichloromethane and buffer as solvent. Laccase-based biocatalysts were applied in the oxidation of alcohols to aldehyde in presence of molecular mediator. Both enzymes, tyrosinase and laccase, performed reactions using dioxygen as the primary oxidant. Data showed that the immobilization procedures increased the enzyme stability in the temperature and pHs conditions assayed, being the LbL systems the most steady biocatalysts. Furthermore, although heterogeneous enzymes were characterized by a slight decrease in catalytic efficiency (lower V_{max} and higher K_m), they showed reactivity comparable to free enzyme when applied in the oxidation of organic compounds, conducting reactions with high yields and conversions of substrate. Moreover, immobilization allows easy recovery of the catalyst from the reaction mixture and its recycling for more consecutive oxidation processes. For these numerous advantages, immobilization procedures are suitable for possible industrial applications, representing an efficient alternative to expensive and polluting chemical procedures for the preparation of these families of bioactive compounds.

RIASSUNTO

Negli ultimi anni, l'uso degli enzimi come catalizzatori naturali ha ricevuto un interesse sempre maggiore per la sintesi di composti organici, specialmente nell'ambito della "green chemistry". Grazie all'alta efficienza chimica ed energetica delle trasformazioni enzimatiche, la biocatalisi è una delle tecnologie più ecocompatibili che lavora in accordo con le emergenti esigenze di usare materie prime sostenibili. La biocatalisi, infatti, previene la formazione di rifiuti conducendo le reazioni con un'alta chemo-, stereo- e regio- selettività in condizioni blande di reazioni, in termini di temperatura, pH, pressione e solvente, lavorando prevalentemente in mezzo acquoso. Questi aspetti limitano i problemi correlati alla formazione di prodotti collaterali dannosi rendendo i processi ecocompatibili. In aggiunta ai numerosi vantaggi, esiste però una serie di problemi pratici che limitano l'uso degli enzimi per applicazioni a livello industriale: gli alti costi di purificazione enzimatica; l'instabilità della struttura degli enzimi una volta che vengono isolati dal loro ambiente naturale; la loro sensibilità alle condizioni di reazione e alla presenza, anche in tracce, di sostanze che possono inibirne l'attività. Inoltre, a differenza dei convenzionali catalizzatori chimici eterogenei, la maggior parte degli enzimi lavora in condizioni omogenee in soluzione acquosa, contaminando così i prodotti di reazione e rendendo impossibile un loro facile recupero e riciclo per più processi catalitici consecutivi. Per superare i limiti associati alla biocatalisi, sono state sviluppate diverse strategie, tra cui la più efficiente è l'immobilizzazione. L'immobilizzazione consiste nel fissare l'enzima sulla superficie o all'interno di supporti solidi inerti e insolubili. In questo modo, mimandone lo stato naturale nelle cellule viventi, dove, per la maggior parte dei casi sono ancorati alle membrane cellulari, i sistemi eterogenei stabilizzano la struttura degli enzimi e ne aumentano l'attività. In questo modo, a differenza di quelli liberi, gli enzimi immobilizzati sono più stabili e resistenti alle variazioni delle condizioni di reazione. L'eterogeneità del sistema permette, inoltre, un facile recupero dei prodotti, il riciclo dei catalizzatori per processi enzimatici a funzionamento continuo, un rapido arresto delle reazioni e una più grande varietà di bioreattori. L'immobilizzazione è caratterizzata comunque da alcuni svantaggi. Rispetto alla sua forma nativa, infatti, l'enzima immobilizzato presenta un'attività catalitica più bassa e una più alta costante di Michaelis-Menten. Queste alterazioni dei parametri cinetici derivano da cambiamenti nella struttura terziaria della proteina indotti dalla procedura d'immobilizzazione applicata e dalla creazione di un microambiente all'interno del quale l'enzima svolge la sua attività che è differente rispetto alla miscela di reazione. La creazione di un microambiente tuttavia ha anche un effetto protettivo nei confronti della molecola proteica,

permettendo all'enzima di rimanere attivo a temperature o valori di pH differenti rispetto all'enzima nella sua forma nativa, estendendo così le sue possibilità di applicazione.

Il presente progetto di ricerca è incentrato sullo sviluppo e caratterizzazione di sistemi di immobilizzazione enzimatica, basati sulla tecnica Layer-by-Layer (LbL), applicati alle biotecnologie farmaceutiche. In particolare la tirosinasi estratta da *Agaricus bisporus* e la laccasi purificata da *Trametes versicolor* sono state immobilizzate attraverso due diverse procedure:

- Immobilizzazione chimica, usando come supporto la resina commerciale Eupergit C250L;
- Immobilizzazione Layer-by-Layer, basata sulla deposizione di polielettroliti a carica opposta su di una superficie in modo da formare microcapsule. Lo strato polielettrolitico ha la funzione di proteggere le proteine da batteri o agenti denaturanti ad alto perso molecolare e permette di regolare l'accesso al sito attivo della proteina; solo substrati di piccole dimensioni possono facilmente diffondere attraverso gli strati e reagire con l'enzima. In dettaglio, il sodio polistirene solfonato (PSS) è stato scelto come polielettrolita a carica negativa, mentre la poliallilammina idrocloruro (PAH) come quello a carica positiva. La deposizione è avvenuta su due diverse superfici, una costituita dagli enzimi immobilizzati per via chimica su Eupergit C250L e l'altra costituita dagli enzimi supportati su particelle di ossido di alluminio (Al_2O_3).

I biocatalizzatori eterogenei così sintetizzati sono stati prima caratterizzati per via cinetica e studiati per valutare la loro stabilità alle variazioni di pH e di temperatura, e poi sono stati impiegati come catalizzatori per la sintesi di molecole organiche ad alto valore aggiunto. Nello specifico, i sistemi basati sulla tirosinasi sono stati usati per la sintesi dei catecoli, molecole con importanti proprietà farmacologiche quali attività antiossidante e antitumorale. La sintesi dei catecoli è stata effettuata sia in soluzione acquosa che in miscela bifasica usando diclorometano e acqua come solventi. I sistemi basati sulla laccasi sono stati invece impiegati nell'ossidazione di alcoli ad aldeidi in presenza di mediatori molecolari. Entrambi gli enzimi, tirosinasi e laccasi, usano ossigeno molecolare come ossidante primario. I risultati ottenuti dimostrano che le procedure di immobilizzazione aumentano la stabilità degli enzimi alle diverse temperature e pH analizzate, con il sistema LbL che manifesta una maggiore efficienza in tutte le condizioni studiate. Inoltre, sebbene gli enzimi immobilizzati siano caratterizzati da una minore efficienza catalitica (minore V_{max} e maggiore K_m), mostrano una reattività comparabile a quella dell'enzima omogeneo quando sono impiegati nell'ossidazione dei composti organici, conducendo reazioni con alte rese e conversioni di substrato. L'immobilizzazione inoltre permette un facile recupero del catalizzatore dalla miscela di reazione e un suo riciclo per più processi ossidativi consecutivi. Grazie ai numerosi vantaggi che offrono, gli enzimi immobilizzati si mostrano così adatti a possibili applicazioni su scala industriale per la sintesi di numerosi composti bioattivi, rappresentando un'efficiente alternativa ai tradizionali processi di sintesi chimica che si avvalgono di procedure costose e basate sull'utilizzo di composti altamente tossici e inquinanti.

LIST OF PAPERS

1) **M. Guazzaroni**, C. Crestini, R. Saladino. "Novel Layer-by-Layer coated tyrosinase: an efficient and selective synthesis of catechols". *Bioorganic & Medicinal Chemistry* **2012**, *20*, 157-166. (IF 2011: 2.978).
2) **M. Guazzaroni**, M. Pasqualini, G. Botta, R. Saladino. "A novel synthesis of bioactive catechols by Layer-by-Layer immobilized Tyrosinase in organic solvent medium". *ChemCatChem* **2012**, *4(1)*, 89-99; (IF 2010: 3.345).
3) R. Perazzini, R. Saladino, **M. Guazzaroni**, C. Crestini. "A novel and efficient oxidative functionalization of lignin by layer-by-layer immobilised Horseradish peroxidase". *Bioorganic & Medicinal Chemistry*, **2011**, *19*, 440-447. (IF 2011: 2.978)
4) **M. Guazzaroni**, C. Crestini, R. Saladino. "Layer-by-Layer immobilized laccase for the synthesis of aldehyde by laccase mediator system" *Manuscript in preparation.*
5) **M. Guazzaroni**. "A Novel Immobilization of Tyrosinases for the Synthesis of Bioactive Phenol Derivatives". *Advances in Natural Substances Chemistry and Biology.* Viterbo, Italy, 19th November 2009 *(oral presentation)*
6) R. Saladino, **M. Guazzaroni**, F. Melone, C. Crestini. "Layer by layer immobilized oxidative enzymes in natural phenolic and polyphenolic compounds modification". Italic 6 - Science & Technology of Biomass: Advances and Challenges. Viterbo, Italy, 5th-8th September, 2011. ISBN 978-88-95688-65-7, pp 290-293 . *(poster presentation)*
7) **M. Guazzaroni**, M. Pasqualini, G. Botta, T. Bozzini, R. Saladino. "A novel synthesis of bioactive catechol by Layer-by-Layer immobilized tyrosinase in organic solvent medium. Italic 6 - Science & Technology of Biomass: Advances and Challenges. Viterbo, Italy, 5th-8th September, 2011. ISBN 978-88-95688-65-7, pp 365-368. *(poster presentation)*
8) **M. Guazzaroni**, M. Pasqualini, G. Botta, T. Bozzini, R. Saladino. "An efficient and selective synthesis of catechol by Layer-by-Layer immobilized tyrosinase". Italic 6 - Science & Technology of Biomass: Advances and Challenges. Viterbo, Italy, 5th-8th September, 2011. ISBN 978-88-95688-65-7, pp 357-360 *(poster presentation)*
9) G. Botta, M. Delfino, **M. Guazzaroni**, T. Bozzini, R. Saladino. "A novel and efficient synthesis of DOPA and DOPA peptides by oxidation of tyrosine residues with tyrosinase". Italic 6 - Science & Technology of Biomass: Advances and Challenges. Viterbo, Italy, 5th-8th September, 2011. ISBN 978-88-95688-65-7, pp 361-364 *(poster presentation)*

10) R. Saladino, **M. Guazzaroni** and C. Crestini. “Immobilized Layer-By-Layer Peroxidase For Dyes Oxidation”. Italic 5 - Science & Technology of Biomass: Advances and Challenges. Villa Monastero, Varenna (Lecco), Italy, 1st -4th September 2009. ISBN 978-88-95688-18-3, pp 246-249 *(poster presentation)*.
11) R. Saladino, **M. Guazzaroni** and C. Crestini. “Porfirins Based Biomimetic Catalysts For Dyes Degradation”. Italic 5 - Science & Technology of Biomass: Advances and Challenges. Villa Monastero, Varenna (Lecco), Italy, 1st -4th September 2009. ISBN 978-88-95688-18-3, pp 250-253 *(poster presentation)*
12) C. Crestini, R. Perazzini, **M. Guazzaroni**, R. Saladino. “Immobilization Of Horseradish Peroxidase And Laccase By The Layer by Layer Method”. XXIII CONGRESSO NAZIONALE DELLA SOCIETA’ CHIMICA ITALIANA - SCI 2009. Sorrento, Italy, 5th -10th July 2009 *(poster presentation)*.
13) R. Saladino, **M. Guazzaroni** and C. Crestini. “Microencapsulated Horseradish Peroxidase For Dyes Degradation”. BIOTECH.ORG – Organic Chemistry and Biotechnology: Challenges and Opportunities. Forte dei Marmi, Italy, 20th -23rd May 2009 *(poster presentation)*
14) R. Saladino, **M. Guazzaroni** and C. Crestini. “Microencapsulated horseradish peroxidase in the activation of hydrogen peroxide for dyes degradation”. ADHOC 2008 - Activation of Dioxygen and Homogeneous Catalytic Oxidation. Venice, Italy, 20th -25th July 2008 *(poster presentation)*

LIST OF TABLES

Table 1.1 The 12 principles of green chemistry publeshed by Anastas and Warner. 1

Table 1.2 Advantages in using oxidative enzyme as biocatalysts. 7

Table 1.3 Oxidoreductase classification. 8

Table 1.4 Some mushroom tyrosinase inhibitors. 14

Table 1.5 Productivity for L-DOPA production using immobilized mushroom tyrosinase. 15

Table 2.1 Pascal's triangle for signal splitting. 33

Table 3.1 Tyrosinase immobilization on alumina spherical particles. 47

Table 3.2 Tyrosinase immobilization on Eupergit®C250L at different conditions. 48

Table 3.3 Kinetic parameters of free (Tyro) and immobilized (Tyro/E, Tyro/E-LbL) tyrosinase. 55

Table 3.4 Reusability of Tyro-immobilized systems. 55

Table 3.5 Oxidation of *para*-alkyl substituted phenols **1-4**. 58

Table 3.6 Oxidation of phenols **7-10**. 60

Table 3.7 Oxidation of phenols **11-14**. 61

Table 3.8 Oxidation of phenols **15-16**. 62

Table 4.1 Purification scheme of tyrosinase with Marín-Zamora method and its variations. 77

Table 4.2 Purification scheme of tyrosinase with the Bouchilloux method. 78

Table 4.3 Specific activity (U mg^{-1}) and contaminant laccase (Lac) of commercial ($Tyro^{S}$) and extracted ($Tyro^{E}$) tyrosinase. 79

Table 4.4 Kinetic parameters of commercial ($Tyro^{S}$) and extracted ($Tyro^{E}$) tyrosinase. 80

Table 4.5 Kinetic parameters of free and immobilized commercial ($Tyro^{S}$) and extracted ($Tyro^{E}$) tyrosinase. 82

Table 4.6 Activity of commercial and extracted tyrosinase at different buffer concentrations. 85

Table 4.7 Optimum buffer expressed as µL μg_{Tyro}^{-1} for free enzyme and µL g_{beads}^{-1} for immobilized enzyme. 85

Table 4.8 Kinetic parameters of free and immobilized Sigma Tyro ($Tyro^{S}$) using *para*-cresol as substrate. 86

Table 4.9 Oxidation of *para*-alkyl substituted phenols **1-2**. 88

Table 4.10 Oxidation of *para*-alkyl substituted phenols **3-4**. 89

Table 4.11 Oxidation of phenols **5-7**. 91

Table 4.12 Oxidation of phenols **8-9**. 92

Table 4.13 Reusability of Tyro-immobilized systems. 93

Table 5.1 ^{31}PNMR attribution. 108

Table 5.2 ^{31}PNMR analysis of lignins and before and after tyrosinase oxidations. 110

Table 5.3 Weight average (M_w) and number average (M_n) molecular weights and polydispersity (M_w/M_n) of lignin samples before and after the enzymatic treatments. 112

Table 5.4 GC-MS analysis of extracted filtrate recovered after LHY lignin oxidation. 113

Table 5.5 GC-MS analysis of extracted filtrate recovered after LOR lignin oxidation. 114

Table 5.6 GC-MS analysis of extracted filtrate recovered after LLS lignin oxidation. 114

Table 6.1 Kinetic parameters of free (Lac) and immobilized laccase (Lac/E, Lac/E-LbL, Lac/Al). 124

Table 6.2 Oxidation of alcohols **1-6**. 129

Table 6.3 Oxidation of alcohols **7-10**. 132

LIST OF FIGURES

Figure 1.1 Chemical immobilization technique: A) covalent binding to solid support; B)intermolecular ross-linking. Physical immobilization technique: C) adsorption on solid support; D) entrapment in polymeric gel; E) encapsulation. 4

Figure 1.2 Layer-by-layer deposition process . 7

Figure 1.3 Classification of oxidative enzyme. 9

Figure 1.4 Oxidation of phenols by tyrosinases. 10

Figure 1.5 On the left the 3D representation of tyrosinase (PDB: 1WX2) with β-sheets in grey, α-helices in light blue and copper atoms in red. On the right magnification of the active site. 11

Figure 1.6 Catalytic cycle for the oxidation of monophenol and diphenol substrates to *o*-quinones by tyrosinase in the presence of O_2. E_{oxy}, E_{met}, and E_{deoxy} are the three types of tyrosinase, respectively. $E_{oxy}D$, $E_{oxy}M$, $E_{met}D$ and $E_{met}M$ are E_{oxy}-Diphenol, E_{oxy}-Monophenol, E_{met}-Diphenol and E_{met}-Monophenol complexes, respectively. 12

Figure 1.7 Action mechanism of reversible (A) and irreversible inhibitors (B). E, Ei, S, I, and P are the enzyme, inactivated enzyme, substrate, inhibitor, and product, respectively; ES is the enzyme-substrate complex, and EI and ESI are the enzyme-inhibitor and enzyme-substrate-inhibitor complexes, respectively. 13

Figure 1.8 A) Ribbon representation of the laccase III from *Trametes versicolor*; B) Copper binding residues of laccase from *Trametes versicolor*. 17

Figure 1.9 Catalytic cycle of laccases showing the mechanism of reduction and oxidation of the enzyme copper sites. 18

Figure 1.10 Schematic representation of laccase-catalyzed redox cycles for substrates oxidation in the absence (a) or in the presence (b) of chemical mediators. 19

Figure 1.11 Oxidation of mediator in the presence of laccases. 20

Figure 2.1 Scheme of Gas Chromatography-Mass Spectrometry (GC-MS) apparatus. 25

Figure 2.2 Scheme of triple quadrupole analyzer. 27

Figure 2.3 (A) Chromatogram obtained after gas chromatography separation of benzyl alcohol, benzaldehyde and acetophenone mixture; (B) mass spectrum of acetophenone molecules. 29

Figure 2.4 Spin states of nuclei in the presence of external magnetic field (B0). 31

Figure 2.5 Chemical shift (in ppm) of 1H and 13C nuclei. 32

Figure 2.6 ^{1}H NMR (A) and ^{13}C NMR of acetophenone. 33

Figure 2.7 ^{1}H NMR of ethanol. 34

Figure 2.8 COSY spectra of ethyl 2-butenoate. 36

Figure 2.9 Scheme of GPC apparatus. 39

Figure 2.10 Chromatogram of a GCP analysis of lignin organosolv. 39

Figure 3.1 Scheme of catechol synthesis by a) chemical method, b) E. coli and c) tyrosinase. 43

Figure 3.2 Role of ascorbic acid in the oxidation of phenols by tyrosinase. 45

Figure 3.3 Scheme of preparation of PSS/PAH-coated tyrosinase/alumina particles: (A) support silanization; (B) coupling with the cross-linker; (C) tyrosinase cross-linking with the support; (D) PAH layer deposition; (E) PSS layer deposition; (F) LbL coating of supported tyrosinase. 46

Figure 3.4 Scheme of immobilization of tyrosinase on Eupergit®C250L: (A) tyrosinase cross-linking with the support; (B) treatment with glycine 3.0 M to block residual epoxy-groups. 48

Figure 3.5 Scheme of preparation of PAH/PSS-coated tyrosinase/Eupergit®C250L: (A) tyrosinase cross-linking with the support; (B) treatment with glycine to block residual epoxy-groups; (C) PAH layer deposition; (D) PSS layer deposition; (E) LbL coating of supported tyrosinase. 49

Figure 3.6 SEM images of Tyro/E (A and B) and Tyro/E-LbL (C and D) at different magnification. 50

Figure 3.7 pH optimum of free (Tyro) and immobilized tyrosinase (Tyro/E and Tyro/E-LbL). Tyrosinase activity was determined using L-Tyrosine as substrate, pH 4.0–9.0 51

Figure 3.8 pH stability of free (Tyro) and immobilized tyrosinase (Tyro/E and Tyro/E-LbL) incubated for 48 h at 25°C in phosphate buffer 0.1 M pH 7.0 (A), pH 6.0 (B) and pH 8.0 (C). Data are the means of three experiments. Standard deviations of data were less than 6%. 51

Figure 3.9 Storage stability of free (Tyro) and immobilized tyrosinase (Tyro/E and Tyro/E-LbL) at (A) -20°C, (B) 4°C and (C) 25°C in Na-phosphate buffer 0.1 M, pH 7.0. Data are the means of three experiments. Standard deviations of data were less than 6%. 52

Figure 3.10 Thermal stability of free (Tyro) and immobilized tyrosinase (Tyro/E and Tyro/E-LbL) at (A) 30°C, (B) 40°C and (C) 50°C in Na-phosphate buffer 0.1 M, pH 7.0. Data are the means of three experiments. Standard deviations of data were less than 7%. 53

Figure 3.11 (A) and (B): SEM images of Tyro/E-LbL at a higher magnification (x15.000) at time zero (A) and after two months (B) upon storage at 4°C. (C): TEM image of a section of Tyr/E-LbL particle upon storage for two months at 4°C. LBL layers are clearly visible in the upper part of the picture. 54

Figure 3.12 Lineweaver-Burk plots of free (Tyro) and immobilized tyrosinase (Tyro/E and Tyro/E-LbL) activity determined at different concentrations of L-Tyrosine (330-1000 μM). Data are the mean values of three experiments with standard deviation less than 1%. 55

Figure 3.13 Phenols selected for the oxidation with free and immobilized tyrosinases. 56

Figure 3.14 Tyrosinase activity at different CH3CN concentrations assayed at 25°C in Na-phosphate buffer 0.1 M, pH 7.0 using L-Tyr as substrate. Activity at 0% v/v CH3CN was chosen as references. Data are the means of three experiments. Standard deviations of data were less than 6%. 57

Figure 3.15 Conversion (%) of *para*-cresol 1 after 5 runs. Each oxidation run was performed for 24h. Results are the mean of three different experiments. 63

Figure 4.1 Lineweaver-Burk plots of commercial (TyroS) and extracted (TyroE) tyrosinase activity determined at different concentrations of L-Tyrosine (330-1000 μM). The data are the mean values of three experiments with standard deviation less than 1%. 80

Figure 4.2 Scheme of immobilization of tyrosinase on Eupergit®C250L: (A) tyrosinase cross-linking with the support; (B) treatment with glycine to block residual epoxy-groups. 81

Figure 4.3 Scheme of preparation of PAH/PSS-coated tyrosinase/Eupergit®C250L: (A) tyrosinase cross-linking with the support; (B) treatment with glycine to block residual epoxy-groups; (C) PAH layer deposition; (D) PSS layer deposition; (E) LbL coating of supported tyrosinase. 81

Figure 4.4 SEM images of $Tyro^S$/E stored in buffer. 83

Figure 4.5 SEM images of $Tyro^S$/E after treatment in CH_2Cl_2. 83

Figure 4.6 SEM image of $Tyro^S$/E-LbL. 83

Figure 4.7 Scanning profile of the tyrosinase-catalyzed end products of *para*-cresol 1 in CH_2Cl_2 at different time. 84

Figure 4.8 Phenols oxidized by free and immobilized tyrosinase. 86

Figure 5.1 Common phenylpropane linkages. 106

Figure 5.2 Lignin oxidation pathways. 107

Figure 5.3 Phosphitylation reaction of hydroxyl groups. 108

Figure 5.4 Role of ascorbic acid in the oxidation of lignin by tyrosinase. 109

Figure 5.5 Gel permeation chromatography of (A) lignin organosolv, (B) lignin hydrolytic and (C) lignin alkali low sulphonate before and after the treatment with free and immobilized tyrosinase. 112

Figure 5.6 Yield percentage of aromatic and non-aromatic compounds recovered from oligomeric constituent of lignin after tyrosinase oxidation. 115

Figure 6.1 Reaction mechanism of primary alcohol oxidation by (A) the ET and HAT route; (B) the TEMPO mechanism. 120

Figure 6.2 Scheme of laccase immobilization on Eupergit®C250L: (A) laccase cross-linking with the support; (B) treatment with glycine to block residual epoxy-groups. 121

Figure 6.3 Scheme of preparation of PAH/PSS-coated laccase/Eupergit®C250L: (A) laccase cross-linking with the support; (B) treatment with glycine to block residual epoxy-groups; (C) PAH layer deposition; (D) PSS layer deposition; (E) LbL coating of supported laccase. 122

Figure 6.4 Scheme of preparation of PSS/PAH-coated laccase/alumina particles: (A) support silanization; (B) coupling with the cross-linker; (C) laccase cross-linking with the support; (D) PAH layer deposition; (E) PSS layer deposition; (F) further PAH layer deposition to complete the LbL coating of supported laccase. 122

Figure 6.5 SEM images of the immobilised laccase before and after PSS/PAH coating on Eupergit® C250L beads (A and B, respectively) and on alumina particles (C and D, respectively). 123

Figure 6.6 TEM images of Lac/E-LbL. 123

Figure 6.7 Lineweaver-Burk plots of free (Lac) and immobilized laccase (Lac/E, Lac/E-LbL, Lac/Al) activity determined at different concentrations of ABTS (4.0-13.0 mM). Data are the mean values of three experiments with standard deviation less than 1%. 124

Figure 6.8 Optimal pH of free (Lac) and immobilized laccase (Lac/E , Lac/E-LbL, Lac/Al). Laccase activity was determined using ABTS as substrate in the range of pH 2.0–7.0. Results are the mean of triplicate assays. 125

Figure 6.9 pH stability of free (Lac) and immobilized laccase (Lac/E, Lac/E-LbL and Lac/Al) incubated for 24 h at 25°C in acetate buffer 0.1 M pH 4 (A) and pH 3 (B). Data are the means of three experiments. Standard deviations of data were less than 6%. 125

Figure 6.10 Storage stability of free (Lac) and immobilized laccase (Lac/E, Lac/E-LbL, Lac/Al) at 4°C in Na-acetate buffer 0.1 M, pH 5.0. Data are the means of three experiments. Standard deviations of data were less than 6%. 126

Figure 6.11 Storage stability of free (Lac) and immobilized laccase (Lac/E, Lac/E-LbL, Lac/Al) at (A) 40°C and (B) at 50°C in Na-acetate buffer 0.1 M, pH 5.0. Data are the means of three experiments. Standard deviations of data were less than 6%. 127

Figure 6.12 Alcohols oxidized by free and immobilized laccase mediator systems. 128

Figure 6.13 Conversion (%) of 2 after 10 runs. Each oxidation run was performed for 10 h. Results are the mean of three different experiments. 133

LIST OF SCHEMES

Scheme 3.1 Oxidation of phenols **1-4**. Reagents and conditions: a) Tyro-based systems, O_2, AA; b) Na-phosphate buffer; c) Na-phosphate buffer/CH_3CN 58

Scheme 3.2 Oxidation of phenols **7-10**. Reagents and conditions: a) Tyro-based systems, O_2, AA; b) Na-phosphate buffer. 59

Scheme 3.3 Oxidation of phenols **11-14**. Reagents and conditions: a) Tyro-based systems, O_2, AA; b) Na-phosphate buffer. 61

Scheme 3.4 Oxidation of phenols **15** and **16**. Reagents and conditions: a) Tyro-based systems, O_2, AA; b) Na-phosphate buffer/CH_3CN; c) Na-phosphate buffer. 62

Scheme 4.1 Oxidation of phenols **1-4**. Reagents and conditions: a) Tyro-based systems, O_2; b) CH_2Cl_2/buffer; c) CH_2Cl_2/buffer/CH_3CN; d) buffer. 87

Scheme 4.2 Oxidation of phenols **5-7**. Reagents and conditions: a) Tyro-based systems, O_2; b) CH_2Cl_2/buffer; c) buffer. 90

Scheme 4.3 Oxidation of phenols **8-9**. Reagents and conditions: a) Tyro-based systems, O_2; b) CH_2Cl_2/buffer; c) buffer; d) CH_2Cl_2/buffer/CH_3CN; e) buffer/CH_3CN. 92

Scheme 6.1 Oxidation of alcohols **1-6**. 128

Scheme 6.2 Oxidation of alcohols **7-10**. 131

Chapter 1

Enzymes as powerful biocatalysts for green chemistry

1.1 Biocatalysis

In recent years, the use of enzymes as natural catalysts has received a steadily increasing amount of attention, especially in the frame of organic synthesis. The worldwide interest in biocatalysts is mainly due to the capability of enzymes to conduct "green chemistry". The "green chemistry" is the design of chemical products and processes that reduce or eliminate the use or generation of waste, toxic and hazardous substances. Principles of green chemistry were outlined by Anastas and Warner in 1998[1] and they provided a guideline for the design, manufacture and use of chemical products with low environmental impact (Table 1.1). Biocatalysis is in agreement with these principles, becoming the greenest chemistry technology that works perfectly with the emerging trend of bio-based sustainable feedstock.

Table 1.1 The 12 principles of green chemistry published by Anastas and Warner.[1]

1. Prevent waste
2. Design safer chemicals and products
3. Design less hazardous chemical syntheses
4. Use renewable feedstocks: use raw materials and feedstocks
5. Use catalysts, not stoichiometric reagents
6. Avoid chemical derivatives
7. Maximize atom economy
8. Use safer solvents and reaction conditions
9. Increase energy efficiency
10. Minimize the potential for accidents
11. Design chemicals and products to degrade after use
12. Analyse in real time to prevent pollution

In fact, biocatalysts can prevent waste generation by performing catalytic processes with high chemo-, stereo- and regio- selectivity under very mild reaction conditions of temperature, pH, pressure and solvent, working predominantly in aqueous systems.

For these reasons, the use of enzymes in industrial applications has increased in recent years in many areas. Currently, the estimated value of world enzyme market is about US $ 1.3 billion and it has been forecasted to grow more than US $ 2 billion. Detergents (37%), textiles (12%), starch (11%), baking (8%) and animal feed (6%) are the main industries, which use about 75% of industrially produced enzymes.[2] Another important growing field for biocatalysts concerns the synthesis of chemical compounds. For example, biocatalysts are used for selective synthesis of enantiomerically pure molecules, ensuring enantioselectivities of > 99% e.e. This aspect becomes increasingly important in the synthesis of advanced pharmaceutical intermediates, since toxicological studies have required for every impurity comprising above 1% of the total content. Again, with respect to pharmaceutical and chemical applications, the importance of biocatalysts is mainly correlated to their ability to work in organic solvent or in ionic liquids. The possibility to use non-conventional reaction media opens the way to the synthesis of water insoluble compounds, as well as for the catalysis of reactions thermodynamically unfavourable in aqueous solution (such as condensation reactions).

1.1.1 Biocatalysis in organic solvent media

Biocatalysis in organic solvents represents the most important non-conventional system, compared to gases,[3] supercritical fluids,[4] ionic liquids[5] and semi-solid systems[6] media studied in the last three decades as possible efficient alternative to aqueous solution for chemical synthesis applications. The replacement of water by an organic solvent has several potential advantages: (i) an enhancement of the solubility of reactants; (ii) a shift of equilibrium in organic media that allow aqueous thermodynamically unfavourable reactions; (iii) an easier recovery of biocatalyst and product; (iv) a lesser conditions of asepsis; (v) an higher thermal stability; (vi) a reduction of product inhibition; (vi) an alteration of selectivity, including substrate specificity, enantio-, prochiral-, regio-, and chemoselectivity. In organic solvent, kinetic constants of reaction do not correlate with solvent parameters such as hydrophobicity, dielectric constant or dipole moment; instead, case-by-case correlations have to be found. The selection of a suitable solvent with regard to activity and stability may be suggested by the log P concept, where P is the partition coefficient of the solvent in an octanol/water biphasic system. Hydrophilic solvents with log P value < 2 often lead to enzyme deactivation if present in high concentrations; apolar solvents with log P ≥ 4 are compatible with enzymes; the influence of solvents with intermediate values of log P (range 2-4) are unpredictable and depend very much on the individual case. The effect of the solvent polarity on enzyme activity and stability depends on the partitioning of water between the enzyme surface and the bulk phase of the organic solvent. In fact, organic solvents affect the dielectric properties of the reaction medium, influencing the non-covalent weak forces responsible for the three dimensional structure of the enzyme. Thus, hydrophilic solvents, such as methanol, strip the water molecules off the enzyme

surface, altering its conformational structure and compromising its activity. Specifically, biocatalysis in organic medium can be provided by (i) increasing concentration of water miscible solvents to the reaction, (ii) working in two-phase systems composed of water and an immiscible solvent and (iii) working in nearly anhydrous organic solvents with minimal amounts of water. In the first two cases, the enzyme may be employed either in the soluble state or immobilized, while in nearly anhydrous organic solvents it have to be in the solid state only. Immobilization may also help to avoid denaturation at the interface in two-phase systems, stabilizing the protein structures. The importance of immobilization processes in biocatalysis has been widely demonstrated both in organic than in aqueous media, being of importance to the stability and activity of enzymes.[7]

1.2 Enzyme immobilization

Although biotechnological applications have grown in recent years and are expected to grow in the future, there are limits in the use of biocatalysts that have yet to be fully solved. They concern the low stability of enzymes, both in aqueous than in organic medium, and the high production costs, worsened by the use of biocatalysts under homogeneous conditions. In fact, when enzyme is used in a soluble form, after the catalysis occurred, it cannot be easily recovered from the mixture preventing from using enzymes in continuous production processes. To overcome these limits, studies are focusing on the development of immobilization technique that can offer the possibility of a wider and more economical exploitation of biocatalysts in industry, waste treatment, medicine, and biosensor technologies. Several studies revealed that enzyme immobilization is a powerful tool to enhance enzyme properties as stability, activity, specificity, selectivity and reduction of inhibition.[8] Moreover, immobilized enzymes can be easily isolated from the reaction mixture (i) minimising or eliminating protein contamination of the product, and (ii) allowing recovery and recycling of biocatalysts for more production cycles.[9] In this way, immobilization enhances the catalytic properties of enzyme and, working in continuous processes, it reduces costs concerning products purification and enzyme manufactures. Nevertheless, immobilized enzymes usually have a lower activity and a higher Michaelis-Menten constant with respect to free enzyme. These alterations result from structural changes introduced by the immobilization procedure and by the creation of a different microenvironment in which the enzyme works.[10] In spite of these disadvantages, the creation of a novel microenvironment may allow to the enzyme to retain activity at different temperatures or pHs than would be predicted for the free enzyme, increasing its biotechnological applications.[11] Immobilization is achieved by fixing enzymes onto or into an inert, insoluble material, by a great variety of methods that can be classified as physical, where weak interactions between support and enzyme exist, and chemical, where covalent bonds are formed with the enzyme. To the physical

methods belong: (a) adsorption (physical, ionic) on a water-insoluble matrix, (c) inclusion (or gel entrapment), (d) microencapsulation with a solid membrane and (e) microencapsulation with a liquid membrane. The chemical immobilization methods include: (a) covalent binding to a solid support and (b) intermolecular cross-linking. However, no single method and support is best for all enzymes and their applications. This is because of the widely different chemical characteristics and composition of enzymes, the different properties of substrates and products, and the different uses to which the product can be applied. Besides, all of the methods present advantages and drawbacks. Adsorption is simple, cheap and effective but frequently reversible; covalent attachment and crosslinking are effective and durable, but expensive and easily worsening the enzyme performance. Consequently, the optimal immobilization conditions for a chosen enzyme and its application would be analysed case-by-case to ensure the highest retention of activity and operational stability. In fact, the method of immobilization has to prevent loss of enzymatic activity and maintain, as possible, the tertiary structure of the protein. The main physical and chemical immobilization techniques are shown in Figure 1.1 and described below.[10]

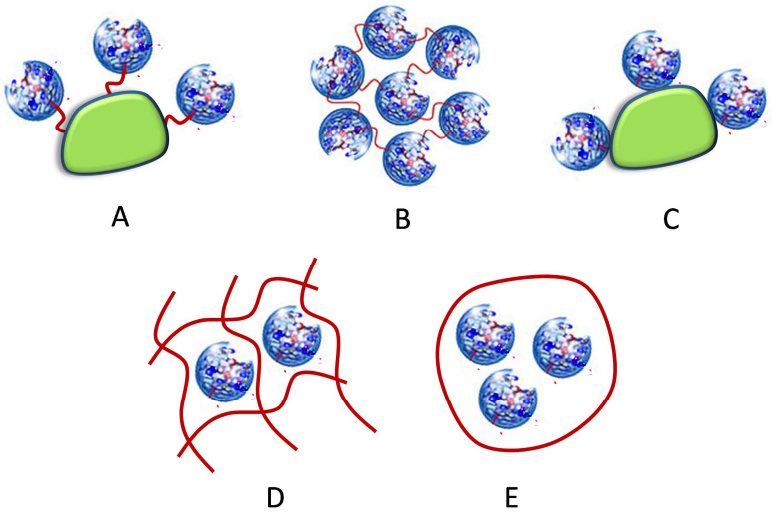

Figure 1.1 Chemical immobilization technique: A) covalent binding to solid support; B) intermolecular cross-linking. Physical immobilization technique: C) adsorption on solid support; D) entrapment in polymeric gel; E) encapsulation.

1.2.1 Chemical methods

1.2.1.1 Covalent binding to solid support

The immobilization of enzymes by covalent attachment to a solid carrier involves formation of a covalent bond between amino acid side chain residues of the protein with reactive groups on the surface of the support (Figure 1.1a). Covalent attachment is often the method of choice when the minimal leaching of the protein from the support is required. Because of the stronger carrier-protein

linkage, the resulting heterogeneous biocatalyst can be more stable than those prepared by adsorption or entrapment. The most common protein functional groups involved in covalent binding are nucleophilic amino (lysine, hisitidine and arginine), thiol (cysteine), hydroxyl groups (serine, threonine and tyrosine) and electrophilic carboxylate groups (aspartic acid and glutamic acid). The carrier-fixed biocatalyst is often more resistant to deactivation by organic reactants or shear and can be recovered by simple filtration. Considerations of the desired properties of the immobilized biocatalyst such as ease of use, mechanical strength, activity density, stability, intended application, cost, and availability help to determine which carriers and methods of attachment are appropriate. When the mass of carrier material is large relative to that of the enzyme, the physical and chemical properties of the carrier will, in large part, determine properties of the resultant immobilized enzyme. Often, the carrier will impart mechanical strength to the enzyme, allowing repetitive recovery by simple filtration of the solid particles and reuse of the system. The degree of porosity and pore volume will determine the resistance to diffusion and molecular size selectivity of the biocatalyst. When used in non-aqueous media, dispersion of the enzyme over a large surface area can greatly increase its activity.[12]

1.2.1.2 Intermolecular cross-linking

Enzymes can be immobilized by chemical cross-linking of reactive amino acid residues with bifunctional reagents, like glutaraldehyde (Figure 1.1b). Cross-linking can be performed on the soluble enzyme protein (cross-linked enzyme, CLE), on a crystallized enzyme protein (cross-linked enzyme crystal, CLEC), or protein enzyme aggregate (cross-linked enzyme aggregate, CLEA). These systems only differ in the protein precursor to be cross-linked and have the obvious advantage that no inert support is involved since the enzyme is auto-immobilized in its own protein mass. Therefore, the specific activity of the biocatalyst is very high, being the enzyme concentration within the biocatalyst close to its theoretical limit of packing value.[13]

1.2.2 Physical method

1.2.2.1 Adsorption

This technique involves the physical adsorption of the enzyme onto the support through short-range interactions like the van der Waals forces (Figure 1.1c). Ionic exchange is a rather simple and effective method for enzyme immobilization since the vast majority of proteins adsorb very fast on anion or cation exchange resins. However, its main drawback is that the enzyme can be easily desorbed from its carrier by fine changes in the reaction medium. Physical adsorption can also denature the enzyme depending on the surface properties of the support material. Many kinds of supports (porous glass,

agarose gels, magnetic particles, etc.) covered with ionic polymers are good candidates to prepare active, stable and selective enzyme biocatalysts useful in several types of industrial reactors.[13]

1.2.2.2 Entrapment

This technique is based on the inclusion of an enzyme in a polymeric matrices network compact enough to retain the enzyme molecules within it (Figure 1.1d). Immobilization occurs by polymerization process of a reactive monomer in the presence of the enzyme. Most popular matrices for gel entrapment are alginate, polyacrylamide, polyurethane and polyvinyl alcohol. Entrapment protects enzymes by preventing direct contact with the environment, minimizing the effects of gas bubbles, mechanical sheer and hydrophobic solvents, but has the disadvantage of mass transfer limitations and low enzyme loading.[13]

1.2.2.3 Encapsulation

Enzyme microcapsules are produced by promoting a polymerization reaction in the surface of drops of enzyme aqueous solution dispersed in a water-immiscible organic solvent (with the aid of a surfactant) (Figure 1.1e). Similar to entrapment, encapsulation protects the enzyme from the external environment but has limited application for the biocatalysis of large substrates, as they are prone to mass transfer limitations.[9a]

1.2.3 Layer-by-layer method

The development of ultrathin organic films technology promises a solution to a variety of tasks of applied biotechnology. For example, biosensors, semipermeable membranes, enzyme immobilization and biocompatible modification of surfaces require the elaboration of thin organic films. A widely applicable and promising new technique to fabricate ultrathin films with determined thickness, composition, and properties is the Layer-by-Layer (LbL) technique, based on the adsorption of oppositely charged macromolecules from the solution onto a substrate (Figure 1.2).[14] The excess or remaining solution after each adsorption step is washed with solvent and thus it is possible to obtain a thin layer of charged species on the surface ready for next adsorption step. Since 1991, a variety of materials such as synthetic polyelectrolytes,[15] proteins,[16] nucleic acids[17] have been employed to collect multilayers on different surfaces. Macroscopic flat wafers, alginate gel beads,[18] submicron-sized colloidal particles[19] have been used as templates for macromolecule, multilayer coating by means of LbL. Applications can be envisaged for nonlinear optical materials formation,[20] patterning,[21] separations,[22] biosensing,[23] and biocatalysis.[24]

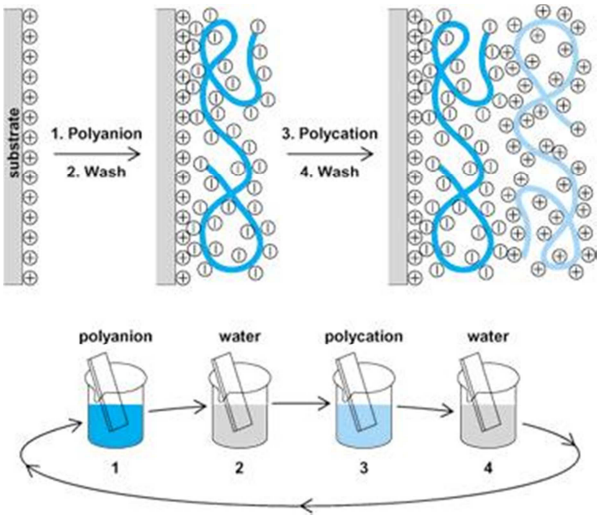

Figure 1.2 Layer-by-layer deposition process
(URL: http://accessscience.com/content/Polyelectrolyte-multilayers/YB041090).

1.3 Oxidative enzymes as biocatalysts

One of the most relevant goals in green chemistry is the development of mild and highly selective reductions and oxidations of complex substrates to yield key intermediates in pharmaceutical, agrichemical and food industries.[25] The use of conventional chemical synthesis is very often quite difficult because of the lack of control and predictability of the product structures and the expense of oxidizing reagents; so that the use of enzymes appears as a suitable alternative, conferring some important advantages in developing oxidative biotransformations (Table 1.2).

Table 1.2 Advantages in using oxidative enzyme as biocatalysts.

1. Oxidation reactions readily achieved or controlled
2. Stereo- and regio- selectivity
3. Addition of functionality
4. Introduction of chirality
5. Increased degree of hydroxylation
6. Increased hydrophobicity and polarity of a molecule
7. Altering its solubility in aqueous systems

The effectiveness of biological oxidizing agents can be attributed partially to their high redox potentials, which enable them to facilitate reaction with chemically stable starting compounds. Hydroxy- and oxo- compounds are important in the pharmaceutical, agrichemical and food industries, and, potentially, biological oxidation reactions can provide feasible alternatives to chemical synthetic routes in many cases.[25] In living systems, oxidative enzymes might have roles in primary or secondary metabolism. Some bacteria are capable of using aromatic hydrocarbons as their only carbon source

(primary metabolism) through monooxygenase or dioxygenase activity, whereas others produce oxidative enzymes that are more clearly involved in secondary metabolite production.[26] The wide variety of oxidizing enzymes known, and the range of their different activities, makes classification very useful to the chemist seeking a biocatalyst for a specific system. Redox enzymes are grouped in the oxidoreductases family, classified as EC 1.# in the EC (Enzyme Commission) number classification of enzymes. According to their coenzyme requirement or to the nature of the oxidizing substrate (the electron acceptor) and the reaction products, oxidoreductases can be further classified into 22 subclasses (Table 1.3 and Figure 1.3). Among these enzymes, oxidases, peroxidases and oxygenases are extensively used in biocatalysis for oxidative biotransformations, since they use oxygen atoms as electron acceptor in their catalytic processes. Specifically, oxidases and peroxidases react with oxygen (as molecular oxygen or peroxide, respectively) producing reactive oxygen intermediates that further react with reducing substrates. Instead, oxygenases introduce one or two oxygen atoms into their substrates and are often more selective than oxidases and peroxidases, particularly in terms of regiospecificity.

Table 1.3 Oxidoreductase classification (http://enzyme.expasy.org/).

EC 1.1 includes oxidoreductases that act on the CH-OH group of donors (alcohol oxidoreductases)
EC 1.2 includes oxidoreductases that act on the aldehyde or oxo group of donors
EC 1.3 includes oxidoreductases that act on the CH-CH group of donors (CH-CH oxidoreductases)
EC 1.4 includes oxidoreductases that act on the CH-NH_2 group of donors (Amino acid oxidoreductases)
EC 1.5 includes oxidoreductases that act on CH-NH group of donors
EC 1.6 includes oxidoreductases that act on NADH or NADPH
EC 1.7 includes oxidoreductases that act on other nitrogenous compounds as donors
EC 1.8 includes oxidoreductases that act on a sulfur group of donors
EC 1.9 includes oxidoreductases that act on a heme group of donors
EC 1.10 includes oxidoreductases that act on diphenols and related substances as donors
EC 1.11 includes oxidoreductases that act on peroxide as an acceptor (peroxidases)
EC 1.12 includes oxidoreductases that act on hydrogen as donors
EC 1.13 includes oxidoreductases that act on single donors with incorporation of molecular oxygen (oxygenases)
EC 1.14 includes oxidoreductases that act on paired donors with incorporation of molecular oxygen
EC 1.15 includes oxidoreductases that act on superoxide radicals as acceptors
EC 1.16 includes oxidoreductases that oxidize metal ions
EC 1.17 includes oxidoreductases that act on CH or CH_2 groups
EC 1.18 includes oxidoreductases that act on iron-sulfur proteins as donors
EC 1.19 includes oxidoreductases that act on reduced flavodoxin as a donor
EC 1.20 includes oxidoreductases that act on phosphorus or arsenic in donors
EC 1.21 includes oxidoreductases that act on X-H and Y-H to form an X-Y bond
EC 1.97 includes other oxidoreductases

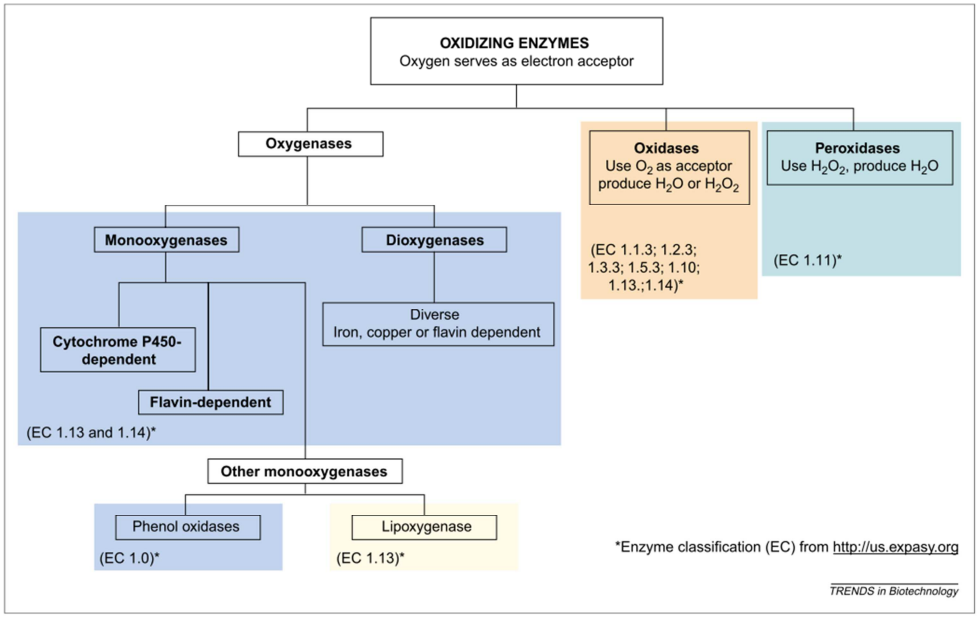

Figure 1.3 Classification of oxidative enzyme (from Burton, 2003).[27]

In this research project, a monooxygenase (tyrosinase) and an oxidase (laccase) were used to perform oxidative biotransformations; their biochemical properties and biotechnological applications are described in the following Sections.

1.4 Tyrosinases

Tyrosinases (phenol monooxygenase, EC 1.14.18.1) are widely diffused copper-containing monooxygenases with two distinct substrate-binding sites, one with high affinity for aromatic compounds, including phenolic substrates, and the other specific for metal-binding agents and molecular oxygen.[28] These enzymes catalyse both the hydroxylation of monophenols to catechols (cresolase or monophenolase activity) and the oxidation of catechols to corresponding *ortho*-quinones (catecholase or diphenolase activity) using molecular oxygen as primary oxidant (Figure 1.4).[29] In nature tyrosinases are widespread in mammals, plants and fungi in which they are responsible of the melanogenesis, the process leading to the formation of the melanin.[30] In mammals, tyrosinases were characterized for their role in the development of melanomas, and for their implication in pigmentation troubles such as albinism and vitiligo.[31] In fungi, tyrosinases are mainly associated with browning and pigmentation. Melanins constitute a mechanism of defence and resistance to stress such as UV radiations, free radicals, γ-rays, dehydration and extreme temperatures, and contribute to the fungal cell-wall resistance against hydrolytic enzymes in avoiding cellular lysis.[32] Fungal pigments are also involved in the formation and stability of spores, in the defence and virulence mechanisms.[33]

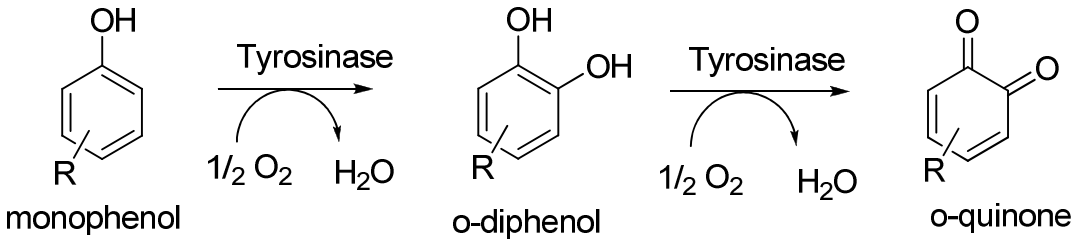

Figure 1.4 Oxidation of phenols by tyrosinases.

In addition, tyrosinases are responsible for the undesired enzymatic browning of fruits and vegetables that takes place during senescence or damage at the time of postharvest handling. However, besides this role in undesired browning, the activity of tyrosinases is needed in other cases (raisins, cocoa, fermented tea leaves) where they produce distinct organoleptic properties. All these involvements of tyrosinases in living being make the identification of novel enzyme inhibitors extremely important.[34] Best-characterized tyrosinases are the fungal *Agaricus bisporus.*

1.4.1 Structural properties of tyrosinases

Tyrosinase from mushroom *Agaricus bisporus* is a heterotetramer H_2L_2 consisting of two heavy (H) and two light (L) chains with a molecular mass of 120 kDa.[35] Robb and Gutteridge[36] identified two types of heavy chains H^{α} and H^{β} for the isozymes, $H_2{}^{\alpha}L_2$ and $H_2{}^{\beta}L_2$, corresponding to α and β, respectively. The two monomeric isoforms of the H chains contain the catalytic sites and occur as monomeric single-chain polypeptides with a molecular mass of 47 kDa; the L chains have an unknown function and occur as subunits with a molecular mass of 13kDa-14kDa.[37] The complete sequence of a tyrosinase clone for *A. bisporus* has been established by Wichers et al.[38] The enzyme tyrosinase has three domains, of which the central one contains two Cu binding sites, called Cu_A and Cu_B (Figure 1.5). The central copper-binding domain is the only highly conserved domain which also shares sequence homology with hemocyanins (Hcs), copper-containing oxygen carriers from the hemolymph of many molluscs and arthropods. Tyrosinase takes α-helical structures with the core of the enzyme, which is formed by a four-helix bundle (α2, α3, α6 and α7 helices). In addition to the helical structures, tyrosinase has a few β-structures, as judged from the backbone torsion angles. In these, only the N- and C-terminal β-strands form a sheet structure.[39,40] The location of cysteine (Cys) also plays an important role in the formation of disulfide linkages, which stabilize protein structure. The number of Cys residues varies from one organism to another.

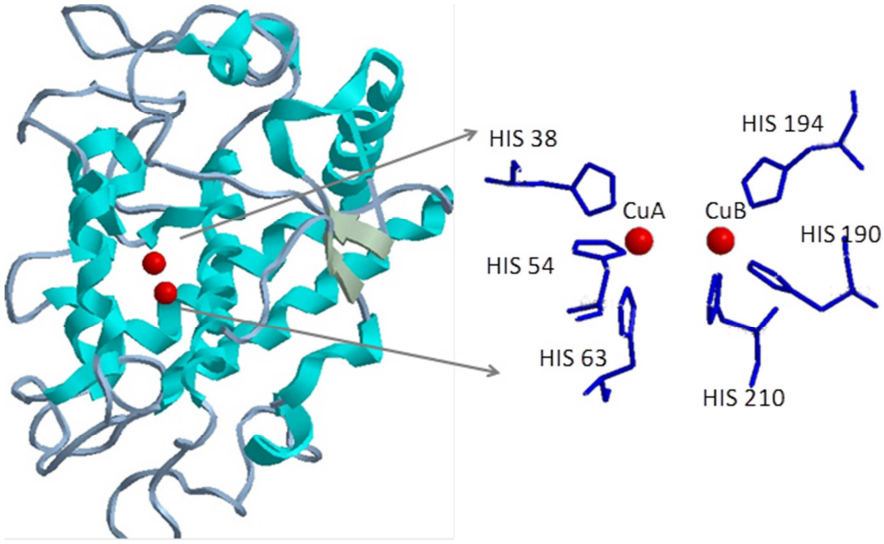

Figure 1.5 On the left the 3D representation of tyrosinase (PDB: 1WX2) with β-sheets in grey, α-helices in light blue and copper atoms in red. On the right magnification of the active site. (Adapted from Decker et al., 2006)[40]

1.4.2 Catalytic cycle

The catalytic dinuclear copper center is lodged in the helical bundle. Each of the two copper ions is coordinated by three histidine (His) residues, which are derived from the four helices of the α-bundle except His54. One copper ion (designated CuA) is coordinated by His38, His54, and His63. His38 and His63 are located in the middle of α2 and α3, respectively. The second copper ion (CuB) is coordinated by His190, His194, and His216. The residues His190 and His194 are at the beginning and in the middle of α6, respectively, and His216 is in the middle of α7. This dicopper center is located at the bottom of the large concavity as a putative substrate-binding pocket, which is formed by the hydrophobic residues. In the catalytic cycle, three types of tyrosinases (*oxy*-, *met*-, and *deoxy*-tyrosinase, Figure 1.6) with different binuclear copper structures of the active site, are involved. The oxygenated form (*oxy*tyrosinase, E_{oxy}) consists of two tetragonal copper(II) atoms, each coordinated by two strong equatorial and one weaker axial N_{His} ligand. The exogenous oxygen molecule is bound as peroxide and bridges the two copper atoms.[41] *Met*tyrosinase (E_{met}), similar to the *oxy*- form, contains two tetragonal copper (II) ions antiferromagnetically coupled through an endogenous bridge, although hydroxide exogenous ligands other than peroxide are bound to the copper site. This derivative can be converted by addition of peroxide to *oxy*tyrosinase, which in turn decays back to *met*tyrosinase when the peroxide is lost. *Deoxy*tyrosinase (E_{deoxy}) has a bicuprous structure [$Cu^{(I)}$-$Cu^{(I)}$] with a coordination arrangement similar to that of the *met*- form, but without the hydroxide bridge.[42] Monophenolic substrate initially coordinates to an axial position of one of the coppers of *oxy*tyrosinase (E_{oxy}).[43] Rearrangement leads to *o*-hydroxylation of monophenol by the bound peroxide, loss of H_2O and formation of the E_{met}-Diphenol complex ($E_{met}D$), as has been experimentally supported by EPR and X-ray studies.[44]

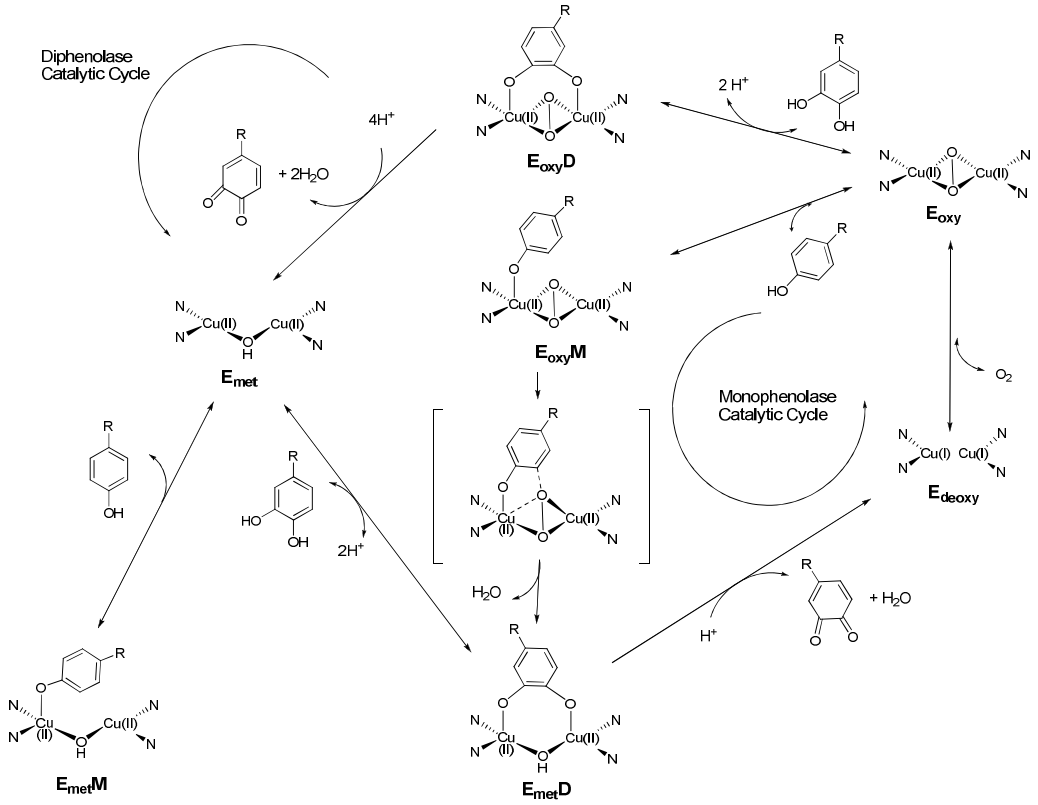

Figure 1.6 Catalytic cycle for the oxidation of monophenol and diphenol substrates to *o*-quinones by tyrosinase in the presence of O_2. E_{oxy}, E_{met}, and E_{deoxy} are the three types of tyrosinase, respectively. E_{oxy}D, E_{oxy}M, E_{met}D and E_{met}M are E_{oxy}-Diphenol, E_{oxy}-Monophenol, E_{met}-Diphenol and E_{met}-Monophenol complexes, respectively. (From Sánchez-Ferrer et al., 1995)[45]

This E_{met}D form can either render free diphenol as a first step in the diphenolase cycle, or undergo oxidation of the diphenolate intermediate bound to the active center, giving a free quinone and a reduced binuclear cuprous enzyme site (E_{deoxy}). *Oxy*tyrosinase is, then, regenerated after the binding of molecular oxygen to E_{deoxy}. If only diphenol is present in the reaction mixture, it binds to the E_{oxy} form to render E_{oxy}-Diphenol complex (E_{oxy}D), which oxidizes the diphenol to *o*-quinone and yields the antiferromagnetically coupled tetragonal Cu(II) form of the enzyme (E_{met}). The latter form transforms another *o*-diphenol molecule to *o*-quinone and it is reduced to the bicuprous E_{deoxy} form. In most situations, a diphenol is necessary as the reducing agent to obtain the *deoxy*- form, the only one capable of reacting with molecular oxygen and continuing in the catalytic action. For this reason, the monophenolase activity presents a characteristic lag time that exists until a sufficient amount of catechol (needed to reduce the *met*-form to the *deoxy*- one) is produced by the small amount of the *oxy*- form generally present in the resting enzyme preparations.[45] In fact, the resting form of tyrosinase, i.e. the enzyme as obtained after purification, is found to be a mixture of > 85% *met*- and < 15% *oxy*- forms.[46] The length of the lag time depends on several factors: the enzyme source; the concentration of monophenol (the lag period being longer when monophenol concentration is

increased); the enzyme concentration (with the lag period diminishing, but never totally disappearing, when the enzyme concentration is increased); and finally, the presence of catalytic amounts of *o*-diphenol or transition metal ions, which completely abolish the lag period.

1.4.3 Substrate stereospecificity and tyrosinase inhibitors

Tyrosinases are able to use monohydroxyphenols (*p*-cresol and tyrosine), dihydroxyphenols (catechol, L-dopa, D-dopa, catechin, and chlorogenic acid) and trihydroxyphenols (pyrogallol) as substrates.[47] The stereospecificity of monophenolase and diphenolase activity of mushroom tyrosinases with several enantiomorphs (D-, L-, and DL-tyrosine, methyltyrosine, dopa, methyldopa, and isoprenaline) of monophenols and *o*-diphenols was assayed by Espin et al.[48] The lower K_m value observed for L-isomers than for D-isomers indicated stereospecificity in the affinity of tyrosinases toward their substrates. They further elucidated that the phenolic compounds containing electron-withdrawing groups are poor substrates for tyrosinases as compared to the electron-donating groups. Moreover, affinity properties ($1/K_m$) and catalytic efficiency (V_{max}/K_m) of tyrosinases increase with a decrease in the size of the side chain in the aromatic ring of their substrates. For the past few decades, tyrosinases inhibitors have been a great concern solely due to the key role of tyrosinases in both mammalian melanogenesis and fruit and fungi enzymatic browning. Tyrosinase inhibitors are classified into two types: reversible inhibitors and irreversible inhibitors (Figure 1.7).

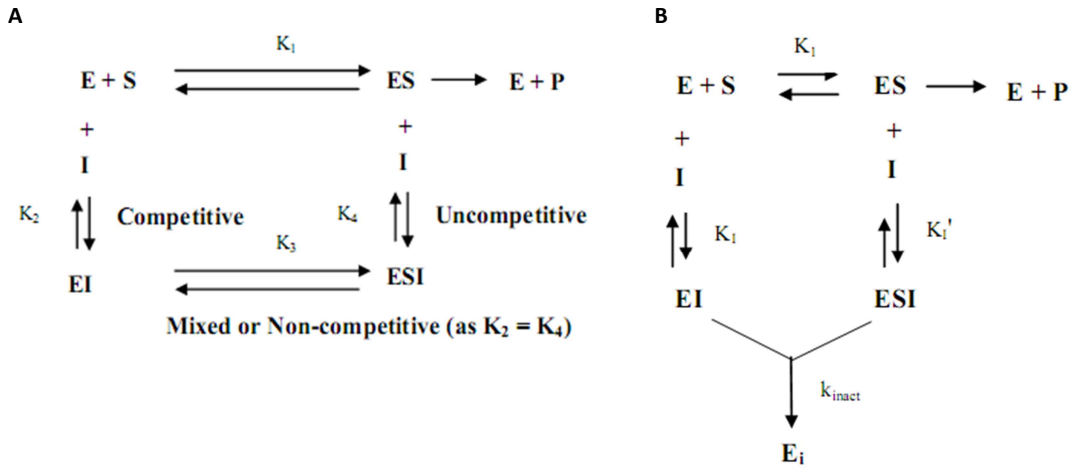

Figure 1.7 Action mechanism of reversible (A) and irreversible inhibitors (B). E, Ei, S, I, and P are the enzyme, inactivated enzyme, substrate, inhibitor, and product, respectively; ES is the enzyme-substrate complex, and EI and ESI are the enzyme-inhibitor and enzyme-substrate-inhibitor complexes, respectively. (From Chang, 2009)[49]

Reversible inhibitors bind to enzyme with non-covalent interactions such as hydrogen bonds, hydrophobic interactions and ionic bonds. In contrast to substrates and irreversible inhibitors, reversible inhibitors generally do not undergo chemical reactions when bound to the enzyme and can be easily removed by dilution or dialysis. There are four kinds of reversible enzyme inhibitors:

competitive inhibitors, uncompetitive inhibitors, mixed type inhibitors and non-competitive inhibitors. A competitive inhibitor is a substance that combines with the active site of the enzyme and prevents substrate binding. An uncompetitive inhibitor can bind only to the enzyme-substrate complex. A mixed (competitive and uncompetitive mixed) type inhibitor can bind with a free enzyme and with the enzyme-substrate complex. A special case among the mixed inhibitors is the non-competitive inhibitors, which bind to a free enzyme and an enzyme-substrate complex with the same equilibrium constant. Irreversible inhibitors covalently modify an enzyme: they often contain reactive electrophilic groups that react with amino acid side chains containing nucleophiles (hydroxyl or sulfhydryl groups) to form covalent adducts. The irreversible inhibitors display a time-dependent inhibition. Tyrosinase inhibitors from both natural and synthetic sources (Table 1.4) have been extensively reviewed by Chang.[49]

Table 1.4 Some mushroom tyrosinase inhibitors. (Adapted from Seo et al., 2003)[29b]

Inhibitor	Source	Type of inhibition
kaempferol	*Crocus sativus*	competitive[a]
quercetin	*Heterotheca inuloides*	competitive[a]
kurarinone	*Sophora flavescens*	noncompetitive[b]
oxyresveratrol	*Morus alba*	noncompetitive[a]
anacardic acid	*Anacardium occidentale*	competitiv[d]
p-coumaric acid	*Panax ginseng*	mixed[c]
aloesin	*Aloe vera*	noncompetitive[a]
3,4-dihydroxycinnamic acid	*Pulsatilla cernua*	noncompetitive[a]
cuminaldehyde	*cumin seed*	noncompetitive[a]
cumic acid	*cumin seed*	noncompetitive[a]
anisaldehyde	*anise oil*	noncompetitive[a]
anisic acid	*anise oil*	noncompetitive[a]
trans-cinnamaldehyde	*Cinnamomum cassia*	competitive[a]
2-hydroxy-4-methoxybenzaldehyde	*Mondia whitei, Rhus vulgaris, Scleroca caffra*	mixed[d]
o-,m-,p-methoxycinnamic acid	Synthetic source	noncompetitive[a]
cinnamaldehyde	Synthetic source	noncompetitive[a]
cinnamic acid	Synthetic source	mixed[a]
kojic acid	Synthetic source	mixed[a]
benzoic acid	Synthetic source	mixed[a]
benzaldehyde	Synthetic source	noncompetitive[a]
p-hydroxybenzaldehyde	Synthetic source	competitive[a]
citral	Synthetic source	noncompetitive[a]

[a] wrt dopa; [b] wrt tyrosine; [c] wrt catechin; [d] wrt chlorogenic acid

1.4.4 Tyrosinases as biocatalysts

The most important biotechnological applications of tyrosinases are a) the biosynthesis of L-DOPA; b) the detection and quantification of phenolic compounds in water samples; c) the removal of phenolic compounds from wastewaters and d) the production of cross-linked protein networks.

a) L-DOPA is an important drug for treatment of Parkinson's disease.[50] Most of the commercially L-DOPA is produced from vanillin and hydantoin by a chemical process that involves eight reaction steps.[51] The possibility to synthesize L-DOPA through a cheaper and environmental process led several investigators to study tyrosinases as useful alternative to chemical synthesis. Interesting results were obtained with immobilized tyrosinases, paving the way for a possible industrial application (Table 1.5).

b) Wastewaters containing phenols and phenolic derivatives are generated by the textile, coal, chemical, petro-chemical, mining and paper industries.[52] Increasingly strict environmental laws are providing an impetus for the development of analytical techniques for fast monitoring of these compounds. Biosensors are currently being developed for the detection of phenols, based on the reaction of these compounds with an immobilized mushroom tyrosinase. The detection and quantification of the reaction within the biosensor can be based on various different principles, such as detection of oxygen consumption,[53] direct reduction of liberated *o*-quinone,[54] the reduction of the *o*-quinone using a redox mediator such as hexacyanoferrate.[55]

Table 1.5 Productivity for L-DOPA production using immobilized mushroom tyrosinase. (From deFaria et al., 2007)[56]

Immobilization method	Productivity/(mg/(L·h))
Adsorption on nylon 6,6	33 (using a single 7-h batch experiment)
Entrapment in copper-alginate gels	4.5 (in batch reactor); 110 (in packed bed reactor when air was used)
Adsorption on sodium aluminosilicate and calcium aluminosilicate (two separate forms of zeolite)	34 (using a single 7-h batch)
Adsorption on polystyrene-polyamino styrene (PSNH) and polymethylchloride styrene (PSCL)	1.4 for the PSNH and 2.33 for the PSCL at 30 °C 3.9 for the PSNH at 60 °C 5.5 for the PSCL at 70 °C (using a batch reactor)
Adsorption on chitosan-based support	54 (on chitosan flakes using glutaraldehyde as crosslinking agent and using a batch reactor)

c) The presence of phenolic compounds in drinking and irrigation water or in cultivated land represents a significant health and environmental hazard. In recent years, methods for the removal and transformation of phenolic compounds have received attention. Numerous conventional methods have been used to remove phenols from industrial wastewaters, all based on chemical or physical principles such as solvent extraction, chemical oxidation and adsorption onto activated carbon.[57] However, these methods typically involve high capital and operating costs and do not remove phenols completely.[58] Further, they can generate secondary effluent problems.[59] Due to the disadvantages of physical and chemical methods, enzymatic approaches have been investigated.[52b] In fact, when tyrosinases oxidize phenols and other aromatic compounds in wastewaters, the oxidized

product will polymerize to insoluble compounds that can be easily removed by filtration or precipitation.[52b]

d) The food industry has an interest in developing new biopolymers with special properties, for use not only as emulsifying and thickening agents, but also in low-calories and low-fat foods. The cross-linking of natural polymers by mushroom tyrosinase has the potential to produce such new biopolymers. Tyrosinases forms *o*-quinones from tyrosine and these *o*-quinones cross-link proteins by reacting with their amino and sulfydryl groups.[60] Halaouli et at.[61] used this capability to form a cross-linked protein network from casein using the tyrosinase from *Pycnoporus sanguineus*. Caffeic acid was supplied as an external phenolic source that was oxidized by tyrosinases, with the *o*-quinone product then acting as the cross-linker in the production of protein-protein conjugates.[62] In addition, a polysaccharide-protein biopolymer was obtained from gelatin and chitosan by tyrosinase cross-linking.[63] In this process, tyrosinases oxidized tyrosine residues of the gelatin, which then reacted with the available amino groups of the chitosan. The gelatin-chitosan gels formed had chemical and physical properties that were different from those of gelatine gels.

1.5 Laccases

Laccases (benzenediol: oxygen oxidoreductase, EC 1.10.3.2) are a multicopper oxidase which catalyses the four-electron reduction of O_2 to H_2O, coupled with one-electron oxidation of four hydrogen-donating substrates, mainly phenols, polyphenols and aromatic derivatives as benzenethiol and anilines.[64] Laccases were first described by Yoshida[65] in 1883 in the exudates of *Rhus vernicifera*, the Japanese lacquer tree, and they were also detected in fungi by Bertrand[66] in 1896. Since then, laccases activity has been found also in some insects[67] and prokaryotes.[68] However, the majority of laccases were isolated from fungi;[69] over 60 fungal strains belonging to Ascomycetes, Deuteromycetes and especially Basidiomycetes show laccase activities. Among the latter group, white-rot fungi are the highest producers of laccases but also litter-decomposing and ectomycorrhizal fungi secret laccases.[64a] Biological functions of laccases are different in the various organisms but they all catalyse polymerization or depolymerization processes. Laccases are involved in cuticle sclerotization in insects;[67,70] in the assembly of UV-resistant spores in *Bacillus* species;[71] in lignification cell walls in plant;[72] spore resistance and pigmentation;[73] lignin biodegradation, humus turnover and detoxification processes in fungi.[64a] Additionally, laccases can protect fungal pathogens from toxic phytoalexins and tannins, and they are an important virulence factor in many fungal diseases.[74]

1.5.1 Structural properties of laccases

Fungal laccases often occur as monomeric proteins, although dimeric and tetrameric laccases have been also described.[75] They are glycoproteins with average molecular mass of 60-70 kDa and carbohydrate contents of 10-30% which may contribute to their high stability. The covalently linked carbohydrate moiety of the enzyme is typically formed by mannose, N-acetylglucosamine and galactose. The amino acid chain contains about 520-550 amino acids arranged in three β-barrel cupredoxin-like domains that surround the catalytic site, consisting of four copper atoms (Figure 1.8). These atoms are classified in three different classes, based on their UV-visible and electronic paramagnetic resonance (EPR) spectroscopic features: Type 1 (T1) or blue copper center, Type 2 (T2) or normal copper and Type 3 (T3) or coupled binuclear copper center. Type 1 (T1) copper shows coordination with two histidines, one cysteine and one methionine as ligands. T1 shows, at its oxidised resting state, an intense absorption band at 600 nm (ε = 5000 $M^{-1}cm^{-1}$) responsible for the blue colour of the protein. T1 also shows a characteristic EPR signal. Type 2 (T2) copper has two histidines and water as ligands. This copper site does not confer colour and it is EPR detectable. Type 3 (T3) copper consists of a pair of Cu atoms coordinates with three histidines and a hydroxyl bridge, which maintains the strong anti-ferromagnetic coupling between the T3 copper atoms.

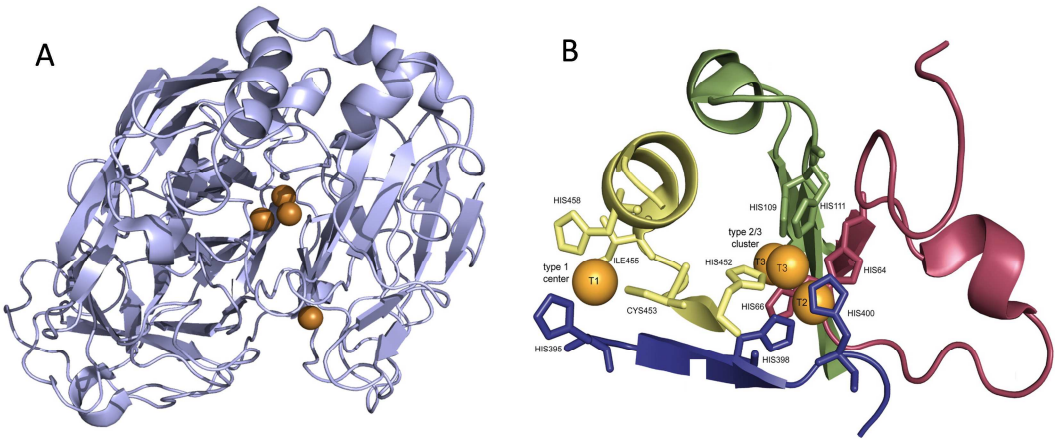

Figure 1.8 A) Ribbon representation of the laccase III from *Trametes versicolor* (URL: http://armstrong.chem.ox.ac.uk/laccase.html); B) Copper binding residues of laccase from *Trametes versicolor*. (Adapted from Sirim et al, 2011)[76]

T3 copper site shows a weak absorbance at 330 nm but it has not detectable EPR signal. T2 and T3 copper sites are close together and form a trinuclear center that is involved in the catalytic mechanism of the enzyme.[69] Until recently, the three-dimensional structure of five fungal laccases has been reported: *Coprinus cinereus* (in a copper Type 2-depleted form),[77] *Trametes versicolor*,[78] *Pycnoporus cinnabarinus*,[79] *Melanocarpus albomyces*[80] and *Rigidoporus lignosus*,[81] the latter four enzymes with a full complement of Cu ions. Moreover, among bacteria, the three-dimensional

structures of the laccase from *Bacillus subtilis*[82] and *Streptomyces coelicolor*[83] have recently been published.

1.5.2 Catalytic cycle of laccases

Laccases catalyse one-electron oxidation processes and four molecules of substrate are oxidized to reduce a dioxygen molecule (O_2) to two water molecules. This cycle is composed by three major steps. In the first one, the substrate oxidation at the mononuclear T1 centre occurs, with the reduction of the copper atom. Then the electrons are transferred to the trinuclear T2/T3 cluster where the molecular oxygen is reduced to water. The O_2 molecule binds to the trinuclear cluster for asymmetric activation and it is postulated that the O_2 binding pocket appears to restrict the access of oxidizing agents other than O_2.[69] In Figure 1.9 is shown the catalytic cycle of laccase. The dioxygen molecule interacts with the completely reduced trinuclear cluster (T2/T3) via a $2e^-$ process to produce the peroxide intermediate which contains the dioxygen anion.

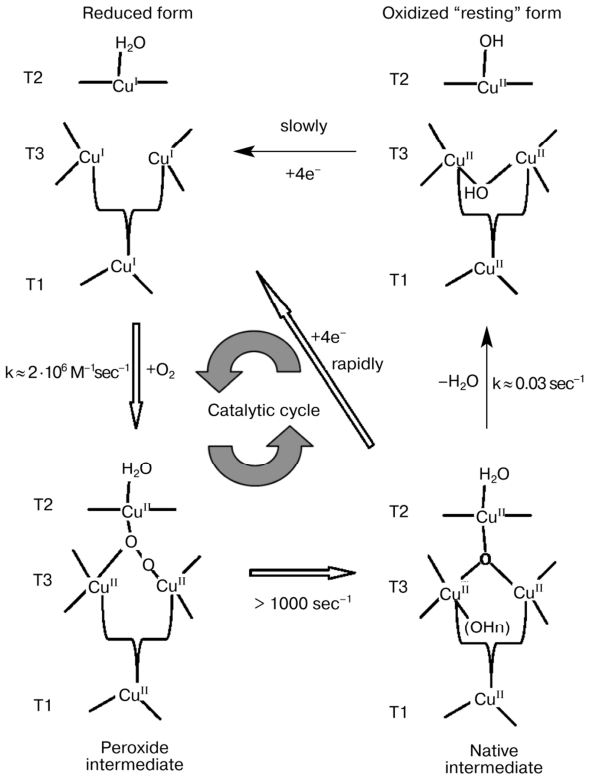

Figure 1.9 Catalytic cycle of laccases showing the mechanism of reduction and oxidation of the enzyme copper sites.

One oxygen atom of the dioxygen anion is bound with the T2 and T3 copper ions and the other oxygen atom is coordinated with another copper ion of T3. Then, the peroxide intermediate undergoes a second $2e^-$ process and the peroxide O-O bond is splitted to produce a native intermediate which is fully oxidized form with three copper centers in the trinuclear site mutually

bridged by the product of full O_2 reduction. This intermediate is either rapidly reduced by substrate in the catalytic reaction, or, in the absence of substrate, slowly decays to the resting state which contains one oxygen atom of the O_2 terminally bound as H_2O to the type 2 copper.

1.5.3 Biotechnological application of laccases

The industrial interest in the application of these enzymes lies in the low substrate selectivity, high value of catalytic constants, use of air oxygen as primary oxidant and high thermal resistance. [84] The reactions catalysed by laccases can be summarized by the schemes shown in Figure 1.10a. Laccases use oxygen as the electron acceptor to remove protons from the phenolic hydroxyl groups. This reaction gives rise to reactive radicals that can undergo a number of non-enzymatic reactions which include (i) covalent coupling to form dimers, oligomers and polymers through C-C, C-O and C-N bonds, (ii) degradation of complex polymers by cleavage of covalent bonds especially alkyl-aryl-bonds (sometimes in the presence of mediators), releasing monomers and (iii) ring cleavage of aromatic compounds.[85] The sole limit to the potential application of laccases in chemical biotransformation is given by their low redox potential [E^0 is in the range of 0.5 to 0.8 V versus NHE (normal hydrogen electrode)] compared to other redox biocatalysts.[86] The redox potential is an essential factor in determining the feasibility of reactions. Enzymes can only oxidize substrates that have lower redox potentials than their own; thus, the action of laccases would be restricted to the oxidation of a limited number of compounds.[27] Nevertheless, in the reactions where the substrate to be oxidized has a higher redox potential than laccases or when the substrate is too large to penetrate into the enzyme active site, the presence of so-called “chemical mediator” may facilitate the reaction.

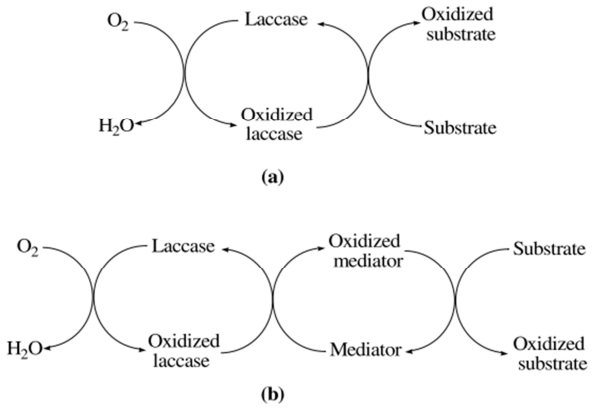

Figure 1.10 Schematic representation of laccase-catalyzed redox cycles for substrates oxidation in the absence (a) or in the presence (b) of chemical mediators.

Mediators are small molecules that act as “electron shuttle”. Once they are oxidized by the enzyme, they diffuse away from the active site and oxidize any substrates (Figure 1.10b).

It has been demonstrated that, depending on their chemical structure, mediators follow three different mechanisms of oxidation (Figure 1.11).

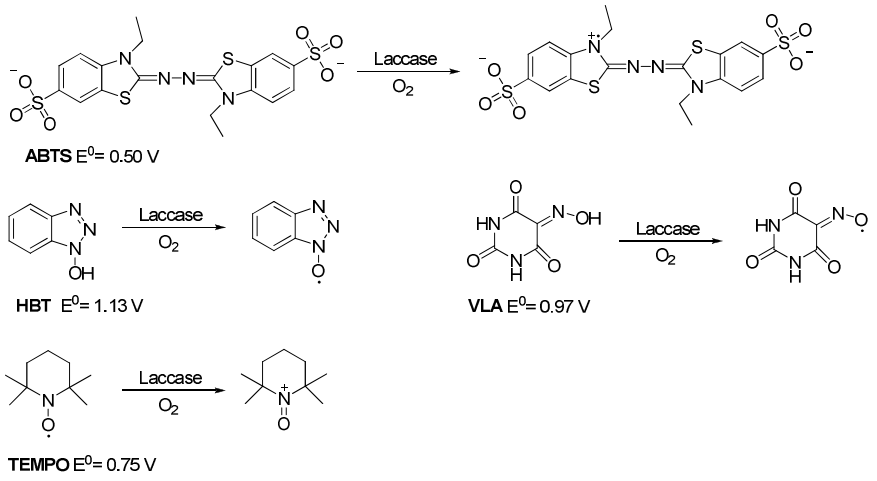

Figure 1.11 Oxidation of mediator in the presence of laccases. (Adapted from Galli et al., 2004)[87]

Compounds as ABTS [2,2'-azinobis-(3-ethylbenzothiazoline-6-sulphonic acid); E^0= 0.5 V[88]] follow the electron-transfer mechanism;[89] N-OH compounds, such as HBT (1-hydroxybenzotriazole; E^0= 1.13 V[90]) and VLA (violuric acid; E^0= 0.97 V[90]) prefer the radical H-abstraction (HAT) pathway;[91] and TEMPO (2,2,6,6-tetramethyl-1-piperidinyloxy free radical, E^0= 0.75 V[92]) undergoes in a one-electron transfer mechanisms to form the oxoammonium ion.[87,93] Laccase mediator systems (LMS) allowed oxidizing "unnatural" substrates increasing the biotechnological applications of laccases, also in fine organic synthesis.[84,94] In fact, LMS was used in delignification and biobleaching of pulp;[95] enzymatic modification of fibers, dye-bleaching in the textile and dye industries;[96] detoxification of pollutants and bioremediation[97] and construction of biosensors and biofuel cells.[98] In organic synthesis, laccases have been employed for the coupling of phenols and steroids,[99] construction of carbon-nitrogen bonds and in the synthesis of complex natural products.[100]

References

[1] Anastas, P.; Warner, J. in *Green Chemistry: Theory and Practice,* **1998**. Oxford University Press, USA.

[2] Leisola, M.; Jokela, J.; Pastinen, O.; Turunen, O.; Schoemaker, H. Industrial use of enzymes. Helsinki University of Technology, Finland, DSM Research, Netherlands. www.hut.fi/Units/Biotechnology/Kem-70.415/INDUSTRIAL_USE_OF_ENZYMES.DOC

[3] Lamare, S.; Legoy, M. *Tibtech* **1993,** *11*, 413-418

[4] a) Kamat, S.; Beckman, E.; Russell, A. *Critic Rev Biotechnol* **1995,** *15*, 41-71; b) Marty, A.; Chulalaksananukul, W.; Willemot, R.M.; Condoret, J.S. *Biotechnol Bioeng* **1992,** *39*, 273-280;

[5] a) Durand, J.; Teuma, E.; Gomez, M. *C R Chim* **2007,** *10*:152-177; b) Ulbert, O.; Belafi-Bako, K.; Tonova, K.; Gubicza, L. *Biocatal Biotransfor* **2005,** *23(3-4)*, 177-183; c) Park, S.; Kazlauskas, R.J. *Curr Opin Biotechnol* **2003,** *14*, 432-437; d) van Rantwijk, F.; Lau, R.M.; Sheldon, R.A. *TIBTECH* **2003,** *21(3),* 131-138;.

[6] a) Ulijn, R.V.; Janssen, A.E.M.; Moore, B.D.; Halling, P.J. *Chem Eur J* **2001,** *7(10)*, 2089-2097; b) Erbeldinger, M.; Ni, X.; Halling, P.J *Biotechnol Bioeng* **1998,** *59(1)*, 68-72.

[7] a) Illanes, A. in *Enzyme Biocatalysis Principles and Applications* (Illanes, A. ed.) **2008**, 20-39. Springer; b) Bommarius, A.S.; Riebel, B.R. in *Biocatalysis foundamentals and applications* (Bommarius, A.S.; Riebel, B.R. ed.) **2004**, 339-372. Wiley-VCH Verlag GmbH, Weinheim; c) Kulo, M.R. in *Enzyme Catalysis in Organic Synthesis A Comprehensive Handbook* (Drauz, K.; Waldmann, H. ed.) **2002,** 1-40. Wiley-VCH Verlag GmbH, Weinheim.

[8] Blanco, R.M.; Terreros, P.; Munoz, N.; Serra, E. *J Mol Catal B Enzym* **2007,** *47(1-2),* 13-20.

[9] a) Brady, D.; Jordaan, J. *Biotechnol Lett* **2009,** *31,* 1639-1650; b) Iyer, P.V.; Ananthanarayan, L. *Process Biochem* **2008,** *43*, 1019-1032.

[10] Krajewska, B. *Enzyme and Microbiol Tech* **2004**, *35*, 126-139.

[11] Spahn, C.; Minteer, S.D. *Recent Patents On Engineering*, **2008**, *2*, 195-200.

[12] Lalonde, J. in *Enzyme Catalysis in Organic Synthesis A Comprehensive Handbook* (Drauz, K.; Waldmann, H. ed.) **2002,** 163-184. Wiley-VCH Verlag GmbH, Weinheim

[13] Illanes, A.; Fernandez-Lafuente, R.; Guisan, J.M.; Wilson, L. in *Enzyme Biocatalysis Principles and Applications* (Illanes, A. ed.) **2008**, 155-204. Springer.

[14] Decher, G.; Hong, J.-D. *Macromol Chem Macromol Symp* **1991,** *46*, 321-327

[15] Decher, G.; Lehr, B.; Lowack, K.; Lvov, Y.; Schmitt, J. *Biosens Bioelectr* **1994,** *9*, 677-683.

[16] a) Lvov, Y.M.; Sukhorukov, G.B. *Membr Cell Biol* **1997,** *11(3)*, 277-303; b) Lvov, Y.M.; Ariga, K.; Ichinose, I.; Kunitake, T. *J Chem Soc Chem Commun* **1995,** *22*, 2313-2314.

[17] Sukhorukov, G.B.; Montrel, M.M.; Petrov, AI.; Shabarchina, L.I.; Sukhorukov, B.I. *Biosens Bioelectr* **1996,** *11(9)*, 913-922.

[18] Pommersheim, R.; Schrezenmeir, J.; Vogt, W. *Macromol Chem Phys* **1994,** *195*, 1557-1567.

[19] Sukhorukov, G.B.; Donath, E.; Davis, S.A.; Lichtenfeld, H.; Caruso, F.; Popov, V.I.;Mohwald H. *Poly Adv Technol* **1998,** *9,* 759-767.

[20] a) Shimazaki, Y., Ito, S., Tsutsumi, N. *Langmuir* **2000**, *16*, 9478-9482; b) Lvov, Y., Yamada, S., Kunitake, T. J. *Thin Solid Films* **1997**, *300*, 107-112.

[21] Zheng, H.; Lee, I.; Rubner, M. F.; Hammond, P. T. *Adv. Mater* **2002**, *14*, 569-572.

[22] a) Malaisami, R.; Bruening, M. L. *Langmuir*, **2005**, *21*, 10587-10592; b) Liu, X.; Bruening, M. L. *Chem Mater* **2004**, *16*, 351-357; c) Wanqin, J.; Toutianoush, A.; Thieke, B. *Langmuir* **2003**, *19*, 2550-2553; d) Kraseman, L.; Thieke, B.J. *Membr. Sci.* **1998**, *150*, 23-30.

[23] a) Wu, Z.; Guan, L.; Shen, G.; Yu, R. *Analyst* **2002**, 391-395; b) Forzani, S.E.; Solis, V.M. *Anal Chem* **2000**, *72*, 5300-5307.

[24] Smuleac, V.; Butterfield, D.A.; Bhattacharyya, D. *Langmuir* **2006**, *22*, 10118-10124.

[25] a) Cirino, P.C.; Arnold, F.H. *Curr Opin Chem Biol* **2002,** *6*, 130-135; b) Duetz, W.A.; van Beilen, J.B.; Witholt, B. *Curr Opin Biotechnol* **2001,** *12*, 419-425; c) Boyd, D.R.; Sharma, N.D.; Allen, C.C. *Curr Opin Biotechnol* **2001,** *12*, 564-573; d) Holland, H.L. *Curr Opin Chem Biol* **1999,** *3*, 22-27

[26] Holland, H.L. in *Organic Synthesis with Oxidative Enzymes*, (Holland, H.L. ed.) **1992,** 5-40. Wiley-VCH Verlag GmbH, Weinheim

[27] Burton, S. *TRENDS Biotechnol* **2003,** *21(12)*, 543-549.

[28] Duchworth, H.W.; Coleman, J.E. *J Biol Chem* **1970,** *245,* 1613-1625.

[29] a) Halaouli, S.; Asther, M.; Sigoillot, J.-C.; Hamdi M.; Lomascolo A. *J Appl Microbiol* **2006**, *100,* 219–232; b) Seo, S-Y.; Sharma, V. K.; Sharma, N. *J Agric Food Chem* **2003**, *51*, 2837-2853

[30] a) Schallreuter, K.U.; Kothari, S.; Chavan, B.; Spencer, J.D. *Exp Dermatol* **2008**, *17*, 395-404; b) Cooksey, C.J.; Garratt, P.J.; Land, E.J.; Pavel, S.; Ramsden, C.A.; Riley, P.A.; Smit N.P.M. *J Biol Chem* **1997**, *272*, 26226-26235.
[31] Riley, P.A. *Int J Biochem Cell Biol* **1997,** *29,* 1235-1239.
[32] Bell, A.A.; Wheeler, M.H. *Ann Rev Phytopathol* **1986,** *24*, 411-451.
[33] a) Jacobson, E.S. *Clin Microbiol Rev* **2000,** *13*, 708-717; b) Soler-Rivas, C., Arpin, N., Olivier, J.M. and Wichers, H.J. *Mycol Res* **1997,** *101*, 375-382; c) Mayer, A.M.; Harel, E. *Phytochem* **1979,** *31*, 193-215.
[34] Martinez, M. V.; Whitaker, J. R. *Trends Food Sci Technol* **1995**, *6*, 195-200.
[35] Strothkemp, K. G.; Jolley, R. L.; Mason, H. S. *Biochem Biophys Res Commun* **1976**, *70*, 519-524.
[36] Robb, D. A.; Gutteridge, S. *Phytochemistry* **1981**, *20*, 1481-1485
[37] a) Flurkey, W. H.; Ingebrigtsen, J. *Chemistry and Technology* (Jen, J.J. ed.) **1989,** 45-54. ACS Symposium series 405. American Chemical Society: Washington, DC, U.S.A; b) Gutteridge, S.; Mason, H. S. In *Biochemical and Clinical Aspects of Oxygen* (Caughy, W.S. ed.) **1979**, 589-602, Academic Press: New York, U.S.A.
[38] Wichers, H. J.; van den Bosch, T.; Gerritsen, Y. A.; Oyevaar, J. I.; Ebbelaar, M. C. E. M.; Recourt, K. *Mushroom Sci* **1995**, *2*, 723-728.
[39] Matoba, Y.; Kumagai, T.; Yamamoto, A.; Yoshitsu, H.; Sugiyama, M. *J Biol Chem* **2006**, *281*, 8981-8990
[40] Decker, H.; Schweikardt, T.; Tuczek, F. *Angew Chem Int Ed* **2006**, *45*, 4546-4550.
[41] Solomon, E.I.; Lowery, M.D. *Science* **1993,** *259*, 1575-1581
[42] Kubowitz, F. *Biochem Z* **1938,** *299*, 32-57.
[43] Wilcox, D.E.; Porras, A.G.; Hwang, Y.T.; Lerch, K.; Winkler, M.E.; Solomon, E.I. *J Am Chem Soc* **1985,** *107*, 4015-4027.
[44] García-Borron, J.C.; Solano, F. *Pigment Cell Res.* **2002**, *15*, 162-173.
[45] Sánchez-Ferrer, A.; Rodríguez-López, J.N.; García-Cánovas, F.; García-Carmona, F. *Biochim Biophys Acta* **1995**, *1247*, 1-11
[46] Jolley, R.L.; Evans, L.H.; Makino, N.; Mason, H.S. *J Biol Chem* **1974,** *249*, 335-345.
[47] Zhang, X.; van Leeuwen, J.; Wichers, H. J.; Flurkey, W. H. *J Agric Food Chem* **1999**, *47*, 374-378.
[48] Espín, J. C.; García-Ruiz, P. A.; Tudela, J.; García-Cánovas, F. *Biochem. J.* **1998**, *331*, 547-551.
[49] Chang, T.-S*. Int J Mol Sci* **2009**, *10*, 2440-2475;
[50] Gelb, D.J.; Oliver, E.; Gilman S. *Arch. Neurol.* **1999,** *56,* 33-39.
[51] D.F. Reinhold, T. Utne, N.L. Abramson, *United States patent* **1987,** 4716246.
[52] a) Yamada, K.; Akiba, Y.; Shibuya, T.; Kashiwada, A.; Matsuda, K.; Hirata, M*. Biotechnol. Progr.* **2005,** *21,* 823-829; b) Chiacchierini, E.; Restuccia, D.; Vinci, G. *Food Sci. Technol. Int.* **2004,** *10,* 373-382.
[53] Campanella, L.; Sammartino, M.P.; Tomassetti, M.; *Sens. Actuat. B: Chem.* **1992,** *7,* 383-388.
[54] a) Apetrei, C.; Rodríguez-Méndez, M.L.; De Saja, J.A. *Electrochimica Acta* **2011**, *56*, 8919-8925; b) Li, J.; Chia, L.S.; Goh, N.K.; Tan, S.N. *Anal. Chim. Acta,* **1998,** *362,* 203-211.
[55] Bonakdar, M.; Vilchez J.L.; Mottola, H.A. *J. Electroanal Chem* **1989,** *266*, 47-55.
[56] de Faria, R.O.; Moure, V.R.; de Almeida Amazonas, M.A.L; Krieger, N.; Mitchell, D.A. *Food Technol Biotechnol* **2007,** *45,* 287-294
[57] Lee, S.G. ; Hong, S.P.; Sung, M.H. *Enzyme Microb Technol* **1996,** *19*, 374-377.
[58] Loh, K.C.; Tan, C.P.P. *Bull. Environ Contam Toxicol* **2000,** *64,* 756-763.
[59] Toscano, G.; Colarieti, M.L.; Greco, G. *Enzyme Microb Technol* **2003,** *33,* 47-54.
[60] Matheis, G.; Whitaker, J.R. *J. Food Biochem* **1987,** *11,*309-327.
[61] Halaouli, S.; Asther, M.; Kruus, K. *J Appl Microbiol* **2005,** *98,* 332-343.
[62] Thalmann, C.R.; Lötzbeyer, T. *Eur Food Res Technol* **2002,** *214,* 276-281
[63] Chen, T.; Embree, H.D.; Wu, L.Q.; Payne, G.F. *Biopolymers* **2002**, *64,* 292-302.
[64] a) Baldrian P. *FEMS Microbiol Rev* **2006**, *30,* 215-242; b) Yaropolov, A.I.; Skorobogat'ko, O.V.; Vartanov, S.S.; Varfolomeyev, S.D. *Appl Biochem Biotechnol* **1994,** *49,* 257-280.
[65] Yoshida, H. *J Chem Soc* **1883**; *43*, 472-86.
[66] Bertrand, G. *C. R. Hebd. Seances Acad Sci* **1896,** *123*, 463-465.
[67] Kramer, K.J.; Kanost, M.R.; Hopkins, T.L.; Jiang, H.; Zhu, Y.C.; Xu R.; Kerwin, J.L.; Turecek, F. *Tetrahedron* **2001**, *57(2),* 385-392.
[68] Claus, H. *Arch Microbiol* **2003,** *179,* 145-50.
[69] Thurston, C.F. *Microbiology* **1994**, *140(1),* 19-26.
[70] Andersen, S.O. *Insect Biochem Mol Biol* **2010**, *40(3),* 166-178.

[71] a) Hullo, M.F.; Moszer, I.; Danchin, A.; Martin-Verstraete, I. *J. Bact.* **2001,** *183*, 5426-5430; b) Martins, L.O.; Soares, C.M.; Pereira, M.M.; Teixera, M.; Costa, T.; Jones, G.H.; Henriques, A.O. *J. Biol. Chem.* **1884,** *277*, 9-18859.

[72] O' Malley, D.M.; Whetten, R.; Bao, W.; Chen, C.L.; Seedorf, R.R. *Plant J* **1993**, *4*, 751-757.

[73] a) Williamson, P.R.; Wakamatsu, K.; Ito, S. *J Bacteriol* **1998**, *180*, 1570-1572; b) Aramayo, R.; Timberlake, W.E. *EMBO J*, **1993,** *12*, 2039-2048.

[74] Mayer, A.M.; Staples, R.C. *Phytochem* **2002,** *60,* 551-565

[75] a) Marques De Souza, C.G.; Peralta, R.M. *J Basic Microbiol* **2003**, *43(4),* 278-286; b) Yaver, D.S.; Xu, F.; Golightly, E.J.; Brown, K.M.; Brown, S.H.; Rey, M.W.; Schneider, P.; Halkier, T.; Mondorf, K.; Dalboge, H. *Appl Environ Microbiol* **1996**, *62*, 834-841.

[76] Sirim, D.; Wagner, F.; Wang, L.; Schmid, R.D.; Pleiss, J. *Database*, **2011,** doi:10.1093/database/bar006.

[77] a) Roggen, E.L.; Ernst, S.; Svendsen, A.; Friis, E.P.; Von, D.O.C. US2002192792, **2003;** b) Svendsen, A.; Xu, F. *US 6184015*, **2001**; c) Ducros, V.; Brzozowski, A.M.; Wilson, K.S.; Brown, S.H.; Ostergaard, P.; Schneider, P.; Yaver, D.S.; Pedersen, A.H.; Davies, G.J. *Nat Struct Biol* **1998**, *5*, 310–316.

[78] a) Piontek, K.; Antorini, M.; Choinowski, T. *J Biol Chem* **2002**, *277(40)*, 37663-37669; b) Bertrand, T.; Jolivalt, C.; Briozzo, P.; Caminade, E.; Joly, N.; Madzak, C.; Mougin, C. *Biochem* **2002,** *41*, 7325-7333.

[79] Antorini, M.; Herpoel-Gimbert, I.; Choinowski, T.; Sigoillot, J.C.; Asther, M.; Winterhalter, K.; Piontek, K. *Biochim Biophys Acta* **2002**, *1594*, 109-114.

[80] Hakulinen, N.; Kiiskinen, L.L.; Kruus, K.; Saloheimo, M.; Paananen, A.; Koivula, A.; Rouvinen, J. *Nat Struct Biol* **2002,** *9,* 601-605.

[81] Garavaglia, S.; Cambria, M.T.; Miglio, M.; Ragusa, S.; Lacobazzi, V.; Palmieri, F.; D'Ambrosio, C.; Scaloni, A.; Rizzi, M. *J Mol Biol* **2004**, *342*, 1519-1531.

[82] Enguita, F.J.; Martins, L.O.; Henriques, A.O.; Carrondo, M.A. *J Biol Chem* **2003**, *278*, 19416-19425.

[83] Skálová, T.; Dohnálek, J.; Østergaard, L.H.; Østergaard, P.R.; Kolenko, P.; Dusková, J.; Stepánková, A.; Hasek, J. *J Mol Biol* **2009**, *385*, 1165-1178.

[84] a) Riva, S. *Trends Biotechnol* **2006**, *24*, 219-226; b) Xu F. *Industrial Biotechnol* **2005**, *1*, 38-50.

[85] Kudanga, T.; Nyanhongo, G.S.; Guebitz, G.M.; Burton, S. *Enzyme Microb Technol* **2011,** *48,* 195-208.

[86] a) Messerschmidt, A. in *Multi-Copper Oxidases* (Messerschmidt, A. ed.) **1997,** 23-80, World Scientific, Singapore; b) Reinhammar, B. in *Multi-Copper Oxidases* (Messerschmidt, A., ed.) **1997,** 167-200, World Scientific, Singapore; c) Jönsson, L.; Sjöström, K.; Häggström, I.; Nyman, P.O. *Biochim Biophys Acta* **1995,** *1251*, 210-215.

[87] Galli, C.; Gentili, P. *J Phys Org Chem* **2004**, *17*, 973-977

[88] a) Abalyaeva, V.V.; Efimov, O.N. *Russ J Electrochem* **2002**, *38*, 1212-1215; b) Bourbonnais, R.; Leech, D.; Paice, M.G. *Biochim Biophys Acta* **1998**, *1379*, 381-390.

[89] a) Marjasvaara, A.; Janis, J.; Vainiotalo, P. *J Mass Spectrom* **2008**, *43,* 470-477; b) Branchi, B.; Galli, C.; Gentili, P. *Org Biomol Chem* **2005**, *3*, 2604-2614; c) Potthast, A.; Rosenau, T.; Fischer, K. *Holzforschung* **2001**, *55*, 47-56; d) Bourbonnais, R.; Paice, M.G.; Freiermuth, B.; Bodie, E.; Borneman, S. *Appl Environ Microbiol* **1997**, *63*, 4627-4632; e) Muheim, A.; Fiechter, A.; Harvey, P. J.; Schoemaker, H. E. *Holzforschung* **1992**, *46,* 121-126.

[90] Li, K.; Xu, F.; Eriksson, K.-E. L. *Appl Environ Microbiol,* **1999**, *65*, 2654-2660.

[91] Crestini, C.; Argyropoulos, D.S. *Bioorg Med Chem* **1998**, *6*, 2161-2169.

[92] Golibev, V.A.; Kozlov, Y.N.; Petrov, A.N.; Purmal, A.P. in *Bioactive spin labels* (Zhdanov, R.I. ed.) **1992,** 119-140, Springer-Verlang, London.

[93] Baiocco, P.; Barreca, A.N.; Fabbrini, M.; Galli, C; Gentili, P. *Org Biomol Chem* **2003,** *1*, 191-197.

[94] Cañas, A.; Camarero, S. *Biotechnol Adv* **2010,** *28,* 694-705.

[95] a) Babot, E.D.; Rico, A.; Rencoret, J.; Kalum, L.; Lund, H.; Romero, J.; del Río, J.C.; Martínez, Á.T.; Gutiérrez, A. *Bioresour Technol* **2011,** *102,* 6717–6722; b) Andreu, G.; Vidal, T. *Bioresour Technol* **2011***, 102(10),* 5932-7; c) Crestini, C.; Melone, F.; Saladino, R. *Bioorg Med Chem* **2011**, *19(16),* 5071-5078; d) Fillata, A.; Coloma, J.F.; Vidal, T. *Bioresour Technol* **2010,** *101(11),* 4104-4110; b).

[96] a) Shi, Y.; Zuo, J. *Adv Mater Research* **2011**, *183 - 185*, 768-772; b) Grassi, E.; Scodeller, P.; Filiel, N.; Carballo, R.; Levina, L. *Int Biodeterior Biodegrad* **2011**, *65(4),* 635-643.

[97] a) Strong, P.J.; Claus. H. *Crit Rev Env Sci Technol* **2011**, *41(4),* 373-434; b) Megharaja, M.; Ramakrishnana, B.; Venkateswarlua, K.; Sethunathand, N.; Naidu, R. *Environ Int* **2011** article in press

[98] a) Martinez-Ortiza, J.; Flores, R.; Vazquez-Duhalt, R. *Biosens Bioelectron* **2011,** *26*, 2626-2631; b) Beneyton, T.; El Harrak, A.; Griffiths, A.D.; Hellwig P.; Taly, V. *Electrochem Commun* **2011,** *13*, 24-27; c) Gil, D.M.A.; Rebelo,

M.J.F. *Eur Food Res Technol* **2010,** *231*, 303-308; d) Montereali, M.R.; Della Seta, L.; Vastarella, W.; Pilloton. R. *J Mol Catal B: Enzym* **2010,** *64,* 189-194.

[99] a) Navarra, C.; Goodwin, C.; Burton, S.; Danieli, B.; Riva. S. *J Mol Catal B: Enzym* **2010,** *65,* 52-57; b) Ponzoni, C.; Beneventi, E.; Cramarossa, M.R.; Raimondi, S.; Trevisi, G.; Pagnoni, U.M.; Riva, S.; Forti, L. *Adv Synth Catal* **2007**, *349*, 1497-1506; c) Nicotra, S.; Cramarossa, M.R.; Mucci, A.; Pagnoni, U.M.; Riva, S.; Forti, L. *Tetrahedron* **2004**, *60,* 595-600.

[100] Barilli, A.; Belinghieri, F.; Passarella, D.; Lesma, G.; Riva, S.; Silvani, A.; Danieli, B. *Tetrahedron Asym* **2004**, *15*, 2921-2925.

Chapter 2

Characterization of organic compounds: instruments at service of biotransformations

In this research project, products recovered from oxidative biotransformations were qualitative and quantitative characterized mainly by: (i) Gas Chromatography-Mass Spectrometry (GC-MS) analysis; (ii) Nuclear Magnetic Resonance (NMR) spectroscopy and (iii) Gel Permeation Chromatography (GPC). In this Chapter, a briefly overview about features and properties of equipped instruments will be given.

2.1 Gas Chromatography-Mass Spectrometry (GC-MS)

Gas chromatography-mass spectrometry (GC-MS) analyses were made using a Varian 450 GC chromatograph coupled to Varian 320 MS spectrometer. Gas chromatography-mass spectrometry (GC-MS) is a method that combines the features of gas-liquid chromatography (GC component) and mass spectrometry (MS component) to identify and quantify volatile and semi volatile organic compounds in complex mixtures (Figure 2.1).[1]

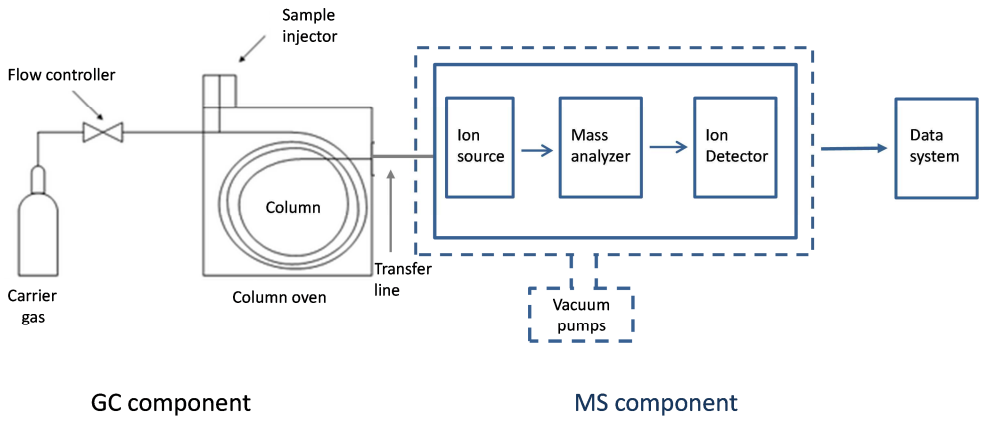

Figure 2.1 Scheme of Gas Chromatography-Mass Spectrometry (GC-MS) apparatus.

Gas chromatograph separates chemical mixtures and mass spectrometer identifies the components at a molecular level. In the gas chromatograph, the gas stream of helium (*mobile phase*) carries the gaseous compounds to be analysed through the silica column (*stationary phase*). Molecules, on the

basis of their chemical and physical properties, interact specifically with the silica packing eluting from the column at different and specific time, known as the *retention time*. The real chromatographic analysis starts with the introduction of the sample onto the column. The injection system in the capillary gas chromatograph should fulfill the following two requirements: (i) the amount injected should not overload the column; (ii) the width of the injected plug should be small compared to the spreading due to the chromatographic process; as a general rule, the volume injected, V_{inj}, and the volume of the detector cell, V_{det}, should be about 1/10 of the volume occupied by the portion of sample containing the molecules of interest (analytes) when they exit the column. The column inlet (or *injector*) provides the means to introduce a sample into a continuous flow of carrier gas. The inlet is a piece of hardware attached to the *column head*. A common inlet type is the S/SL (Split/Splitless) injector. A sample is introduced into a heated small chamber via a syringe through a *septum*; the heat facilitates volatilization of the sample and sample matrix. The carrier gas then either sweeps the entirety (*splitless* mode) or a portion (*split* mode) of the sample into the column. In split mode, a part of the sample/carrier gas mixture in the injection chamber is exhausted through the *split vent*. Split injection is preferred when working with samples with high analyte concentrations (>0.1%) whereas splitless injection is best suited for trace analysis with low amounts of analytes (<0.01%). In splitless mode the split valve opens after a pre-set amount of time to purge heavier elements that would otherwise contaminate the system. This pre-set (splitless) time should be optimized, the shorter time (e.g., 0.2 min) ensures less tailing but loss in response, the longer time (2 min) increases tailing but also signal. Thus volatilized sample is carried by the gas through the column. The column is contained in a temperature controlled oven. The rate at which a sample passes through the column is directly proportional to the temperature of the column. The higher the column temperature, the faster the sample moves through the column. However, the faster a sample moves through the column, the less it interacts with the stationary phase, and the less the analytes are separated. In general, the column temperature is selected to compromise between the length of the analysis and the level of separation. A method which holds the column at the same temperature for the entire analysis is called "isothermal." Most methods, however, increase the column temperature during the analysis, the initial temperature, rate of temperature increase (the temperature "ramp") and final temperature is called the "temperature program." A temperature program allows analytes that elute early in the analysis to separate adequately, while shortening the time it takes for late-eluting analytes to pass through the column. Thus isolated molecules are then transferred by the transfer line to the mass spectrometry where the Electron Ionization source (EI) breaks molecules into ionized fragments.

The EI source uses an electron beam, generated from a tungsten filament, to ionize gas-phase atoms or molecules by subtractions of electron (Eq. 2.1).

Eq. 2.1 $$M + e^- \rightarrow M^{+\cdot} + 2e^-$$

The EI ionization yields reproducible molecular fragmentation patterns independent of the make and model of the MS. This allows the creation of standard libraries containing searchable spectra. The EI source consists of an ion volume, a filament assembly, electron collimating magnets, and ion focusing lenses, all supported by a heated ion block. The ion volume is an open cylinder with two side holes. Vaporized sample and carrier gas from the GC enters the ion volume through the transfer line in one of the holes. An electron beam, generated at the heated filament, enters the ion volume through the other hole. The accelerated electrons collide with the sample molecules inside the ion volume and generate molecular ions. The resulting ions fragment into differently charged or neutral fragments. These generated ions enter the triple quadrupole mass analyzer (Figure 2.2). In a triple quadrupole system, the mass analyzer consists of three quadrupole rod assemblies (Q1, Q2, and Q3). Collision induced dissociation, (CID) or MS/MS applications are done in the curved Q2 of triple quadrupole systems. The ions are accelerated into Q2, which is filled with a collision gas, usually argon. The fast moving ions collide with the argon molecules and dissociate. The product ions, from these interactions, go to Q3 and neutral molecules do not reach the detector.

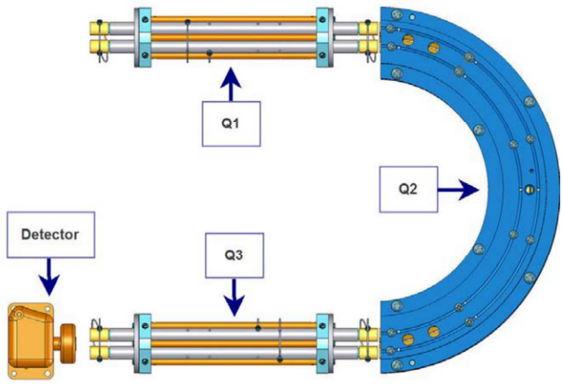

Figure 2.2 Scheme of triple quadrupole analyzer.[2]

This reduces the background noise and increase the signal to noise ratio. Q3 can either guide the ions to the detector or act as a mass filter for the fragment ions produced by CID. Triple quadrupole systems can be used for MS modes of operation (full scan or SIM) or for MS/MS modes of operation (SRM or MRM, product scan, precursor scan, neutral loss/gain scan). During MS operation of a triple quadrupole system, the RF and DC voltages are controlled so that Q1 acts as mass filter and Q2 and

Q3 are ion guides that transmit all masses to the detector. During MS/MS operations Q1 is a mass filter of the ions entering the system, Q2 is the collision cell, and Q3 is a mass filter for the product ion of the collisions. The ions enter the on-axis detector. Positive and negative ions are detected with similar efficiency due to the on-axis geometry of the detector. Extended Dynamic Range is an option that automatically adjusts the detector for the best signal to noise ratio and provides an "absolute" measure of ion counts. To use GC-MS, the organic compounds must be in solution for injection into the gas chromatograph. The solvent must be volatile and organic (for example, hexane or dichloromethane). Depending on the ionization method, analytical sensitivities of 1 to 100 pg *per* component are routine. GC-MS has a few limitations. In general, only substances that vaporize below 300 °C (and therefore are stable up to that temperature) can be measured quantitatively. The samples are also required to be salt-free; they should not contain ions. Determining positional substitution on aromatic rings is often difficult. Certain isomeric compounds cannot be distinguished by mass spectrometry (for example, naphthalene versus azulene), but they can often be separated chromatographically. Quantitative accuracy is controlled by the overall analytical method calibration. Using isotopic internal standards, accuracy of ±20% relative standard deviation is typical.

2.1.1 Applications of GC-MS

GC-MS is a technique that can be used to separate volatile organic compounds (VOCs) and pesticides. Portable GC units can be used to detect pollutants in the air, and they are currently used for vapor intrusion investigations. As such, the GC-MS instrument is very useful for the determination of molecular weights and (sometimes) the elemental compositions of unknown organic compounds in complex mixtures. Among other applications, GC-MS is widely used for the quantitation of pollutants in drinking and wastewater. It is the basis of official EPA methods. It is also used for the quantitation of drugs and their metabolites in blood and urine. Both pharmacological and forensic applications are significant. GC-MS can be used for the identification of unknown organic compounds both by matching spectra with reference spectra and by a priori spectral interpretation. The identification of reaction products by synthetic organic chemists is another routine application, as is the analysis of industrial products for control of their quality.[3]

2.1.1.1 Qualitative analysis

Generally chromatographic data is presented as a graph of detector response (y-axis) against retention time (x-axis), which is called a chromatogram. This provides a spectrum of peaks for a sample representing the analytes present in a sample eluting from the column at different times. Retention time can be used to identify analytes if the method conditions are constant. Moreover, the presence of mass spectrometer ensures the unequivocal identification of the analytes represented by

the peaks. A mass spectrum is intensity vs. *m/z* (mass-to-charge ratio) plot representing a chemical analysis. Hence, the mass spectrum of a sample is a pattern representing the distribution of ions by *m/z* in a sample. In Figure 2.3a is reported a typical gas chromatogram obtained after separation of mixture containing benzyl alcohol, benzaldehyde and acetophenone. Each analyte is represented by a single peak characterized by a specific retention time (5.304 min, 6.381 min and 6.935 min, respectively).

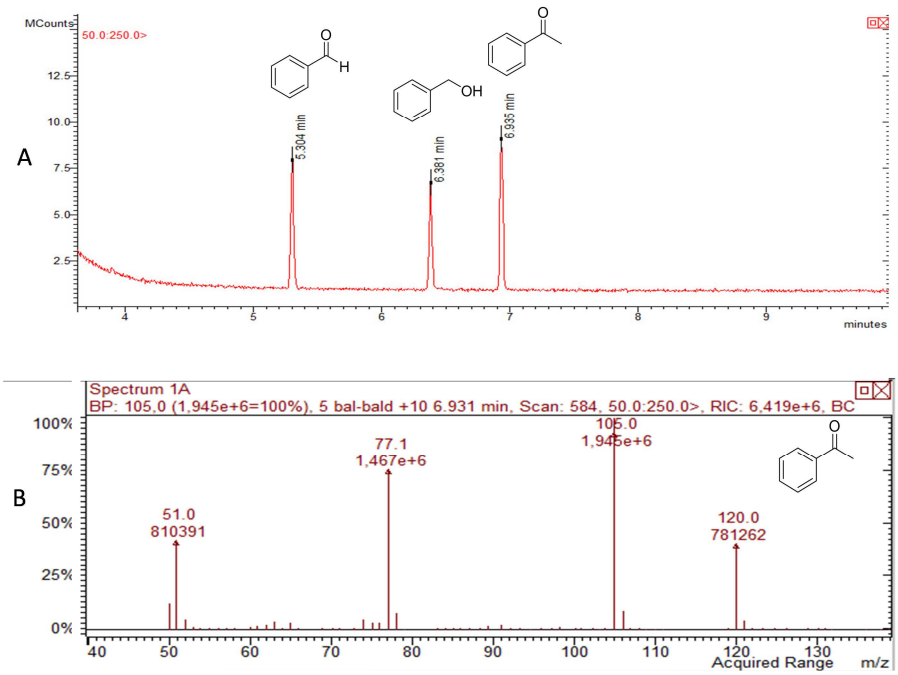

Figure 2.3 (A) Chromatogram obtained after gas chromatography separation of benzyl alcohol, benzaldehyde and acetophenone mixture; (B) mass spectrum of acetophenone molecules.

In Figure 2.3b is reported the mass spectrum of acetophenone, characterized by distinct sets of peaks:

- Molecular ion (or parent ion): is the radical cation $M^{+\cdot}$ resulting by removing one electron from the molecule and it corresponds to the molecular mass of analytes (i.e. 120 m/z). The molecular ion peak does not always appear or can be weak. The height of the molecular ion peak diminishes with branching and with increasing mass in a homologous series. Molecular ion peaks are also often preceded by an M-1 or M-2 peak resulting from loss of hydrogen radical or dihydrogen.
- Isotope peaks: more peaks are visible with m/e ratios larger than the molecular ion peak due to isotope distributions. The value of 120 in the acetophenon example corresponds to the monoisotopic mass of a molecule of toluene entirely composed of the most abundant isotopes (^{1}H and ^{12}C). The so-called M+1 peak corresponds to a fraction of the molecules with one higher isotope incorporated (^{2}H or ^{13}C) and the M+2 peak has two higher isotopes. The natural abundance of the higher isotopes is low for frequently encountered elements such as

hydrogen, carbon and nitrogen and the intensity of isotope peaks subsequently low and the intensity quickly diminishes with total mass.

- Fragmentation peaks: peaks with mass less than the molecular ion are the result of fragmentation of the molecule. These peaks are called daughter peaks. The peak with the highest ratio is called the base peak which is not necessarily the molecular ion. Many reaction pathways exist for fragmentation but only newly formed cations will show up in the mass spectrum and not radical fragments or neutral fragments.
- Metastable peaks: peaks resulting from molecular fragments with lower kinetic energy because are characterized by non-integer mass values.

2.1.1.2 Quantitative analysis

The area under a peak is proportional to the amount of analyte present in the chromatogram. By calculating the area of the peak using the mathematical function of integration, the concentration of an analyte in the original sample can be determined. Concentration can be calculated using a calibration curve created by finding the response for a series of concentrations of analyte, or by determining the relative response factor of an analyte. The relative response factor is the expected ratio of an analyte to an internal standard (or external standard) and is calculated by finding the response of a known amount of analyte and a constant amount of internal standard (a chemical added to the sample at a constant concentration, with a distinct retention time to the analyte).

2.2 Nuclear Magnetic Resonance (NMR)

Nuclear magnetic resonance spectroscopy (NMR) analyses were made using a Bruker 200 MHz and a Bruker 400 MHz instrument. NMR is a technique that exploits the magnetic properties of certain atomic nuclei to determine physical and chemical properties of atoms or the molecules in which they are contained.[4] It relies on the phenomenon of nuclear magnetic resonance and can provide detailed information about the structure, dynamics, reaction state, and chemical environment of molecules. The NMR phenomenon is based on the fact that nuclei of atoms have magnetic properties that can be utilized to yield chemical information. The nuclei of many elemental isotopes have a characteristic spin (**I**). Some nuclei have integral spins (e.g. ^{2}H, ^{14}N; I = 1), some have fractional spins (e.g. ^{1}H, ^{13}C, ^{15}N, ^{19}F, ^{31}P; I = 1/2), and a few have no spin, I = 0 (e.g. ^{12}C, ^{16}O, ^{32}S). Isotopes of particular interest and use to organic chemists are ^{1}H, ^{13}C, ^{15}N, ^{19}F and ^{31}P, all of which have I = 1/2. Since the atomic nucleus has a charge, a spinning nucleus generates a small electric current to which a small magnetic field is connected. The resulting spin-magnet has a magnetic moment (**μ**) proportional to the spin. For the four common nuclei noted above, the magnetic moments are: ^{1}H μ = 2.7927, ^{19}F μ = 2.6273,

^{31}P μ = 1.1305 and ^{13}C μ = 0.7022. In the presence of an external magnetic field (B_0), two spin states exist, +1/2 and -1/2. Spin states which are oriented parallel to the external field (+1/2) are lower in energy than in the absence of an external field. In contrast, spin states whose orientations oppose the external field (-1/2) are higher in energy than in the absence of an external field (Figure 2.4).

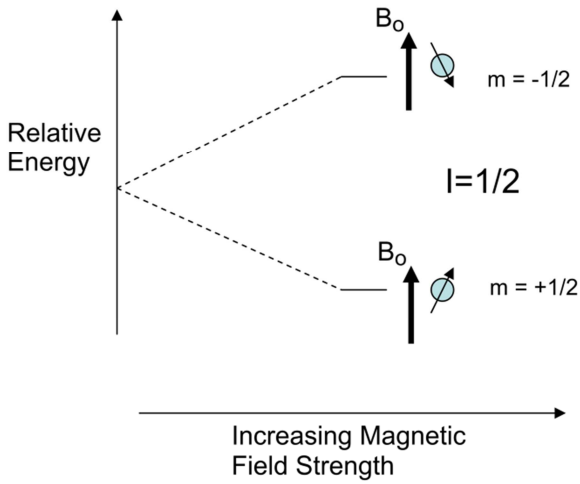

Figure 2.4 Spin states of nuclei in the presence of external magnetic field (B_0).

Modern NMR spectrometers use powerful magnets having fields of 1 to 20 Tesla (T). Even with these high fields, the energy difference between the two spin states is less than 0.1 cal/mole. For NMR purposes, the small energy difference (ΔE) between the two spin states is usually given as a frequency in units of MHz (10^6 Hz), ranging from 20 to 900 MHz, depending on the magnetic field strength and the specific nucleus being studied. Irradiation of a sample with radio frequency (rf) energy corresponding exactly to the spin state separation of a specific set of nuclei will cause excitation of those nuclei in the +1/2 state to the higher -1/2 spin state. When this transition occurs, the nuclei are in resonance with the applied radiation, hence the name Nuclear Magnetic Resonance. The absorption of energy during this transition forms the basis of the NMR method. Unlike infrared and UV-Visible spectroscopy, where absorption peaks are uniquely located by a frequency or wavelength, the location of different NMR resonance signals is dependent on both the external magnetic field strength and the rf frequency. Since no two magnets will have exactly the same field, resonance frequencies will vary accordingly and an alternative method for characterizing and specifying the location of NMR signals is needed. One method of solving this problem is to report the location of an NMR signal in a spectrum relative to a reference signal from a standard compound added to the sample. Such a reference standard should be chemically unreactive and easily removed from the sample after the measurement. Also, it should give a single sharp NMR signal that does not interfere with the resonances normally observed for organic compounds. Tetramethylsilane, $(CH_3)_4Si$, usually referred to as TMS, meets all these characteristics, and has become the reference compound of

choice for proton and carbon NMR. This association with the reference signal is called the chemical shift (δ), measured in parts per million (ppm) (Figure 2.5). As a general rule, protons and carbons adjacent to electronegative atoms are more "deshielding" thus they feel a more intense magnetic field and move them "downfield" to higher ppm values.

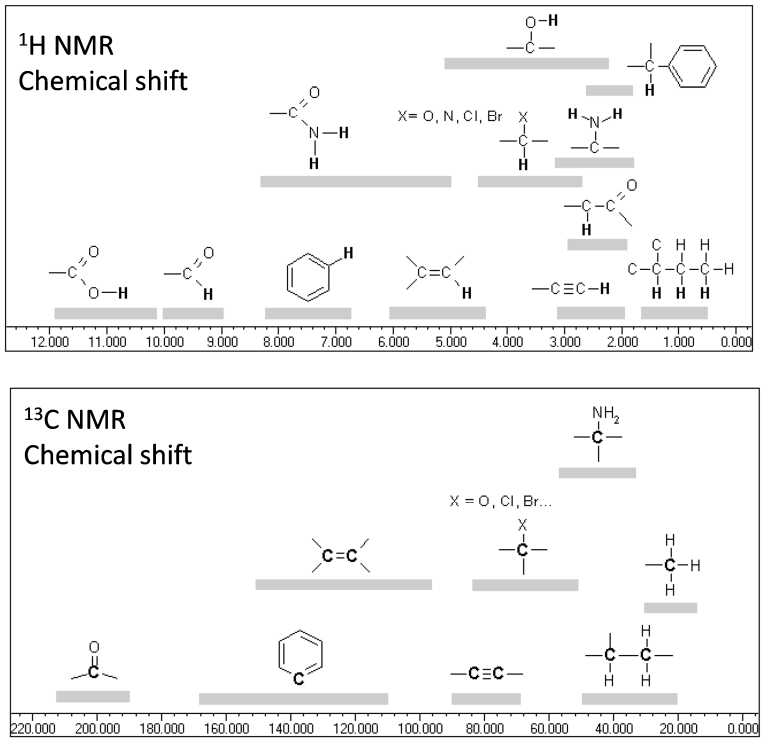

Figure 2.5 Chemical shift (in ppm) of ^{1}H and ^{13}C nuclei.

The ppm scale is another form of standardization that allows one to compare directly the spectra obtained on NMR instruments with different magnetic fields. After the samples have been referenced to the TMS resonance at 0 ppm the actual NMR peak position in Hz is divided by the resonance frequency of the spectrometer, which is in MHz obtaining a a part per million (ppm) (eq 2.2).

Eq. 2.2

$$\delta\ (ppm) = \frac{Chemical\ shift\ respect\ to\ (CH_3)_4Si\ in\ Hz}{Resonance\ frequency\ in\ MHz}$$

The proton NMR chemical shift range is 0-12 ppm, while the carbon one is 0-220 ppm (Figure 2.6). Moreover, in ^{1}H NMR the shape and size of peaks are indicators of the chemical structure because the peak intensity is proportional to the number of proton generating the signal. For example acetic acid, CH_3COOH has two peaks in ^{1}H-NMR, δ = 2 ppm with area = 3 (corresponding to CH_3 proton), and a second at δ = 12 with area = 1 (corresponding to COOH proton). Some of the most useful information for structure determination in a one-dimensional NMR spectrum comes from J-coupling or scalar

coupling between NMR active nuclei. This coupling arises from the interaction of different spin states through the chemical bonds of a molecule and results in the splitting of NMR signals. These splitting patterns can be complex or simple and, likewise, can be straightforwardly interpretable or deceptive. This coupling provides detailed insight into the connectivity of atoms in a molecule.

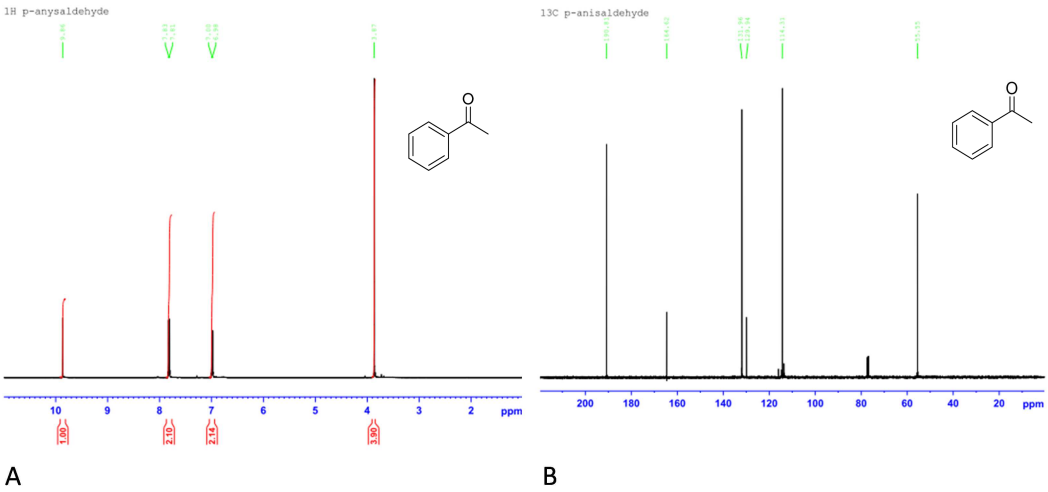

Figure 2.6 ^{1}H NMR (A) and ^{13}C NMR of acetophenone.

Coupling to *n* equivalent (spin ½) nuclei splits the signal into an *n*+1 multiplet with intensity ratios following Pascal's triangle as described in Table 2.1. Note that coupling between nuclei that are chemically equivalent (that is, have the same chemical shift) has no effect of the NMR spectra and couplings between nuclei that are distant (usually more than three bonds apart for protons in flexible molecules) are usually too small to cause observable splittings.

Table 2.1 Pascal's triangle for signal splitting.

Multiplicity	Intensity Ratio
Singlet (s)	1
Doublet (d)	1:1
Triplet (t)	1:2:1
Quartet (q)	1:3:3:1
Quintet	1:4:6:4:1
Sextet	1:5:10:10:5:1
Septet	1:6:15:20:15:6:1

Long-range couplings over more than three bonds can often be observed in cyclic and aromatic compounds, leading to more complex splitting patterns. For example, as shown in the proton spectrum for ethanol (CH_3OH) reported in Figure 2.7, the CH_3 group (3) is split into a *triplet* with an

intensity ratio of 1:2:1 by the two neighboring CH_2 protons. Similarly, the CH_2 (2) is split into a *quartet* with an intensity ratio of 1:3:3:1 by the three neighboring CH_3 protons.

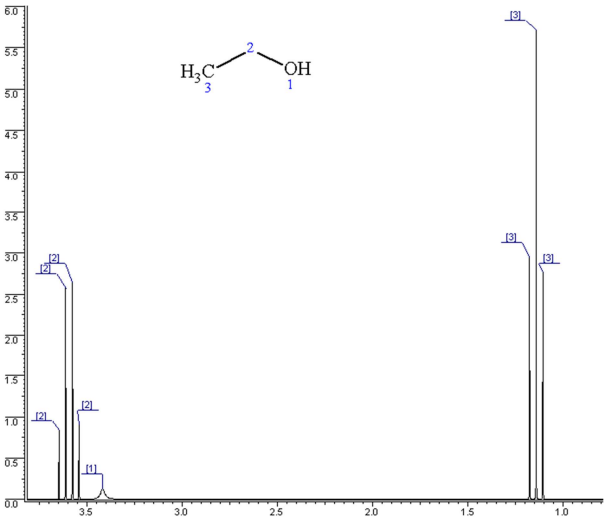

Figure 2.7 ^{1}H NMR of ethanol.

2.2.1 Two-dimensional nuclear magnetic resonance (2D-NMR)

Two-dimensional nuclear magnetic resonance spectroscopy (2D NMR) is a set of nuclear magnetic resonance spectroscopy methods which give data plotted in a space defined by two frequency axes rather than one.[5] Types of 2D NMR include correlation spectroscopy (COSY), J-spectroscopy, exchange spectroscopy (EXSY), Nuclear Overhauser effect spectroscopy (NOESY) total correlation spectroscopy (TOCSY) and heteronuclear correlation experiments, such as HSQC, HMQC, and HMBC. Two-dimensional NMR spectra provide more information about a molecule than one-dimensional NMR spectra and are especially useful in determining the structure of a molecule, particularly for molecules that are too complicated to work with using one-dimensional NMR. Each experiment consists of a sequence of radio frequency (RF) pulses with delay periods in between them. It is the timing, frequencies, and intensities of these pulses that distinguish different NMR experiments from one another. Almost all two-dimensional experiments have four stages: the preparation period, where a magnetization coherence is created through a set of RF pulses; the evolution period, a determined length of time during which no pulses are delivered and the nuclear spins are allowed to freely precess (rotate); the mixing period, where the coherence is manipulated by another series of pulses into a state which will give an observable signal; and the detection period, in which the free induction decay signal from the sample is observed as a function of time, in a manner identical to one-dimensional FT-NMR. The two dimensions of a two-dimensional NMR experiment are two frequency axes representing a chemical shift. Each frequency axis is associated with one of the two time variables, which are the length of the evolution period (the *evolution time*) and the time elapsed

during the detection period (the *detection time*). There are each converted from a time series to a frequency series through a two-dimensional Fourier transform. A single two-dimensional experiment is generated as a series of one-dimensional experiments, with a different specific evolution time in successive experiments, with the entire duration of the detection period recorded in each experiment. The end result is a plot showing an intensity value for each pair of frequency variables. The intensities of the peaks in the spectrum can be represented using a third dimension. More commonly, intensity is indicated using contour lines or different colors.

2.2.1.1 Homonuclear 2D NMR experiment

Homonuclear 2D NMR experiments occur when magnetization transfer take place between nuclei of the same type, through J-coupling of nuclei connected by up to a few bonds.

Correlation spectroscopy (COSY)

The first and most popular two-dimension NMR experiment is the homonuclear correlation spectroscopy (COSY) sequence, which is used to identify spins which are coupled to each other. It consists of a single RF pulse (p1) followed by the specific evolution time (t1) followed by a second pulse (p2) followed by a measurement period (t2). The two-dimensional spectrum that results from the COSY experiment shows the frequencies for a single isotope, most commonly hydrogen (^{1}H) along both axes. COSY spectra show two types of peaks.[6] *Diagonal peaks* have the same frequency coordinate on each axis and appear along the diagonal of the plot; while *cross peaks* have different values for each frequency coordinate and appear off the diagonal. Diagonal peaks correspond to the peaks in a 1D-NMR experiment, while the cross peaks indicate couplings between pairs of nuclei. Cross peaks result from a phenomenon called magnetization transfer, and their presence indicates that two nuclei are coupled which have the two different chemical shifts that make up the cross peak's coordinates. Each coupling gives two symmetrical cross peaks above and below the diagonal. That is, a cross-peak occurs when there is a correlation between the signals of the spectrum along each of the two axes at these values. One can thus determine which atoms are connected to one another (within a small number of chemical bonds) by looking for cross-peaks between various signals. An easy visual way to determine which couplings a cross peak represents is to find the diagonal peak which is directly above or below the cross peak, and the other diagonal peak which is directly to the left or right of the cross peak. The nuclei represented by those two diagonal peaks are coupled. As example, Figure 2.8 shows the COSY spectra of ethyl 2-butenoate. Peak marked A in the top left corner indicates a coupling interaction between the H at 6.9 ppm and the H at 1.8 ppm. This corresponds to the coupling of the CH_3 group and the adjacent H on the alkene. Similarly, the peak marked B indicates a coupling interaction between the H at 4.15 ppm and the H at 1.25 ppm. This corresponds to the coupling of the CH_2 and the CH_3 in the ethyl group.

Exclusive correlation spectroscopy (ECOSY)

ECOSY was developed for the accurate measurement of small J-couplings. It uses a system of three active nuclei (SXI spin system) to measure an unresolved coupling with the help of a larger coupling which is resolved in a dimension orthogonal to the small coupling.

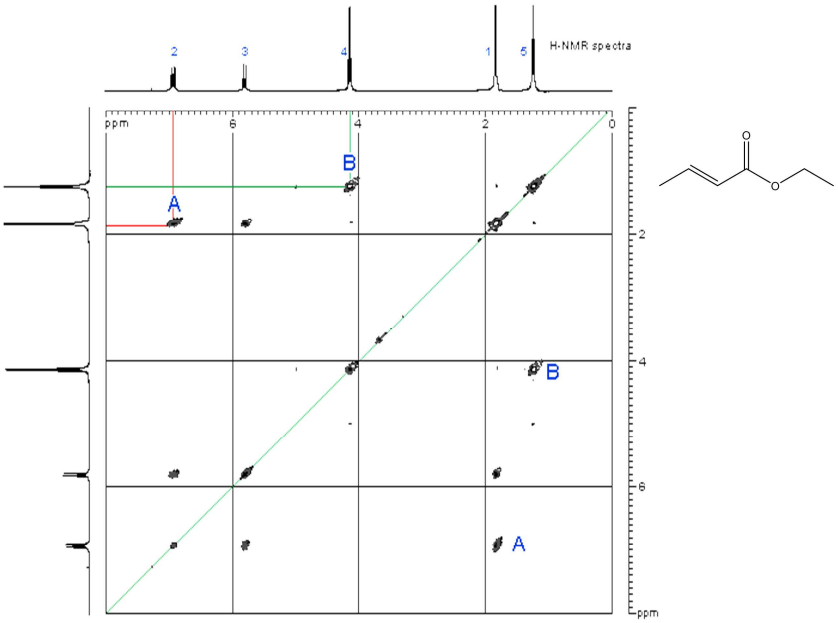

Figure 2.8 COSY spectra of ethyl 2-butenoate.[7]

Total correlation spectroscopy (TOCSY)

The TOCSY experiment is similar to the COSY experiment, in that cross peaks of coupled protons are observed.[8] However, cross peaks are observed not only for nuclei which are directly coupled, but also between nuclei which are connected by a chain of couplings. This makes it useful for identifying the larger interconnected networks of spin couplings. This ability is achieved by inserting a repetitive series of pulses which cause *isotropic mixing* during the mixing period. Longer isotropic mixing times cause the polarizaton to spread out through an increasing number of bonds.

Incredible natural-abundance double-quantum transfer experiment (INADEQUATE)

INADEQUATE is a method often used to find ^{13}C couplings between adjacent carbon atoms.[9] Because the natural abundance of ^{13}C is only about 1%, only about 0.01% of molecules being studied will have the two nearby ^{13}C atoms needed for a signal in this experiment. However, correlation selection methods are used (similar to DQF COSY) to prevent signals from single ^{13}C atoms, so that the double ^{13}C signals can be easily resolved. Each coupled pair of nuclei gives a pair of peaks on the INADEQUATE spectrum which both have the same vertical coordinate, which is the sum of the chemical shifts of the nuclei; the horizontal coordinate of each peak is the chemical shift for each of the nuclei separately.

Nuclear Overhauser effect spectroscopy (NOESY)

In NOESY, the Nuclear Overhauser cross relaxation between nuclear spins during the mixing period is used to establish the correlations. The spectrum obtained is similar to COSY, with diagonal peaks and cross peaks, however the cross peaks connect resonances from nuclei that are spatially close rather than those that are through-bond coupled to each other. NOESY spectra also contain extra *axial peaks* which do not provide extra information and can be eliminated through a difference experiment by reversing the phase of the first pulse. One application of NOESY is in the study of large biomolecules such as in protein NMR, which can often be assigned using sequential walking.

2.2.1.2 Heteronuclear 2D NMR experiment

Heteronuclear correlation spectroscopy gives signals based upon coupling between nuclei of different types.

Heteronuclear single-quantum correlation spectroscopy (HSQC)

HSQC detects correlations between nuclei of two different types which are separated by one bond. This method gives one peak per pair of coupled nuclei, whose two coordinates are the chemical shifts of the two coupled atoms.[10] HSQC works by transferring magnetization from the *I* nucleus (usually the proton) to the *S* nucleus (usually the heteroatom); this first step is done because the proton has a greater equilibrium magnetization and thus this step creates a stronger signal. The magnetization then evolves and then is transferred back to the *I* nucleus for observation. An extra spin echo step can then optionally be used to decouple the signal, simplifying the spectrum by collapsing multiplets to a single peak. The undesired uncoupled signals are removed by running the experiment twice with the phase of one specific pulse reversed; this reverses the signs of the desired but not the undesired peaks, so subtracting the two spectra will give only the desired peaks. Heteronuclear multiple-quantum correlation spectroscopy (HMQC) gives an identical spectrum as HSQC, but using a different method. The two methods give similar quality results for small to medium sized molecules, but HSQC is considered to be superior for larger molecules.

Heteronuclear multiple-bond correlation spectroscopy (HMBC)

HMBC detects heteronuclear correlations over longer ranges of about 2-4 bonds.[11] The difficulty of detecting multiple-bond correlations is that the HSQC and HMQC sequences contain a specific delay time between pulses which allows detection only of a range around a specific coupling constant. This is not a problem for the single-bond methods since the coupling constants tend to lie in a narrow range, but multiple-bond coupling constants cover a much wider range and cannot all be captured in a single HSQC or HMQC experiment. In HMBC, this difficulty is overcome by omitting one of these delays from an HMQC sequence. This increases the range of coupling constants that can be detected, and also reduces signal loss from relaxation. The cost is that this eliminates the possibility of

decoupling the spectrum, and introduces phase distortions into the signal. There is a modification of the HMBC method which suppresses one-bond signals, leaving only the multiple-bond signals.

2.3 Gel Permeation Chromatography (GPC)

The Gel Permeation Chromatography (GPC) analyses were performed using a Shimadzu LC 20AT liquid chromatograph with a SPD M20A ultraviolet diode array (UV) and a system of columns connected in series (Varian PL gel MIXED-D 5 µm, 1-40 K and PL gel MIXED-D 5 µm, MW 500-20 K). Gel permeation chromatography (GPC), also known as Size Exclusion Chromatography (SEC), is a chromatographic technique that employs specialized columns to separate natural and synthetic polymers, biopolymers, proteins or nanoparticles on the basis of size.[12] Separation occurs via the use of porous beads packed in a column. The smaller molecules spend more time traveling through the pores of the gel and are eluted later than the larger molecules which spend less time in the pores. Thus elution volume (or elution time) is proportional to molecular size. There is a limited range of molecular weights that can be separated by each column and therefore the size of the pores for the packing should be chosen according to the range of molecular weight of analytes to be separated. For polymer separations the pore sizes should be on the order of the polymers being analysed. If a sample has a broad molecular weight range it may be necessary to use several GPC columns in tandem with one another to fully resolve the sample. Gel permeation chromatography is conducted almost exclusively in chromatography columns. The experimental design is not much different from other techniques of liquid chromatography (Figure 2.9). Samples are dissolved in an appropriate solvent, in the case of GPC these tend to be organic solvents, and after filtering the solution is injected onto a column. The separation of multi-component mixture takes place in the column packed with gels (stationary phase). The pore size of a gel must be chosen to guarantee an efficient separation of analytes. Moreover, other desirable properties of the gel forming agents are the absence of ionizing groups and, in a given solvent, low affinity for the substances to be separated. Commercial gels like Sephadex, Bio-Gel (cross-linked polyacrylamide), agarose gel and Styragel are often used based on different separation requirements. The eluent (mobile phase) should be a good solvent for the polymer, should permit high detector response from the polymer and should wet the packing surface. The most common eluents for polymers are tetrahydrofuran (THF), *o*-dichlorobenzene and trichlorobenzene for crystalline polyalkines, *m*-cresol and *o*-chlorophenol for crystalline condensation polymers such as polyamides and polyesters.

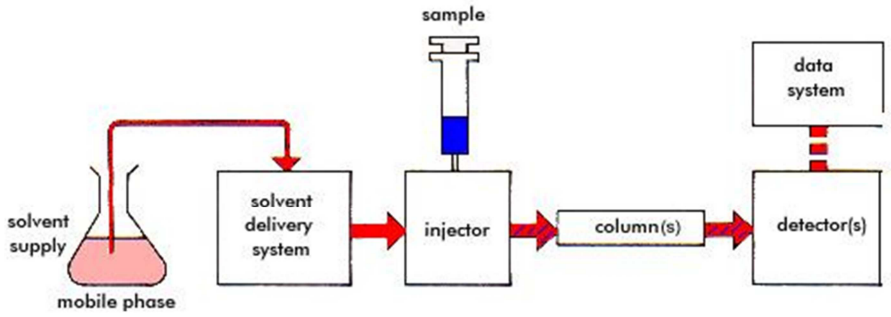

Figure 2.9 Scheme of GPC apparatus.

The constant supply of fresh eluent to the column is accomplished by the use of a pump (piston or peristaltic pumps). Molecules such eluted from the column were analyzed by detector. Often multiple detectors are used to gain additional information about the polymer sample. The resulting chromatogram is therefore a weight distribution of the polymer as a function of retention volume (Figure 2.10).

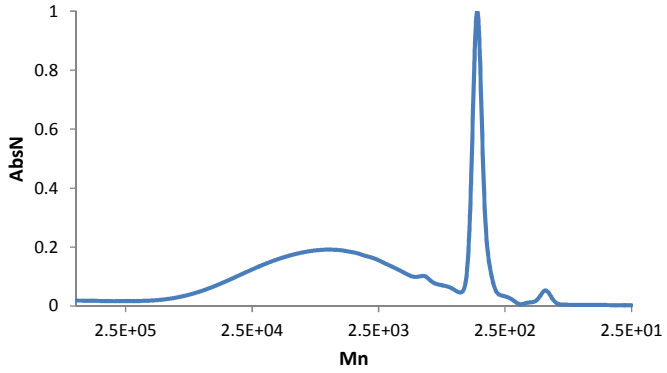

Figure 2.10 Chromatogram of a GCP analysis of lignin organosolv.

Benoit et al.[13] proposed that the hydrodynamic volume, V_η, which is proportional to the product of [η] and M, where [η] is the intrinsic viscosity of the polymer in the GPC eluent, may be used as the universal calibration parameter.[14] A plot of log [η]M versus elution volume (or elution time) for a particular solvent, column, and instrument provides a universal calibration curve which can be used for any polymer in that solvent so long as the Mark-Houwink constants are known for the polymer-solvent pair. By determining the retention volumes (or times) of monodisperse polymer standards (e.g. solutions of monodispersed polystyrene in THF), a calibration curve can be obtained by plotting the logarithm of the molecular weight versus the retention time or volume. Once the calibration is obtained, the gel permeation chromatogram of any other polymer can be obtained in the same solvent and the molecular weights (usually M_n and M_w) and the complete molecular weight distribution for the polymer can be determined.

2.3.1 Applications

GPC analysis allows characterization of polymers by parameters:[15]

- Number average molecular weight (M_n), is the statistical average molecular weight of all the polymer chains in the sample, and it is defined by:

$$M_n = \frac{\sum N_i M_i}{\sum N_i} \qquad \textbf{Eq. 2.3}$$

  Where M_i is the molecular weight of a chain and N_i is the number of chains of that molecular weight.

- Weight average molecular weight (M_w) (or molar mass distribution), that describes the relationship between the number of moles of each polymer species (N_i) and the molar mass (M_i) of that species.

$$M_w = \frac{\sum N_i {M_i}^2}{\sum N_i M_i} \qquad \textbf{Eq. 2.4}$$

  Compared to M_n, M_w takes into account the molecular weight of a chain in determining contributions to the molecular weight average. The more massive the chain, the more the chain contributes to M_w

- Higher average molecular weight (M_z) is given by:

$$M_w = \frac{\sum N_i M^3}{\sum N_i {M_i}^2} \qquad \textbf{Eq. 2.5}$$

  For all synthetic polymers: $M_n < M_w < M_z$

- The polydispersity index (PDI): it is a measure of the distribution of molecular mass in a given polymer sample and is defined by:

$$PDI = \frac{M_w}{M_n} \qquad \textbf{Eq. 2.6}$$

  It indicates the distribution of individual molecular masses in a batch of polymers. The larger the PDI, the broader the molecular weight. A monodisperse polymer where all the chain lengths are equal (such as protein) has a PDI value of 1. The best controlled synthetic polymers (narrow polymer used for calibrations) have a PDI of 1.02 to 1.10. Step polymerization reactions typically yield values of 2.0, whereas chain reactions yield PDI value of 1.5-20. A polymer material is denoted by the term *polydisperse* if its chain lengths vary over a wide range of molecular masses.

As a separation technique, GPC has many advantages. First of all, it has a well-defined separation time due to the fact that there is a final elution volume for all unretained analytes. Additionally, since the analytes do not interact chemically or physically with the column, there is a lower chance for analyte loss to occur. For investigating the properties of polymer samples in particular, GPC can be very advantageous. However, GPC has disadvantages, too. First, there are a limited number of peaks that can be resolved within the short time scale of the GPC run. Also, as a technique, GPC requires around at least a 10% difference in molecular weight for a reasonable resolution of peaks to occur. In regards to polymers, the molecular masses of most of the chains will be too close for the GPC separation to show anything more than broad peaks. Another disadvantage of GPC for polymers is that filtrations must be performed before using the instrument to prevent dust and other particulates from ruining the columns and interfering with the detectors. Although useful for protecting the instrument, the pre-filtration of the sample has the possibility of removing higher molecular weight sample before it can be loaded on the column.

References

[1] a) Ronald, A. H. in *Handbook of instrumental techniques for analytical chemistry* (Frank, S. ed), **1997,** 609-626, Prentice Hall; b) Rouessac, F.;in *Chemical Analysis: Modern Instrumentation Methods and Techniques,* **2007,** cap. 2 and 16, Wiley; c) Kitson, F.G.; Larsen, B.S., McEwen, C.N. in *Gas Chromatography and Mass Spectrometry: A Practical Guide* **1996,** 3-35, Academic Press, 1st edition; d) Rabin, S.; Stillian, J.; Barreto, V.; Friedman, K.; Toofan, K. *Journal of Chromatography, **1993,** 640, 97-109;* e) Pavia, D.L.; Lampman, G.M.; Kritz, G.S.; Engel, R.G. in *Introduction to Organic Laboratory Techniques (4th Ed.)* **2006,** 797-817 Thomson Brooks/Cole; f) Harris, D.C. in *Quantitative chemical analysis* **1999**. 675-712, Freeman W.H.)

[2] Varian 300 Series Quadrupole LC/MS and GC/MS Hardware Operation Manual **2008**

[3] a) Adlard, E.R.; Handley, A.J. in *Gas chromatographic techniques and applications **2001,*** Sheffield Academic, London; b) Eiceman, G.A. In *Encyclopedia of Analytical Chemistry: Applications, Theory, and Instrumentation (Meyers, R.A.ed.)* **2000,** 10627, Wiley; c) Weber, A.; Maurer, H.W.; Pfleger, K. in *Mass Spectral and GC Data of Drugs, Poisons, Pesticides, Pollutants and Their Metabolites* **2007,** Wiley-VCH

[4] a) Keeler, J. in *Understanding NMR Spectroscopy* **2005,** 5-23, Wiley; b) Edwards, J.C. Principles of NMR
URL: http://www.process-nmr.com/nmr1.htm; c) Bovey, F.A.; Jelinski, L.; Mirau, P.A. *Nuclear Magnetic Resonance Spectroscopy*, **1988,** Academic Press, NY; d) Atta-ur-Rahman, *Nuclear Magnetic Resonance, Basic Principles*, **1986,** Springer-Verlag, NY; e) Skoog, D.A.; Holler, F.J.; Crouch, S.R. in *Principles of Instrumental Analysis* **2007,** chapter 19, BrooksCole

[5] a) Martin, G.E; Zekter, A.S. in *Two-Dimensional NMR Methods for Establishing Molecular Connectivity* **1988,** 59.: VCH Publishers, Inc New York; b) Akitt, J.W.; Mann, B.E. in *NMR and Chemistry* **2000**, 273, Stanley Thornes Cheltenham, UK; c) Keeler, J. in *Understanding NMR Spectroscopy* (2nd ed.) **2010,** 184-187, Wiley.

[6] Keeler, J. in *Understanding NMR Spectroscopy* (2nd ed.) **2010,** 190-191, Wiley

[7] URL: http://www.chem.ucalgary.ca/courses/351/Carey5th/Ch13/ch13-2dnmr-1.html

[8] Keeler, J. in *Understanding NMR Spectroscopy* (2nd ed.) **2010,** 223-227, Wiley.

[9] Keeler, J. in *Understanding NMR Spectroscopy* (2nd ed.) **2010,** 206-208, Wiley.

[10] Keeler, J. in *Understanding NMR Spectroscopy* (2nd ed.) **2010,** 209-215, Wiley.

[11] Keeler, J. in *Understanding NMR Spectroscopy* (2nd ed.) **2010,** 208-209, 220, Wiley.

[12] a) Skoog, D.A. in *Principles of Instrumental Analysis*, **2006,** Chapter 28, Thompson Brooks/Cole; b) Sandler, S.R.; Karo, W.; Bonesteel, J.; Pearce, E.M. Polymer Synthesis and Characterization: A Laboratory Manual **1998,** Academic Press, San Diego; c) Helmut, D. Gel Chromatography, Gel Filtration, Gel Permeation, Molecular Sieves: A Laboratory Handbook **1969,** Springer-Verlag; d) Pasch, H. *Adv Polym Sci* **2000**, *150*, 1-66; e) Cowie, J.M.G.; Arrighi, V. Polymers: Chemistry and Physics of Modern Materials, **2008,** CRC Press; f) Odian G. Principles of Polymerization, **1991,** Wiley Interscience Publication.

[13] Grubisic, Z.; Rempp, P.; Benoit, H. *J Poly. Sci, Part C: Polym Lett,* **1967,** *5*, 753-759.

[14] Coleman, M.M.; Painter, P.C. in *Fundamentals of Polymer Science* **1998,** 353-370, CRC Press

[15] URL: http://www.ias.ac.in/initiat/sci_ed/resources/chemistry/MolWeight.pdf

Chapter 3

Immobilized tyrosinase for catechol synthesis: aqueous biotransformation

3.1 Introduction

Tyrosinases (Tyro; EC 1.14.18.1), polyphenol oxidases widely diffused in nature, catalyse the oxidation of phenols to catechols (cresolase or monophenolase activity) and that of catechols to corresponding *ortho*-quinones (catecholase or diphenolase activity).[1] Both catechols and *ortho*-quinones derivatives are characterized by several biological activities, including antioxidant and antitumoral properties.[2] The transformation of phenols to catechols and quinones is usually difficult to perform by chemical methods under environmental friendly conditions (Figure 3.1).[3]

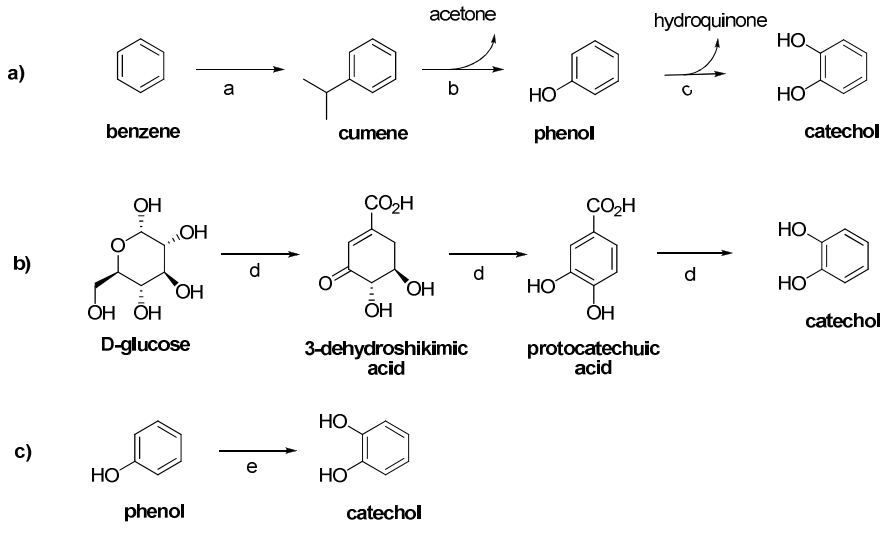

(a) propylene, solid H_3PO_4 catalyst, 200-260°C, 400-600 psi; (b) 80-130°C then SO_2, 60-100°C;
(c) 70% H_2O_2, EDTA, Fe^{2+} or Co^{2+}, 70-80°C; (d) E. coli AB2834/pKD136/pKD9.069A, 37°C;
(e) tyrosinase, O_2, room temperature

Figure 3.1 Scheme of catechol synthesis by a) chemical method, b) E. coli and c) tyrosinase. (Adapted from Frost et al., 1998)[7]

While some catechol is distilled from coal tar, the dominant method of their production begins with Friedel-Crafts alkylation of petroleum-derived benzene to afford cumene (Figure 3.1a). Subsequent Hock-type, air oxidation of the cumene leads to formation of acetone and phenol. The phenol is then oxidized using 70% hydrogen peroxide either in the presence of transition metal catalysts or in formic

acid solution where performic acid is the actual oxidant. The catechol and hydroquinone mixture that is generated is separated into its pure components by successive distillations.[4] Chemical products derived from the purified catechol include pharmaceuticals (L-DOPA, adrenaline, papaverine), flavors (vanillin, eugenol, isoeugenol), agrochemicals (carbofuran, propoxur), polymerization inhibitors and antioxidants (4-tert-butylcatechol, veratrol) compounds.[4] Several aspects of contemporary catechol manufacture are environmentally problematic. Petroleum is a non-renewable resource that has been historically plagued by inadvertent releases into the environment. The benzene starting material is carcinogenic and intermediate phenol is toxic.[5] Moreover, hydrogen peroxide used as the oxidant in catechol synthesis is a highly energetic and corrosive material which requires special safety precautions to ensure safe storage and handling.[6] A choosing route has been elaborated by Frost et al.[7] using D-glucose as starting material; this approach is a multistep reaction pathway involving a genetically modified bacterium as catalyst (Figure 3.1b). Briefly, catechol is synthesized by the introduction of *Klebsiella pneumoniae aroZ* and *aroY* genes encoding 3-dehydroshikimate dehydratase and protocatechuate decarboxylase, respectively, into 3-dehydroshikimate-synthesizing *Escherichia coli* constructs. Carbon flow directed into the shikimate pathway is thus diverted at 3-dehydroshikimate into synthesis of catechol. The third alternative route is rapresented by tyrosinase-based biocatalyst that, involving a one-step reaction pathway, directly oxidized phenols to catechols, under O_2 at room temperature (Figure 3.1c). Thus, tyrosinases represent the most useful, efficient and simplest green alternative to chemical treatments.[8] The sole limit of this approach would be correlated with the subsequent conversion of catechol to quinone mediated by the catecholase activity of the enzyme. Quinones are high reactive compounds that can both inactivate the enzyme through a covalent bond to the protein structure, then autoxidize producing insoluble brown pigments.[9] These drawbacks can be easily overcome through two different procedures: working in reducing condition or in biphasic medium in the presence of organic solvent (see Chapter 4). In the first case, a reducing agent, such as ascorbic acid, was added to reaction mixture to reduce the eventually synthesized quinones, thus ensuring the total conversion of phenols to catechols (Figure 3.2).[10] The application of tyrosinases in industrial chemistry is further increased by the possibility to immobilize the enzymes on stable and low cost supports.[11] Examples of the immobilization of tyrosinases on carbon nanotube,[12] copolymer matrices,[13] chitosan,[14] gold nanoparticles,[15] alumina sol-gel,[16] membrane alginate, polyacrylamide and gelatine gels[17] have been reported in the production of L-dopa,[18] in the removal of phenolic compounds from wastewater,[19] and in other industrial applications.[20] However, some of these immobilization methods are rather complicated and do not give good enzyme stability or retention.[21] Recently, the Layer-by-Layer (LbL) technique was reported as a general and versatile tool for the controlled productions of multilayer surface coatings on a large

variety of surfaces.[22] This method is based on the consecutive deposition of alternatively charged polyelectrolytes onto a surface.[23]

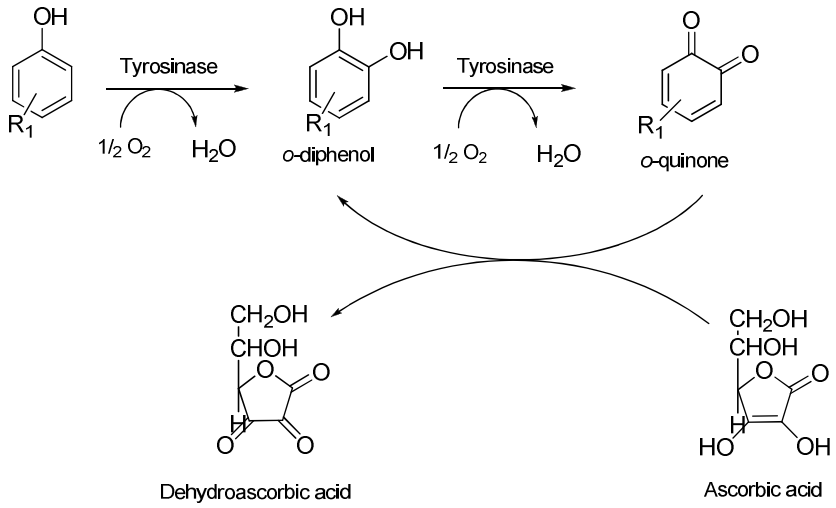

Figure 3.2 Role of ascorbic acid in the oxidation of phenols by tyrosinase. (Adapted from Espín et al., 2001)[10a]

The polyelectrolyte films have the ability to protect encapsulated protein from high-molecular-weight denaturing agents or bacteria and to allow regulation of the permeability towards small substrates, which can enter the multilayer and react with the catalytic site of the enzyme.[24] Specifically, in this chapter, the synthesis of immobilized biocatalysts and their use in the catechol synthesis in aqueous medium will be described. Tyrosinase was immobilized by three different methods: the first based on the chemo-physical procedure consisting, first, in the immobilization of mushroom tyrosinase on alumina particles and then in the coating of the biocatalyst by the LbL technique; the second based on the chemical immobilization of tyrosinase on the epoxy-resin Eupergit®C250L; and the third based again on the chemo-physical procedure consisting, first, in the immobilization of tyrosinase on Eupergit®C250L and then in their coating by the LbL procedure. The novel biocatalysts were applied for the selective synthesis of catechol derivatives by oxidation of substituted phenols, including biologically active compounds, under friendly environmental conditions. The reactions were performed in buffer at room temperature with dioxygen as primary oxidant in the presence of ascorbic acid (AA). Since it is also known that high concentrations of ascorbic acid can inhibit tyrosinase, its concentration requires to be optimized for a good compromise between high enzymatic activity and high yield in catechols.[25] The comparison between the efficiency and selectivity of tyrosinases with and without the LbL procedure, as well as the possibility to recycle the biocatalysts for more runs, are also reported.

3.2 Results and discussions

3.2.1 Optimization of tyrosinase immobilization

Immobilization of tyrosinase on alumina spherical particles (Al_2O_3, 3 mm diameter) led to the synthesis of heterogeneous biocatalyst showing very low activity. Since tyrosinase has not been supported yet on alumina, several conditions were analyzed and compared; the ratio between the enzyme and the particles (mg g^{-1}) and the glutaraldehyde concentration were investigated to optimize the procedure. The supporting method consisted of different stages (Figure 3.3).[26] In the first one, amino-groups were made available on the surface of the support by two successive silanizations of Al_2O_3 with 2% (v/v) γ-aminopropyltriethoxysilane in acetone at 45°C for 24 h. The second stage provides a cross-linking agent for enzyme immobilization by treatment of Al_2O_3 with 2% (v/v) aqueous glutaraldehyde (50% v/v) for 2 h. The third stage consisted of enzyme immobilization putting in contact tyrosinase (50.0-400.0 mg, 13900 U mg^{-1}) suspended in Na-phosphate buffer 0.1 M, pH 7.0 with activated alumina (100.0 g).

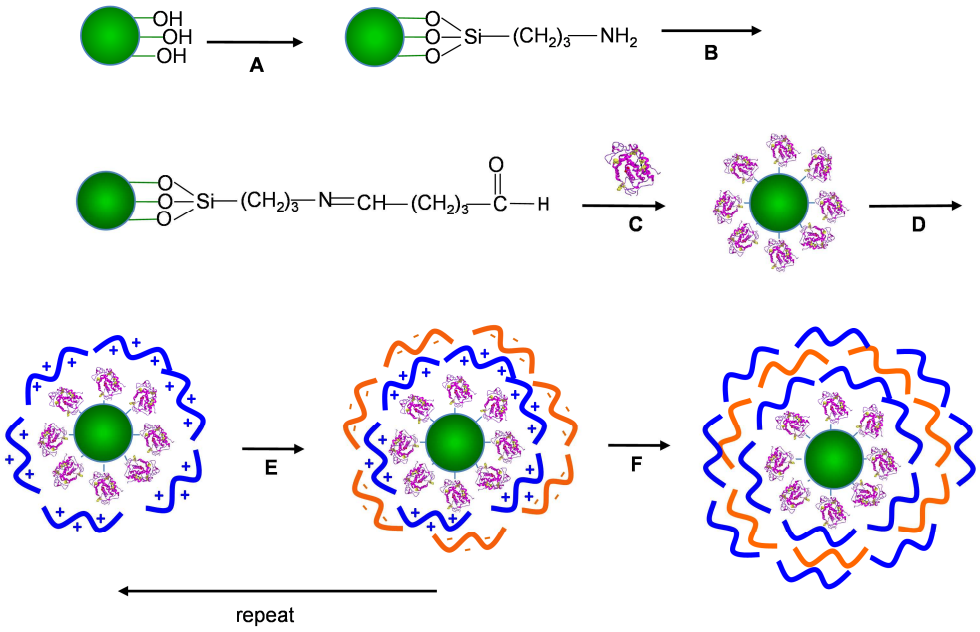

Figure 3.3 Scheme of preparation of PSS/PAH-coated tyrosinase/alumina particles: (A) support silanization; (B) coupling with the cross-linker; (C) tyrosinase cross-linking with the support; (D) PAH layer deposition; (E) PSS layer deposition; (F) LbL coating of supported tyrosinase.

In the last step, the particles were coated with LbL procedures: particles were first suspended in positively charged polyallylamine hydrochloride (PAH) (2.0 mg ml^{-1} in 0.5 M NaCl, pH 6.5), and then treated with negatively charged polystyrene sulphonate (PSS) (2.0 mg ml^{-1} in 0.5 M NaCl, pH 6.5). The procedure was repeated until the formation of three layers. The deposition procedure started with

the positive PAH layer because at pH 6.5 tyrosinase was negatively charged (tyrosinase Isoelectric Point = 4.5[27]). The effectiveness of the immobilization procedure was investigated in terms of Immobilization Yield (Eq. 3.1), where U_a is the total activity of enzyme added in the solution and U_r is the activity of the residual enzyme recovered in the washing solutions, and Activity Yield (Eq. 3.2), where U_x is the activity of the immobilized enzyme assayed by dopachrome method.[28]

Eq. 3.1
$$\boldsymbol{Immobilization\ Yield}\ (\%) = \frac{\boldsymbol{U_a - U_r}}{\boldsymbol{U_a}} \times \mathbf{100}$$

Eq. 3.2
$$\boldsymbol{Activity\ Yield}\ (\%) = \frac{\boldsymbol{U_x}}{\boldsymbol{U_a - U_r}} \times \mathbf{100}$$

As reported in Table 3.1, the Immobilization Yield increased with the ratio of enzyme (mg) to support (g), while the Activity Yield was very low in all cases studied (Table 3.1, entries 1-3). In the literature is reported that tyrosinase exhibited low activity when it was immobilized in excess of glutaraldehyde.[29] This behavior is correlated with the presence of residual aldehyde sites available to bind the substrate, product, or reaction intermediates. For this reason, the effect of less concentration of glutaraldehyde and the influence of the deactivation of unreacted aldehyde groups with glycine were also studied.

Table 3.1 Tyrosinase immobilization on alumina spherical particles.[a]

Entry	Ratio Tyro/support (mg g^{-1})	% Glutaraldehyde (50% v/v)	Glycine 3.0 M	% Immobilization Yield (mg bounded Tyro)	Activity Yield (%)
1	0.5	2	no	95 (0.5)	< 8
2	1.5	2	no	72 (1.1)	< 8
3	4.0	2	no	50 (2.0)	< 8
4	4.0	1	no	47 (1.9)	< 8
5	4.0	1	yes	47 (1.9)	< 8

[a] Immobilization conditions: 100.0 g Al_2O_3 and tyrosinase were taken in 250.0 mL of phosphate buffer solution for 48 h. After incubation biocatalysts were coated with three layers of PAH-PSS-PAH.

The immobilization performed with 1% (v/v) of glutaraldehyde (50% v/v) showed a 47% of Immobilization Yield, demonstrating that 2% (v/v) glutaraldehyde was in excess; however the Activity Yield was still very low (Table 3.1, entry 4 versus 3). Moreover, the deactivation of aldehyde groups with glycine 3.0 M did not affect the enzymatic activity that was minor than 8% (Table 3.1, entry 5). Despite these data, it was not possible obtain a good biocatalysts using Al_2O_3 particles as carrier. On the other hand, promising results were obtained supporting tyrosinase on resin beads of Eupergit®C250L. Since in the literature the immobilization of tyrosinase on Eupergit®C250L has not been reported, optimal conditions were first determined using a modification of previously reported

procedures used for other enzymes; then the novel biocatalyst was assayed for its stability and catalytic properties.[30] The ratio between the enzyme and the resin (mg g^{-1}), the incubation time and pH were investigated to optimize the yield of immobilization. As a general procedure, the enzyme (1.0-6.0 mg, 13900-83400 U) was suspended in Na-phosphate buffer (pH 5.0-8.0) (7.0-9.0 mL) in the presence of a defined amount of resin (1.0 g) for 24-48 h at room temperature. The immobilized system (Tyro/E) was washed with water to remove excess of protein and treated with glycine 3.0 M to block residual epoxy-groups (Figure 3.4).

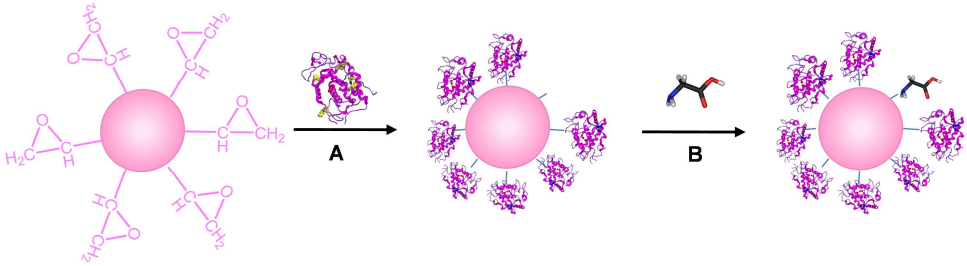

Figure 3.4 Scheme of immobilization of tyrosinase on Eupergit®C250L: (A) tyrosinase cross-linking with the support; (B) treatment with glycine 3.0 M to block residual epoxy-groups.

The effectiveness of the immobilization procedure was investigated in terms of Immobilization Yield (Eq. 3.1) and Activity Yield (Eq. 3.2) by the analysis of the residual enzymatic activity in the waste waters after the reaction with the support. As reported in Table 3.2, the Activity Yield increased with the amount of the enzyme in contact with the resin (entries 1-5), reaching the maximum value of 38% (that corresponds to an Immobilization Yield of 66%) at 5:1 enzyme/support ratio (entry 4). When the amount of enzyme was further increased, the recovered Activity Yield decreased to 31%; nevertheless the bound protein was slightly higher (entry 5 versus entry 4).

Table 3.2 Tyrosinase immobilization on Eupergit®C250L at different conditions.

Entries	Ratio Tyro/support (mg/g)	Incubation time (h)	pH	% Immobilization Yield (mg bounded Tyro)	Activity Yield (%)
1	1	24	7	74 (0.74)	16
2	2	24	7	76 (1.52)	20
3	4	24	7	70 (2.80)	30
4	5	24	7	66 (3.30)	38
5	6	24	7	68 (4.08)	31
6	5	48	7	77 (3.85)	30
7	5	24	5	58 (2.90)	23
8	5	24	6	60 (3.00)	30
9	5	24	8	56 (2.80)	26

Similar results were obtained for the immobilization of cyclodextrin glucosyltransferase[31] and lipase[32] on Eupergit®, probably because the close packing of the enzymes on the support surface that limits

the access of substrate. Once defined the optimum value of the enzyme/support ratio, the immobilization was performed at different times (24 and 48 h). Data reported in Table 3.2 show the highest Immobilization Yield at 48 h with a value of 77% respect to 66% at 24 h; even if a longer incubation time led to a reduction of the Activity Yield (30% and 38%, respectively for 48 h and 24 h) (entry 6 versus entry 4). The influence of pH on the immobilization procedure was also studied in the range of 5.0-8.0. The optimum binding was achieved with sodium phosphate buffer at pH 7.0 (Table 3.2 entries 5 versus 7-9). With the aim to further increase the stability of Tyro/E, the LbL technique was applied by coating Tyro/E (synthesized according to procedure reported in Table 3.2, entry 4) through a sequential deposition of charged polyelectrolytes. Briefly, Tyro/E was first suspended in positively charged polyallylamine hydrochloride (PAH) (2 mg ml^{-1} in 0.5 M NaCl), and then treated with negatively charged polystyrene sulphonate (PSS) (2 mg ml^{-1} in 0.5 M NaCl). The procedure was repeated until the formation of three layers (Figure 3.5).

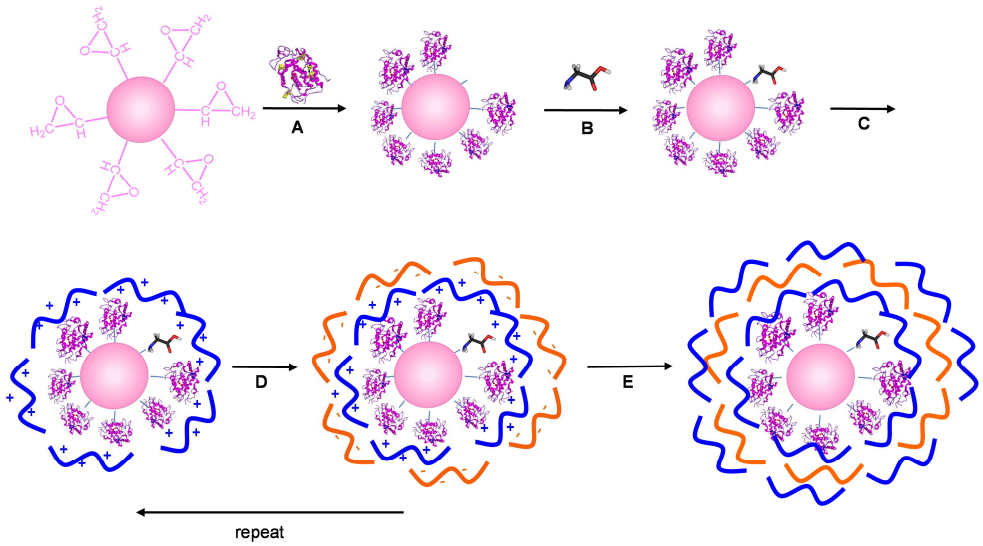

Figure 3.5 Scheme of preparation of PAH/PSS-coated tyrosinase/Eupergit®C250L: (A) tyrosinase cross-linking with the support; (B) treatment with glycine to block residual epoxy-groups; (C) PAH layer deposition; (D) PSS layer deposition; (E) LbL coating of supported tyrosinase.

Even in this case, the coating started with the deposition of positively charged PAH to ensure electrostatic interaction with negatively charged tyrosinase. The immobilized LbL enzyme (Tyro/E-LbL) retained about 87% of the activity (15165 U g_{beads}^{-1}) with reference to Tyro/E. A set of scanning electron microscopy (SEM) photographs showing the morphology of the surface of Tyro/E and Tyro/E-LbL particles is reported in Figure 3.6. Tyro/E shows particles with a regular shape and an average diameter value of 100-150 µm (Figure 3.6a). A low number of irregular fragments were observed which are probably formed by a mechanical damage of particles during the sample preparation. At larger magnification the particles show an irregular surface characterized by grumes

of different dimension (Figure 3.6b). About Tyro/E-LbL, although the presence of polyelectrolyte does not alter the average diameter of beads (100-150 µm, Figure 3.6c), the coating modifies the morphology of particle surface that appears more smooth than Tyro/E (Figure 3.6d).

Immobilized tyrosinases (Tyro/E and Tyro/E-LbL) were then characterized for their pH and storage stability, kinetic properties and reusability.

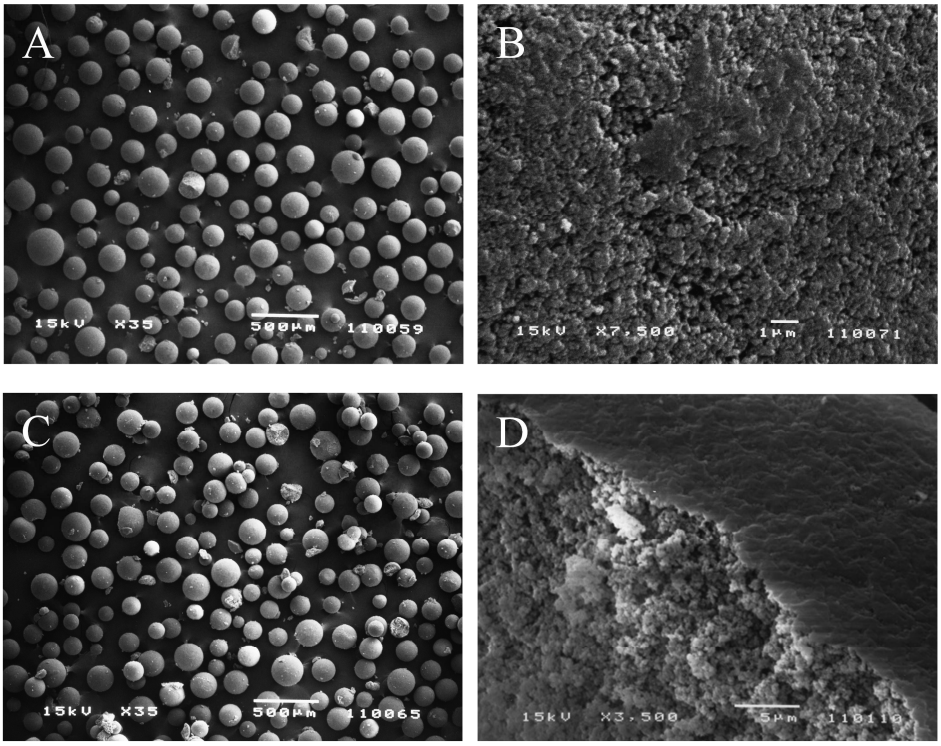

Figure 3.6 SEM images of Tyro/E (A and B) and Tyro/E-LbL (C and D) at different magnification.

3.2.2 Effect of pH on tyrosinase activity

The pH/activity curves related to free (Tyro) and immobilized tyrosinase (Tyro/E and Tyro/E-LbL) at 25°C are shown in Figure 3.7. The activity was measured using L-tyrosine (L-Tyr) as substrate; tyrosinase activity was expressed as relative percentage activity respect to that at time zero. Irrespective to immobilization procedure, tyrosinase showed the optimum pH 7.0 that is the same value selected for the immobilization of the enzyme. Noteworthy, Tyro/E and Tyro/E-LbL were more active than the free enzyme in the range of pH studied, achieving 90% of optimal activity at pH 6.0 and 82% and 92%, respectively, at pH 8.0. Changes in pH-activity profile after immobilization, eventually involving the shift of the optimal pH value, have been reported during immobilization of tyrosinase on others support.[18,33] The stability of tyrosinase incubated for 48 h at 25°C in various pH buffers (pH 6.0-8.0) was reported in Figure 3.8.

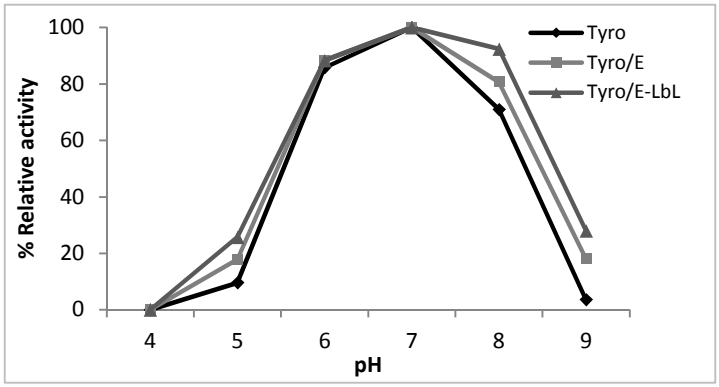

Figure 3.7 pH optimum of free (Tyro) and immobilized tyrosinase (Tyro/E and Tyro/E-LbL). Tyrosinase activity was determined using L-Tyrosine as substrate, pH 4.0–9.0

At pH 7.0 tyrosinase was very stable and more than 80% of the initial activity was retained after 48 h of incubation (Figure 3.8a). Notable, even if at pH 6.0 and 8.0 tyrosinase showed high activity (more than 70% respect to optimal pH 7.0, Figure 3.7), storage in these buffer solutions caused a quick decreased in enzyme activity.

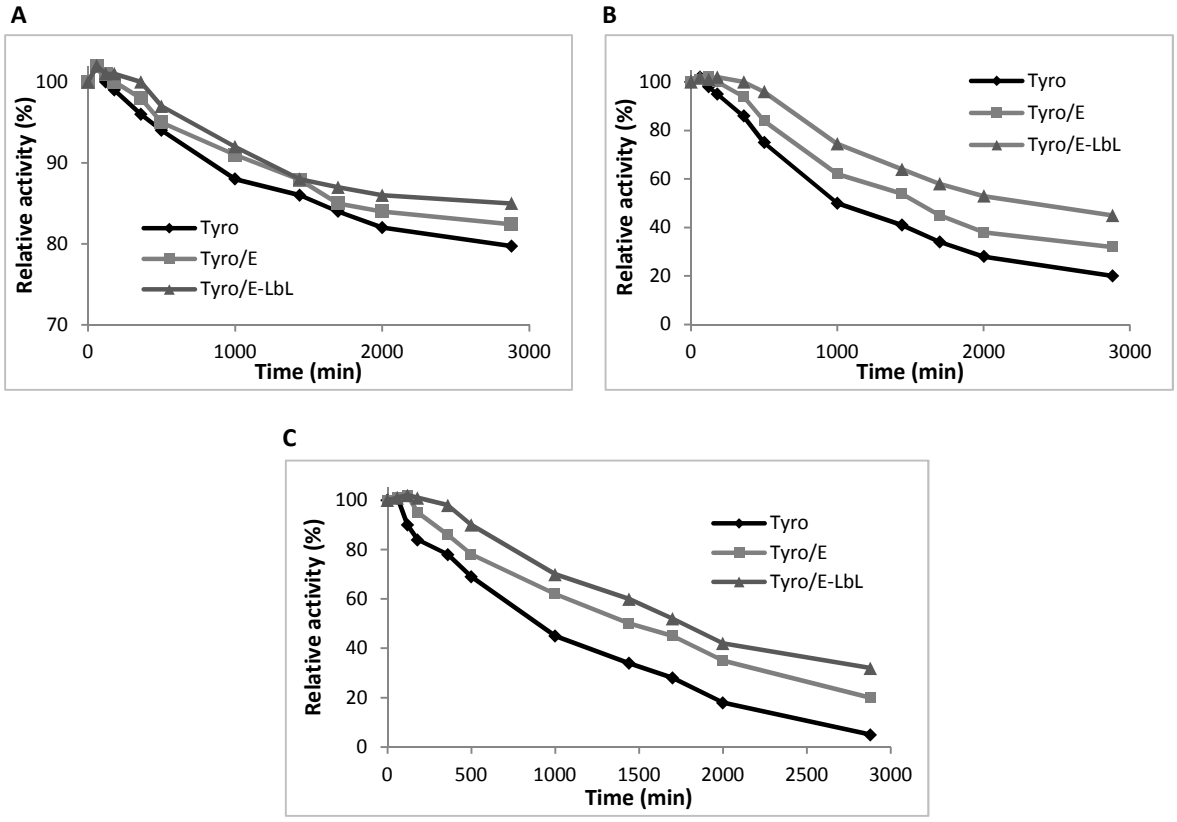

Figure 3.8 pH stability of free (Tyro) and immobilized tyrosinase (Tyro/E and Tyro/E-LbL) incubated for 48 h at 25°C in phosphate buffer 0.1 M pH 7.0 (A), pH 6.0 (B) and pH 8.0 (C). Data are the means of three experiments. Standard deviations of data were less than 6%.

Specifically, tyrosinase was inactivated more rapidly at pH 8.0 than pH 6.0 (Figure 3.8c and Figure 3.8b, respectively). For each case reported, immobilized tyrosinase maintained higher activity respect to free enzyme; LbL represents the best immobilization procedures.

3.2.3 Storage and thermal stability

The storage stability of free and immobilized tyrosinase was evaluated by storing the enzyme in Na-phosphate buffer buffer 0.1 M, pH 7.0 at -20°C, 4°C and 25°C for 25 days (Figure 3.9a, Figure 3.9b and Figure 3.9c, respectively). The activity was measured at specific times by the dopachrome method after cooling or warming the enzyme solution at room temperature; tyrosinase activity was expressed as relative percentage activity respect to that at time zero.

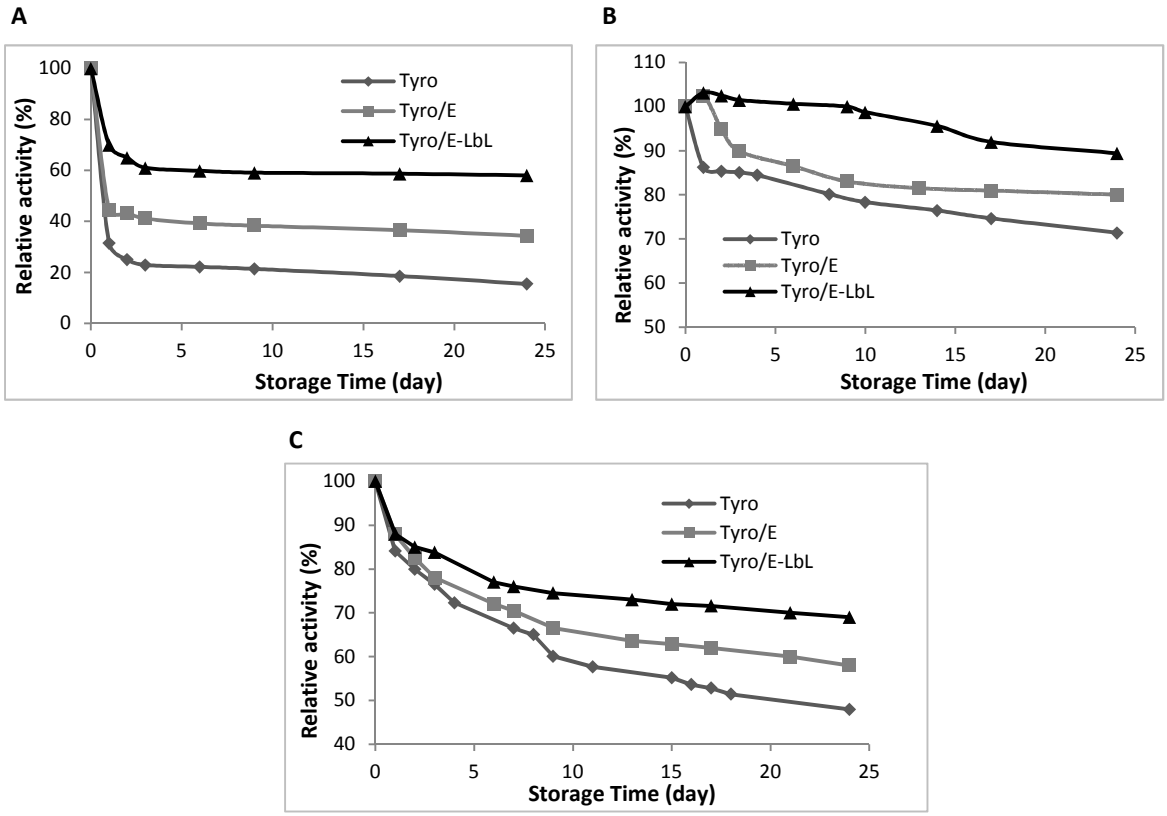

Figure 3.9 Storage stability of free (Tyro) and immobilized tyrosinase (Tyro/E and Tyro/E-LbL) at (A) -20°C, (B) 4°C and (C) 25°C in Na-phosphate buffer 0.1 M, pH 7.0. Data are the means of three experiments. Standard deviations of data were less than 6%.

At each of the temperature studied, Tyro/E and Tyro/E-LbL were more stable than free enzyme. The temperature of 4°C was achieved as the optimum storage conditions where immobilized tyrosinases maintained more than 80% of their activity over 25 days (Figure 3.9b). The presence of the polyelectrolyte coating exerted its beneficial role on maintaining the structural stability of the enzyme especially at -20°C where the enzyme increased its activity respect to free enzyme by 43%, compared to 21% at 25°C and 20% at 4°C. The thermal stability of tyrosinase was also evaluated by storing the

enzyme in Na-phosphate buffer 0.1 M, pH 7.0 at higher temperature: 30°C, 40°C and 50°C (Figure 3.10a, Figure 3.10b and Figure 3.10c, respectively). Again, immobilization procedures enhanced the enzymatic stability, especially at higher temperature. The activity of free tyrosinase, in fact, decreased very quickly at 40°C and 50°C where it disappeared completely after 120 h and 6 h of incubation, respectively. Tyro/E-LbL decreased its activity more slowly and remained at almost 83% (40°C) and 60% (50°C) of its initial value at the same incubation time. At 30°C tyrosinases showed a similar pattern to storing at 25°C.

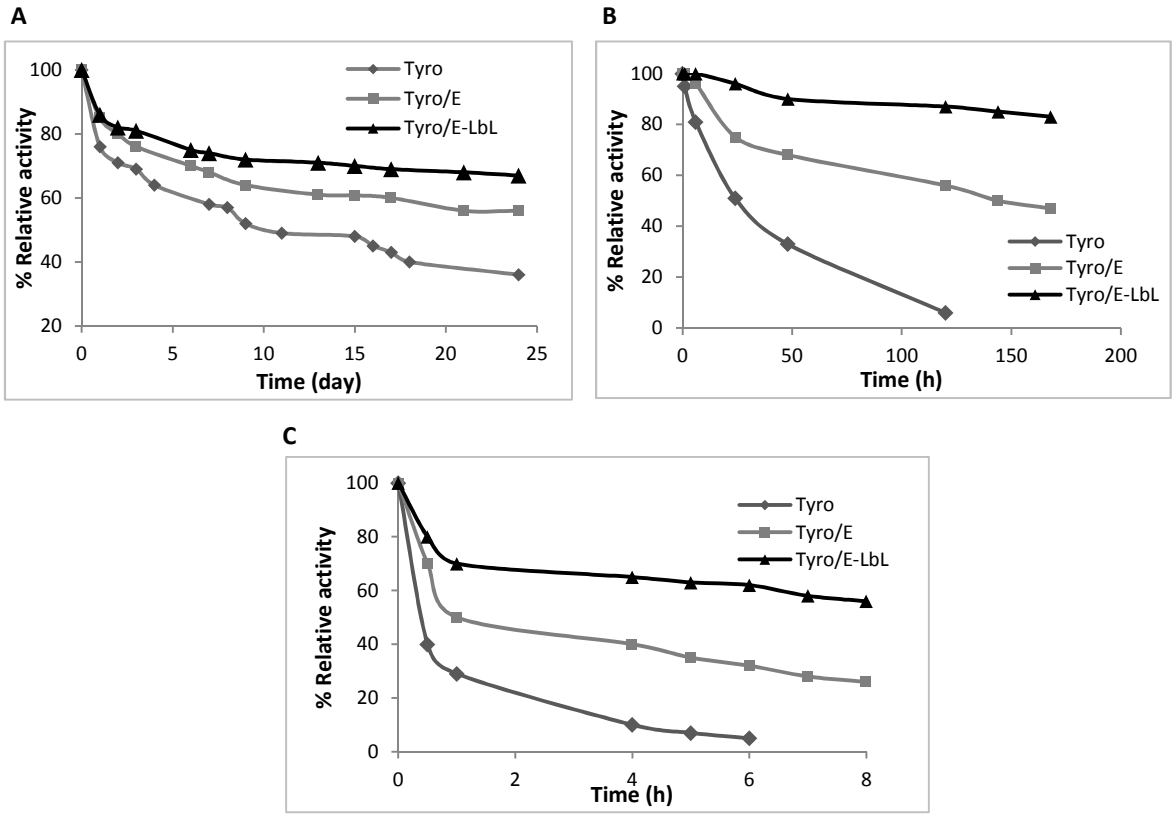

Figure 3.10 Thermal stability of free (Tyro) and immobilized tyrosinase (Tyro/E and Tyro/E-LbL) at (A) 30°C, (B) 40°C and (C) 50°C in Na-phosphate buffer 0.1 M, pH 7.0. Data are the means of three experiments. Standard deviations of data were less than 7%.

Immobilized enzymes showed an increased stability and resistance to thermal and pH denaturation dependent on both (i) the multipoint attachment of enzymes to solid supports that stiffened the protein structure[34] and (ii) the presence of polyelectrolyte layers that create a microenvironment inside the capsules that protect the enzyme from denaturing agent. The increased resistance to thermal and pH denaturation could be a potential advantage in chemical applications. To further confirm the integrity of Tyro/E-LbL over time, a SEM comparison of freshly prepared capsules and two months stored ones was carried out at a higher magnification (x15.000). As reported in Figure 3.11a and Figure 3.11b, the surface morphology of the particles is not significantly altered during the storage period. In addition, the stability of the system was confirmed by Transmission Electron

Microscopy (TEM) analysis of a section of the particles after two months of storage, which shows a substantial integrity of the polyelectrolyte layers (Figure 3.11c). This fact, coupled with the maintenance of the catalytic activity for multiple subsequent reactions (see below) confirms a substantial stability of the system. The enhanced stability of enzyme activities within LbL assembly was previously discussed in details by Onda et al. [35]

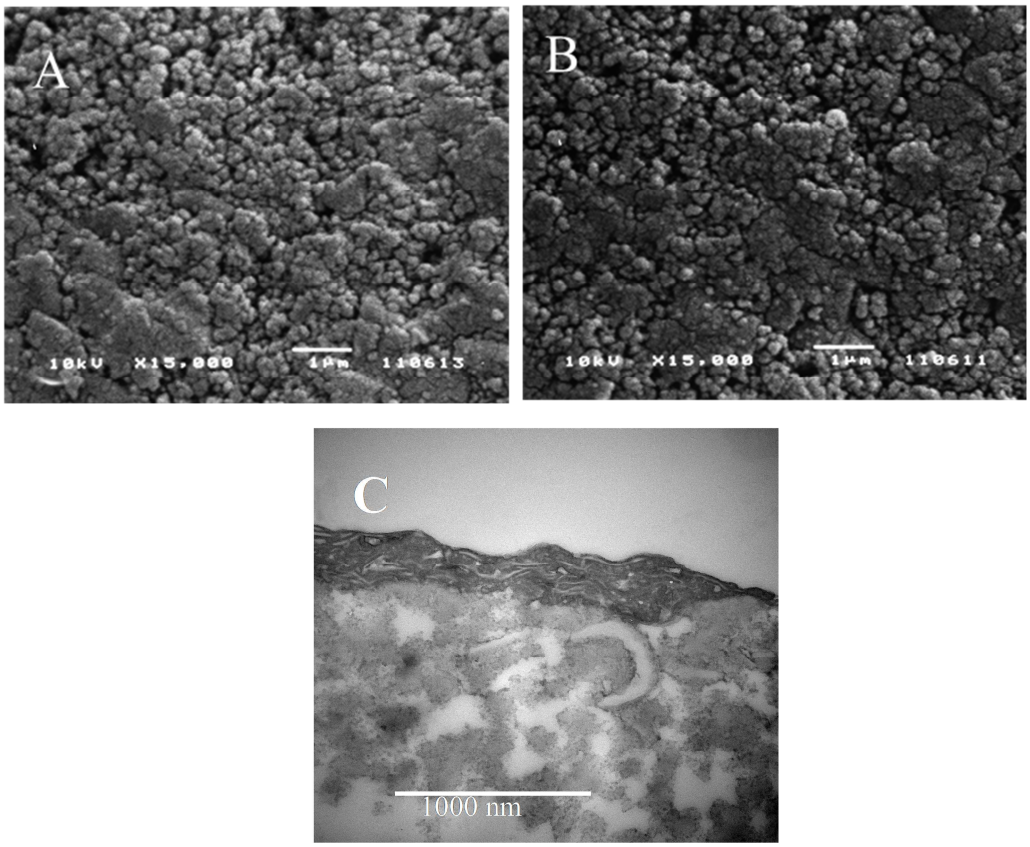

Figure 3.11 (A) and (B): SEM images of Tyro/E-LbL at a higher magnification (x15.000) at time zero (A) and after two months (B) upon storage at 4°C. (C): TEM image of a section of Tyr/E-LbL particle upon storage for two months at 4°C. LBL layers are clearly visible in the upper part of the picture.

3.2.4 Kinetic assay

Kinetic parameters of free and immobilized tyrosinases were examined by measuring the enzyme activity at different concentrations of L-tyrosine (L-Tyr; range 330-1000 μM) and plotting data to a double reciprocal plot (Lineweaver-Burk plot) (Table 3.3 and Figure 3.12).[36] Irrespective to procedures used for the immobilization, V_{max} decreased and K_m increased for supported tyrosinases, leading to a partial reduction of the catalytic efficiency (V_{max}/K_m) with respect to free enzyme. Similar trends in K_m values were reported for tyrosinase immobilized on other carriers and are attributed to alteration of three-dimensional structure and mass transfer limitations.[37]

Table 3.3 Kinetic parameters of free (Tyro) and immobilized (Tyro/E, Tyro/E-LbL) tyrosinase.

Entry	Enzyme	K_m (μM)	V_{max} [a] ($x10^{-3}$)	V_{max}/K_m [b] ($x10^{-6}$)
1	Tyro	180	6.02	33.4
2	Tyo/Eup	270	4.11	15.2
3	Tyro/E-LbL	300	3.20	10.7

[b] V_{max} was defined as ΔAbs min^{-1} μg_{enzyme}^{-1}; [b] V_{max}/K_m was defined as ΔAbs min^{-1} μg_{enzyme}^{-1} μM^{-1}. Each experiment was conducted in triplicate. Average errors in kinetic parameters were ± 2-4% for K_m and ±1-3% for V_{max}.

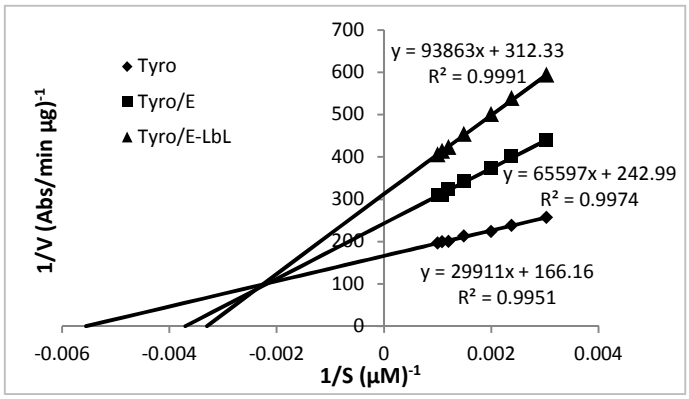

Figure 3.12 Lineweaver-Burk plots of free (Tyro) and immobilized tyrosinase (Tyro/E and Tyro/E-LbL) activity determined at different concentrations of L-Tyrosine (330-1000 μM). Data are the mean values of three experiments with standard deviation less than 1%.

3.2.5 Recycle and reusability

Recycle and reusability assay was performed using L-Tyr as substrate. The oxidations were followed spectrophotometrically at 475 nm. After reaching absorbance plateau, the immobilized biocatalyst was recovered, washed and reused with fresh added substrate. One unit of enzyme activity was defined as the increase in absorbance of 0.001 at defined wavelength, temperature and pH. For successive runs, the enzyme activity measured in the first oxidation was used as the reference value. As shown in Table 3.4, Tyro/E-LbL was more stable than Tyro/E, retaining 75% of activity after 5 runs.

Table 3.4 Reusability of Tyro-immobilized systems.

Run	Tyro/E [a]	Tyro/E-LbL [a]
1	90	91
2	76	86
3	68	80
4	63	79
5	56	75
6	45	71

[a] Reusability is expressed as percentage of activity in each runs respect to that measured in the first reference oxidation.

This behaviour suggests that the LbL coating process effectively stabilizes the enzyme from inactivating agents. Different examples of the stabilization effect of LbL were reported in literature.[38]

3.2.6 Oxidation of phenols

With the aim to evaluate the synthetic relevance of immobilized tyrosinases, a large panel of phenols (Figure 3.13) was oxidized, including *para*-cresol **1**, 4-ethyl phenol **2**, 4-*tert*-butyl phenol **3**, 4-*sec*-butyl phenol **4**, 2,4-di-*tert*-butyl phenol **5**, *para*-nitrophenol **6**, *meta*-cresol **7**, 3,4-dimethyl phenol **8**, 4-chloro phenol **9,** 4-chloro-2-methyl phenol **10**, 2-methoxy-4-methyl phenol **11**, 2-methoxy phenol **12**, 3-(4-hydroxyphenyl)propionic acid **13**, 4-hydroxyphenylacetic acid **14**, bis(4-hydroxyphenyl)methane **15** and tyrosol **16**.

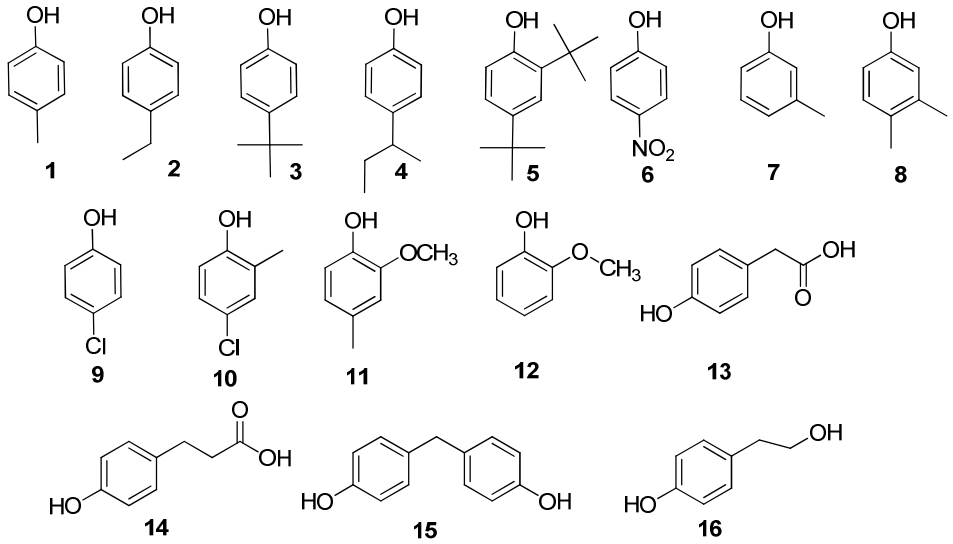

Figure 3.13 Phenols selected for the oxidation with free and immobilized tyrosinases.

As general procedure, phenol (0.05 mmol) and tyrosinase (263 - 526 U) were placed in Na-phosphate buffer 0.1 M, pH 7.0 (5.0 mL) at room temperature for 24 h in the presence of ascorbic acid (AA) (1.5 equivalents).[39] For low soluble phenols (**3, 5, 15**) the substrates were dissolved in CH_3CN (1.0 mL) and then added to the reaction mixture. The amount of CH_3CN (corresponding to 16% v/v) was chosen in order to allow substrate dissolution and ensure a high enzymatic activity. As reported in Figure 3.14, in fact, tyrosinase activity was high at low concentration of CH_3CN (90% activity at 16% v/v) but it was reduced drastically at less than 30% for CH_3CN > 50% v/v. This activity trend is dependent on the effect of the amount (v/v) of hydrophilic solvents (log P < 2) on the conformational structure of the enzyme: polar solvents, as CH_3CN (log P CH_3CN = -0.33), compete with water molecules to interact with amino acid residues located on the surface of the enzyme. Thus at high

concentration, CH_3CN strip the water molecules off the tyrosinase surface, altering its conformational structures and compromising its activity.

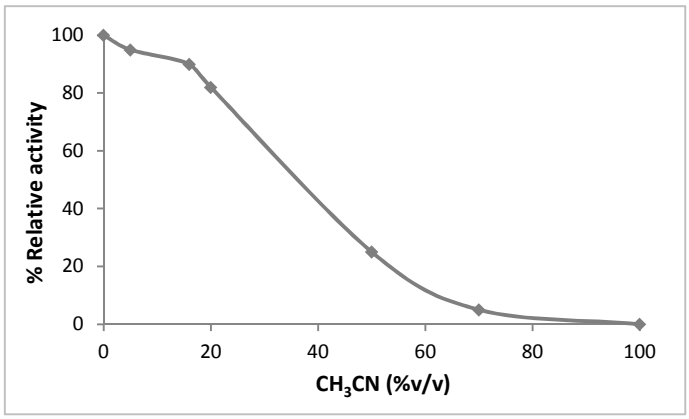

Figure 3.14 Tyrosinase activity at different CH_3CN concentrations assayed at 25°C in Na-phosphate buffer 0.1 M, pH 7.0 using L-Tyr as substrate. Activity at 0% v/v CH_3CN was chosen as references. Data are the means of three experiments. Standard deviations of data were less than 6%.

As selected cases, oxidations of **1-4** in absence of ascorbic acid were also performed as references. Initially, the oxidation of **1** with both free and immobilized tyrosinases was studied. Under reducing conditions catechol **1a** was obtained as the only recovered product in quantitative yield and conversion of substrate (Scheme 3.1, Table 3.5, entry 1). Similar results were obtained with Tyro/E and Tyro/E-LbL as catalysts (Table 3.5, entries 2-3). Thus, the reactivity and selectivity of tyrosinase was completely retained after the immobilization procedures. The oxidations of **1** performed in absence of ascorbic acid (AA) showed a lower selectivity for compound **1a** that was recovered in low yield (15-22%) besides to pyrogallol derivative **1b** and dimers **1c-d** (Table 3.5, entries 4-6). In accordance with data reported in the literature, the formation of dimers **1c-d**, characterized by the formation of C-C cross-linkage between two phenol units, can be ascribed to reactive *ortho*-quinones intermediates by a non-enzymatic mechanism; however, the occurrence of a radical mechanism involving a phenoxy radical intermediate generated by residual laccase activity, cannot be completely ruled out.[40] The oxidation of **2** in reducing condition confirmed the high reactivity of immobilized tyrosinases, the catechol **2a** being again obtained as the only recovered product in quantitative yield and conversion of substrate (Scheme 3.1, Table 3.5, entries 8-9). Moreover the same reactions performed without ascorbic acid performed dimers **2c-d** as the main products beside to low amount of pyrogallol derivatives **2b** and catechol **2a** (Table 3.5, entries 10-12). Noteworthy, Tyro/E and Tyro/E-LbL were efficient and selective biocatalysts also in the oxidation of *para*-alkyl substituted phenols characterized by a high steric hindrance, as in the case of bulky substituted phenols **3** and **4**. As reported in Table 3.5, the oxidation of **3** required the addition a small amount of CH_3CN (0.1 mL) to increase the solubility of substrate.

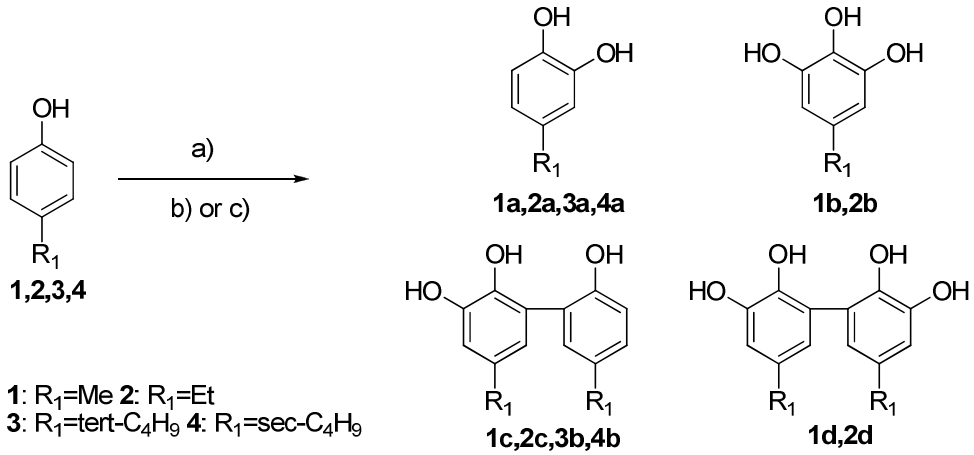

Scheme 3.1 Oxidation of phenols 1-4. ***Reagents and conditions:*** **a) Tyro-based systems, O_2, AA; b) Na-phosphate buffer; c) Na-phosphate buffer/CH_3CN**

Table 3.5 Oxidation of *para*-alkyl substituted phenols 1-4.[a]

Entry	Substrate	Biocatalysts	Products	Conversion (%) [b]	Yield (%) [b]
1	**1**	Tyro	**1a**	>99	>99
2	**1**	Tyro/E	**1a**	94	94
3	**1**	Tyro/E-LbL	**1a**	97	97
4	**1**	Tyro	**1a(1b)[1d]** [c]	95	22(10)[26]
5	**1**	Tyro/E	**1a(1b)[1c]{1d}** [c]	87	15(18)[27]{25}
6	**1**	Tyro/E-LbL	**1a(1b)[1c]{1d}** [c]	84	18(17)[25]{23}
7	**2**	Tyro	**2a**	>99	>99
8	**2**	Tyro/E	**2a**	95	95
9	**2**	Tyro/E-LbL	**2a**	98	98
10	**2**	Tyro	**2a(2b)[2c]{2d}** [c]	90	18(15)[33]{19}
11	**2**	Tyro/E	**2a(2b)[2c]** [c]	92	36(42)[14]
12	**2**	Tyro/E-LbL	**2a(2b)[2c]{2d}** [c]	92	18(16)[28]{16}
13	**3**	Tyro	**3a** [d]	>99	>99
14	**3**	Tyro/E	**3a** [d]	92	92
15	**3**	Tyro/E-LbL	**3a** [d]	95	95
16	**3**	Tyro	**3a(3b)** [c] [d]	63	10(48)
17	**3**	Tyro/E	**3a(3b)** [c] [d]	60	14(44)
18	**3**	Tyro/E-LbL	**3a(3b)** [c] [d]	60	14(40)
19	**4**	Tyro	**4a**	96	96
20	**4**	Tyro/E	**4a**	92	92
21	**4**	Tyro/E-LbL	**4a**	94	95
22	**4**	Tyro	**4a(4b)** [c]	44	8(34)
23	**4**	Tyro/E	**4a(4b)** [c]	42	10(30)
24	**4**	Tyro/E-LbL	**4a(4b)** [c]	41	14(24)

[a] Reaction conditions: substrate (0.05 mmol), AA (1.5 eq.) and tyrosinase (263 U) were taken in 5.0 mL of Na-phosphate buffer solution for 24 h; [b] Conversion and yield were calculated by GC-MS analysis using dodecane as internal standard; [c] Oxidation performed without AA as reference; [d] Oxidation performed in Na-phosphate buffer/CH_3CN.

In these latter cases, irrespective to experimental conditions, catechols **3a** and **4a** were synthesized in yield higher than 90% (Scheme 3.1, Table 3.5, entries 13-15 and 19-21). Even for compounds **3** and **4**, reactions performed without ascorbic acid afforded dimer **3b** and **4b** as main product with no selectivity toward catechols that were recovered in very low amount (Table 3.5, entries 16-18 and 22-24). As general rule, these reaction pathways confirm that in non-reducing condition the selective synthesis of catechol was impeded by reacting quinones that produce dimers and insoluble brown pigments as main recovery product. Unlike compounds **1**-**4**, 2,4-di-*tert*-butyl phenol **5** was stable under all of the conditions tested, probably due to known inhibition effect exerted by the steric encumbering of the bulky *ortho*-substituent.[41] Similar result was obtained in the case of **6** where the presence of an electron withdrawing group in *para*-position inhibited tyrosinase oxidation. A substituent in the *meta*-position on the aromatic ring, as in in the case of 3-methyl phenol **7** and 3,4-dimethylphenol **8**, showed a slightly inhibitory effect. In these latter cases, twice amount of enzyme was required (526 U) to produce catechols **1a** and **8a** in 42-48% and 80-84% yield with Tyro/E and Tyro/E-LbL, respectively; Tyro/E-LbL being the best biocatalyst (Scheme 3.2, Table 3.6, entries 2-3 and 5-6). Catechols were obtained as the only recovered products. The highest yield observed in the case of **8a** suggests that the inhibitory effect of the *meta*-substituent can be partially balanced by the presence of a *para*-substituent with an inductive electron-donor effect. Next the oxidation of chloro phenol derivatives, 4-chloro phenol **9** and 4-chloro-2-methyl phenol **10** was analysed. Treatment of **9** with Tyro/E and Tyro/E-LbL (263 U) afforded catechol **9a** in quantitative yield and conversion of substrate (Scheme 3.2, Table 3.6, entries 8-9).

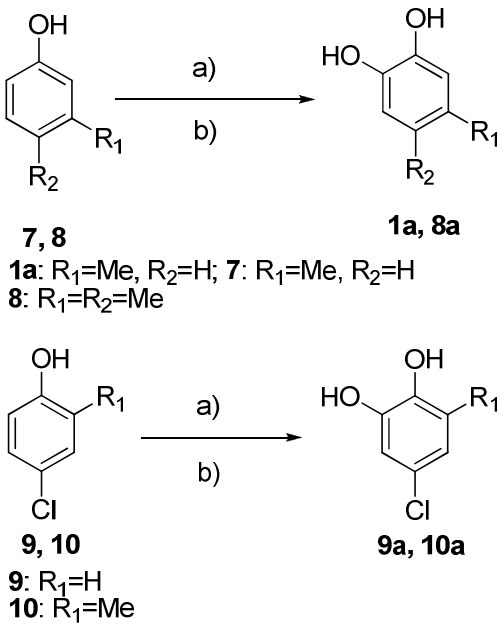

Scheme 3.2 Oxidation of phenols 7-10. ***Reagents and conditions:*** **a) Tyro-based systems, O_2, AA; b) Na-phosphate buffer.**

Table 3.6 Oxidation of phenols 7-10.[a]

Entry	Substrate	Biocatalysts	Products	Conversion (%)[b]	Yield (%)[b]
1	**7**	Tyro	**1a**	52	52
2	**7**	Tyro/E	**1a**	42	42
3	**7**	Tyro/E-LbL	**1a**	48	48
4	**8**	Tyro	**8a**	88	88
5	**8**	Tyro/E	**8a**	80	80
6	**8**	Tyro/E-LbL	**8a**	84	84
7	**9**	Tyro	**9a** [c]	>99	>99
8	**9**	Tyro/E	**9a** [c]	94	>99
9	**9**	Tyro/E-LbL	**9a** [c]	97	>99
10	**10**	Tyro	**10a**	>99	>99
11	**10**	Tyro/E	**10a**	82	82
12	**10**	Tyro/E-LbL	**10a**	89	89

[a] Reaction conditions: substrate (0.05 mmol), AA (1.5 eq.) and tyrosinase (526 U) were taken in 5.0 mL of phosphate buffer solution for 24 h; [b] Conversion and yield were calculated by GC-MS analysis using dodecane as internal standard; [c] Oxidation performed with 263 U of tyrosinase.

A similar result was obtained with the free enzyme (Table 3.6, entry 7). As expected, twice amount of tyrosinase (526 U) was required for the oxidation of **10**, due to the presence of the *ortho*-substituent. Despite this request, the catechol **10a** was isolated in high yield (Scheme 3.2, Table 3.6, entries 11-12), confirming the beneficial role of the electron-donor substituent in the *para*-position of the aromatic ring. Even for compounds **7-10** reactions performed without ascorbic acid afforded dimeric compounds as main recovered product beside to very low amount of catechols (data not shown). Note that, phenol derivatives characterized by an electron-donor *ortho*-substituent, as in the case of 2-methoxy-4-methyl phenol **11** and 2-methoxy phenol **12**, while requesting a twice amount of enzyme (526 U), afforded the corresponding catechols **11a** and **12a** in significant yield (Scheme 3.3, Table 3.7**,** entries 2-3 and 5-6). Again, the Tyro/E-LbL was the best biocatalyst. The synthesis of catechol derivatives characterized by a potential biological activity was then studied. Since acidic catechols are interesting compounds in pharmaceutical field, thanks to their antibacterial,[42] antimicrobial[43] and antioxidant[44] activities, the oxidation of two phenolic acid derivatives, 3-(4-hydroxyphenyl)propionic acid **13** and 4-hydroxyphenylacetic acid **14** was further evaluated. Irrespective to experimental conditions used, the catechols **13a** and **14a** were obtained in high yield as the only recovered products, confirming again the validity of the reducing condition (Scheme 3.3, Table 3.7, entries 8-9 and 11-12).

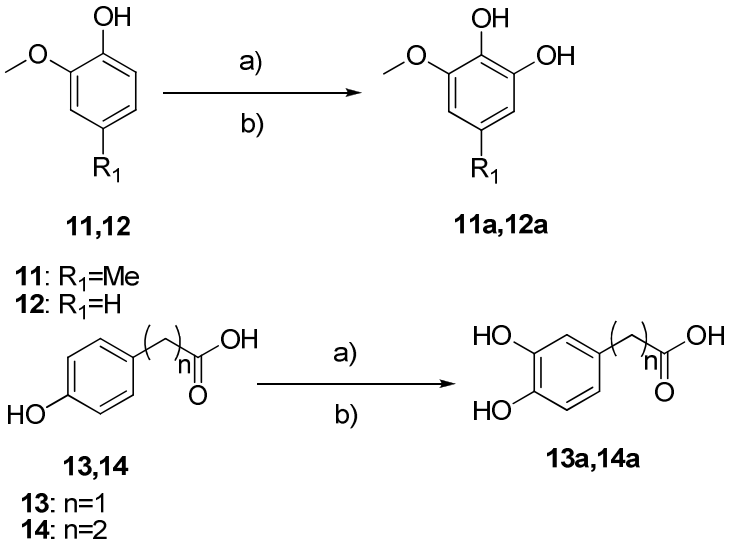

Scheme 3.3 Oxidation of phenols 11-14. ***Reagents and conditions*****: a) Tyro-based systems, O_2, AA; b) Na-phosphate buffer.**

Table 3.7 Oxidation of phenols 11-14.[a]

Entry	Substrate	Biocatalysts	Products	Conversion (%)[b]	Yield (%) [b]
1	**11**	Tyro	**11a** [c]	80	80
2	**11**	Tyro/E	**11a** [c]	73	73
3	**11**	Tyro/E-LbL	**11a** [c]	78	78
4	**12**	Tyro	**12a** [c]	84	84
5	**12**	Tyro/E	**12a** [c]	73	73
6	**12**	Tyro/E-LbL	**12a** [c]	79	79
7	**13**	Tyro	**13a**	88	88
8	**13**	Tyro/E	**13a**	75	75
9	**13**	Tyro/E-LbL	**13a**	84	84
10	**14**	Tyro	**14a**	48	88
11	**14**	Tyro/E	**14a**	37	77
12	**14**	Tyro/E-LbL	**14a**	40	80

[a] Reaction conditions: substrate (0.05 mmol), AA (1.5 eq.) and tyrosinase (263 U) were taken in 5.0 mL of phosphate buffer solution for 24 h; [b] Conversion and yield were calculated by GC-MS analysis using dodecane as internal standard; [c] Oxidation performed with 526 U of tyrosinase.

In a similar way, the oxidation of bis(4-hydroxyphenyl)methane **15** proceeded with high conversion of substrate to afford the mono-catechol and bis-catechol derivatives **15b** and **15a**, respectively, in appreciable yield (Scheme 3.4, Table 3.8, entries 1-3). In accordance with the selectivity of the free enzyme, immobilized tyrosinases afforded **15a** as the main reaction product, Tyro/E-LbL being the best biocatalys. Moreover, the reaction performed with twice amount of enzyme and for longer reaction time (48 h) produced **15a** as the only recovered product in quantitative yield (Table 3.8, entries 4-5). This transformation is of synthetic interest since polyhydroxylated diphenylmethane derivatives are characterized by antiviral,[45] antioxidant,[46] and antimicrobial activities.[47] Finally, the synthesis of 3,4-dihydroxyphenylethanol (hydroxytyrosol), a low molecular weight component in

virgin olive oil and in mill wastes, was studied.[10a] This compound shows several biological activity, including antimicrobial,[48] hypoglycaemic,[49] antioxidant,[49] cardiovascular properties,[50] inhibition of platelet aggregation[51] and inhibition of lipoxygenases,[52] or induction of apoptosis.[53]

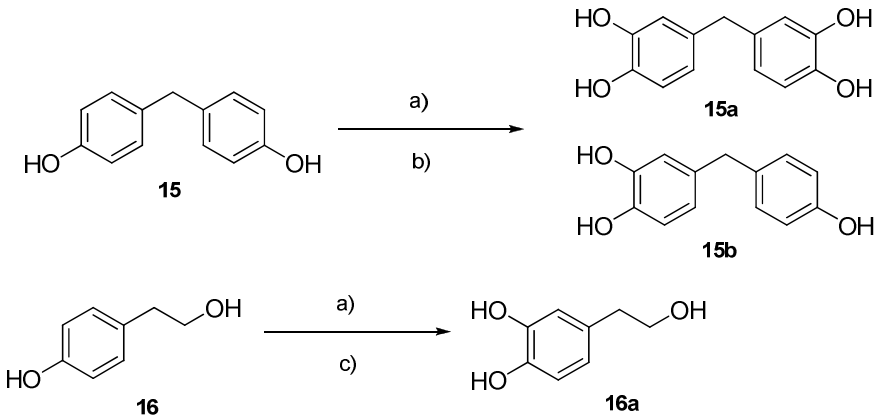

Scheme 3.4 Oxidation of phenols 15 and 16. ***Reagents and conditions:*** **a) Tyro-based systems, O_2, AA; b) Na-phosphate buffer/CH_3CN; c) Na-phosphate buffer.**

Table 3.8 Oxidation of phenols 15-16.[a]

Entry	Substrate	Biocatalysts	Products	Conversion (%) [b]	Yield (%) [b]
1	**15**	Tyro	**15a(15b)** [c]	>99	65(34)
2	**15**	Tyro/E	**15a(15b)** [c]	95	53(41)
3	**15**	Tyro/E-LbL	**15a(15b)** [c]	98	66(32)
4	**15**	Tyro/E	**15a** [c], [d]	>99	>99
5	**15**	Tyro/E-LbL	**15a** [c], [d]	>99	>99
6	**16**	Tyro	**16a**	85	85
7	**16**	Tyro/E	**16a**	70	70
8	**16**	Tyro/E-LbL	**16a**	77	77

[a] Reaction conditions: substrate (0.05 mmol), AA (1.5 eq.) and tyrosinase (263 U) were taken in 5.0 mL of phosphate buffer solution for 24 h; [b] Conversion and yield were calculated by GC-MS analysis using dodecane as internal standard; [c] Oxidation performed in Na-phosphate buffer/CH_3CN; [d] Oxidation performed with 526 U of tyrosinase for 48 h.

When 2-(4-hydroxy phenyl)ethanol (tyrosol) **16** was treated with Tyro/E and Tyro/E-LbL under previously reported conditions, catechol **16a** was obtained in 70% and 77% yield, respectively (Scheme 3.4, Table 3.8, entries 7-8). In this latter case, free enzyme showed reactivity slightly higher than immobilized biocatalysts (Table 3.8, entry 6 versus entries 7-8). With the aim to evaluate the reusability of immobilized tyrosinases *para*-cresol **1** was selected as representative phenol derivative. Compound **1** (0.05 mmol) was oxidized with immobilized tyrosinase systems (263 U) (Tyro/E and Tyro/E-LbL) in buffer medium under previously reported experimental conditions. After 24 h, the immobilized biocatalyst was recovered, washed and reused with fresh added substrate and ascorbic acid.

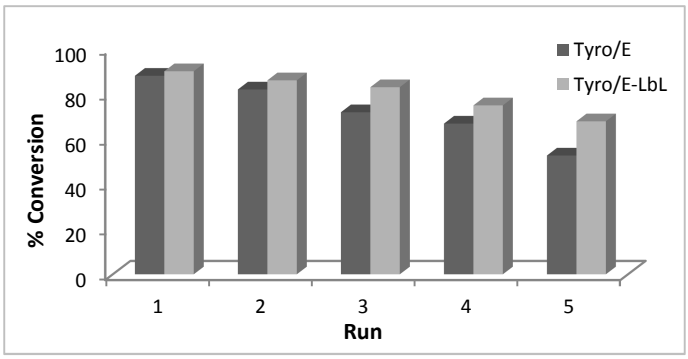

Figure 3.15 Conversion (%) of *para*-cresol 1 after 5 runs. Each oxidation run was performed for 24h. Results are the mean of three different experiments.

As shown in Figure 3.15, the immobilized laccase retained significant activity after 5 runs, mainly for polyelectrolyte covered-system (Tyro/E-LbL) that showed more than 70% of substrate conversion in reference to Tyro/E.

3.3 Conclusions

The alumina particles were low efficient support for tyrosinase immobilization, while new and efficient heterogeneous biocatalysts were synthesized by immobilization on Eupergit®C250L and coating by LbL. With respect to the free enzyme used as reference, tyrosinase retained the catalytic activity and selectivity after immobilization. It is interesting to note that in all of the cases studied, Tyro/E-LbL was more efficient than Tyro/E, suggesting a stabilization effect exerted by the polyelectrolyte coating. Tyro/E and Tyro/E-LbL were stable enough to perform at least five recycling experiments with similar conversion and selectivity. The stability of tyrosinase at different pH and temperatures was also found to be increased in the presence of the support; Tyro/E-LbL being the most stable and reusable catalyst. These data supported the hypothesis that polyelectrolytes act by creating an inner microenvironment that stabilizes the enzyme by denaturing agents, such as changes in temperature and pH, showing a positive effect on maintenance of the catalytic properties of enzyme.[38] Oxidative reactions performed in reducing condition afforded catechol with high selectivity, unlike reactions carried out without ascorbic acid that produced dimeric compounds as the main recovered products. About the selectivity of the oxidations, tyrosinase activity was affected by the electronic effect exerted by substituents on the aromatic ring. Tyrosinase showed decreasing catalytic efficiency from *para*- to *meta*- and *ortho*- substituted phenols; the reactivity decreases upon a transition of substituent from electron-donating to electron-withdrawing groups.[41,54]

Para-substituted phenols with electron releasing group [alkylphenols (**1-4**) > chlorophenols (**9**) > alcohol phenol (**16**) > acidic phenols (**13, 14**)] were efficiently oxidized, even in the case of highly

encumbering substituents (**3, 4, 15**). *Meta*-substituted (**7, 8**) and *ortho*-substituted phenols (**10-12**) required a twice amount of enzyme to yield the corresponding catechols in high yield, probably due to both the effect exerted by the substituent on the electronic distribution of the aromatic ring[41] and the steric encumbering for the formation of the first intermediate with the Cu atom in the active site of the enzyme. Substrates with strong electron-withdrawing substituent (**6**) or with large-size substituent group (**5**) inhibited tyrosinase activity. Since catechols are biologically active compounds difficult to synthesize by traditional chemical procedure under environmental friendly conditions, the use of immobilized tyrosinases in reducing reaction condition open a novel synthetic alternative for this interesting family of substances.

3.4 Experimental Section

Mushroom tyrosinase from *Agaricus bisporus* (Tyro), Eupergit®C250L, poly(sodium 4-styrenesulfonate) (PSS, MW 70000), poly(allylamine hydrochloride) (PAH, MW 56000), L-tyrosine (L-Tyr), ascorbic acid, 2,2'-azino-bis(3-ethylbenzothiazoline-6-sulphonic acid) (ABTS), bovine serum albumin (BSA), ethyl acetate (EtOAc), acetonitrile (CH_3CN), sodium sulphate anhydrous (Na_2SO_4), dodecane, pyridine, hesamethyldisilazane (HMDS), trimethylchlorosilane (TMCS) and phenols were purchased from Sigma-Aldrich. All spectrophotometric measurements were made with a Varian Cary50 UV-Vis spectrophotometer equipped with a single cell peltier thermostatted cell holder. Spectrophotometric data were analyzed with Cary WinUV software. All experiments were carried out in triplicate using free and immobilized tyrosinase.

3.4.1 Tyrosinase immobilized on alumina spherical particles and coated with polyelectrolyte layers

Tyrosinase was treated with activated alumina pellets in accordance with previously reported procedures.[26] The adopted immobilization technique consisted of four different stages. In the first one, aminoalkylation, amino-groups were made available on the surface of the support by silanization of Al_2O_3 with 2% (v/v) γ-aminopropyltriethoxysilane in acetone a 45°C for 20 h. The silanized supports were washed once with acetone and silanized again for 24 h. They were then washed several times with deionized water and dried through air. The second stage provides a cross-linking agent for enzyme immobilization by treatment of Al_2O_3 with 2% (v/v) aqueous glutaraldehyde (50% v/v) for 2 h. The particles were then washed again with deionized water and dried through air. The third stage, grafting, consisted of enzyme immobilization putting in contact tyrosinase (50.0-400.0 mg, 6950-55600 U) suspended in Na-phosphate buffer 0.1 M, pH 7.0 (250.0 ml) with activated alumina

(100.0 g). The particles were then washed several times with phosphate buffer 0.1 M, pH 7.0 until no enzymatic activity was found in the washing solution. The amount in milligrams and the units of coupled tyrosinase were calculated by the difference between the amount/units loaded and that recovered in the washings by conventional Bradford and activity assay. In the last step, the particles were first washed three times with 0.1 M NaCl and then the sequential deposition of polyelectrolyte layers onto the alumina particles was performed. The supports were immersed for 20 min inside each polyelectrolyte solution (2.0 mg/ml PAH or PSS in 0.5 M NaCl). The pH of the PAH solution was adjust to 6.5, ensuring the protonation of more than 90% of the amino groups (NH_3^+ form).[55] Since the alumina pellets with immobilized enzyme were negatively charged, microcapsules consisting of three layers were created starting with the positively charged polyelectrolyte (PAH^+, PSS^-, PAH^+). After each layer, the excess of polyelectrolyte was removed by washing with 0.1 M NaCl. The red particles of LbL immobilized tyrosinase were obtained by simple filtration from the reaction mixture.

3.4.2 Tyrosinase immobilization on Eupergit®C250L

The immobilization of tyrosinase was performed by a modification of literature procedure used for laccase immobilization on Eupergit®C250L.[30] Dry Eupergit®C250L (1.0 g) was added to different amount of buffer 0.1 M (pH 5.0-8.0) containing tyrosinase (Tyro, 1.0-5.0 mg, 13900 U/mg). The mixture was incubated for 24-48 h at room temperature with orbital shaking. At the end of the coupling period, the resin beads were filtered, washed with buffer (5 x 8.0 mL) until no activity was detected in the washing. The obtained beads were incubated with glycine (3.0 M) for 2 h to block residual epoxy groups,[56] then washed with buffer and finally air-dried and stored at 4°C. The amount in milligrams and the units of coupled tyrosinase (Tyro/E) were calculated by the difference between the amount/units loaded and that recovered in the washings by conventional Bradford and activity assay.

3.4.3 Tyrosinase immobilization on Eupergit®C250L and coating with Layer-by-Layer method

Tyro/E, synthesized using the optimal experimental conditions described above, was coated with the Layer-by-Layer method (LbL) in accordance to literature procedures.[57] Briefly, PAH and PSS solutions (2.0 mg/mL in 0.5 M NaCl) were alternately added to Tyro/E system: each polyelectrolyte layer was adsorbed for 20 min at room temperature with orbital shaking and then washed with 0.5 M NaCl to remove excess of polyelectrolytes. The pH of the PAH solution was adjust to 6.5, ensuring the protonation of more than 90% of the amino groups (NH_3^+ form).[55] The deposition of polyelectrolytes

started with PAH and was repeated to obtain three layers (PAH-PSS-PAH). Immobilized tyrosinase (Tyro/E-LbL) was air-dried and stored at 4°C.

3.4.4 Determination of protein concentration

Protein concentration was determined spectrophotometrically at 595 nm according to Bradford procedure using BSA as standard.[58]

3.4.5 Activity assay

Tyrosinase assay was performed by the dopachrome method as previously described.[28] Briefly, L-Tyr solution (1.0 mL, 2.5 mM), Na-phosphate buffer 0.1 M, pH 7.0 (1.9 mL) was incubated under vigorous stirring at 25°C for 10 min. Then, an appropriate amount of free or immobilized enzyme in Na-phosphate buffer (100.0 µl) was added to the mixture and the initial rate was immediately measured as linear increase in optical density at 475 nm, due to dopachrome formation. One unit of enzyme activity was defined as the increase in absorbance of 0.001 per minute at pH 7.0, 25°C in a 3.0 mL reaction mixture containing 0.83 mM of L-tyrosine and 67.0 mM of Na-phosphate buffer pH 7.0. The specific activity of biocatalysts was also analyzed in the pH range of 4.0-9.0.

3.4.6 Kinetic assay

Kinetic parameters, K_m and V_{max} and V_{max}/K_m, were determined by measuring enzyme activity at different concentrations of L-Tyr (330.0-1000.0 µM) and plotting data to a double reciprocal plot (Lineweaver-Burk plot).[36] Reactions were carried out by means of the same procedure as for activity assay, using Tyro (53.0 µg), Tyro/E (70.0 µg) and Tyro/E-LbL (70.0 µg), and measuring absorbance at 475 nm as described above.

3.4.7 Stability assay

Tyrosinase (53.0 µg for Tyro and 70.0 µg for Tyro/E and Tyro/E-LbL) in Na-phosphate buffer 0.1 M, pH 7.0 was stored at three temperatures (-20°C, +4°C, 25°C). At different times (0-25 days), aliquots were taken and the activity was determined at room temperature by the dopachrome method. For each sample, tyrosinase activity was expressed as relative percentage activity respect to that at time zero.

3.4.8 Transmission Electron Microscopy (TEM) measurements

Samples were prepared at the Interdepartmental Centre of Electron Microscopy of Tuscia University, Viterbo, Italy, using conventional procedures. For Transmission Electron Microscopy (TEM), samples were fixed with 2,5% glutaraldehyde in 0.1 M cacodylate buffer pH 7.2 overnight at 4°C. After rinsing in the same buffer, they were post-fixed in cacodylate-buffered 1% osmium tetroxide for 1 h and then washed in distilled water. Specimens were dehydrated in a graded ethanol series and embedded in LRWhite resin. Thin sections were cut with Reichert Ultracut ultramicrotome using a diamond knife, collected on copper grids, stained with uranyl acetate and lead citrate, and observed with a JEOL 1200 EX II electron microscope. Micrographs were acquired by the Olympus SIS VELETA CCD camera equipped the iTEM software.

3.4.9 Scanning Electron Microscopy (SEM) measurements

Samples were prepared at the Interdepartmental Centre of Electron Microscopy of Tuscia University, Viterbo, Italy, using conventional procedures. For Scanning Electron Microscopy (SEM), samples were sputter-coated with gold in a Balzers MED 010 unit and observed with a JEOL JSM 5200 electron microscope. Micrographs were taken by a Mamiya camera applied to the microscope using TMAX 100 ASA films.

3.4.10 Enzyme recycling

In characterization studies, immobilized enzymes (Tyro/E and Tyro/E-LbL) were recycled as follow: L-Tyr (0.83 mM), immobilized Tyro (70.0 µg) and Na-phosphate buffer 0.1 M, pH 7.0 (3.0 mL) were placed in vials at 25°C. At specific time, solutions were removed to measure absorbance at 475 nm and then returned to the vials as rapidly as possible. After reaching plateau, enzyme was washed with buffer, recycled and reused again. One unit of enzyme activity was defined as the increase in absorbance of 0.001 at defined wavelength, temperature and pH. For each run, tyrosinase activity was expressed as relative percentage activity respect to that at first run. In phenols oxidation, immobilized enzyme (Tyro/E and Tyro/E-LbL) was recycled as follow: *para*-cresol **1** (0.05 mmol), immobilized Tyro (263 U) and ascorbic acid (1.5 eq.) were placed in Na-phosphate buffer 0.1 M, pH 7.0 (5.0 mL). After 24 h, tyrosinase was recovered by filtration, washed and reused with fresh substrate and ascorbic acid. For each run, the reaction mixture was extracted with EtOAc and analysed by GC-MS using dodecane as internal standard.

3.4.11 Phenols oxidation

A panel of phenols (Figure 3.13) were oxidized, including *para*-cresol **1**, 4-ethyl phenol **2**, 4-*tert*-butyl phenol **3**, 4-*sec*-butyl phenol **4**, 2,4-di-*tert*-butyl phenol **5**, *para*-nitrophenol **6**, *meta*-cresol **7**, 3,4-dimethyl phenol **8**, 4-chloro phenol **9**, 4-chloro-2-methyl phenol **10**, 2-methoxy-4-methyl phenol **11**, 2-methoxy phenol **12**, 3-(4-Hydroxyphenyl)propionic acid **13**, 4-hydroxyphenylacetic acid **14**, bis(4-hydroxyphenyl)methane **15** and tyrosol **16**. As a general procedure, phenol (0.05 mmol), tyrosinases (263.0-526.0 U) and ascorbic acid (1.5 eq) were placed in Na-phosphate buffer 0.1 M, pH 7.0 (5.0 mL) in vigorous stirring at room temperature. For insoluble aqueous phenols **3, 5, 15** substrates were dissolved in CH_3CN (1.0 mL) and then added to the buffer solutions. Oxidations were performed using homogeneous and heterogeneous conditions. Reactions were monitored by thin layer chromatography (TLC). After the disappearance of the substrate, the reaction mixture was acidified with a solution of HCl 1.0 N and extracted twice with EtOAc. The organic extracts were treated with a saturated solution of NaCl and dried over anhydrous Na_2SO_4, then filtered and concentrated under vacuum to yield coloured crude. In the case of immobilized enzyme, biocatalyst was first recovered by filtration and the solution was subjected to the same work up described above.

3.4.12 Identification and characterization of oxidation products

All products were identified by ^{1}H NMR, ^{13}C NMR and GC-MS. ^{1}H NMR and ^{13}C NMR were recorded on a Bruker 200 MHz spectrometer using $CDCl_3$ as solvent. All chemical shift are expressed in parts per million (δ scale). GC-MS analysis were performed on a 450GC-320MS Varian apparatus using a SPB column (25 m×0.25 mm and 0.25 mm film thickness) and an isothermal temperature profile of 100°C for 2 min, followed by a 10°C/min temperature gradient to 280°C for 25 min. The injector temperature was 280°C. Chromatography-grade helium was used as the carrier gas with a flow of 2.7 mL/min. Mass spectra were recorded with an electron beam of 70 eV. For GC-MS analysis, the coloured residue obtained after extraction was treated with pyridine, HMDS and TMCS (HMDS:TMCS, 2:1 v/v) under vigorous stirring at room temperature for 30 min, then allowed to stand for 5 min.[59]

4-Methylcatechol (4-Methyl-1,2-benzenediol) (1a).

Oil. ^{1}HNMR[60] (200 MHz, $CDCl_3$) δ_H (ppm) 2.24 (3H, s, CH_3), 5.04 (1H, br. s., OH), 5.18 (1H, br. s., OH), 6.61- 6.76 (3H, m, Ph-H). ^{13}CNMR[60] (50MHz, $CDCl_3$) δ_C (ppm) 20.8 (CH_3), 115.3 (CH), 116.2 (CH), 121.5 (CH), 131.1 (C), 141.0 (C), 143.3 (C). MS, (m/z): 268 (M^+), 253 (M-CH3), 238 [M-$(CH_3)_2$], 223 [M-$(CH_3)_3$], 195 [M-$Si(CH_3)_3$], 179 [M-$OSi(CH_3)_3$], 164 [M- $OSi(CH_3)_4$], 149 [M-$OSi(CH_3)_5$], 134 [M-$OSi(CH_3)_6$], 106 [M-$OSi_2(CH_3)_6$], 90 [M-$O_2Si_2(CH_3)_6$].

5-Methylpyrogallol (5-methyl-1,2,3-benzenetriol) (1b).

Oil. ^{1}HNMR[61] (200 MHz, $CDCl_3$) δ_H (ppm) 2.20 (3H, s, CH_3), 5.00 (s, 1H), 5.05 (s, 1H), 8.20 (3H, s, OH). ^{13}CNMR (50MHz, $CDCl_3$) δ_C (ppm) 22.1 (CH_3), 109.0 (2xCH), 131.2 (C), 137.1(C), 146.1 (2xC). *MS, m/z:* 356 (M^+), 341 (M-CH_3), 313]M-$(CH_3)_3$], 283 [M-$Si(CH_3)_3$], 267 [M-$OSi(CH_3)_3$], 252 [M-$OSi(CH_3)_4$], 237 [M-$OSi(CH_3)_5$].

Dimer (1c).

Oil. ^{1}HNMR (200 MHz, $CDCl_3$) δ_H (ppm) 2.19 (3H, s, CH_3), 2.42 (3H, s, CH_3), 6.51 (3H, b.s., OH), 6.61-7.12 (5H, m, Ph-H). ^{13}CNMR (50MHz, $CDCl_3$) δ_C (ppm) 16.0 (CH_3), 22.1 (CH_3), 116.6 (CH), 118.2 (CH), 122.0 (C), 125.6 (C), 127.0 (CH), 127.2 (C), 131.2 (CH), 133.1 (CH), 136.7 (C), 141.3 (C), 150.1 (C), 158.2 (C). *MS, m/z:* 446 (M^+), 431 (M-CH_3), 329 [M-$Si(CH_3)_3$], 313 [M-$OSi(CH_3)_3$], 298 [M-$OSi(CH_3)_4$], 268 [M-$OSi(CH_3)_6$], 180 [M-$O_2Si_2(CH_3)_6$].

5,5'-Dimethyl-[1,1'-Biphenyl]-2,2',3,3'-tetrol (1d).

Oil. ^{1}HNMR (200 MHz, $CDCl_3$) δ_H (ppm) 2.41 (6H, s, 2xCH_3), 6.62-6.91 (4H, m, Ph-H). ^{13}CNMR (50MHz, $CDCl_3$) δ_C (ppm) 22.1 (2xCH_3), 117.2 (2xCH), 122.1 (2xC), 132.0 (2xCH), 138.1 (2xC), 141.3 (2xC), 150.3 (2xC). *MS, m/z:* 534 (M^+), 519 (M-CH_3), 417 [M-$Si(CH_3)_3$], 401 [M-$OSi(CH_3)_3$], 386 [M-$OSi(CH_3)_4$], 371 [M-$OSi(CH_3)_5$], 268 [M-$O_2Si_2(CH_3)_6$].

4-Ethylcatechol (4-ethyl-1,2-Benzenediol) (2a).

Oil. ^{1}HNMR[62] (200 MHz, $CDCl_3$) δ_H (ppm) 1.04 (3H, m, CH_3), 2.36 (2H, m, CH_2), 6.00-7.25 (3H, m, Ph-H). ^{13}CNMR (50MHz, $CDCl_3$) δ_C (ppm) 15.2 (CH_3), 28.1 (CH_2), 116.5 (CH), 117.4 (CH), 124.2 (CH), 139.3 (C), 145.7 (C), 148.4 (C). *MS, m/z:* 282 (M^+), 267 [M-CH_3], 252 [M-$(CH_3)_2$], 237 [M-$(CH_3)_3$], 209 [M-$Si(CH_3)_3$], 193 [M-$OSi(CH_3)_3$], 179 [M-$OSi(CH_3)_4$], 164 [M-$OSi(CH_3)_5$], 148 [M-$OSi(CH_3)_6$], 120 [M-$OSi_2(CH_3)_6$].

5-Ethyl-1,2,3-Benzenetriol (2b).

Oil. ^{1}HNMR (200 MHz, $CDCl_3$) δ_H (ppm) 1.22 (3H, m, CH_3), 2.62 (2H, m, CH_2), 6.62 (2H, m, Ph-H), 8.14 (3H, b.s., OH). ^{13}CNMR (50MHz, $CDCl_3$) δ_C (ppm) 15.2 (CH_3), 29.3 (CH_2), 111.1 (2xCH), 136.2 (C), 138.0 (C), 142.3 (2xC). *MS, m/z:* 370 (M^+), 355 (M-CH_3), 282 [M-$OSi(CH_3)_3$], 267 [M-$OSi(CH_3)_5$], 251 [M-$OSi(CH_3)_6$], 209 [M-$O_2Si_2(CH_3)_6$], 194 [M-$O_2Si_2(CH_3)_9$].

Dimer (2c).

Oil. ^{1}HNMR (200 MHz, $CDCl_3$) δ_H 1.21 (3H, m, CH_3), 1.32 (3H, m, CH_3), 2.71 (2H, m, CH_2), 2.82 (2H, m, CH_2), 6.4-7.2 (5H, m, Ph-H). ^{13}CNMR (50MHz, $CDCl_3$) δ_C (ppm) 15.2 (CH_3), 15.7 (CH_3), 27.2 (CH_2), 28.3 (CH_2), 106.4 (C), 107.2 (C), 112.3 (CH), 114.1 (CH), 128.3 (C), 130.1 (CH), 134.1 (CH), 134.6 (C), 135.1 (C), 136.2 (CH), 143.1 (C), 155.2 (C). *MS, m/z:* 474 (M^+), 459 (M-CH_3), 429 (M-$CH_3)_3$, 341 [M-$OSi(CH_3)_3$], 326 [M-$OSi(CH_3)_4$], 311 [M-$OSi(CH_3)_5$].

5,5'-Diethyl-[1,1'-Biphenyl]-2,2',3,3'-tetrol (2d).

Oil. ^{1}HNMR (200 MHz, $CDCl_3$) δ_H (ppm) 1.22 (6H, m, 2xCH_3), 2.73 (4H, m, 2xCH_2), 6.4-7.2 (4H, m, Ph-H). ^{13}CNMR (50MHz, $CDCl_3$) δ_C (ppm) 15.6 (2xCH3), 28.3 (2xCH_2), 102.2 (2xC), 114.0 (2xCH), 134.3 (2xC),

136.1 (2xC), 138.3 (2xCH), 143.2 (2xC). *MS, m/z:* 562 (M^+), 517 ($M-CH_3)_3$, 489 [$M-Si(CH_3)_3$], 474 [$M-OSi(CH_3)_3$], 459 [$M-OSi(CH_3)_4$], 444 [$M-OSi(CH_3)_5$], 430 [$M-OSi(CH_3)_6$], 385 [$M-O_2Si_2(CH_3)_6$].

4-*tert*-Butylcatechol (4-*tert*-Butylbenzene-1,2-diol) (3a).

Oil. ^{1}HNMR (200 MHz, $CDCl_3$) δ_H (ppm) 1.33 (9H, s, CH_3), 6.63-7.11 (3H, m, Ph-H). ^{13}CNMR (50MHz, $CDCl_3$) δ_C (ppm) 31.2 (3xCH_3), 34.5 (C), 116.5 (CH), 116.9 (CH), 122 (CH), 144.3 (C), 146.2 (C), 147.1 (C). *MS, m/z:* 310 (M^+), 295 ($M-CH_3$), 280 [$M-(CH_3)_2$], 265 [$M-(CH_3)_3$], 237 [$M-Si(CH_3)_3$], 222 [$M-OSi(CH_3)_3$], 207 [$M-OSi(CH_3)_4$], 192 [$M-OSi(CH_3)_5$], 176 [$M-OSi(CH_3)_6$], 148 [$M-OSi_2(CH_3)_6$].

5,5'-bis(1,1-dimethylethyl)-[1,1'-Biphenyl]-2,2',3-triol (3b).

Oil. ^{1}HNMR (200 MHz, $CDCl_3$) δ_H (ppm) (200 MHz $CDCl_3$) δ (ppm) 1.20 (9H, s, CH_3), 1.22 (9H, s, CH_3), 6.51 (3H, s, OH), 6.68-7.47 (5H, m, Ph-H). ^{13}CNMR (50MHz, $CDCl_3$) δ_C (ppm) 31.2 (3xCH_3), 31.5 (3xCH_3), 34.5 (C), 35.9 (C) 116.5 (CH), 118.9 (CH), 122.7 (C), 127.4 (C), 128.5 (CH), 130.2 (CH), 131.7 (CH), 135.5 (C), 151.4 (C), 152.2 (C), 155.8 (C), 157.1 (C). *MS, m/z:* 472 (M^+), 442 [$M-(CH_3)_2$], 427 [$M-(CH_3)_3$], 399 [$M-Si(CH_3)_3$], 354 [$M-OSi(CH_3)_5$], 338 [$M-OSi(CH_3)_6$], 295 [$M-O_2Si_2(CH_3)_6$], 280 [$M-O_2Si_2(CH_3)_7$].

4-*sec*-Butylcatechol (4-(1-methylpropyl)-1,2-Benzenediol) (4a).

Oil. ^{1}HNMR (200 MHz, $CDCl_3$) δ_H (ppm) 1.10 (3H, m, CH_3), 1.22 (3H, m, CH_3), 1.53 (2H, m, CH_2), 3.23 (1H, m, CH), 6.52-6.84 (3H, m, Ph-H). ^{13}CNMR (50MHz, $CDCl_3$) δ_C (ppm) 11.2 (CH_3), 22.3 (CH_3), 31.2 (CH_2), 43.1 (CH), 113.3 (CH), 114.1 (CH), 124.4 (CH), 136.2 (C), 145.1 (C), 147.0 (C). *MS, m/z:* 310 (M^+), 295 ($M-CH_3$), 280 [$M-(CH_3)_2$], 237 [$M-Si(CH_3)_3$], 222 [$M-OSi(CH_3)_3$], 207 [$M-OSi(CH_3)_4$], 192 [$M-OSi(CH_3)_5$], 149 [$M-OSi_2(CH_3)_6$], 133 [$M-O_2Si_2(CH_3)_6$].

Dimer (4b)

Oil. ^{1}HNMR (200 MHz $CDCl_3$) δ (ppm) 1.09 (3H, m, CH_3), 1.12 (3H, m, CH_3), 1.21 (3H, m, CH_3), 1.32 (3H, m, CH_3), 1.52 (2H, m, CH_2), 1.63 (2H, m, CH_2), 3.09 (1H, m, CH), 3.21 (1H, m, CH), 6.6 (3H, s, OH), 6.8-7.5 (5H, m, Ph-H). ^{13}CNMR (50MHz $CDCl_3$) δ (ppm) 11.1 (2xCH_3), 21.9 (2xCH_3), 31.1 (2xCH_2), 43.5 (CH), 45.0 (CH), 115.7 (CH), 116.1 (CH), 121.6 (C), 126.1 (C), 130.5 (CH), 131.3 (CH), 134.7 (CH), 135.3 (C), 150.2 (C), 152.9 (C), 154.3 (C), 156.0 (C). *MS, m/z:* 458 (M^+), 443 ($M-CH_3$), 428 [$M-(CH_3)_2$], 340 [$M-OSi(CH_3)_5$], 324 [$M-OSi(CH_3)_6$], 281 [$M-O_2Si_2(CH_3)_6$], 265 [$M-O_2Si_2(CH_3)_7$].

4,5-Dimethylcatechol (4,5-Dimethyl-1,2,-Benzenediol) (8a).

Oil. ^{1}HNMR[63] (200 MHz, $CDCl_3$) δ_H (ppm) 2.20 (s, 6H,CH_3), 6.51 (s, 2H, Ph-H). ^{13}CNMR (50MHz, $CDCl_3$) δ_C (ppm) 19.7 (2xCH_3), 118.9 (2xCH), 130.1 (2xC), 143.9 (2xC). *MS, m/z:* 282 (M^+), 267 ($M-CH_3$), 252 [$M-(CH_3)_2$], 237 [$M-(CH_3)_3$], 210 [$M-Si(CH_3)_3$], 194 [$M-OSi(CH_3)_3$], 179 [$M-OSi(CH_3)_4$], 164 [$M-OSi(CH_3)_5$], 149 [$M-OSi(CH_3)_6$], 105 [$M-O_2Si_2(CH_3)_6$].

4-Chlorocatechol (4-chloro-1,2-Benzenediol) (9a).

Oil. ^{1}HNMR (200 MHz, $CDCl_3$) δ_H (ppm) 6.72-6.83 (3H, m, Ph-H), 8.10 (2H, br.s, OH). ^{13}CNMR (50MHz, $CDCl_3$) δ_C (ppm) 113.0 (CH), 117.3 (CH), 125.4 (CH), 127.2 (C), 145.0 (C), 152.3 (C). *MS, m/z:* 288 (M^+),

273 (M-CH_3), 258 (M-$(CH_3)_2$), 243 (M-$(CH_3)_3$), 215 (M-$Si(CH_3)_3$), 199 [M-$OSi(CH_3)_3$], 184 [M-$OSi(CH_3)_4$], 169 [M-$OSi(CH_3)_5$], 126 [M-$OSi_2(CH_3)_6$].

5-Chloro-3-methylcatechol (5-chloro-3-methyl-1,2-Benzenediol) (10a).

Oil. ^{1}HNMR (200 MHz, $CDCl_3$) δ_H (ppm) 2.10 (3H, s, CH_3), 6.53-6.74 (2H, s, Ph-H), 7.52 (2H, br.s, OH). ^{13}CNMR (50MHz $CDCl_3$) δ_C (ppm) 17.2 (CH_3), 116.3 (CH), 123.2 (C), 125.4 (C), 126.3 (CH), 140.2 (C), 151.0 (C)**.** *MS*, *m/z*: 302 (M^+), 287 (M-CH_3), 272 [M-$(CH_3)_2$], 229 [M-$Si(CH_3)_3$], 213[M-$OSi(CH_3)_3$], 198 [M-$OSi(CH_3)_4$], 168 [M-$OSi(CH_3)_6$].

3-methoxy-5-methyl-1,2-Benzenediol (11a).

Oil. ^{1}HNMR[64] (200 MHz, $CDCl_3$) δ_H (ppm) 2.19 (3H, s, CH_3), 3.80 (3H, s, OCH_3), 6.27- (2H, m, Ph-H). ^{13}CNMR (50MHz, $CDCl_3$) δ_C (ppm) 22.0 (CH_3), 56.6 (CH_3), 106.2 (CH), 111.1 (CH), 131.2 (C), 133.6 (C), 145.4 (C), 145.8 (C). *MS*, *m/z*: 298 (M^+), 283 (M-CH_3), 268 [M-$(CH_3)_2$], 253 [M-$Si(CH_3)_3$], 225 [M-$Si(CH_3)_3$], 209 [M-$OSi(CH_3)_3$], 194 [M-$OSi(CH_3)_4$], 179 [M-$OSi(CH_3)_5$], 164 [M-$OSi(CH_3)_6$].

3-methoxy-1,2-Benzenediol (12a).

Oil. ^{1}HNMR (200 MHz, $CDCl_3$) δ_H (ppm) 3.79 (3H, s, CH_3), 6.54-6.80 (3H, m, Ph-H), 8.08 (2H, b.s., OH). ^{13}CNMR (50MHz, $CDCl_3$) δ_C (ppm) 56.2 (CH_3), 105.4 (CH), 111.1 (CH), 122.8 (CH), 138.9 (C), 147.6 (C), 148.7 (C). *MS, m/z:* 284 (M^+), 269 (M-CH_3), 254 [M-$(CH_3)_2$], 239 [M-$(CH_3)_3$], 211 [M-$Si(CH_3)_3$], 195[M-$OSi(CH_3)_3$], 180 [M-$OSi(CH_3)_4$], 165 [M-$OSi(CH_3)_5$], 106 [M-$O_2Si_2(CH_3)_6$].

3,4-Dihydroxy-Benzenepropanoic acid (13a)

Oil. ^{1}HNMR[65] (200 MHz, $CDCl_3$) δ_H (ppm) 2.47 (2H, m, CH_2), 2.70 (2H, m, CH_2), 6.50-6.65 (3H, m, Ph-H). ^{13}CNMR (50MHz, $CDCl_3$) δ_C (ppm) 31.5 (CH_2), 37.2 (CH_2), 116.3 (CH), 116.4 (CH), 120.5 (CH), 133.8 (C), 144.1 (C), 146.2 (C), 177.1 (C). *MS, m/z:* 384 (M^+), 369 (M-CH_3), 354 [M-$(CH_3)_2$], 339 [M-$(CH_3)_3$], 311 [M- $Si(CH_3)_3$], 295 [M-$OSi(CH_3)_3$], 280 [M-$OSi(CH_3)_4$], 265 [M-$OSi(CH_3)_5$], 222 [M-$OSi_2(CH_3)_6$].

3,4-dihydroxy-Benzeneacetic acid (14a)

Oil. ^{1}HNMR (200 MHz, $CDCl_3$) δ_H (ppm) 3.56 (2H, s, CH_2), 6.49-7.10 (3H, m Ph-H), 9.4 (3H, b.s., OH). ^{13}CNMR (50MHz, $CDCl_3$) δ_C (ppm) 41.2 (CH_2), 114.5 (CH), 116.8 (CH), 120.6 (CH), 126.1 (C), 145.2 (C), 145.4 (C), 175.0 (C). *MS, m/z:* 384 (M^+), 369 (M-CH_3), 354 (M-$(CH_3)_2$), 339 [M- $(CH_3)_3$], 311 [M-$Si(CH_3)_3$], 295 [M-$OSi(CH_3)_3$], 280 [M-$OSi(CH_3)_4$], 265 [M-$OSi(CH_3)_5$], 222 [M-$OSi_2(CH_3)_6$].

4-(*Para*-hydroxybenzyl)-pyrocatechol (4-[(4-hydroxyphenyl)methyl]-1,2-Benzenediol) (15a).

Oil. ^{1}HNMR (200 MHz, $CDCl_3$) δ_H (ppm) 4.10 (2H, m, CH_2), 6.51-7.22 (7H, m. Ph-H). ^{13}CNMR (50MHz, $CDCl_3$) δ_C (ppm) 42.2 (CH), 115.5 (CH), 116.1 (2xCH), 116.5 (CH), 121.3 (CH), 130.2 (2xC), 133.5 (C), 134.5 (C), 144.2 (C), 145.3 (C), 156.1 (C). *MS*, *m/z*: 432 (M^+), 417 (M-CH_3), 402 [M-$(CH_3)_2$], 359 [M-$Si(CH_3)_3$], 343 [M-$OSi(CH_3)_3$], 329 [M-$OSi(CH_3)_4$], 314 [M-$OSi(CH_3)_5$], 298 [M-$OSi(CH_3)_6$].

4,4'-Methylenedi-pyrocatechol (4,4'-methylenebis-1,2-Benzenediol) (15b).

Oil. ^{1}HNMR (200 MHz, $CDCl_3$) δ_H (ppm) 4.12 (2H, m, CH_2), 6.62 -7.10 (6H, m. Ph-H), 8.13 (4H, s, OH). ^{13}CNMR (50MHz, $CDCl_3$) δ_C (ppm) 40.2 (CH_2), 115.5 (2xCH), 116.2 (2xCH), 121.1 (2xCH), 135.4 (2xC),

144.3 (2xC), 145.2 (2xC). *MS*, *m/z*: 520 (M^+), 505 (M-CH_3), 447 [M-$Si(CH_3)_3$], 431 [M-$OSi(CH_3)_3$], 417 [M-$OSi(CH_3)_4$], 343 [M-$O_2Si_2(CH_3)_6$], 329 [M-$O_2Si_2(CH_3)_7$].

3,4-Dihydroxyphenylethanol (hydroxytyrosol) (16a).

Oil. ^{1}H NMR[66] (200 MHz, acetone-d_6) δ_H (ppm) 2.65 (2H, m, CH_2), 3.67 (2H, mt, CH_2), 6.54-6.72 (3H, m, Ph-H), 7.67 (2H, br s, 2H); ^{13}C NMR (50MHz, acetone-d_6) δ_C (ppm) 39.7 (CH_2), 64.2(CH_2), 115.9 (CH), 116.8 (CH), 121.0 (CH), 131.9 (C), 144.0 (C), 145.6 (C); *MS*, *m/z*: 386 (M^+), 371 (M-CH_3), 356 (M-$Si(CH_3)_2$), 341(M-$Si(CH_3)_3$), 269 (M-$Si(CH_3)_3$), 253 (M-$OSi(CH_3)_3$), 238 (M-$OSi(CH_3)_4$), 223 (M-$OSi(CH_3)_5$), 208 (M-$OSi(CH_3)_6$)

References

[1] a) Halaouli, S.; Asther, M.; Sigoillot, J.-C.; Hamdi, M.; Lomascolo, A. *J. Appl. Microbiol.* **2006**, *100,* 219–232; b) Seo, S- Y.; Sharma, V. K.; Sharma, N. *J. Agric. Food Chem.* **2003**, *51*, 2837-2853.

[2] a) Perron, N. R.; García, C. R.; Pinzón, J. R.; Chaur, M. N.; Brumaghim, J. L. *J Inorg Biochem* **2011,** *105,* 745-753; b) Perron, N. R.; Brumaghim, J. L. *Cell Biochem Biophys* **2009,** *53*, 75-100; c) Ginja Teixeira, J.; Barrocas Dias, C.; Martins Teixeira, D. *Electroanalysis* **2009**, *21*, 2345-2353.

[3] a) Xiao, Z.-P.; Ma, T.-W.; Fu, W.-C.; Peng, X.-C.; Zhang, A.H.; Zhu, H.-L. *Eur J Med Chem* **2010,** *45*, 5064-5070; b) Bansal, V. K.; Kumar, R.; Prasad, R.; Prasad, S. Niraj, *J Mol Catal A: Chem* **2008,** *284,* 69-76.

[4] (a) Szmant, H. H. *Organic Building Blocks of the Chemical Industry* (Szmant, H.H. ed.), **1989,** 512-519, Wiley-Interscience, New York; b) Franck, H.-G.; Stadelhofer, J. W. *Industrial Aromatic Chemistry* **1988,** 183-190, Springer-Verlag, New York; (c) Varagnat, I. In *Kirk-Othmer Encyclopedia of Chemical Technology* (Grayson, M. Ed.), **1981,** *13*, 39-69, Wiley-Interscience, New York.

[5] Lewis, R. J. *Hazardous Chemicals Desk Reference*, **1991,** Van Nostrand Reinhold, New York.

[6] Kirchner, J. R. In *Kirk-Othmer Encyclopedia of Chemical Technology* (Grayson, M. Ed.), **1981,** *13*, 12-38, Wiley-Interscience, New York.

[7] Frost, J.W.; Draths, K.M. *US patent* 5272073, **1993**.

[8] a) Marín-Zamora, M. E.; Rojas-Melgarejo, F.; García-Cánovas, F.; García-Ruiz, P. A. *J Biotechnol* **2009,** *139,* 163-168; b) Mayer, A. M. *Phytochem* **2006,** *67,* 2318-2331.

[9] a) Ramsden, C.A.; Stratford, M.R.L.; Riley, P.A. *Org Biomol Chem,* **2009**, *7*, 3388-3390; b) Muñoz-Muñoz, J.L.; García-Molina, F.; García-Ruiz, P.A.; Molina-Alarcón, M.; Tudela, J.; García-Canovas, F.; Rodriguez-Lopez, J.N. *Biochem J* **2008** *416,* 431-440.

[10] a) Espín, J.C.; Soler-Rivas, C.; Cantos, E.; Tomás-Barberán, F.A.; Wichers, H.J. *J Agric Food Chem,* **2001**, *49 (3)*, 1187-1193; b) Brown, R.S.; Male, K. B.; Luong, J.H.T. *Anal Biochem* **1994**, *222*, 131-139.

[11] Sheldon, R.A. *Adv Synth Catal* **2007**, *349*, 1289-1307.

[12] Majid, Z.A.; Sabri, N.A.M.; Buang, N.A.; Shahir, S. *J Fundam Sciences* **2010,** *6*, 51-55.

[13] Arslan, A.; Kiralp, S.; Toppare, L.; Yagci, Y. *Int J Biol Macromol* 2005, **35**, 163-167.

[14] Jaafar, A.; Musa, A.; Nadarajah,, K.; Lee, Y. H.; Hamidah, S. *Sens. Actuators, B* **2006**, *114*, 604-609.

[15] Sanz, V.C.; Mena, M.L.; Gonzalez-Cortes, A.; Yanez-Sedeno, P.; Pingarron, J.M. *Anal Chim Acta,* **2005**, *528*, 1-8.

[16] Zejli**,** H.; Hidalgo-Hidalgo de Cisneros**,** J.L.; Naranjo-Rodriguez**,** I.; LU, B.; Temsamani, K.R.; Marty, J.L. *Anal Chim Acta* **2008,** *612*, 198-203.

[17] a) Munjal, N.; Sawhney, S.K. *Enzyme Microb Technol* **2002**, *30*, 613–619; b) Duran, N.; Rosa, M.A.; D'Annibale, A.; Gianfreda, L. *Enzyme Microb Technol* **2002**, *31*, 907-931.

[18] Tuncagil, S.; Kayahan, S.K.; Bayramoglu, G.; Arica, M.Y.; Toppare, L. *J Mol Catal B: Enzym* **2009**, *58*, 187-193.

[19] a) Yin, H.; Zhou, Y.; Xu, J.; Ai, S.; Cui, L.; Zhu, L. *Anal Chim Acta* **2010**, *659*, 144-150; b) Hanifah, S.A.; Heng, L.Y.; Ahmad, M. *Anal Sci* **2009,** *25,* 779.

[20] a) Anghileri, A.; Lantto, R.; Kruus, K.; Arosio, C.; Freddi, G. *J Biotechnol* **2007**, *127,* 508-519; b) Thalmann, C.R.; Lötzbeyer, T. *Eur Food Res Technol* **2002,** *214,* 276-281; c) Chen, T.; Embree, H.D.; Wu, L.Q.; Payne, G.F. *Biopolymers*, **2002,** *64*, 292-302; d) Huang, T.H.; Kuwana, T.; Warsinke, A. *Biosens Bioelectron* **2002,** *17*, 1107-1113.

[21] Yahsi, A.; Sahin, F.; Demirel, G.; Tumturk, H. *Int J Biol Macromol* **2005,** *36*, 253-258.

[22] a) Ariga, K.; Lvov, Y.M.; Kawakami, K.; Ji, Q.; Hill, J.P. *Adv Drug Deliv Rev.* **2011**, *63*, 762-71; b) Ariga,K.; Ji, Q.; Hill, J.P. *Adv Polym Sci* **2010**, *229*, 51-87; c) Schönhoff, M. Curr Opin Colloid Interface Sci **2003,** *8*, 86-95; d) G. Decher, *Nachr Chem Tech Lab* **1993**, *41*, 793.

[23] Decher, G.; Schmitt*, J Prog Colloid Polym Sci* **1992**, *89*, 160.

[24] Held, C.; Kandelbauer, A.; Schroeder, M.; Cavaco-Paulo, A.; Gubitz, G.M. *Environ Chem Lett* **2005,** *3*, 74-77.

[25] a) de Faria, R.O.; Rotuno-Moure, V.; Lopes de Almeida, M.A.; Krieger, N.; Mitchell, D.A. *Food Technol Biotechnol* **2007,** *45*, 287-294; b) Ho, P.Y.; Chiou, M.S.; Chao, A.C. *Appl Biochem Biotechnol* **2003,** *111,* 139-152; c) Ros, J.R.; Rodriguez-Lopez, J.N.; García-Cánovas, F. *Biochim Biophys Acta* **1995**, *1204*, 33-42; d) Andrawis, A.; Varda, K. *J. Food Biochem* **1990,** *14*, 103-115.

[26] a) Abadulla, E.; Tzanov, T.; Costa, S.; Robra, K.-H.; Cavaco-Paulo, A.; Gübitz, G. M. *Appl Environ Microb* **2000**, *66*, 3357-3362; b) Cho, Y.K.; Bailey, J.E. *Biotechnol Bioeng* **1979**, *21*, 461-476.

[27] Gerritsen, Y.A.M.; Chapelon, C.G.J.; Wichers, H.J. *Phytochemistry* **1994,** *35(3),* 573-577

[28] Masamoto, Y.; Iida, S.; Kubo, M. *Planta Med* **1980,** *40*, 361-365.

[29] Pialis, P.; Hamann, M.C.J.; Saville, B.A. *Biotechnology and Bioengineering* **1996,** *51*, 141-147.

[30] a) Baratto, L.; Candido, A.; Marzorati, M.; Sagui, F.; Riva, S.; Danieli, B. *J Mol Catal B: Enzym* **2006**, *39,* 3; b) Rauch, P.; Ferri, E.N.; Girotti, S.; Rauchova, H.; Carrea, G.; Bovara, R.; Fini, F.; Roda, A. *Anal Biochem* **1997,** *245*, 13.
[31] Martın, M.T.; Plou, F.J.; Alcalde, M.; Ballesteros, A. *J Mol Catal.B: Enzym* **2003,** *21*, 299-308.
[32] Knezevic, Z.; Milosavic, N.; Bezbradica, D.; Jakovljevic, Z.; Prodanovic. R. *Biochem Eng J* **2006**, *30*, 269-278.
[33] a) Aytar, B. S.; Bakir, U. *Process Biochem* **2008,** *43*, 125–131; b) Acharya, C.; Kumar, V.; Sen R.; Kundu, S.C. *Biotechnol J* **2008**, *3*, 226-233.
[34] Klibanov, A.M *Anal. Biochem* **1979,** *93*, 1-25.
[35] Onda, M.; Ariga, K.; Kunitake, T. *J Biosci Bioeng* **1999,** *87,* 69-75.
[36] Lineweaver, H.; Burk, D. *JACS* **1934,** *56*, 658-661.
[37] a) Huang, C.L.; Cheng, W.C.; Yang, J.C.; Chi, M.C.; Chen, J.H.; Lin, H.P.; Lin, L.L. *J Ind Microbiol Biotechnol* **2010**, *37,* 717-725; b) Chitrangada, A.; Veerendra, K.; Ramkrishna, S.; Subhas, C.K. *Biotechnol J* **2008**, *3*, 226-233.
[38] Sukhorukov, G.; Fery, A.; Möhwald, H. *Prog Polym Sci* **2005**, *30,* 885-897.
[39] Espin, G. J. C. , Tomas, B. F. , Garcia, V.M.C. , Ferreres, A. F., Soler, R. C., Wichers, H. J. US 20030180833, EP1310562A1, 2003.
[40] Dawson, C.R.; Tarpley, W.B. *Ann N Y Acad Sci*, **1963**, *100,* 937-950.
[41] Kazandjiand, R.; Klibanov, A.M. *J Am Chem Soc* **1985**, *107*, 5448-5450.
[42] Moreno-Álvarez, S.A.; Martínez-Castañón, G.A.; Niño-Martínez, N.; Reyes-Macías, J.F.; Patiño-Marín, N.; Loyola-Rodríguez, J.P.; Ruiz, F. *J Nanopart Res* **2010**, *12(8),* 2741-2746.
[43] Chanwitheesuka**,** A.; Teerawutgulraga, A.; Kilburnb, J.D.; Rakariyathama, N. *Food Chemistry*, **2007,** *100(3),* 1044-1048.
[44] Satoa**,** Y.; Itagaki, S.; Kurokawaa, T.; Ogura, J.; Kobayashia, M.; Hirano, T.; Sugawaraa, M. *Int J Pharm* **2011,** *403(1-2),* 136-138.
[45] Costia, R.; Di Santo, R.; Artico, M.; Massa, S.; Ragno, R.; Loddo, R.; La Colla, M.; Tramontano, E.; La Colla, P. ; Pani, A. *Bioorg Med Chem* **2004**, *12,* 199.
[46] Tuerker, B.H.; Ilhami, G.; Abdullah, M.; Sueleyman, G.; Ertan, S. *J Enz Inhibition Med Chem* **2010**, *25(5),* 685.
[47] Colon, M.; Guevara, P.; Gerwick, W.H. *J Nat Prod* **1987**, *50(3),* 368-374.
[48] Yangui, T.; Dhouib, A.; Rhouma A.; Sayadi, S. *Food Chem* **2009, *117***, 1-8
[49] Hamdena, K.; Alloucheb, N.; Damakb, M.; Elfekia, A. *Chem Biol Interact* **2009,** *180(3),* 421-432.
[50] a) Bertelli, A.; Das, D. *J Cardiovasc Pharmacol* **2009,** *54(6),* 468-476; b) Rietjens, S. J.; Bast, A.; de Vente, J.; Haenen, G. R. M. M. *Am J Physiol Heart Circ Physiol* **2007,** *292*, H1931-H193.
[51] González Correa, J. A.; López-Villodresa, J. A.; Asensia, R.; Espartero, J. L.; Rodríguez-Gutiéreza, G.; De La Cruza, J. P. *Br J Nutr* **2009**, *101*, 1157-1164.
[52] Fki, I.; Sahnoun, Z.; Sayadi, S. *J Agric Food Chem,* **2007**, *55(3)*, 624-631.
[53] Han, J.; Talorete, T. P. N.; Yamada, P.; Isoda, H. *Cytotechnol* **2009,** *59(1)*, 45-53.
[54] Sakuma, K.; Ogawa, M.; Sugibayashi, K.; Yamada, K.; Yamamoto, K. *Arch Pharm Res* **1999,** *22(4)*, 335-339.
[55] Djugnat, C.; Sukhorukov, G.B. *Langmuir*, **2004**, *20(17)*, 7265-7269.
[56] Mateo, C.; Abian, O.; Fernandez-Lorente, G.; Predoche, J.; Fernandez-Lafuente, R.; Guisan, J. M. *Biotechnol Prog* **2002,** *18,* 629-634.
[57] a) Perazzini, R.; Saladino, R.; Guazzaroni, M.; Crestini, C. *Bioorg Med Chem* **2011**, *19,* 440-447; b) Tiourina, O.P.; Antipov, A.A.; Sukhorukov, G.B.; Larionova, N.I.; Lvov, Y.; Möhwald, H. *Macromol Biosci* **2001,** *1,* 209.
[58] a) Sedmak, J.J.; Grossberg, S.E. *Anal Biochem* **1977**, *79,* 544; b) Bradford, M.M. *Anal Biochem* **1976,** *72,* 248.
[59] a) Rodríguez-López, J.N.; Gómez-Fenoll, L.; Penalver, M.J.; García-Ruíz, P.A.; Varón, V.; Martínez-Ortíz, F.; García-Cánovas, F.; Tudela, *J Biochim Biophys Acta* **2001**, *1548*, 238**–**256; b) Sweely, C. C.; Bentlry, R.; Makita, M.; Wells, W. W. *J Am Chem Soc,* **1963,** *85*, 2497-2507.
[60] Chernyak, N.; Dudnik, A. S.; Huang, C.; Gevorgyan, V. *J Am Chem Soc* **2010**, *132*, 8270-8272.
[61] Chantarasriwong, O.; Cho, W.C.; Batova, A.; Chavasiri, W.; Moore, C.; Rheingold, A.L.; Theodorakis, E.A. *Org Biomol Chem* **2009**, *7,* 4886-4894.
[62] Nakayama, S.; Ikeda, F. *US Patent* 5102906, 4985458, **1988.**
[63] Pezzella, A.; Lista, L.; Napolitano, A.; d'Ischia, M. *Tetrahedron Lett* **2005,** *46,* 3541-3544.
[64] Silke, P.; Spitelle, P. *J Nat Prod* **2006**, *69*, 1809-1812.
[65] Deng, L.; Sundriyal, S.; Rubio, V.; Shi, Z.-Z.; Song, Y. *J Med Chem*, **2009**, *52(21)*, 6539-6654.
[66] Pouységu, L.; Sylla, T.; Garnier, T.; Rojas, L. B.; Charris, J.; Deffieux, D.; Quideau, S. *Tetrahedron* **2010,** *66,* 5908-5917.

Chapter 4

Immobilized tyrosinase for catechol synthesis: biphasic organic/aqueous biotransformation

4.1 Introduction

As introduced in Chapter 3, the biotechnological potential of tyrosinases (polyphenol oxidases, EC 1.14.18.1) are mainly correlated with their ability to synthesized catechol derivatives; using dioxygen as primary oxidant. Tyrosinases catalysed both the hydroxylation of phenols to catechols (cresolase or monophenolase activity) and the oxidation of catechols to *ortho*-benzoquinones (catecholase or diphenolase activity).[1] As described, catechols are characterized by several biological activities, and are well recognized as antioxidant compounds.[2] Their synthesis is usually difficult to perform by chemical methods, so tyrosinases are studied as efficient and eco-friendly alternative to traditional processes.[3] Investigations showed that a wide range of substrates can be transformed to desired catechols in conventional aqueous-based systems.[4] However, the limitation in the use of tyrosinases in water medium is correlated with the successive conversion of catechol to quinone mediated by the catecholase activity of tyrosinase (Figure 1.4). Quinones are high reactive compounds that can easily polymerize producing insoluble brown pigments able to inactivate the enzyme by covalent bonds.[5] Another approach to overcome this drawback, in addition to the reducing conditions obtained adding ascorbic acid in the reaction medium (as described in Chapter 3),[6] was given by the use of organic solvents as opposed to conventional aqueous medium.[7] Developments in the field of non-aqueous enzymology revealed numerous advantages: (i) increased solubility of hydrophobic substrates, (ii) improved stability of enzyme in water-immiscible organic solvents, (iii) enhanced degree of selectivity and (iv) limited *ortho*-benzoquinone polymerization.[8] Moreover, the use of organic solvent media provides higher oxygen solubility, which in turn reduces the availability of the oxygen as a limiting factor.[9] Kazandjina and Klibanov[10] reported that polyphenol oxidase in chloroform was still 10-times more active than in aqueous medium, thanks to the increased solubility of oxygen and of the phenolic substrates. Recently, the use of organic solvents as potential reaction media for tyrosinase activity has been reported, particularly, for the production of natural stable pigments of selected colour intensity, due to limited *ortho*-quinone polymerization.[5b]

The selection of the appropriate organic solvent as a reaction medium for enzyme biocatalysis depends on several factors such as solvent hydrophobicity, density, viscosity, surface tension, toxicity, flammability, waste disposal, and cost.[11] Solvent hydrophobicity is represented as the logarithm of the partition coefficient (log P), where P is defined as the partitioning of a given solvent between water and 1-octanol in a two-phase system.[12] Solvents with a log P value lower than 2 (hydrophilic solvent) were reported not to be suitable for tyrosinase biocatalysis, as they strongly distorted the essential water layer required to maintain the enzyme in its native catalytically active conformation. Water shows a central role in enzymatic catalysis (i) participating in all non-covalent interactions, including electrostatic, hydrogen bonding, van der Waals and hydrophobic, which maintain the catalytically active enzyme conformation and (ii) playing a crucial role in enzyme dynamics. Generally, water is considered to maintain conformational flexibility in the protein molecules. Mechanistically, the role of water as a lubricant stems from its ability to form hydrogen bonds with the functional groups of the protein molecules, which were bound to each other, thereby "unlocking" the structure. Solvents with a log P value between 2 and 2.5 (weakly hydrophobic solvent) showed higher enzymatic conversions since they did not interfere with the essential water coat surrounding the enzyme molecule in its active site.[5b,13] Apolar solvents with log P ≥ 4 are compatible with enzymes, leaving the essential layer of water molecules on the polar surface regions unperturbed. Moreover, the interest in tyrosinase biocatalysis can be increased by the possibility to immobilize the enzyme on inert supports. The immobilization, in fact, favours the reusability, enhances stability of the enzyme, and facilitates purification of the products. Tyrosinase has been so far immobilized on various types of supports by different methods, such as physical adsorption, covalent cross-linking and microcapsule entrapment.[14] On the other hand, only few examples are reported on the use of immobilized tyrosinase in organic solvents for the synthesis of catechols.[5,15] Specifically, in this chapter the preparation of biocatalysts by immobilization of tyrosinase on Eupergit®C250L and their use in biphasic synthesis of catechols will be described. Eupergit®C250L is a commercially available and low cost epoxy-activated acrylic resin, which has been successfully used for covalent binding of several oxidases such as laccase,[16] glucose oxidase[17] and pyranose oxidase.[18] To further increase the stability of the catalyst, the Layer-by-Layer (LbL) technique, first introduced by Decher et al.,[19] was also applied. This method is based on consecutive deposition of alternatively charged polyelectrolytes on the active species.[20] LbL is an effective tool for the stabilization of enzymes since the polyelectrolyte films show the ability to protect proteins from high-molecular-weight denaturing agents, modifying the permeability towards substrates which can enter the multilayer and react with the catalytic site.[21] Both tyrosinases cross-linked on Eupergit® C250L and the biocatalyst covered with the LbL technique, were used for the oxidation of a large panel of phenols in organic mixed solvent, dichloromethane/buffer (CH_2Cl_2/buffer), to afford the corresponding catechols in high yield. The

comparison between the efficiency and selectivity of tyrosinase with or without the LbL procedure, as well as the possibility to recycle the biocatalysts for more runs, are also reported. To further reduce costs associated with biocatalysis, tyrosinase partially purified from mushrooms *Agaricus bisporous* was used to study the biphasic biotransformation.

4.2 Results and Discussions

4.2.1 Tyrosinase extraction

In literature numerous methods for extracting and purifying tyrosinases from edible mushroom *Agaricus bisporous* have been reported.[22] Among these, two procedures were chosen and compared to obtain a partial purification of tyrosinase: Marín-Zamora and Bouchilloux approach. Marín-Zamora et al.[23] described a single step method to extract tyrosinase from starting lyophilized mushroom in presence of *para*-nitrophenol (PNP). Briefly, 3.0 kg of fresh mushroom were frozen at -20°C at least one day and then lyophilized. The obtained 210.0 mg of lyophilized-ground mushroom were added to 5.6 ml of a 30 mM aqueous solution of PNP (pH 7.0) and magnetically stirred for 30 min at 4 °C. The extraction medium was then centrifuged at 6000 rpm for 5 min. The supernatant which contained the tyrosinase activity was collected and equilibrated to pH 5.5 by adding 35.0 µl of a 0.9 M aqueous solution of NaH_2PO_4 and 0.1 M of H_3PO_4. This solution was assayed for tyrosinase activity by the dopachrome method using L-tyrosine (L-Tyr) as substrate.[24] All experiments were carried out in triplicate. One unit of enzyme activity (U) was defined as the increase in absorbance of 0.001 per minute at 25°C (3.0 ml reaction mixture) in Na-phosphate buffer, pH 7.0. Protein concentration was determined spectrophotometrically at 595 nm according to the Bradford method using bovine serum albumin (BSA) as a standard.[25] As reported in Table 4.1, with a single step extraction, tyrosinase showed a very low activity (150.0 U mg^{-1}) probably due to the presence of residual PNP that could act as competitive inhibitor, binding to the active site of the enzyme (Table 4.1, entry 1).

Table 4.1 Purification scheme of tyrosinase with Marín-Zamora method and its variations. [a]

Entry	Fraction	Total protein (mg)	Total activity (U)	Specific activity[b] (U mg^{-1})	Yield (%)
1	Extraction	24.3	3645.0	150.0	100.0
2	$(NH_4)_2SO_4$ precipitation	8.5	2677.5	315.0	73.0
3	Dialysis	2.0	2548.0	1274.0	69.0
4	Freeze-drying	2.0	2324.4	1162.2	63.0

[a] Tyrosinase activity was measured using L-Tyr as substrates. The amount (mg) of protein was measured with the Bradford method; [b] The specific activity (U mg^{-1}) was defined as the ratio between the enzymatic activity and the amount (mg) of enzyme

With the aim to further increase the specific activity of tyrosinase, further purification steps have been added to the Marín-Zamora method. Specifically, the solution obtained after extraction with 30 mM aqueous solution of PNP was first subjected to ammonium sulphate [$(NH_4)_2SO_4$] precipitation (35-70%) and then dialyzed against water. These additional two steps allow recovering a more reactive enzyme with a specific activity of 315.0 U mg^{-1} and 1274.0 U mg^{-1} respectively (Table 4.1, entries 2 and 3). The solution obtained after dialysis was freeze-dried for better preservation of the enzyme activity (Table 4.1, entry 4). Since freeze-drying process caused a small loss of the specific activity (Table 4.1, entry 4 versus 3) and PNP act as inhibitor of tyrosinase, subsequent extraction experiment was carried out using the Bouchilloux et al.[26] procedure (with slight modifications). In this method enzyme purification started from fresh mushroom and ascorbic acid, instead of PNP, was used to prevent the browning of mushroom extracts. Briefly, the sporocarps were washed with 20 mM ascorbic acid and then sliced and frozen at least 1 day before extraction. 3.0 kg of frozen sporocarp were homogenized twice in 4.0 L of acetone at -20°C in a blender for 1 min. The obtained solid pulp was filtered and homogenized with 3.0 L of 30% v/v acetone in water for 2-3 min. Edible mushroom contains a considerable amount of various phenolic substances, which are readily oxidized during the homogenizing process. Upon oxidation and successive polymerization of the mushroom phenolic content, macromolecules of melanins are formed. The starting acetone washing of the homogenized extract allows collecting the phenolic compounds in the organic solvent limiting the melanin production. This acetone extraction represents the first purification step characterized by tyrosinase with specific activity of 372.2 U mg^{-1} (Table 4.2, entry 1). The mixture obtained after acetone washing was centrifuged and then 1.5 volumes of acetone were added drop wise to the supernatant, under vigorous stirring. The mixture was allowed to settle at 4°C for 2-3 h and centrifuged. Recovered tyrosinase had a specific activity of 1030.9 U mg^{-1} (Table 4.2, entry 2); this first precipitation step was necessary to remove undesirable compounds from crude extract.

Table 4.2 Purification scheme of tyrosinase with the Bouchilloux method.[a]

Entry	Fraction	Total protein (mg)	Total activity (U)	Specific activity [b]	Yield (%)
1	30% v/v acetone extraction	2,292.5	853,268.5	372.2	100.0
2	Acetone precipitation	492.4	496,893.8	1,030.9	58.0
3	$(NH_4)_2SO_4$ precipitation	77.6	118,440.9	1,526.3	14.0
4	Dialysis	6.3	17,778.6	2,822.0	2.1
5	Freeze-drying	6.3	16,178.4	2,568.0	2.0

[a] Tyrosinase activity was measured using L-Tyr as substrates. The amount (mg) of protein was measured with the Bradford method; [b] The specific activity (U mg^{-1}) was defined as the ratio between the enzymatic activity and the amount (mg) of enzyme.

The precipitate was dissolved in water, subjected to precipitation with calcium acetate 1% of saturation and frozen at -20°C. According to Bouchilloux et al., addition of calcium acetate was shown to give no increase in specific activity. Samples obtained from several successive days were frozen at this stage. They were then thawed, mixed and centrifuged. Ammonium sulphate powder $(NH_4)_2SO_4$ was added to the collected supernatant to make a 35% saturated solution. The resulting solution was allowed to stand for 30 min at 4°C and centrifuged at 9000xg for 20 min. $(NH_4)_2SO_4$ was added to supernatant to make a 70% saturated solution. The solution was allowed to stand for 2h at 4°C and centrifuged. At this stage, collected tyrosinase showed a specific activity of 1526.3 U mg^{-1}, about four-fold higher than the crude extract (Table 4.2, entry 3 versus 1). The precipitate collected after centrifugation was dissolved in a minimal volume of cold water and then dialyzed against water and concentrated by means of Vivaflow®50 equipped with a polyethersulfone (PES) membrane (10,000 MWCO). The resulting solution was freeze-dried thus obtaining an enzymatic powder with a specific activity of 2568.0 U mg^{-1} (Table 4.2, entry 5). This tyrosinase was more active than that extracted by Marín-Zamora procedure (2568.0 U mg^{-1} and 1162.2 U mg^{-1}), so the Bouchilloux method was used as reference process for further tyrosinase purifications.

4.2.2 Evaluation of the enzymatic activity and kinetic parameters of tyrosinase

With the aim to evaluate the usage of extracted tyrosinase in biocatalytic systems, to further reduce the costs associated with biotransformations, enzyme activity and kinetic properties of tyrosinase purified by Bouchilloux procedure ($Tyro^E$) was compared with the commercially available mushroom tyrosinase (purchased from Sigma-Aldrich, $Tyro^S$). Tyrosinase activity was assayed by the dopachrome method using L-tyrosine (L-Tyr) as substrate.[24] The specific activity (U mg^{-1}) is defined as the ratio between the enzymatic activity and the amount (mg) of enzyme. Both tyrosinases showed a significant value of enzymatic activity, the commercial enzyme being more reactive than the extracted one (Table 4.3, entries 1 and 2).

Table 4.3 Specific activity (U mg^{-1}) and contaminant laccase (Lac) of commercial ($Tyro^S$) and extracted ($Tyro^E$) tyrosinase.[a]

Entry	Enzyme	Specific activity (U mg^{-1})[b]	Tyro/Lac activity ($x10^3$)[c]
1	$Tyro^S$	13881	2300
2	$Tyro^E$	2568	23

[a] Tyrosinase and laccase activity was assayed using L-Tyr and ABTS as substrate, respectively; [b] The specific activity (U mg^{-1}) was defined as the ratio between the enzymatic activity and the amount (mg) of enzyme; [c] Tyro/Lac activity was defined as the ratio between the specific activity of tyrosinase and that of laccase.

Since tyrosinase preparations usually contain laccase as contaminant, the activity of residual laccase was also evaluated by conventional 2,2'-azino-bis(3-ethylbenzthiazoline-6-sulphonic acid) (ABTS)

assay.[27] Values of the ratio between tyrosinase and laccase activity (Tyro/Lac) are reported in Table 4.3. The amount of laccase was found to be higher in the case of extracted enzyme ($2300x10^3$ for $Tyro^S$ and $23x10^3$ for $Tyro^E$) as expected since a partial purification method was applied for tyrosinase extraction from *A. bisporous*. The kinetic parameters (K_m, V_{max} and V_{max}/K_m) of $Tyro^S$ and $Tyro^E$ were determined measuring the enzyme activity at different concentrations of L-Tyr (330-1000 μM) and plotting data to a double reciprocal plot (Lineweaver-Burk plot) (Table 4.4 and Figure 4.1).[28] $Tyro^E$ showed a K_m value higher than $Tyro^S$, suggesting a reduced affinity for the substrate. This pattern was confirmed by the value of the maximum reaction rate (V_{max}) that is lower for $Tyro^E$. Furthermore, the value of V_{max}/K_m for $Tyro^S$ was higher than $Tyro^E$ (Table 4.4, entry 1 versus entry 2). Due to the high cost of the commercial enzyme, both tyrosinases were studied to compare their efficiency and selectivity and to evaluate the possible use of extracted tyrosinase in catechol synthesis.

Table 4.4 Kinetic parameters of commercial ($Tyro^S$) and extracted ($Tyro^E$) tyrosinase.

Entry	Enzyme	K_m (μM)	V_{max} [a] ($x10^{-3}$)	V_{max}/K_m [b] ($x10^{-6}$)
1	$Tyro^S$	180	6.02	33.4
2	$Tyro^E$	257	4.00	16.1

[a] V_{max} was defined as ΔAbs min^{-1} μg_{enzyme}^{-1}. [b] V_{max}/K_m was defined as ΔAbs min^{-1} μg_{enzyme}^{-1} μM^{-1}. Each experiment was conducted in triplicate. Average errors in kinetic parameters were ± 2-4% for K_m and ±1-3% for V_{max}.

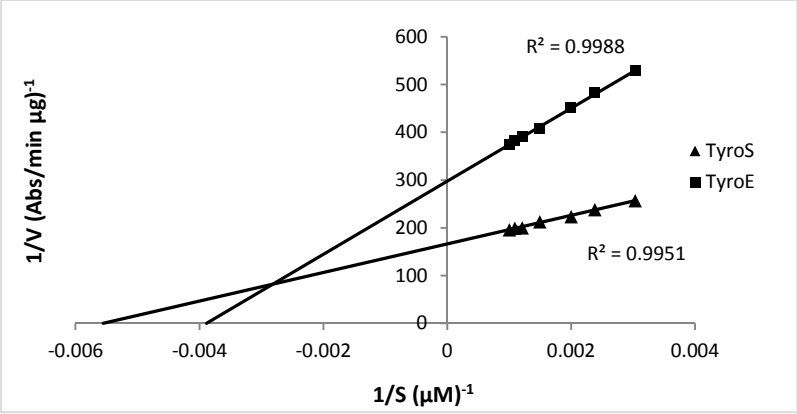

Figure 4.1 Lineweaver-Burk plots of commercial ($Tyro^S$) and extracted ($Tyro^E$) tyrosinase activity determined at different concentrations of L-Tyrosine (330-1000 μM). The data are the mean values of three experiments with standard deviation less than 1%.

4.2.3 Tyrosinase immobilization procedure

Initially, the immobilization of $Tyro^S$ and $Tyro^E$ was performed on the epoxy-activated acrylic beads of Eupergit®C250L, using the previously reported procedures optimized as described in Chapter 3.[29] Briefly, the appropriate enzyme (5.0 mg, 69405 U of $Tyro^S$ and 12840 U of $Tyro^E$, respectively) was suspended in buffer (Na-phosphate buffer 0.1 M, pH 7.0) in the presence of Eupergit®C250L (1.0 g)

for 24 h at room temperature. The immobilized systems (Tyro^S/E and Tyro^E/E, respectively) were washed with water to remove excess of protein and treated with glycine to block residual epoxy-groups (Figure 4.2).

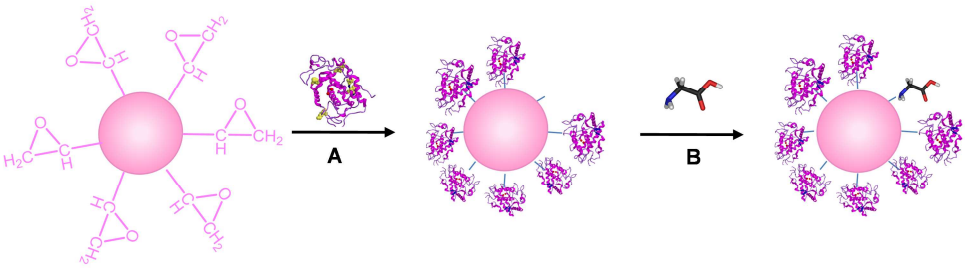

Figure 4.2 Scheme of immobilization of tyrosinase on Eupergit®C250L: (A) tyrosinase cross-linking with the support; (B) treatment with glycine to block residual epoxy-groups.

The effectiveness of the immobilization procedure was investigated in terms of Immobilization Yield and Activity Yield (Eq. 3.1 and Eq. 3.2, Chapter 3) by the analysis of the residual enzymatic activity in the waste waters after the reaction with the support. Under these experimental conditions 45807 U of Tyro^S and 8474 U of Tyro^E were immobilized. Tyro^S/E and Tyro^E/E retained about 38% of their native activity (17407 U g^{-1} for Tyro^S/E and 3135 U g^{-1} for Tyro^E/E).

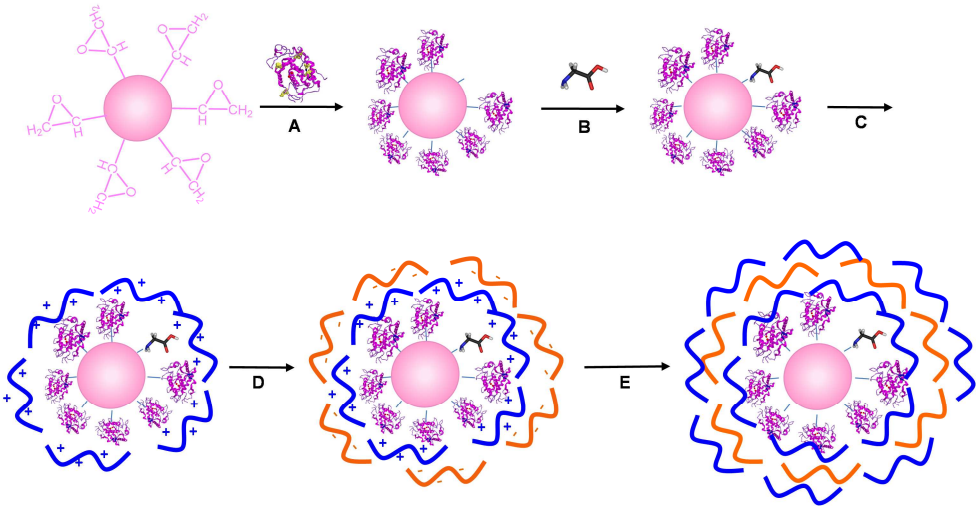

Figure 4.3 Scheme of preparation of PAH/PSS-coated tyrosinase/Eupergit®C250L: (A) tyrosinase cross-linking with the support; (B) treatment with glycine to block residual epoxy-groups; (C) PAH layer deposition; (D) PSS layer deposition; (E) LbL coating of supported tyrosinase.

With the aim to further increase the stability of Tyro^S/E and Tyro^E/E, the LbL technique was applied by coating the particles through a sequential deposition of alternatively charged polyelectrolytes. Briefly, biocatalysts were suspended in positively charged polyallylamine hydrochloride (PAH) (2.0 mg ml^{-1} in 0.5 M NaCl, pH 6.5), filtrated and then treated with negatively charged polystyrene sulphonate (PSS)

(2.0 mg ml^{-1} in 0.5 M NaCl, pH 6.5) (Figure 4.3). This procedure was repeated until the formation of three layers. The coating started with the deposition of the positive PAH to ensure electrostatic interaction with negatively charged tyrosinase (tyrosinase Isoelectric Point = 4.5[30]). The immobilized LbL enzymes retained about 87% of the activity with respect to $Tyro^S$/E and $Tyro^E$/E (15144 U g^{-1} for $Tyro^S$/E-LbL and 2727 U g^{-1} for $Tyro^E$/E-LbL). Novel immobilized tyrosinases were characterized in terms of their kinetic properties using L-Tyr (330-1000 µM) as substrate (Table 4.5). Irrespective to procedures used for the immobilization, V_{max} decreased and K_m increased for supported tyrosinases, leading to a partial reduction of the catalytic efficiency with respect to free enzyme. Similar trends in K_m values were reported in Chapter 3 and are attributed to a possible mass transfer limitations.[31] $Tyro^S$-based heterogeneous biocatalysts were more reactive than $Tyro^E$ systems, confirming the previously reported kinetic parameters (Table 4.4).

Table 4.5 Kinetic parameters of free and immobilized commercial ($Tyro^S$) and extracted ($Tyro^E$) tyrosinase. [a]

Entry	Enzyme	K_m (µM)		V_{max} [b] ($x10^{-3}$)		V_{max}/K_m [c] ($x10^{-6}$)	
		$Tyro^S$	$Tyro^E$	$Tyro^S$	$Tyro^E$	$Tyro^S$	$Tyro^E$
1	Free	180	257	6.02	4.00	33.4	16.1
2	Tyro/E	270	320	4.11	2.10	15.2	6.6
3	Tyro/E-LbL	300	385	3.20	1.53	10.7	3.9

[a] Kinetic properties were determined using L-Tyr (330-1000 µM) as substrate; [b] V_{max} was defined as ΔAbs min^{-1} μg_{enzyme}^{-1}; [c] V_{max}/K_m was defined as ΔAbs min^{-1} μg_{enzyme}^{-1} μM^{-1}. Each experiment was conducted in triplicate. Average errors in kinetic parameters were ± 2-4% for K_m and ±1-3% for V_{max}.

Note that the difference in reactivity of commercial with respect to extracted tyrosinase is more pronounced in the case of immobilized enzymes. In order to evaluate the stability of immobilized biocatalysts in organic solvent medium for the selective synthesis of catechols, a set of Scanning Electron Microscopy (SEM) photographs were taken to compare the morphology of the surface of particles after storage in buffer and in dichloromethane medium. $Tyro^S$/E particles kept in buffer showed a very regular shape and an average value of diameter in the order of 150 µm (Figure 4.4a). A low number of irregular fragments, probably formed by a mechanical damage of particles during the preparation of the sample, was observed as also reported in Chapter 3. At a larger magnification the particles show an irregular surface characterized by grumes of different dimension (Figure 4.4b). A similar behaviour was observed for $Tyro^S$/E after treatment with CH_2Cl_2 suggesting the stability of the resin in organic medium (Figure 4.5) and confirming its suitability for biphasic biotransformations

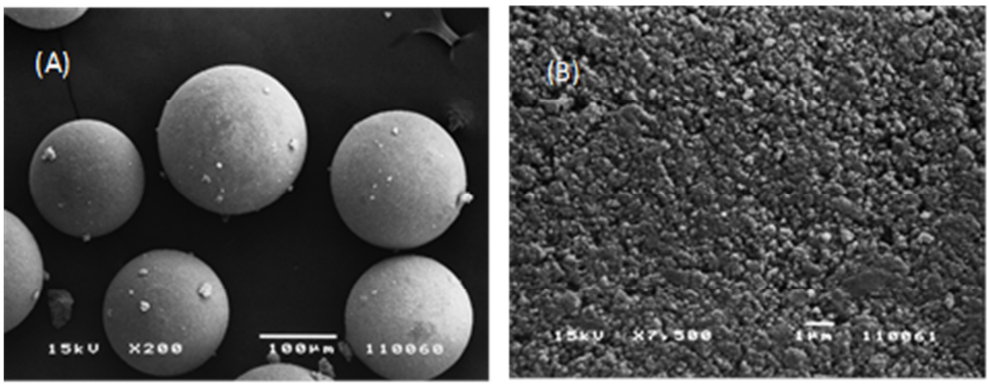

Figure 4.4 SEM images of Tyro^S/E stored in buffer.

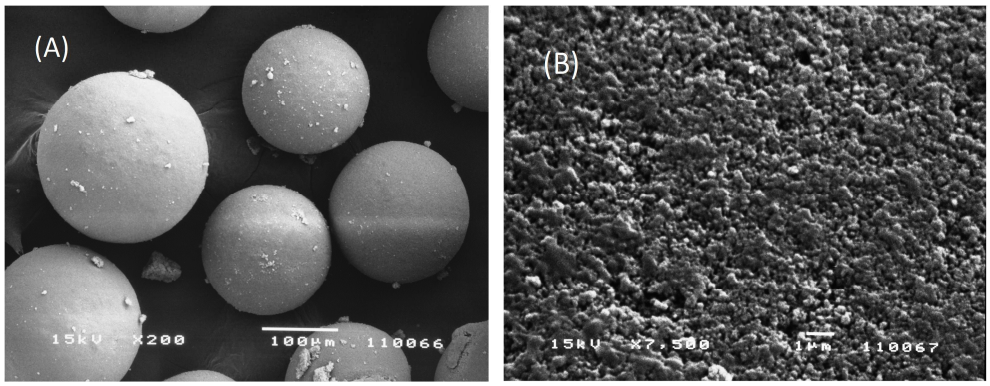

Figure 4.5 SEM images of Tyro^S/E after treatment in CH_2Cl_2.

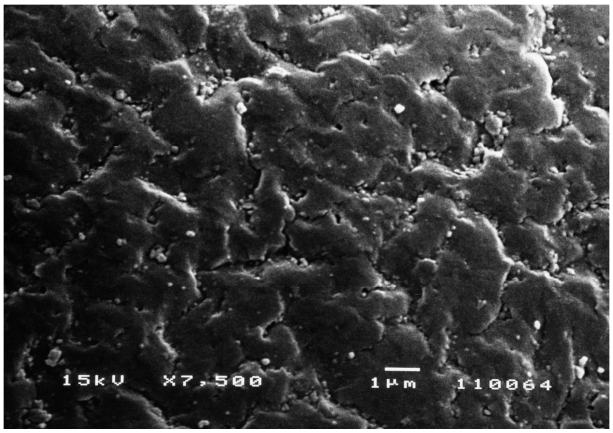

Figure 4.6 SEM image of Tyro^S/E-LbL.

In Figure 4.6 was shown the SEM photograph of Tyro^S/E-LbL after treatment in CH_2Cl_2. As can be seen, the ultrathin coating layers cover the surface of the particles and maintain the characteristic smooth feature described in Figure 3.6d in buffer medium.

4.2.4 Optimization of water requirement for the oxidation in organic solvent

The fundamental role of water for protein function and for their three dimensional structure maintenance is well-recognized and has been reviewed by several authors.[32] In low water content media the relationships between the solvation process and the enzyme kinetics have been reported,[33] the hydration of the active site of the enzyme playing a critical role in substrate recognition and transformation.[34] Water molecules can interact with the protein surface and occupy internal cavities and deep clefts, optimizing spatial configurations and minimizing energetic pathways.[35] Because of the uncertainty of the effect of this process in organic solvents, the amount of added buffer has to be optimized for any specific catalytic system. For this reason, the dependence of the reaction rate versus the concentration buffer was evaluated. In particular, *para*-cresol **1** was selected as a representative phenol substrate. Since oxidative reactions carried out to determine the optimal hydration conditions were followed spectrophotometrically, the absorption peak of *ortho*-quinone was first determined. Briefly, biocatalysts (2.7 μg Tyro^S and 12.00 μg Tyro^E) and buffer (10.0 uL) were added to CH_2Cl_2 solution of substrate (20 mM, 2.5 ml), and the mixture was shaken for 2-4 h. Thereafter, the UV spectrum (800-300 nm) of the CH_2Cl_2 solution was measured; the spectrophotometric scanning profile (Figure 4.7) showed clear distinct absorbance peak at 389 nm, corresponding to the enzymatically-catalysed end product of *para*-cresol **1**.

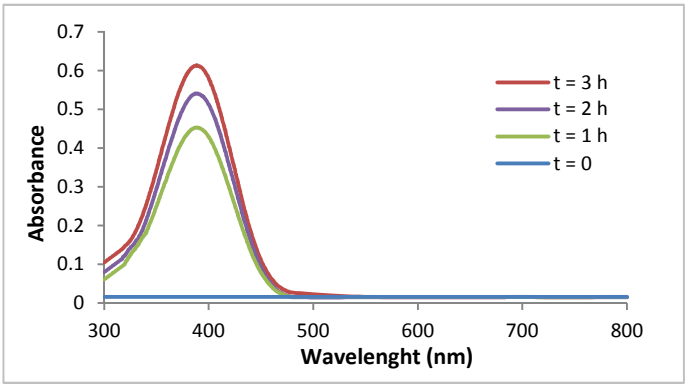

Figure 4.7 Scanning profile of the tyrosinase-catalyzed end products of *para*-cresol 1 in CH_2Cl_2 at different time.

After this preparatory study, the optimal hydration condition was determined. Biocatalysts (2.7 μg Tyro^S, 30.0 mg Tyro^S/E or Tyro^S/E-LbL, 12.0 μg Tyro^E, 30.0 mg Tyro^E/E or Tyro^E/E-LbL) were suspended in Na-phosphate buffer (0.1 M, pH 7.0, 10.0-70.0 μL) and added to CH_2Cl_2 solution of *para*-cresol **1** (20 mM, 2.5 ml) at 25 °C. After 30 min, absorbance at 389 nm was read to determine tyrosinase activity (Table 4.6). From these data the correlation between the volume of buffer (μl) and the amount of free enzyme (μg) or the amount of resin beads (g) was found, as reported in Table 4.7. Data show that Tyro^S/E required more buffer per μg of enzyme (9.3 μL μg_{Tyro}^{-1}) respect to Tyro^E

(2.9 µL μg_{Tyro}^{-1}) to reach the highest value of activity (7587 U mg^{-1} for $Tyro^S$ and 1772 U mg^{-1} for $Tyro^E$). In the case of immobilized tyrosinases, a major amount of buffer (defined as µL per gram of support, µL g_{beads}^{-1}) was required in the presence of the polyelectrolyte layers [the optimal amount of buffer was 500 µL g_{beads}^{-1} for $Tyro^S$/E (2067 U g^{-1}_{beads}) and 1000 µL g_{beads}^{-1} for $Tyro^S$/E-LbL (1798 U g^{-1}_{beads}), while it was 1000 µL g_{beads}^{-1} for $Tyro^E$/E (420 U g^{-1}_{beads}) and 2000 µL g_{beads}^{-1} for $Tyro^E$/E-LbL (365 U g^{-1}_{beads}).

Table 4.6 Activity of commercial and extracted tyrosinase at different buffer concentrations.[a]

Buffer (µl)	Commercial Tyro activity			Extracted Tyro activity		
	$Tyro^S$ (U mg^{-1}_{Tyro})	*$Tyro^S$/E* (U g^{-1}_{beads})	*$Tyro^S$/E-LbL* (U g^{-1}_{beads})	*$Tyro^E$* (U mg^{-1}_{Tyro})	*$Tyro^E$/E* (U g^{-1}_{beads})	*$Tyro^E$/E-LbL* (U g^{-1}_{beads})
10	3508	1865	975	410	-	-
15	4112	**2067**	1106	524	104	-
20	6951	1905	1502	845	264	105
25	**7587**	1764	1654	1323	280	194
30	7434	1074	**1798**	1614	**420**	269
35	7312	970	1598	**1772**	340	290
45	4200	340	1065	1372	300	350
60	2010	210	980	650	184	**365**
70	1090	120	650	420	102	336

[a] One unit of enzyme activity was defined as the increase in absorbance of 0.001 at 389 nm and 25°C in a solution of CH_2Cl_2/Na-phosphate buffer 0.1 M, pH 7, using 2.69 µg $Tyro^S$, 12 µg $Tyro^E$ and 30 mg $Tyro^S$/E or $Tyro^S$/E-LbL or $Tyro^E$/E or $Tyro^E$/E-LbL. Each experiment was conducted in triplicate with an average errors of ± 2-3% for free enzymes and 4-5% for immobilized enzymes.

Table 4.7 Optimum buffer expressed as µL μg_{Tyro}^{-1} for free enzyme and µL g_{beads}^{-1} for immobilized enzyme.

Entry	Enzyme	Free Tyro (µL μg_{Tyro}^{-1})	Tyro/E (µl g_{beads}^{-1})	Tyro/E-LbL (µl g_{beads}^{-1})
1	$Tyro^E$	2.9	1000	2000
2	$Tyro^S$	9.3	500	1000

The kinetic parameters in CH_2Cl_2/buffer were determined in the selected case of $Tyro^S$ by measuring the tyrosinase activity at different concentrations of compound **1** (2-15 mM), using the amount of the buffer previously optimized. Measurements in buffer were also performed as references. As reported in Table 4.8, in the case of **1** the K_m of free and immobilized $Tyro^S$ was higher in buffer than in CH_2Cl_2, the $Tyro^S$/E showing the highest affinity for substrate in the organic solvent (Table 4.8, entry 2 versus entries 1 and 3).[36] This result showed that phenols concentration of 20 mM used in oxidative reactions are sufficient to achieve saturating condition. About the catalytic efficiency (V_{max}/K_m), free and immobilized $Tyro^S$ were more reactive in CH_2Cl_2 than in buffer, showing a significant value of the acceleration factor (defined as the ratio between V_{max}/K_m in CH_2Cl_2 and in buffer) in the range of 1.30-4.96.

Table 4.8 Kinetic parameters of free and immobilized Sigma Tyro (Tyro^S) using *para*-cresol as substrate.

Entry	Enzyme	V_{max} [a] ($x10^{-4}$)		K_m (mM)		V_{max}/K_m [b] ($x10^{-4}$)		Acceleration factor[c]
		CH_2Cl_2	*buffer*	*CH_2Cl_2*	*buffer*	*CH_2Cl_2*	*buffer*	
1	Free	350	410	1.50	8.60	233	47	4.96
2	Tyro/E	114	40	1.31	1.50	87	26	3.52
3	Tyro/E-LbL	45	60	3.40	6.00	13	10	1.30

[a] V_{max} was defined as ΔAbs min^{-1} μg_{enzyme}^{-1}; [b] V_{max}/K_m was defined as ΔAbs min^{-1} μg_{enzyme}^{-1} μM^{-1}. [c] Acceleration factor was defined as the ratio of V_{max}/K_m in CH_2Cl_2 to that in buffer. Each experiment was conducted in triplicate. Average errors in kinetic parameters were ± 2-4% for K_m and ± 1-3% for V_{max}.

Tyro^S/E was the most reactive immobilized system. These data are in accordance with the general effects showed by organic solvents on the magnitude of the acceleration factors for the oxidation of simple hydrophobic substrates.[8b-c] In fact, hydrophobic substrates are retained in the organic solvent with higher efficiency than in the buffer, thus less amount of substrate is available for the active site giving rise to a higher catalytic efficiency and acceleration factor.[9]

4.2.5 Oxidation of phenols

A panel of phenols (Figure 4.8) was oxidized, including *para*-cresol **1**, 4-ethyl phenol **2**, 4-*tert*-butyl phenol **3**, 4-*sec*-butyl phenol **4**, 4-methoxy phenol **5**, and 4-chloro phenol **6**; 4-chloro-2-methyl phenol **7**; *meta*-cresol **8** and bis(4-hydroxyphenyl)methane **9**.

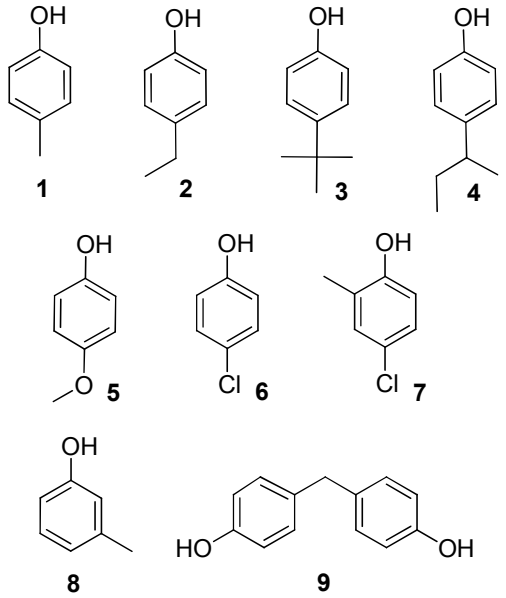

Figure 4.8 Phenols oxidized by free and immobilized tyrosinase.

As a general procedure the appropriate phenol (0.05 mmol), tyrosinases (in the range of 600-2400 U) and the optimal amount of the Na-phosphate buffer 0.1 M, pH 7.0 were placed in 2.5 mL of CH_2Cl_2 at 25°C, under O_2 in vigorous stirring. For insoluble aqueous phenols **3**, **4**, **9** substrates were dissolved in

CH_3CN (100.0 µL) and then added to CH_2Cl_2/buffer solutions. Reactions in aqueous system were carried out under similar experimental conditions. Initially we studied the oxidation of **1** with both free and immobilized tyrosinases. The oxidation of **1** (0.05 mmol) with Tyro^S (263 U) in CH_2Cl_2/buffer (2.5 mL/176 µL; pH 7.0) at room temperature under O_2 atmosphere for 18 h, afforded catechol **1a** as the main reaction product in 49% yield and 97% conversion of substrate, besides low amount of pyrogallol derivative **1b**. Dimers **1c-d**, characterized by the formation of C-C cross-linkage between two phenol units, were also detected in appreciable amount (Scheme 4.1, Table 4.9, entry 1).

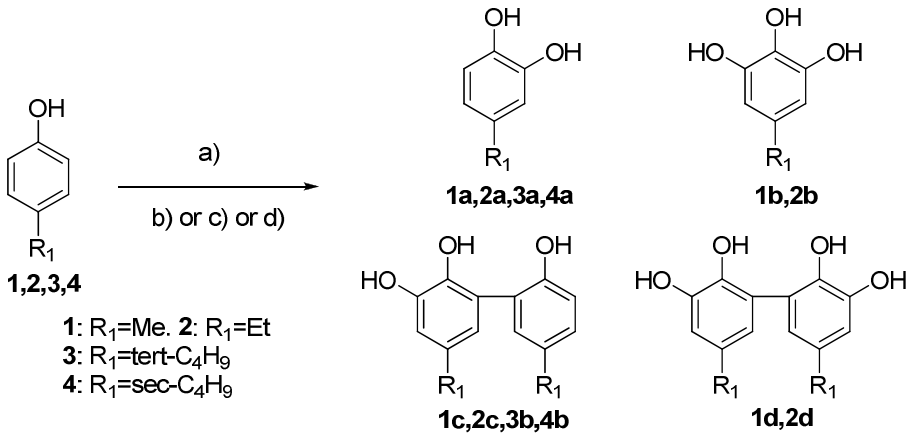

Scheme 4.1 Oxidation of phenols 1-4. ***Reagents and conditions:*** **a) Tyro-based systems, O_2; b) CH_2Cl_2/buffer; c) CH_2Cl_2/buffer/CH_3CN; d) buffer.**

Pyrogallol **1b** is a product of further oxidation of **1a**. Pyrogallol derivatives are potent antioxidants characterized by several biological activities.[37] In accordance with data reported in the literature, the formation of dimers **1c-d** can be ascribed to reactive *ortho*-quinones intermediates through a nonenzymatic mechanism, even if the occurrence of a radical mechanism involving a phenoxy radical intermediate generated by residual laccase activity, cannot be completely ruled out.[38] The oxidation of **1** (0.05 mmol) with Tyro^S/E (263 U) in CH_2Cl_2/buffer (2.5 mL/13µl; pH 7.0) at room temperature under O_2 atmosphere for 18 h afforded **1a** in 72% yield and 90% conversion of substrate. Again low amount of **1b** and **1c** was detected (Table 4.9, entry 2). About the effect of the LbL coating, compound **1a** was again obtained as the main reaction product by treatment of **1** with Tyro^S/E-LbL, in 78% yield and 85% conversion of substrate (Scheme 4.1, Table 4.9, entry 3). In homogeneous condition, catechol **1a** was recovered in lower yield when the same reaction was performed in buffer as reference (Table 4.9, entry 4 versus entry 1). In this latter case, a high amount of **1b** was obtained, compound **1d** being the only isolated dimer (Table 4.9, entry 4). The low mass balance of the reaction further suggests the formation of some over-oxidized products, not recovered under our experimental conditions. Even in heterogeneous conditions, tyrosinase was more selective in organic solvent than in buffer to afford catechol **1b** (Table 4.9, entries 5,6 versus 2,3).

Table 4.9 Oxidation of *para*-alkyl substituted phenols 1-2.[a]

Entry	Substrate	Biocatalysts	Products	Conversion (%)[b]	Yield (%)[b]
1	**1**	Tyro^S	**1a(1b)[1c]{1d}** [c]	97	49(4)[7]{25}
2	**1**	Tyro^S/E	**1a(1b)[1c]** [c]	90	72(7)[10]
3	**1**	Tyro^S/E-LbL	**1a[1c]** [c]	85	78[6]
4	**1**	Tyro^S	**1a(1b)[1d]** [c],[d]	95	22(10)[26]
5	**1**	Tyro^S/E	**1a(1b)[1c]{1d}** [d]	87	15(18)[27]{25}
6	**1**	Tyro^S/E-LbL	**1a(1b)[1c]{1d}** [d]	84	18(17)[25]{23}
7	**1**	Tyro^E	**1a(1b)[1c]{1d}**	89	60(10)[12]{7}
8	**1**	Tyro^E/E	**1a(1b)[1c]**	91	53(25)[12]
9	**1**	Tyro^E/E-LbL	**1a(1b)**	98	67(29)
10	**1**	Tyro^E	**1a(1b)[1c]** [d]	90	19(39)[30]
11	**1**	Tyro^E/E	**1a(1b)[1c]{1d}** [d]	89	13(19)[31]{26}
12	**1**	Tyro^E/E-LbL	**1a(1b)[1c]{1d}** [d]	91	15(19)[31]{26}
13	**2**	Tyro^S	**2a(2b)** [c]	70	58(9)
14	**2**	Tyro^S	**2a(2b)[2c]{2d}** [c],[d]	90	18(15)[33]{19}
15	**2**	Tyro^E	**2a(2b)**	73	60(10)
16	**2**	Tyro^E/E	**2a(2b)**	91	67(8)
17	**2**	Tyro^E/E-LbL	**2a(2b)**	98	84(12)
18	**2**	Tyro^E	**2a(2b)[2c]{2d}**[d]	92	15(11)[30]{15}
19	**2**	Tyro^E/E	**2a(2b)[2c]** [d]	92	36(42)[14]
20	**2**	Tyro^E/E-LbL	**2a(2b)[2c]{2d}**[d]	92	18(16)[28]{16}

[a] Reaction conditions: substrate (0.05 mmol) and tyrosinase (263 U) were taken in 2.5 mL of CH_2Cl_2/buffer for 24 h; [b] Conversion and yield were calculated by GC-MS analysis using dodecane as internal standard; [c] Oxidation performed in 18 h; [d] Oxidation performed in buffer as reference.

Note that, in several of the cases studied, the reactivity and selectivity of tyrosinase was found to be increased after the immobilization, suggesting a beneficial effect of the support and of the LbL coating on the activity and selectivity of the catalyst (Table 4.9, entries 2,3 versus entry 1). The oxidation of **1** with Tyro^E was performed under similar experimental conditions using higher reaction time (24 h) to afford **1a** in 60% yield and 89% conversion of substrate, besides low amount of **1b** and of dimers **1c-d** (Scheme 4.1, Table 4.9, entry 7). Tyro^E/E-LbL showed a slightly higher reactivity than Tyro^E/E affording **1a** as the main reaction product in 67% yield (Table 4.9, entries 9 and 8). In both cases **1b** was obtained in significant amount suggesting a high reactivity of the catalytic systems. Since there are only few chemical procedures available to synthesize pyrogallol derivatives, the use of immobilized tyrosinase open a possible new synthetic entry to this family of compounds.[39] In a similar way, extracted tyrosinase showed a lower selectivity in homogeneous than in heterogeneous conditions performing the oxidation in buffer, in which cases **1b** and **1c** became the main reaction products (Table 4.9, entry 10-12). These first analyses demonstrated as Tyro^S and Tyro^E showed a similar selectivity for compound **1** under both homogeneous and heterogeneous conditions. For successive oxidations, the comparison between commercial and extracted tyrosinases was first conducted in homogeneous condition; if the enzyme selectivity was confirmed for the substrates, then it would

have been used the low price $Tyro^E$/E and $Tyro^E$/E-LbL as the only heterogeneous catalysts. The oxidation of **2** with $Tyro^S$ showed a higher selectivity in CH_2Cl_2/buffer than in buffer alone to afford catechol **2a** (58% yield), further confirming the benign role of the organic solvent to inhibit the dimerization processes that are operative in aqueous medium (Scheme 4.1, Table 4.9, entry 13 versus 14). Pyrogallol **2b** was isolated in low yield. Similar behaviour was shown by $Tyro^E$ (**2a** in 60% yield and **2b** in 10% yield), confirming that two tyrosinases had the same selectivity, although the oxidations with $Tyro^E$ were conducted in 24 hours (Table 4.9, entry 15). Noteworthy, the highest yield of catechol for immobilized systems was obtained with $Tyro^E$/E-LbL where **2a** was isolated in 84% yield besides to pyrogallol **2b** (Table 4.9, entry 17 versus 16). According to previous results, oxidation of **2** was more selective in CH_2Cl_2/buffer than in aqueous medium (Table 4.9, entries 18-20 versus 15-17). The efficacy of Tyro-based systems in the oxidation of *para*- alkyl substituted phenols decreased by increasing the steric hindrance of the substituent, as evaluated in the case of bulky substituted compounds **3** and **4**. Irrespective to experimental conditions, a relatively low conversion of substrate was observed to yield the corresponding catechols **3a** and **4a** as the only recovered product. In these latter cases, oxidations were performed with twice amount of tyrosinases (526 U) in the presence of a low amount of CH_3CN (100.0 µl) to increase the solubility of substrates. Again, $Tyro^E$/E and $Tyro^E$/E-LbL were the best catalysts (with the only exception of phenol **4**) (Scheme 4.1, Table 4.10, entries 1-16). Oxidations performed in buffer/CH_3CN showed high conversion (58-63%) of substrate but a low selectivity, affording dimers as the main products (Table 4.10, entries 1-16).

Table 4.10 Oxidation of *para*-alkyl substituted phenols 3-4.[a]

Entry	Substrate	Biocatalysts	Products	Conversion (%) [b]	Yield (%) [b]
1	**3**	$Tyro^S$	**3a**	22	22
2	**3**	$Tyro^S$	**3a(3b)**[c]	63	10(48)
3	**3**	$Tyro^E$	**3a**	21	21
4	**3**	$Tyro^E$/E	**3a**	37	37
5	**3**	$Tyro^E$/E-LbL	**3a**	39	39
6	**3**	$Tyro^E$	**3a(3b)**[c]	62	10(46)
7	**3**	$Tyro^E$/E	**3a(3b)**[c]	58	12(44)
8	**3**	$Tyro^E$/E-LbL	**3a(3b)**[c]	60	14(40)
9	**4**	$Tyro^S$	**4a**	39	38
10	**4**	$Tyro^S$	**4a**[c]	44	8(34)
11	**4**	$Tyro^E$	**4a**	37	37
12	**4**	$Tyro^E$/E	**4a**	55	44
13	**4**	$Tyro^E$/E-LbL	**4a**	36	36
14	**4**	$Tyro^E$	**4a(4b)**[c]	42	8(30)
15	**4**	$Tyro^E$/E	**4a(4b)** [c]	41	10(29)
16	**4**	$Tyro^E$/E-LbL	**4a(4b)** [c]	40	14(24)

[a] Reaction conditions: substrate (0.05 mmol, dissolved in 100.0 µl CH_3CN), and tyrosinase (526 U) were taken in 2.5 mL of CH_2Cl_2/buffer for 48 h; [b] Conversion and yield were calculated by GC-MS analysis using dodecane as internal standard; [c] Oxidation performed in buffer/CH_3CN as reference.

The low conversion of **3** and **4** in organic solvent medium are in accordance with previously reported kinetic data; the low reactivity of bulky phenols is correlated with the reduction of conformational flexibility, caused by the hydrophobic solvent that restricts the access of substrate at the active site of enzyme.[9] This high selectivity was further confirmed in the oxidation of 4-methoxy phenol **5** bearing an electron donating group in the *para*-position of the aromatic ring. Even for compound **5**, Tyro^{E} and Tyro^{S} showed similar behaviour, with higher selectivity in organic solvent than in buffer (Scheme 4.2, Table 4.11, entries 1-4).

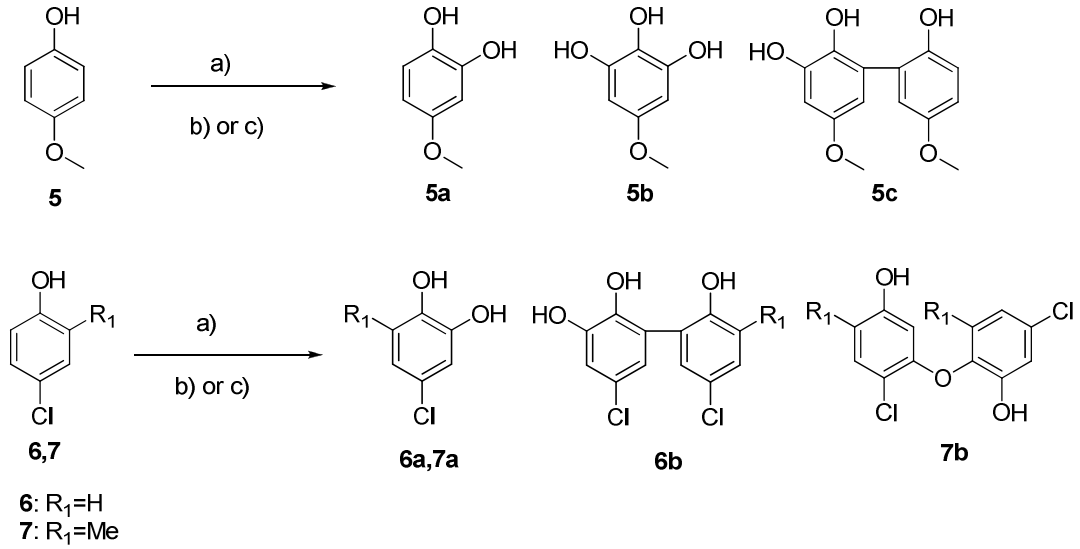

Scheme 4.2 Oxidation of phenols 5-7. ***Reagents and conditions:*** **a) Tyro-based systems, O_2; b) CH_2Cl_2/buffer; c) buffer.**

Both Tyro^{E}/E and Tyro^{E}/E-LbL afforded catechol **5a** as the main reaction in 77 and 60% yield, respectively, besides to minor amount of pyrogallol **5b** and dimer **5c** (Table 4.11, entries 5,6 versus 7,8). As showed for previous compounds, immobilized systems were more selective than Tyro^{E} (Table 4.11, entries 3-5). Reactions performed in buffer afforded again dimeric compounds as the main products (Table 4.11, entries 7,8). A similar reaction pathway was observed in the oxidation of 4-chloro phenol **6**, where the catechol **6a** was the only recovered product in organic solvent medium, with the exception of Tyro^{E}/E where a low amount of **6b** was also detected (Scheme 4.2, Table 4.11, entries 9-12). The highest yield of **6a** was again obtained with Tyro^{E}/E-LbL (Table 4.11, entry 15). In buffer medium dimer **6b** was the main reaction product (Table 4.11, entries 13-16). On the other hand, in CH_2Cl_2/buffer 4-chloro-2-methyl phenol **7** showed a low reactivity toward Tyro^{E} and Tyro^{S} to afford **7a** in negligible yield and conversion of substrate, probably due to the steric encumbering of the *ortho*-substituent7 (Scheme 4.2, Table 4.11, entries 17,18). In buffer medium, dimer **7b** were detected as the main product (Table 4.11, entries 19,20). This compound was characterized by the formation of C-O-C cross-linkage, ascribing to reactive *ortho*-quinones intermediates through a nonenzymatic mechanism or phenoxy radical mechanism generated by residual laccase activity.[38]

Table 4.11 Oxidation of phenols 5-7. [a]

Entry	Substrate	Biocatalysts	Products	Conversion (%)[b]	Yield (%)[b]
1	**5**	$Tyro^S$	**5a(5b)[5c]**	99	35(23)[31]
2	**5**	$Tyro^S$	**5a(5b)[5c]** [c]	96	17(28)[51]
3	**5**	$Tyro^E$	**5a(5b)[5c]**	99	37(12)[41]
4	**5**	$Tyro^E$	**5a(5b)[5c]** [c]	97	15(30)[49]
5	**5**	$Tyro^E$/E	**5a(5c)**	99	77(21)
6	**5**	$Tyro^E$/E-LbL	**5a(5b)**	99	60(38)
7	**5**	$Tyro^E$/E	**5a(5b)[5c]** [c]	96	19(34)[41]
8	**5**	$Tyro^E$/E-LbL	**5a(5b)[5c]** [c]	95	20(36)[39]
9	**6**	$Tyro^S$	**6a**	75	74
10	**6**	$Tyro^E$	**6a**	73	73
11	**6**	$Tyro^E$/E	**6a(6b)**	75	63(11)
12	**6**	$Tyro^E$/E-LbL	**6a**	93	75
13	**6**	$Tyro^S$	**6a(6b)** [c]	80	20(56)
14	**6**	$Tyro^E$	**6a(6b)** [c]	76	22(54)
15	**6**	$Tyro^E$/E	**6a(6b)** [c]	74	19 (54)
16	**6**	$Tyro^E$/E-LbL	**6a(6b)** [c]	73	20(50)
17	**7**	$Tyro^S$	**7a**	>5	traces
18	**7**	$Tyro^E$	**7a**	>5	traces
19	**7**	$Tyro^S$	**7a(7b)** [c]	45	5(30)
20	**7**	$Tyro^E$	**7a(7b)** [c]	30	6(21)

[a] Reaction conditions: substrate (0.05 mmol) and tyrosinase (263 U) were taken in 2.5 mL of CH_2Cl_2/buffer for 24 h; [b] Conversion and yield were calculated by GC-MS analysis using dodecane as internal standard; [c] Oxidation performed in buffer as reference.

The inhibition effect was not observed in CH_2Cl_2/buffer in the case of 3-methyl phenol **8**. In this latter case, the catechol **1a** was isolated in 62-86% yield and quantitative conversion of substrate, $Tyro^E$/E-LbL being the best catalyst (Scheme 4.3, Table 4.12, entries 1-7). Pyrogallol **1b** was obtained as by-product in low yield. Finally, we evaluated the oxidation of a diphenyl methane derivative, the bis(4-hydroxyphenyl)methane **9**. The reaction proceeded with high conversion of substrate to afford selectively the mono-catechol derivative **9a** in the presence of traces of bis-catechol **9b** (only identified by GC-MS analysis; Scheme 4.3, Table 4.12, entries 9-12); a low amount of CH_3CN (100.0 µl) was required to increase the solubility of **9**. In the case of oxidations performed in aqueous medium the low mass balance of the reaction suggests the formation of unrecovered over-oxidized products (Table 4.12, entries 13-16). $Tyro^E$ and immobilized tyrosinases showed a similar reactivity. This transformation is of synthetic interest because polyhydroxylated diphenylmethane derivatives are characterized by antiviral,[40] antioxidant,[41] and antimicrobial activities.[42]

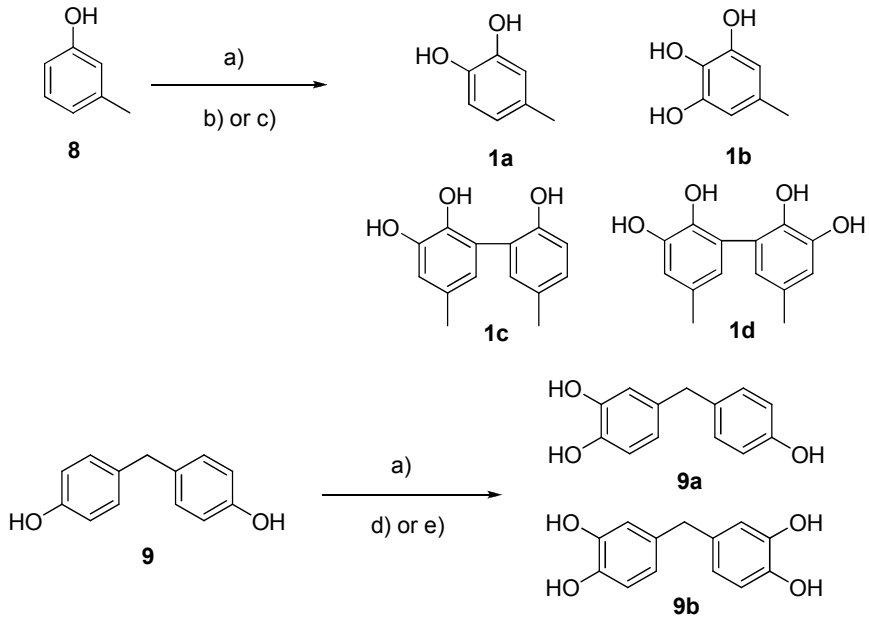

Scheme 4.3 Oxidation of phenols 8-9. ***Reagents and conditions:*** **a) Tyro-based systems, O_2; b) CH_2Cl_2/buffer; c) buffer; d) CH_2Cl_2/buffer/CH_3CN; e) buffer/CH_3CN.**

Table 4.12 Oxidation of phenols 8-9. [a]

Entry	Substrate	Biocatalysts	Products	Conversion (%)[b]	Yield (%)[b]
1	**8**	$Tyro^S$	**1a**	92	74
2	**8**	$Tyro^E$	**1a**	94	62
3	**8**	$Tyro^E$/E	**1a(1b)**	98	84(13)
4	**8**	$Tyro^E$/E-LbL	**1a(1b)**	98	86(11)
5	**8**	$Tyro^S$	**(1c)[1d]** [c], [d]	37	(20)[14]
6	**8**	$Tyro^E$	**1a(1c)[1d]** [c], [d]	35	6(10)[18]
7	**8**	$Tyro^E$/E	**1a(1c)[1d]** [c], [d]	32	6(10)[24]
8	**8**	$Tyro^E$/E-LbL	**1a(1c)(1d)** [c], [d]	30	6(8)[15]
9	**9**	$Tyro^S$	**9a(9b)** [e]	83	79(3)
10	**9**	$Tyro^E$	**9a(9b)** [e]	82	78(4)
11	**9**	$Tyro^E$/E	**9a(9b)** [e]	82	78(3)
12	**9**	$Tyro^E$/E-LbL	**9a(6b)** [e]	77	74(3)
13	**9**	$Tyro^S$	**9a(9b)** [f]	80	58(10)
14	**9**	$Tyro^E$	**9a(9b)** [f]	80	54(15)
15	**9**	$Tyro^E$/E	**9a(9b)** [f]	70	40(16)
16	**9**	$Tyro^E$/E-LbL	**9a(9b)** [f]	75	38(18)

[a] Reaction conditions: substrate (0.05 mmol) and tyrosinase (263 U) were taken in 2.5 mL of CH_2Cl_2/buffer for 24. [b] Conversion and yield were calculated by GC-MS analysis using dodecane as internal standard; [c] Oxidation performed with 526 U of tyrosinase; [d] Oxidation performed in buffer as references; [e] Oxidation performed in CH_2Cl_2/buffer/CH_3CN; [f] Oxidation performed in buffer/CH_3CN as reference.

With the aim to evaluate the reusability of immobilized tyrosinases *para*-cresol **1** was selected as representative phenol derivative. Compound **1** (0.05 mmol) was oxidized with immobilized tyrosinase systems (263 U) ($Tyro^S$/E, $Tyro^S$/E-LbL, $Tyro^E$/E, $Tyro^E$/E-LbL) in CH_2Cl_2/buffer medium under previously reported experimental conditions. The oxidations were followed spectrophotometrically at 389 nm.

After 30 min, the immobilized biocatalyst was recovered, washed and reused with fresh added substrate. For successive runs, the enzyme activity measured in the first oxidation was used as the reference value. One unit activity (U) was defined as the increase in absorbance of 0.001 at 389 nm, 25°C, in CH_2Cl_2/Na-phosphate buffer 0.1 M at pH 7.0. Recycling in organic medium was compared to aqueous one. As shown in Table 4.13, the immobilized Tyro^S systems retained a significant activity after 5 runs, that was higher in CH_2Cl_2/buffer medium than in aqueous medium (Table 4.13, entries 1-5). Moreover, the presence of the polyelectrolyte coating further stabilized the enzyme (Table 4.13, column 1 versus column 2).

Table 4.13 Reusability of Tyro-immobilized systems. [a]

Number of reuse	Tyro^S/E		Tyro^S/E-LbL		Tyro^E/E		Tyro^E/E-LbL	
	CH_2Cl_2	*buffer*	*CH_2Cl_2*	*buffer*	*CH_2Cl_2*	*buffer*	*CH_2Cl_2*	*buffer*
1	84	72	86	74	88 [b]	68	90	70
2	70	38	79	54	79	52	81	60
3	50	12	59	23	55	20	62	27
4	39	8	47	10	41	9	45	10
5	32	4	37	7	32	3	38	5

[a] Reusability is expressed as percentage of activity in each runs respect to that measured in the first reference oxidation.

Similar results were obtained with Tyro^E-based systems (Table 4.13, entries 1-5, columns 3-4). Thus, as a general trend, LbL based biocatalysts were more stable and maintained higher activity with respect to Eupergit®C250L systems. This behaviour suggests that microcapsules create an internal microenvironment able to protect the enzyme from denaturing agents.[43] Moreover, microcapsules may keep water inside, ensuring hydration required for enzyme activity and stability.[44]

4.3 Conclusions

Tyrosinase showed to be an efficient catalyst for the oxidation of phenols to corresponding catechols in organic medium and mild experimental conditions. The enzyme retained the catalytic activity and selectivity after immobilization on Eupergit®C250L and successive coating by LbL technique. Even if the free enzymes afford better kinetic parameters, in some of the cases studied, immobilized systems were more selective than parent enzyme to yield catechols, suggesting a stabilization effect exerted by the support. This pattern was further remarked by recycling experiments which showed that the best stabilization effect was in the presence of the polyelectrolyte coating. Moreover, the immobilized systems were more stable in organic medium than in water. It is well known that polyelectrolytes can influence the activity of oxidative enzymes, for example by acting as surfactants or stabilizing the enzyme in a right conformation.[45] These effects can be further modulated by the

presence of organic solvent. Although the mechanism by which polyelectrolytes PSS and PAH may affect the selectivity of tyrosinase was not studied in detail, in agreement with data previously reported in the literature, it is reasonable to suggest that they may inhibit the dimerization of quinones formed by secondary processes.[46] About the structure activity relationships, *para*-substituted phenols with small electron releasing group were efficiently oxidized (**1, 2, 5** and **6**) affording catechol as mainly recovered product beside to small amount of pyrogallol derivative. Conversely, in the presence of bulky substituent (**3** and **4**) the catalytic efficiency of tyrosinase was very low, requiring twice amount of enzyme to yield the corresponding catechols in high yield. No reactivity was observed in the case of *ortho*-substituted phenols (**7**). This inhibition effect was probably due to a steric encumbering of the *ortho*-substituent for the formation of the first intermediate ($E_{oxy}M$) in the catalytic cycle of tyrosinase. As general trend, in organic solvent medium, tyrosinase exhibited a substrate structure-dependent reactivity similar to that described in Chapter 3 for aqueous biotransformations in reducing conditions. Moreover, both systems, aqueous and biphasic one, allowed to oxidize phenols to the corresponding catechols with high selectivity and conversion of substrates, reducing the formation of dimers and brown pigments that were obtained as main product when reactions were conducted in buffer. Differences between the two types of biotransformations solely concern the reduction of conformational flexibility of tyrosinase observed in biphasic medium. The hydrophobic solvent, in fact, restricts the access of bulky-substituted compounds at the active site of enzyme, thus influencing the reactivity of tyrosinase that was affected by the chemical structure of the substrate.[9] On the other hand, the organic solvent granted the oxidations of hydrophobic or low soluble phenols that would not be performed in water. For this reason, the choice between two systems depends on the chemical properties of substrates: phenols with high steric encumbrance can be efficiently oxidized in aqueous medium, while small and apolar compounds in organic one.

4.4 Experimental Section

Mushroom tyrosinase was either purchased from Sigma-Aldrich ($Tyro^S$) or extracted ($Tyro^E$) from *A. bisporous*. Eupergit®C250L, poly(sodium 4-styrenesulfonate) (PSS, MW 70000), poly(allylamine hydrochloride) (PAH, MW 56000), L-tyrosine (L-Tyr), 2,2'-azino-bis(3-ethylbenzthiazoline-6-sulphonic acid) (ABTS), bovine serum albumin (BSA), ammonium sulphate ($(NH_4)_2SO_4$), dichloromethane (CH_2Cl_2), ethyl acetate (EtOAc), petroleum ether (EtP), acetonitrile (CH_3CN), sodium sulphite (Na_2SO_3), sodium sulphate anhydrous (Na_2SO_4), dodecane, pyridine, hesamethyldisilazane (HMDS), trimethylchlorosilane (TMCS) and phenols were purchased from Sigma-Aldrich. Water used during extraction was degassed and stored at 4°C until use. All spectrophotometric measurements were

made with a Varian Cary50 UV-Vis spectrophotometer equipped with a single cell peltier thermostatted cell holder. Dichloromethane was dried on anhydrous sodium sulphate prior to use. All experiments were carried out in triplicate using free and immobilized Sigma-Aldrich tyrosinase ($Tyro^S$) and free and immobilized extracted tyrosinase ($Tyro^E$) in dichloromethane/buffer system and in aqueous medium. Buffer used was a sodium phosphate buffer (Na-phosphate) pH 7.0, 0.1 M.

4.4.1 Extraction of tyrosinase

The mushroom tyrosinase was partially purified from commercial *Agaricus bisporus* using two procedures with slight modifications.[23,24] In the first extraction procedure, 3.0 kg of fresh mushroom were frozen at -20°C at least one day and then lyophilized. The obtained 210.0 mg of lyophilized-ground mushroom were added to 5.6 ml of a 30 mM aqueous solution of *para*-nitrophenol (PNP) (pH 7.0) and magnetically stirred for 30 min at 4 °C. The extraction medium was centrifuged at 6000 rpm for 5 min and the solution obtained was first subjected to ammonium sulphate [$(NH_4)_2SO_4$] precipitation (35-70%) and then dialyzed against water. In the second extraction procedure, the sporocarps were cleaned to remove earthy residues and then washed with 20 mM ascorbic acid maintained at 4°C. After they had been dried, the sporocarps were sliced and frozen at -20°C at least 1 day before extraction. 1.0 kg of frozen sporocarp was homogenized twice in 1.2 L of acetone at -20°C in a blender for 1 min. The obtained solid pulp was filtered through a Buchner funnel and homogenized with 1.0 L of 30%v/v acetone in water for 2-3 min. The mixture was centrifuged at 9000xg for 20 min. To the supernatant, 1.5 volumes of acetone at -20°C were added dropwise under vigorous stirring. The mixture was allowed to settle at 4°C for 2-3 h; most of the supernatant fluid was decanted and discarded, the remainder was centrifuged and the precipitate was dissolved in water and subjected to precipitation with calcium acetate 1% of saturation. The turbid mixture was frozen at -20°C. Samples obtained from several days were stored frozen at this stage. They were then thawed, mixed and centrifuged. Ammonium sulphate powder ($(NH_4)_2SO_4$) was added to the collected supernatant to make a 35% saturated solution. The resulting solution was allowed to stand for 30 min at 4°C and centrifuged at 9000xg for 20 min. $(NH_4)_2SO_4$ was added to supernatant to make a 70% saturated solution. The solution was allowed to stand for 2 h at 4°C and centrifuged. The precipitate was dissolved in a minimal volume of cold water and then dialyzed against water and concentrated by means of Vivaflow®50 equipped with a polyethersulfone (PES) membrane (10000 MWCO). The resulting enzyme solution was lyophilized and stored at -20°C.

4.4.2 Tyrosinase immobilization on Eupergit®C250L

The enzyme immobilization was performed as reported in Chapter 3.[29a-b] Dry Eupergit®C250L (1.0 gr) was added to Na-phosphate buffer 0.1 M, pH 7.0 (8.0 ml) containing tyrosinase (5.0 mg, 69405 U for $Tyro^S$ and 12840 U for $Tyro^E$) for 24 h. At the end of the coupling period, the beads were filtered and washed (5 x 8 ml) with Na-phosphate buffer 0.1 M, pH 7.0. The obtained beads were incubated with glycine (3.0 M) for 2 h to block residual epoxy groups,[47] then washed with buffer and finally air-dried and stored at 4°C. The amount in milligrams and the units of coupled tyrosinase ($Tyro^S$/E and $Tyro^E$/E, respectively) were calculated by the difference between the amount/units loaded and that recovered in the washings by conventional Bradford and activity assay.

4.4.3 Tyrosinase immobilization on Eupergit®C250L covered with Layer-by-Layer method

Both $Tyro^S$/E and $Tyro^E$/E, synthesized as described above, were coated with the Layer-by-Layer method (LbL) by a modification of literature procedures.[48] Briefly, PAH and PSS solutions (2 mg ml^{-1} in 0.5 M NaCl) were alternately added to Eupergit®-supported tyrosinase: each polyelectrolyte layer was adsorbed for 20 min at room temperature with orbital shaking and then washed with 0.5 M NaCl. The pH of the PAH solution was adjust to 6.5, ensuring the protonation of more than 90% of the amino groups (NH_3^+ form).[49] The deposition of polyelectrolytes was repeated three times (in the sequence PAH-PSS-PAH) and the obtained immobilized tyrosinases ($Tyro^S$/E-LbL and $Tyro^E$/E-LbL) were air-dried and stored at 4°C.

4.4.4 Determination of protein concentration

Protein concentration was determined spectrophotometrically at 595 nm according to the Bradford method using bovine serum albumin (BSA) as a standard.[25]

4.4.5 Activity assay

Tyrosinase assay was performed by the dopachrome method as previously described.[24] Briefly, 1.0 mL of 2.5 mM of L-Tyr solution in water was mixed with 1.9 mL of Na-phosphate buffer 0.1 M, pH 7.0 and incubated at 25°C for 10 min. Then, an appropriate amount of free or immobilized enzyme in 100.0 µl of Na-phosphate buffer was added to the mixture and the initial rate was immediately measured as linear increase in optical density at 475 nm, due to dopachrome production. One unit of enzyme activity was defined as the increase in absorbance of 0.001 per minute at pH 7.0, 25°C in a 3.0 mL reaction mixture containing 0.83 mM of L-Tyr and 67 mM of Na-phosphate buffer pH 7.0. To evaluate the contaminant laccase in enzyme preparation, the laccase activity was determined spectrophotometrically using 2,2'-azino-bis(3-ethylbenzthiazoline-6-sulphonic acid) (ABTS) as the

substrate.[27] The assay mixture contained 0.5 mM ABTS, Na-phosphate buffer 0.1 M, pH 7.0 and the enzyme was incubated at 25°C. The oxidation was followed by an absorbance increase at 415 nm for 1 min. One activity unit was defined as the amount of enzyme that oxidised 1 μmol_{ABTS}/min.

4.4.6 Optimization of water requirement

Para-cresol **1** was used as standard phenolic substrate.[15b] Compound **1** (5.0 mg, 0.05 mmol), the biocatalysts (2.7 μg $Tyro^S$, 30.0 mg $Tyro^S$/E or $Tyro^S$/E-LbL, 12 μg $Tyro^E$, 30.0 mg $Tyro^E$/E or $Tyro^E$/E-LbL) and CH_2Cl_2 (2.5 mL) were placed in vials at 25°C under O_2, and Na-phosphate buffer 0.1 M, pH 7.0 (in the range of 10.0-70.0 μL) was added. The reaction mixture was vigorously stirred for 30 min. Every 15 min, aliquots were removed and their absorbance at 389 nm due to *ortho*-quinone produced were measured and returned to the vials as rapidly as possible. One unit of enzyme activity was defined as the increase in absorbance of 0.001 at 389 nm, 25°C, CH_2Cl_2 and Na-phosphate buffer 0.1 M, pH 7.0.

4.4.7 Kinetic assay

Kinetic parameters (K_m, V_{max} and V_{max}/K_m) were determined by measuring enzyme activity at different concentrations of substrate and plotting data to a double reciprocal plot (Lineweaver–Burk plot).[28] Studying the catalytic properties of enzymes in the organic solvent media, reactions were carried out by means of the same procedure as for the optimization of hydration described above, using different concentrations of *para*-cresol **1** (in the range of 2-15 mM) and optimum of aqueous buffer. Absorbance was measured at 389 nm as described above. Reactions in aqueous system were carried out under similar experimental conditions.[5] To compare the catalytic properties of commercial and extracted tyrosinase, reactions were carried out by means of the same procedure as for the activity assay, using different concentrations of L-Tyr (330-1000 μM) and 53.0 μg of $Tyro^S$ and $Tyro^E$ and 88.0 μg of immobilized commercial and extracted tyrosinases. Absorbance was measured at 475 nm as described above.

4.4.8 Scanning Electron Microscopy (SEM) measurements

Samples were prepared at the Interdepartmental Centre of Electron Microscopy, Tuscia University, Viterbo, Italy, using conventional procedures. For Scanning Electron Microscopy (SEM), samples were sputter-coated with gold in a Balzers MED 010 unit and observed with a JEOL JSM 5200 electron microscope. Micrographs were taken by a Mamiya camera applied to the microscope using TMAX 100 ASA films.

4.4.9 Enzyme recycling

Immobilized enzymes were recycled as follow: 5.0 mg of *para*-cresol, 10.0 mg of immobilized Tyro, optimal buffer and 2.5 mL of CH_2Cl_2 were placed in vials at 25°C under O_2. The reaction mixture was vigorously shaken for 30 min. Every 15 min, aliquots were removed to measure their absorbance at 389 nm and returned to the vials as rapidly as possible. After 30 min the biocatalyst was washed, recycled and reused again. Reactions in aqueous system were carried out under similar experimental conditions. For each run, tyrosinase activity was expressed as relative percentage activity respect to that at first run.

4.4.10 Phenols oxidation. General procedure

A large panel of phenols (Figure 4.8) have been oxidized, including *para*-mono substituted phenols *para*-cresol **1**, 4-ethyl phenol **2**, 4-*tert*-butyl phenol **3**, 4-*sec*-butyl phenol **4**, 4-methoxy phenol **5**, and 4-chloro phenol **6**; *ortho*, *para*-disubstituted phenol 4-chloro-2-methyl phenol **7**; *meta*-substituted phenol *meta*-cresol **8** and the bisphenol methane derivative bis(4-hydroxyphenyl)methane **9**. The reactions were performed under both homogeneous and heterogeneous conditions in CH_2Cl_2/buffer and in aqueous system as reference. As a general procedure the appropriate phenol (0.05 mmol), tyrosinases (in the range of 600-2400 U) and the optimal amount of the Na-phosphate buffer 0.1 M, pH 7.0 were placed in 2.5 mL of CH_2Cl_2 at 25°C, under O_2 in vigorous stirring. For insoluble aqueous phenols **3**, **4**, **9** substrates were dissolved in CH_3CN (100.0 µL) and then added to CH_2Cl_2/buffer solutions. Reactions in aqueous system were carried out under similar experimental conditions. The reaction was monitored by thin layer chromatography (TLC). After the disappearance of the substrate, different work-up procedures were used depending on the reaction conditions. In the case of organic medium, the enzyme was recovered by decantation (free enzymes) or filtration (immobilized enzymes) and the organic layer was treated with an equal volume of sodium sulphite solution 1% w/w to reduce benzoquinones to catechols.[5] The mixture was stirred for 5 min and the phases were separated. The aqueous phase was acidified with HCl 1.0 N and extracted twice with EtOAc. The organic extracts (CH_2Cl_2 and EtOAc) were treated with a saturated solution of NaCl and dried over anhydrous Na_2SO_4, then filtered and concentrated under vacuum to yield coloured crude. In the case of aqueous medium, sodium sulphite was added on reaction mixture and stirred for 5 min. Solution was then acidified with HCl 1.0 N, extracted twice with EtOAc and the organic phase treated as described above.

4.4.11 Identification and characterization of oxidative products

All products were identified by ^{1}HNMR, ^{13}CNMR and GC-MS. ^{1}HNMR and ^{13}CNMR were recorded on a Bruker 200 MHz spectrometer using $CDCl_3$ as solvent. All chemical shift are expressed in parts per million (δ scale). GC-MS analysis were performed on a 450GC-320MS Varian apparatus using a SPB column (25 m × 0.25 mm and 0.25 mm film thickness) and an isothermal temperature profile of 100°C for 2 min, followed by a 10 °C/min temperature gradient to 280°C for 25 min. The injector temperature was 280°C. Chromatography-grade hellum was used as the carrier gas with a flow of 1.0 mL/min. Mass spectra were recorded with an electron beam of 70 eV. Quantitative analyses were performed using dodecane as internal standard. For GC-MS analysis, the coloured residue obtained after extraction was treated with pyridine, HMDS and TMCS (HMDS:TMCS, 2:1 v/v) under vigorous stirring at room temperature for 30 min, then allowed to stand for 5 min.[50]

4-Methylcatechol (4-Methyl-1,2-benzenediol) (1a).

Oil. ^{1}HNMR[51] (200 MHz, $CDCl_3$) δ_H (ppm) 2.24 (3H, s, CH_3), 5.04 (1H, br. s., OH), 5.18 (1H, br. s., OH), 6.61- 6.76 (3H, m, Ph-H). ^{13}CNMR[51] (50MHz, $CDCl_3$) δ_C (ppm) 20.8 (CH_3), 115.3 (CH), 116.2 (CH), 121.5 (CH), 131.1 (C), 141.0 (C), 143.3 (C). *MS, (m/z):* 268 (M^+), 253 (M-CH_3), 238 [M-$(CH_3)_2$], 223 [M-$(CH_3)_3$], 195 [M-$Si(CH_3)_3$], 179 [M-$OSi(CH_3)_3$], 164 [M-$OSi(CH_3)_4$], 149 [M-$OSi(CH_3)_5$], 134 [M-$OSi(CH_3)_6$], 106 [M-$OSi_2(CH_3)_6$], 90 [M-$O_2Si_2(CH_3)_6$].

5-Methylpyrogallol (5-methyl-1,2,3-benzenetriol) (1b).

Oil. ^{1}HNMR[52] (200 MHz, $CDCl_3$) δ_H (ppm) 2.20 (3H, s, CH_3), 5.00 (s, 1H), 5.05 (s, 1H), 8.20 (3H, s, OH). ^{13}CNMR (50MHz, $CDCl_3$) δ_C (ppm) 22.1 (CH_3), 109.0 (2xCH), 131.2 (C), 137.1(C), 146.1 (2xC). *MS, m/z:* 356 (M^+), 341 (M-CH_3), 313]M-$(CH_3)_3$], 283 [M-$Si(CH_3)_3$], 267 [M-$OSi(CH_3)_3$], 252 [M-$OSi(CH_3)_4$], 237 [M-$OSi(CH_3)_5$].

Dimer (1c).

Oil. ^{1}HNMR (200 MHz, $CDCl_3$) δ_H (ppm) 2.19 (3H, s, CH_3), 2.42 (3H, s, CH_3), 6.51 (3H, b.s., OH), 6.61-7.12 (5H, m, Ph-H). ^{13}CNMR (50MHz, $CDCl_3$) δ_C (ppm) 16.0 (CH_3), 22.1 (CH_3), 116.6 (CH), 118.2 (CH), 122.0 (C), 125.6 (C), 127.0 (CH), 127.2 (C), 131.2 (CH), 133.1 (CH), 136.7 (C), 141.3 (C), 150.1 (C), 158.2 (C). *MS, m/z:* 446 (M^+), 431 (M-CH_3), 329 [M-$Si(CH_3)_3$], 313 [M-$OSi(CH_3)_3$], 298 [M-$OSi(CH_3)_4$], 268 [M-$OSi(CH_3)_6$], 180 [M-$O_2Si_2(CH_3)_6$].

5,5'-Dimethyl-[1,1'-Biphenyl]-2,2',3,3'-tetrol (1d).

Oil. ^{1}HNMR (200 MHz, $CDCl_3$) δ_H (ppm) 2.41 (6H, s, 2xCH_3), 6.62-6.91 (4H, m, Ph-H). ^{13}CNMR (50MHz, $CDCl_3$) δ_C (ppm) 22.1 (2xCH_3), 117.2 (2xCH), 122.1 (2xC), 132.0 (2xCH), 138.1 (2xC), 141.3 (2xC), 150.3 (2xC). *MS, m/z:* 534 (M^+), 519 (M-CH_3), 417 [M-$Si(CH_3)_3$], 401 [M-$OSi(CH_3)_3$], 386 [M-$OSi(CH_3)_4$], 371 [M-$OSi(CH_3)_5$], 268 [M-$O_2Si_2(CH_3)_6$].

4-Ethylcatechol (4-ethyl-1,2-Benzenediol) (2a).

Oil. ^{1}HNMR[53] (200 MHz, $CDCl_3$) δ_H (ppm) 1.04 (3H, m, CH_3), 2.36 (2H, m, CH_2), 6.00-7.25 (3H, m, Ph-H). ^{13}CNMR (50MHz, $CDCl_3$) δ_C (ppm) 15.2 (CH_3), 28.1 (CH_2), 116.5 (CH), 117.4 (CH), 124.2 (CH), 139.3 (C), 145.7 (C), 148.4 (C). *MS, m/z:* 282 (M^+), 267 (M-CH_3), 252 [M-$(CH_3)_2$], 237 [M-$(CH_3)_3$], 209 [M-$Si(CH_3)_3$], 193 [M-$OSi(CH_3)_3$], 179 [M-$OSi(CH_3)_4$], 164 [M-$OSi(CH_3)_5$], 148 [M-$OSi(CH_3)_6$], 120 [M-$OSi_2(CH_3)_6$].

5-Ethyl-1,2,3-Benzenetriol (2b).

Oil. ^{1}HNMR (200 MHz, $CDCl_3$) δ_H (ppm) 1.22 (3H, m, CH_3), 2.62 (2H, m, CH_2), 6.62 (2H, m, Ph-H), 8.14 (3H, b.s., OH). ^{13}CNMR (50MHz, $CDCl_3$) δ_C (ppm) 15.2 (CH_3), 29.3 (CH_2), 111.1 (2xCH), 136.2 (C), 138.0 (C), 142.3 (2xC). *MS, m/z:* 370 (M^+), 355 (M-CH_3), 282 [M-$OSi(CH_3)_3$], 267 [M-$OSi(CH_3)_5$], 251 [M-$OSi(CH_3)_6$], 209 [M-$O_2Si_2(CH_3)_6$], 194 [M-$O_2Si_2(CH_3)_9$].

Dimer (2c).

Oil. ^{1}HNMR (200 MHz, $CDCl_3$) δ_H 1.21 (3H, m, CH_3), 1.32 (3H, m, CH_3), 2.71 (2H, m, CH_2), 2.82 (2H, m, CH_2), 6.4-7.2 (5H, m, Ph-H). ^{13}CNMR (50MHz, $CDCl_3$) δ_C (ppm) 15.2 (CH_3), 15.7 (CH_3), 27.2 (CH_2), 28.3 (CH_2), 106.4 (C), 107.2 (C), 112.3 (CH), 114.1 (CH), 128.3 (C), 130.1 (CH), 134.1 (CH), 134.6 (C), 135.1 (C), 136.2 (CH), 143.1 (C), 155.2 (C). *MS, m/z:* 474 (M^+), 459 (M-CH_3), 429 (M-$CH_3)_3$, 341 [M-$OSi(CH_3)_3$], 326 [M-$OSi(CH_3)_4$], 311 [M-$OSi(CH_3)_5$].

5,5'-Diethyl-[1,1'-Biphenyl]-2,2',3,3'-tetrol (2d).

Oil. ^{1}HNMR (200 MHz, $CDCl_3$) δ_H (ppm) 1.22 (6H, m, 2xCH_3), 2.73 (4H, m, 2xCH_2), 6.4-7.2 (4H, m, Ph-H). ^{13}CNMR (50MHz, $CDCl_3$) δ_C (ppm) 15.6 (2xCH3), 28.3 (2xCH_2), 102.2 (2xC), 114.0 (2xCH), 134.3 (2xC), 136.1 (2xC), 138.3 (2xCH), 143.2 (2xC). *MS, m/z:* 562 (M^+), 517 (M-$CH_3)_3$, 489 [M-$Si(CH_3)_3$], 474 [M-$OSi(CH_3)_3$], 459 [M-$OSi(CH_3)_4$], 444 [M-$OSi(CH_3)_5$], 430 [M-$OSi(CH_3)_6$], 385 [M-$O_2Si_2(CH_3)_6$].

4-*tert*-Butylcatechol (4-tert-Butylbenzene-1,2-diol) (3a).

Oil. ^{1}HNMR (200 MHz, $CDCl_3$) δ_H (ppm) 1.33 (9H, s, CH_3), 6.63-7.11 (3H, m, Ph-H). ^{13}CNMR (50MHz, $CDCl_3$) δ_C (ppm) 31.2 (3xCH_3), 34.5 (C), 116.5 (CH), 116.9 (CH), 122 (CH), 144.3 (C), 146.2 (C), 147.1 (C). *MS, m/z:* 310 (M^+), 295 (M-CH_3), 280 [M-$(CH_3)_2$], 265 [M-$(CH_3)_3$], 237 [M-$Si(CH_3)_3$], 222 [M-$OSi(CH_3)_3$], 207 [M-$OSi(CH_3)_4$], 192 [M-$OSi(CH_3)_5$], 176 [M-$OSi(CH_3)_6$], 148 [M-$OSi_2(CH_3)_6$].

5,5'-bis(1,1-dimethylethyl)-[1,1'-Biphenyl]-2,2',3-triol (3b).

Oil. ^{1}HNMR (200 MHz, $CDCl_3$) δ_H (ppm) (200 MHz $CDCl_3$) δ (ppm) 1.20 (9H, s, CH_3), 1.22 (9H, s, CH_3), 6.51 (3H, s, OH), 6.68-7.47 (5H, m, Ph-H). ^{13}CNMR (50MHz, $CDCl_3$) δ_C (ppm) 31.2 (3xCH_3), 31.5 (3xCH_3), 34.5 (C), 35.9 (C) 116.5 (CH), 118.9 (CH), 122.7 (C), 127.4 (C), 128.5 (CH), 130.2 (CH), 131.7 (CH), 135.5 (C), 151.4 (C), 152.2 (C), 155.8 (C), 157.1 (C). *MS, m/z:* 472 (M^+), 442 [M-$(CH_3)_2$], 427 [M-$(CH_3)_3$], 399 [M-$Si(CH_3)_3$], 354 [M-$OSi(CH_3)_5$], 338 [M-$OSi(CH_3)_6$], 295 [M-$O_2Si_2(CH_3)_6$], 280 [M-$O_2Si_2(CH_3)_7$].

4-*sec*-Butylcatechol (4-(1-methylpropyl)-1,2-Benzenediol) (4a).

Oil. ^{1}HNMR (200 MHz, $CDCl_3$) δ_H (ppm) 1.10 (3H, m, CH_3), 1.22 (3H, m, CH_3), 1.53 (2H, m, CH_2), 3.23 (1H, m, CH), 6.52-6.84 (3H, m, Ph-H). ^{13}CNMR (50MHz, $CDCl_3$) δ_C (ppm) 11.2 (CH_3), 22.3 (CH_3), 31.2

(CH_2), 43.1 (CH), 113.3 (CH), 114.1 (CH), 124.4 (CH), 136.2 (C), 145.1 (C), 147.0 (C). *MS, m/z:* 310 (M^+), 295 (M-CH_3), 280 [M-$(CH_3)_2$], 237 [M-$Si(CH_3)_3$], 222 [M-$OSi(CH_3)_3$], 207 [M-$OSi(CH_3)_4$], 192 [M-$OSi(CH_3)_5$], 149 [M-$OSi_2(CH_3)_6$], 133 [M-$O_2Si_2(CH_3)_6$].

Dimer (4b)

Oil. ^{1}HNMR (200 MHz $CDCl_3$) δ (ppm) 1.09 (3H, m, CH_3), 1.12 (3H, m, CH_3), 1.21 (3H, m, CH_3), 1.32 (3H, m, CH_3), 1.52 (2H, m, CH_2), 1.63 (2H, m, CH_2), 3.09 (1H, m, CH), 3.21 (1H, m, CH), 6.6 (3H, s, OH), 6.8-7.5 (5H, m, Ph-H). ^{13}CNMR (50MHz $CDCl_3$) δ (ppm) 11.1 (2xCH_3), 21.9 (2xCH_3), 31.1 (2xCH_2), 43.5 (CH), 45.0 (CH), 115.7 (CH), 116.1 (CH), 121.6 (C), 126.1 (C), 130.5 (CH), 131.3 (CH), 134.7 (CH), 135.3 (C), 150.2 (C), 152.9 (C), 154.3 (C), 156.0 (C). *MS, m/z:* 458 (M^+), 443 (M-CH_3), 428 [M-$(CH_3)_2$], 340 [M-$OSi(CH_3)_5$], 324 [M-$OSi(CH_3)_6$], 281 [M-$O_2Si_2(CH_3)_6$], 265 [M-$O_2Si_2(CH_3)_7$].

4-Methoxycatechol (4-methoxy-1,2-Benzenediol) (5a).

Oil. ^{1}HNMR (200 MHz, $CDCl_3$) δ_H (ppm) 3.72 (3H, s, CH_3), 6.41-6.73 (3H, m, Ph-H), 6.94 (2H, b.s., OH). ^{13}CNMR (50MHz, $CDCl_3$) δ_C (ppm) 56.3 (CH_3), 101.4 (CH), 108.3 (CH), 115.6 (CH), 140.4 (C), 146.0 (C), 154.4 (C). *MS, m/z:* 284 (M^+), 269 (M-CH_3), 254 [M-$(CH_3)_2$], 239 [M-$(CH_3)_3$], 196 [M-$OSi(CH_3)_3$], 181 [M-$OSi(CH_3)_4$], 166 [M-$OSi(CH_3)_5$], 150 [M-$OSi(CH_3)_6$].

5-methoxy-1,2,3-Benzenetriol (5b).

Oil. ^{1}HNMR (200 MHz, $CDCl_3$) δ_H (ppm) 3.71 (3H, s, CH_3), 6.10 (2H, s, Ph-H), 9.11 (3H, b.s., OH). ^{13}CNMR (50MHz, $CDCl_3$) δ_C (ppm) 57.3 (CH_3), 95.2 (2xCH), 131.5 (C), 147.3 (2xC), 151.4 (C). *MS, m/z* : 372 (M^+), 357 (M-CH_3) 342 [M-$(CH_3)_2$], 255 [M-$Si(CH_3)_3$], 224 [M-$OSi(CH_3)_4$], 209 [M-$OSi(CH_3)_5$], 194 [M-$OSi(CH_3)_6$].

Dimer (5c).

Oil. ^{1}HNMR (200 MHz, $CDCl_3$) δ_H (ppm) 3.32 (3H, s, CH_3), 3.74 (3H, s, CH_3), 6.23-6.72 (3H, m, Ph-H), 6.94 (3H, s, OH), 7.10-7.32 (2H, m, Ph-H). ^{13}CNMR (50MHz $CDCl_3$) δ_C (ppm) 55.3 (2xCH_3), 103.4 (CH), 111.2 (CH), 114.5 (CH), 117.0 (CH), 117.5 (C), 120.3 (CH), 121.2 (C), 136.4 (C), 150.2 (C), 154.3 (C), 156.0 (C), 157.9 (C). *MS, m/z* : 478 (M^+), 432 [M-$(OCH_3)_2$], 401 [M-$(O_2(CH_3)_3$], 386 [M-$(O_2(CH_3)_4$], 371 [M-$(O_2(CH_3)_5$], 343 [M-$(O_2Si(CH_3)_5$], 328 [M-$(O_3Si(CH_3)_5$], 313 [M-$(O_3Si(CH_3)_6$], 270 [M-$(O_3Si_2(CH_3)_7$].

4-Chlorocatechol (4-chloro-1,2-Benzenediol) (6a).

Oil. ^{1}HNMR (200 MHz, $CDCl_3$) δ_H (ppm) 6.72-6.83 (3H, m, Ph-H), 8.10 (2H, s, OH). ^{13}CNMR (50MHz, $CDCl_3$) δ_C (ppm) 113.0 (CH), 117.3 (CH), 125.4 (CH), 127.2 (C), 145.0 (C), 152.3 (C). *MS, m/z:* 288 (M^+), 273 (M-CH_3), 258 [M-$(CH_3)_2$], 243 [M-$(CH_3)_3$], 215 [M-$Si(CH_3)_3$], 199 [M-$OSi(CH_3)_3$], 184 [M-$OSi(CH_3)_4$], 169 [M-$OSi(CH_3)_5$], 126 [M-$OSi_2(CH_3)_6$].

5,5'-Dichloro-(1,1'-Biphenyl)-2,2',3-triol (6b).

Oil. ^{1}HNMR (200 MHz, $CDCl_3$) δ_H (ppm) 6.71-7.23 (5H, m, Ph-H), 7.62 (3H, s, OH). ^{13}CNMR (50MHz, $CDCl_3$) δ_C (ppm) 111.2 (C), 114.2 (C), 114.5 (CH), 117.3 (CH), 126.5 (C), 127.4 (C), 129.3 (CH), 130.2

(CH), 135.1 (CH), 137.2 (C), 152.3 (C), 155.0 (C). *MS, m/z:* 486 (M^+), 471 (M-CH_3), 353 [M-$OSi(CH_3)_3$], 338 [M-$OSi(CH_3)_4$], 236 [M-$OSi_2(CH_3)_6$].

5-Chloro-3-methylcatechol (5-chloro-3-methyl-1,2-Benzenediol) (7a).

Oil. ^{1}HNMR (200 MHz, $CDCl_3$) δ_H (ppm) 2.10 (3H, s, CH_3), 6.53-6.74 (2H, s, Ph-H), 7.52 (2H, s, OH). ^{13}CNMR (50MHz $CDCl_3$) δ_C (ppm) 17.2 (CH_3), 116.3 (CH), 123.2 (C), 125.4 (C), 126.3 (CH), 140.2 (C), 151.0 (C)**.** MS, m/z: 302 (M^+), 287 (M-CH_3), 272 [M-$(CH_3)_2$], 229 [M-$Si(CH_3)_3$], 213 [M-$OSi(CH_3)_3$], 198 [M-$OSi(CH_3)_4$], 168 [M-$OSi(CH_3)_6$].

Dimer (7b)

Oil. ^{1}HNMR (200 MHz, $CDCl_3$) δ_H (ppm) 2.29 (3H, s, CH_3), 2.35 (3H, s, CH_3), 4.40 (2H, s, CH_2), 6.49-6.70 (4H, m, Ph-H), 6.90 (2H, bs, OH). ^{13}CNMR (50MHz $CDCl_3$) δ_C (ppm) 16.2 (CH_3), 17.6 (CH_3), 102.1 (CH), 113.9 (C), 121.6 (CH), 122.2 (C), 126.2 (C), 127.6 (CH), 128.2 (CH), 129.4 (C), 140.0 (C), 150.7 (C), 154.2 (C), 157.7 (C)**.**

MS, m/z: 426 (M^+), 411 (M-CH_3), 353 [M-$Si(CH_3)_3$], 337 [M-$OSi(CH_3)_3$], 321 [M-$OSi(CH_3)_4$], 307 [M-$OSi(CH_3)_5$], 247 [M-$O_2Si_2(CH_3)_6$].

4-(Para-hydroxybenzyl)-pyrocatechol (4-[(4-hydroxyphenyl)methyl]-1,2-Benzenediol) (9a).

Oil. ^{1}HNMR (200 MHz, $CDCl_3$) δ_H (ppm) 4.10 (2H, m, CH_2), 6.51-7.22 (7H, m. Ph-H). ^{13}CNMR (50MHz, $CDCl_3$) δ_C (ppm) 42.2 (CH), 115.5 (CH), 116.1 (2xCH), 116.5 (CH), 121.3 (CH), 130.2 (2xC), 133.5 (C), 134.5 (C), 144.2 (C), 145.3 (C), 156.1 (C). *MS*, m/z: 432 (M^+), 417 (M-CH_3), 402 [M-$(CH_3)_2$], 359 [M-$Si(CH_3)_3$], 343 [M-$OSi(CH_3)_3$], 329 [M-$OSi(CH_3)_4$], 314 [M-$OSi(CH_3)_5$], 298 [M-$OSi(CH_3)_6$].

4,4'-Methylenedi-pyrocatechol (4,4'-methylenebis-1,2-Benzenediol) (9b).

MS, m/z: 520 (M^+), 505 (M-CH_3), 447 [M-$Si(CH_3)_3$], 431 [M-$OSi(CH_3)_3$], 417 [M-$OSi(CH_3)_4$], 343 [M-$O_2Si_2(CH_3)_6$], 329 [M-$O_2Si_2(CH_3)_7$].

References

[1] a) Halaouli, S.; Asther, M.; Sigoillot, J.C.; Hamdi, M.; Lomascolo, A. *J Appl Microbiol* **2006**, *100,* 219-232; b) Seo, S-Y.; Sharma, V. K.; Sharma, N. *J Agric Food Chem* **2003**, *51*, 2837-2853; c) Duchworth, H.W.; Coleman, J.E. *J Biol Chem* **1970**, *245*, 1613-1625.

[2] a) Shimizu, T.; Nakanishi, Y.; Nakahara, M.; Wada, N.; Moro-Oka, Y.; Hirano, T.; Konishi, T.; Matsugo, S. *J Clin Biochem Nutr* **2010,** *47(3)*, 181-190; b) Zheng, L.T.; Ryu, G.M.; Kwon, B.M.; Lee, W.H.; Suk, K. *Eur J Pharm* **2008**, *588*, 106-113; c) Nolan, L.C.; O'Connor, K.E. *Biotech Lett* **2008**, *30*, 1879-1891.

[3] a) Xiao, Z.-P.; Ma, T.-W.; Fu, W.-C.; Peng, X.-C.; Zhang, A.H.; Zhu, H.-L. *Eur J Med Chem* **2010,** *45*, 5064-5070; b) Bansal, V. K.; Kumar, R.; Prasad, R.; Prasad, S. Niraj, *J Mol Catal A: Chem* **2008,** *284,* 69-76.

[4] a) Marín-Zamora, M.E.; Rojas-Melgarejo, F.; García-Cánovas, F.; García-Ruiz, P.A. *J Biotechnol* **2009,** *139,* 163-168; b) Ullrich, R.; Hofrichter, M. *Cell Mol Life Sci* **2007,** *64*, 271-293; c) de Faria, R.O.; Rotuno-Moure, V.; Lopes de Almeida, M.A.; Krieger, N.; Mitchell, D.A. *Food Technol Biotechnol* **2007,** *45*, 287-294; d) Carvalho, G.M.J.; Alves, T.L.M.; Freire, D.M.G. *Appl Biochem Biotechnol* **2000,** *84–86*, 791-800.

[5] a) Ramsden, C.A.; Stratford, M.R.L.; Riley, P.A. *Org. Biomol. Chem.,* **2009**, *7*, 3388-3390; b) Muñoz-Muñoz, J.L.; García-Molina, F.; García-Ruiz, P.A.; Molina-Alarcón, M.; Tudela, J.; García-Canovas, F.; Rodriguez-Lopez, J.N. *Biochem J* **2008** *416,* 431-440; c) Estrada, P.; Sanchez-Muniz, R.; Acebal, C.; Arche, R.; Castillon, M.P. *Biotechnol Appl Biochem* **1991**, *14*, 12-20.

[6] Espín, J.C.; Soler-Rivas, C.; Cantos, E.; Tomás-Barberán, F.A.; Wichers, H.J. *J Agric Food Chem* **2001**, *49(3),* 1187-1193.

[7] Kazandjiand, R.; Klibanov, A.M. *J Am Chem Soc* **1985**, *107*, 5448-5450.

[8] a) Kermasha, S.; Bao, H.; Bisakowski, B.; Yaylayan, V. *J Mol Catal B: Enzymatic* **2002,** *19-20,* 335-345; b) Kermasha, S.; Bao, H.; Bisakowski, B. *J Mol Catal B: Enzym* **2001**, *11*, 929-938; c) Kermasha, S.; Tse, M. *J Chem Technol Biotechnol* **2000**, *75*, 475-483.

[9] Burton, S.G.; Duncan, J.R.; Kaye, P.T.; Rose, P.D. *Biotech Bioeng* **1993,** *42,* 938-944.

[10] Kazandjina, R.Z.; Klibanov, A.M. *J Am Chem Soc* **1985,** *107,* 5448-5450.

[11] Dordick, S.J. *Enzyme Microb Technol* **1989,** *11,* 194-211.

[12] Rekker, R.F.; de Kort, H.M. *Eur J Med Chem* **1979,** *14, 4*79-488.

[13] a) Lanne, C.; Boeren, S.; Vos, K.; Veerger, C. *Biotech Bioeng* **1987**, *30,* 80–87; b) Zaks, A.; Klibanov, A.M. *Proc Natl Acad Sci USA* **1985**, *82,* 3192-3196.

[14] Durán, N.; Rosa, M.A.; D'Annibale, A.; Gianfreda, L. *Enzyme Microb Technol* **2002**, *31,* 907-931.

[15] a) Warrington, J.C.; Saville, B.A. *Biotechnol Bioeng* **1999**, *65*, 325-333; b) Estrada, P.; Baroto, W.; Castillon, M.P.; Acebal, C.; Arche, R. *J Chem Tech Biotechnol* **1993**, *56(1),* 59-65.

[16] a) Ilabahen, P.; Roland, L.; Kitti, M.; Dietmar, H.; Thomas, R.; Antje, P. *Holzforschung* **2009**, *63(6),* 715-720; b) Russo, M.E.; Giardina, P.; Marzocchella, A.; Salatino, P.; Sannia, G. *Enzyme Microb Technol* **2008**, *42(6),* 521-530; c) Baratto, L.; Candido, A.; Marzorati, M.; Sagui, F.; Riva, S.; Danieli, B. *J Mol Catal B: Enzymatic* **2006,** *39(1-4),* 3-8.

[17] a) Mislovicova, D.; Turjan, J.; Vikartovska, A.; Paetoprsty, V. *J Mol Catal B: Enzymatic* **2009**, *60(1-2),* 45-49; b) Mislovicova, D.; Michalkova, E.; Vikartovska, A. *Process Biochem.* **2007**, *42(4),* 704-709.

[18] Sukyai, P.; Rezìc, T.; Lorenz, C.; Mueangtoom, K.; Lorenz, W.; Haltrich, D.; Ludwig, R. *J Biotechnol* **2008**, *135,* 281-290.

[19] Decher, G. *Science* **1997**, *277*, 1232-1237.

[20] Decher, G.; Schmitt, J. *Prog Colloid Polym Sci* **1992**, *89*, 160-164.

[21] Held, C.; Kandelbauer, A.; Schroeder, M.; Cavaco-Paulo, A.; Gubitz, G.M. *Environ Chem Lett* **2005**, *3,* 74-77.

[22] a) Jolley, R.L.; Evans, L.H.; Makino, N.; Mason, H.S. *J Biol Chem **1974,** 249*, 335-345; b) Nelson, R.M.; Mason, H.S. *Methods Enzymol* **1970,** *17a*, 626-632; c) Duckworth, H.W.; Coleman, J.E. *J Biol Chem **1970,** 245*, 1613-1625.

[23] Marín-Zamora, M.E.; Rojas-Melgarejo, F.; Garcìa-Canovas, F.; Garcıa-Ruiz, P.A. *J Biotechnol* **2006,** *126,* 295-303.

[24] Masamoto, Y.; Iida, S.; Kubo, M. *Planta Med* **1980**, *40*, 361-365

[25] a) Sedmak, J.J.; Grossberg, S.E. *Anal Biochem* **1977**, *79,* 544-552; b) Bradford, M.M. *Anal Biochem* **1976**, 72*,* 248-254.

[26] a) MarongU, B.; Piras, A.; Porcedda, S.; Tuveri, E.; Sanjust, E.; Meli, M.; Sollai, F.; Zucca, P.; Rescigno, A. *J Agric Food Chem* **2007**, *55,* 10022-10027; b) Bouchilloux, S.; McMahill, P.; Mason, H.S. *J Biol Chem* **1963**, *238*, 1699-1707.

[27] Wolfender, B.S.; Willson, R.L. *J Chem Soc, Perkin Trans 2* **1982**, 805-810.
[28] Lineweaver, H.; Burk, D. *J Am Chem Soc* **1934,** *56*, 658-666.
[29] a) Katchalski-Katzir, E.; Kraemer, D.M. *J Mol Catal B: Enzym* **2000**, *10,* 157-176; b) Rauch, P.; Ferri, E.N.; Girotti, S.; Rauchova, H.; Carrea, G.; Bovara, R.; Fini, F.; Roda, A. *Anal Biochem* **1997,** *245*, 133-140.
[30] Gerritsen, Y.A.M.; Chapelon, C.G.J.; Wichers, H.J. *Phytochemistry* **1994,** *35(3),* 573-577
[31] a) Huang, C.L.; Cheng, W.C.; Yang, J.C.; Chi, M.C.; Chen, J.H.; Lin, H.P.; Lin, L.L. *J Ind Microbiol Biotechnol* **2010**, *37,* 717-725; b) Acharya, C.; Kumar, V.; Sen, R.; Kundu, S.C. *Biotechnol J* **2008**, *3*, 226-233; c) Arslan, A.; Kiralp, S.; Toppare, L.; Yagci, Y. *Int J Biol Macromol* **2005**, *35*, 163-167.
[32] Frauenfelder, H.; Fenimore, P.W.; McMahon, B.H. *Biophys Chem* **2002**, *98,* 35-48.
[33] Pocker, Y. *Cell Mol Life Sci* **2000**, *57*, 1008-1017.
[34] Levy, Y.; Onuchic, J.N. *Annu Rev Biophys Biomol Struct* **2006**, *35,* 389-415.
[35] Zhong, D. *Adv Chem Phys* **2009**, *143*, 83-149.
[36] a) Tuncagil, S.; Kayahan, S.K.; Bayramoglu, G.; Arica, M.Y.; Toppare, L. *J Mol Catal B:Enzym* **2009,** *58,* 187-193; b) Puri, M.; Kaur, H.; Kennedy, J.F. *J Chem Tech Biotech* **2005,** *80,* 1160-1165; c) Quan, D.; Kim, Y.; Shin, W. *J Electroanal Chem* **2004,** *561*, 181-189.
[37] Ziyatdinova, G.K.; Gainetdinova, A.A.; Budnikov, G.K. *J Anal Chem* **2010**, *65(9),* 929-934.
[38] Dawson, C.R.; Tarpley, W.B. *Ann N Y Acad Sci*, **1963**, *100,* 937-950.
[39] Xiao, Z-P.; Ma, T-W.; Fu, W-C.; Peng, X-C.; Zhang, A-H.; Zhu, H-L. *Eur J Med Chem* **2010**, *45(11),* 5064-5070.
[40] Costi, R.; Di Santo, R.; Artico, M.; Massa, S.; Ragno, R.; Loddo, R.; La Colla, M.; Tramontano, E.; La Colla, P.; Pani, A. *Bioorg Med Chem* **2004**, *12,* 199-215.
[41] Balaydin, H.T.; Gülçin, I.; Menzek, A.; Göksu, S.; Şahin, E. *J Enz Inhibition Med Chem* **2010**, *25(5),* 685-695.
[42] Colon, M.; Guevara, P.; Gerwick, W.H. *J Nat Prod* **1987**, *50(3),* 368-374.
[43] Sukhorukov, G.; Fery, A.; Möhwald, H. *Prog Polym Sci* **2005**, *30,* 885-897.
[44] Gao, C.Y.; Donath, E.; Möhwald, H.; Shen, J. *Angew Chem Int Ed* **2002**, *41,* 3789-3793.
[45] a) Tudorache, M.; Mahalu, D.; Teodorescu, C.; Stan, R.; Bala, C.; Parvulescu, V.I. *J Mol Catal B: Enzym* **2011**, *69(3-4),* 133-139; b) Dotzauer, D.M.; Abusaloua, A.; Miachon, S.; Dalmon, J.-A.; Bruening, M.L. *Appl Catal B: Environ* **2009**, *91(1-2),* 180-188.
[46] Shinkai, S.; Kusano, Y.; Manabe, O. *J Chem Soc Perk T1* **1980**, *7*, 1622-16625.
[47] Mateo, C.; Abian, O.; Fernandez-Lorente, G.; Predoche, J.; Fernandez-Lafuente, R.; Guisan J.M. *Biotechnol Prog* **2002**, *18,* 629-634.
[48] a) Perazzini, R.; Saladino, R.; Guazzaroni, M.; Crestini, C. *Bioorg Med Chem* **2010**, *19*, 440-447; b) Tiourina, O.P.; Antipov, A.A.; Sukhorukov, G.B.; Larionova, N.I.; Lvov, Y.; Möhwald, H. *Macromol Biosci* **2001**, *1,* 209-214.
[49] Djugnat, C.; Sukhorukov, G.B. *Langmuir*, **2004**, *20(17)*, 7265-7269.
[50] a) Rodríguez-López, J.N.; Gómez-Fenoll, L.; Penalver, M.J.; García-Ruíz, P.A.; Varón, V.; Martínez-Ortíz, F.; García-Cánovas, F.; Tudela, J. *Biochim Biophys Acta* **2001**, *1548*, 238-256; b) Sweely, C.C.; Bentlry, R.; Makita, M.; Wells, W.W. *J Am Chem Soc* **1963**, *85*, 2497-2507.
[51] Chernyak, N.; Dudnik, A.S.; Huang, C.; Gevorgyan, V. *J Am Chem Soc* **2010**, *132*, 8270–8272.
[52] Chantarasriwong, O.; Cho, W.C.; Batova, A.; Chavasiri, W.; Moore, C.; Rheingold, A.L.; Theodorakis, E.A. *Org Biomol Chem* **2009**, *7,* 4886-4894.
[53] Nakayama, S.; Ikeda, F. *US Patent* 5102906, 4985458, **1988**.

Chapter 5

Tyrosinase in lignin oxidative functionalization

5.1 Introduction

Lignin is a characteristic chemical and morphological component of the xylem, the vascular tissue of the higher plants (gymnosperms and angiosperms) specialized for liquid transport and mechanical strength. Lignin seals the water conducting system against the hydraulic pressure produced by the transport of water from the soil to the leaves and needles, so reinforcing plants to withstand the forces of gravity and wind. Moreover, it operates for re-orientating stems and branches in response to changes in mechanical stressed and light levels.[1] Finally, lignin plays an important function in plant natural defense against degradation by impeding penetration of destructive enzymes through the cell wall.[2] On the biochemical features, lignin is a polyphenolic material formed by enzymatic polymerization of coniferyl, sinapyl and coumaryl alcohols. These phenylpropanoid units are linked to each other in irregular order via ether linkages and carbon-carbon bonds (Figure 5.1).[3] The traditionally held biosynthesis process, which consists essentially of random radical coupling reactions, sometimes followed by the addition of water, of primary, secondary, and phenolic hydroxyl groups to quinonemethide intermediates, leads to the formation of a three-dimensional polymer that lacks the regular and ordered repeating units found in other natural polymers such as cellulose and proteins.[4] Lignin resists attack by most microorganisms; in nature only basidiomycetes white-rot fungi are able to degrade lignin efficiently, by an enzymatic process.[5] Some white-rot basidiomycetes (*Phlebia* spp. and *Pleorotus* spp.) preferentially attack lignin more readily than hemicellulose and cellulose in wood tissue. This process of selective delignification leaves cellulose-enriched white material. It is considerable interest in the industrial application of these fungi, because many uses of wood involve preferentially removing lignin, such as in biopulping. Many white-rot fungi (*Trametes versicolor, HeterobasidIum annosum* and *Irpex lacteus*), however, exhibit a pattern of simultaneous decay characterized by degradation of all cell wall components with formation of radial cavities.[6] White-rot fungi secrete a pool of oxidative enzymes that are involved in degradation of cell-wall components. The four major groups of enzymes for the degradation of lignin are lignin peroxidases (EC 1.11.1.14), manganese dependent peroxidases (EC 1.11.1.13), versatile peroxidases (EC 1.11.1.16) and laccases (EC 1.10.3.2); so oxidative enzymes are potential tools for modification of wood lignin.[7]

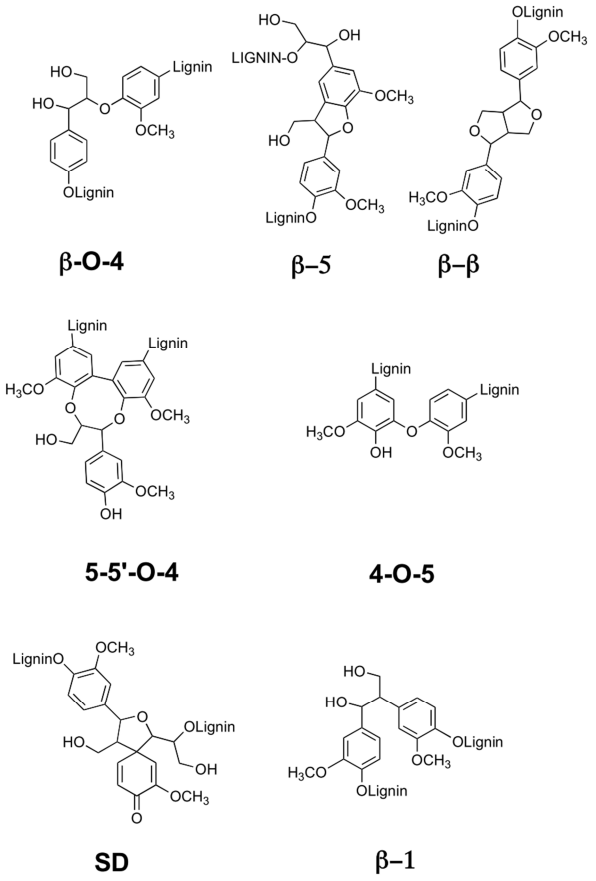

Figure 5.1 Common phenylpropane linkages.

The effect of laccase and peroxidase oxidation has been extensively investigated, while few studies have been reported about the tyrosinase activity. Laccases and peroxidases catalyze the oxidation of lignin through formation of phenoxy radicals causing phenolic oxidative coupling, alkyl-arylether bond cleavage, aromatic ring cleavage and side chain oxidations (Figure 5.2).[8] Tyrosinases are copper-containing enzyme able to catalyze the hydroxylation of monophenols to *ortho*-diphenols and the oxidation of *ortho*-diphenols to *ortho*-quinones.[9] Unlike peroxidases and laccases, tyrosinases do not act through radical pathway. Previously reported data demonstrated that the effect exerted by tyrosinases on lignin depolymerization was negligible. In these studies the lignin modification process was monitored by measuring the consumption of O_2 and by studying the changes in molecular-weight distributions (GPC analysis) and in the total amount of phenolic hydroxyls groups.[10] These kinds of studies can give valuable information about the effects of an enzyme on the whole fiber substrate. However, studies concerning the possible role of tyrosinases in the lignin side chain modification have not been performed. In this chapter, the role of tyrosinases in the oxidation of lignin was investigated by quantifying the changes of particular functional groups after enzyme treatment (^{31}PNMR analysis) and by studying the changes in molecular-weight distributions (GPC analysis). Specifically, the Phosphorous Nuclear Magnetic Resonance (^{31}PNMR) is a technique that allows the recognition of the

different phenolic hydroxyl groups contents (syringyl, guaiacyl and *p*-hydroxyphenyl), the determination of hydroxyl aliphatic groups, the distinction between the condensed forms 4-O-5', 5-5' and diphenylmethoxy and, finally, the carboxylic groups content.

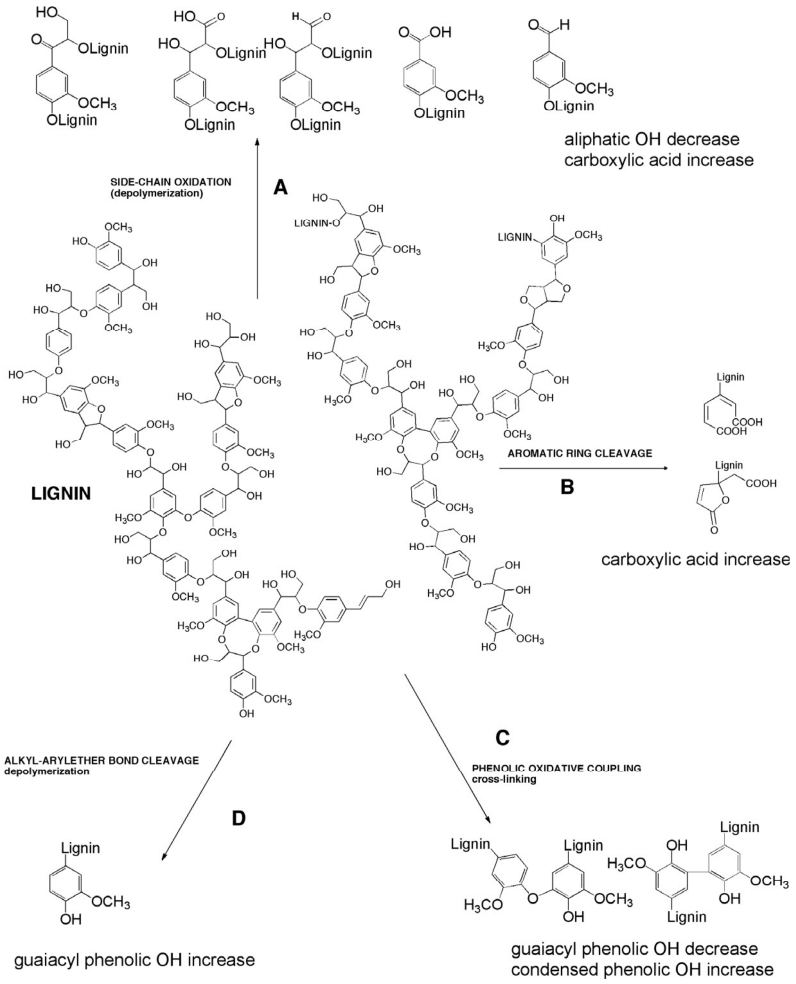

Figure 5.2 Lignin oxidation pathways (from Perazzini et al., 2010)[8].

The analysis requires the derivatization of hydroxyl groups with the phosphitylation reagent, 2-chloro-4,4',5,5'-tetramethyl-1,3,2-dioxaphospholane. The phosphitylation reaction is reported in Figure 5.3. This reagent allows the overall distribution of hydroxyl groups present in a lignin sample to be determined. It has been found to be particularly useful in the discrimination between the condensed structures, in which the bond involves the phenolic hydroxyl, and the uncondensed phenolic units, and in resolving the primary and secondary hydroxyls.[11] The presence of four methyl groups in the 2-chloro-4,4',5,5'-tetramethyl-1,3,2-dioxaphospholane reagent affects the spin-lattice relaxation profiles of the phosphorus atoms attached on lignin and increase the stability of the phosphitylated lignin: thus the analysis is reproducible also some hours after the derivatization reaction.

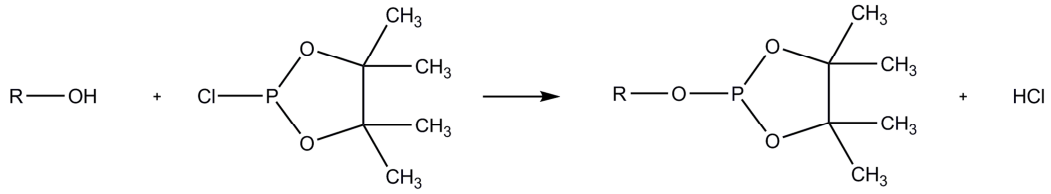

Figure 5.3 Phosphitylation reaction of hydroxyl groups.

Usually, the analysis is realized in the presence of the relaxation reagent chromium(III) acetylacetonate. With the use of an internal standard it is possible to make a quantitative analysis to quantify the spin-lattice relaxation of the various hydroxylic functional groups present in lignin.[12] In Table 5.1 the ^{31}P chemical shift of phosphorus nuclei labeling hydroxyl groups in different environments in lignin are reported.

Table 5.1 ^{31}PNMR attribution (from Argyropoulos, 1995).[13]

OH groups	Chemical shift
Aliphatic	149.0-146.0
Diphenilmethane	144.27-142.78
4-O-5’	142.78-141.24
5-5’	141.72-140.24
Guaiacylic	140.24-138.8
p-OH phenylic	138.8-137.4
COOH	135.5-134.0

Instead, the Gel Permeation Chromatography (GPC) is a technique that allows the chromatographic fraction of macromolecules according to molecular size.[14] In this technique, gels are used as stationary phase and acts as a molecular sieve. When an aqueous solution of macromolecules is allow moving through a column containing the gel, a chromatographic separation takes place; molecules of low molecular weight are able to penetrate into the gel particle pores but large molecules are excluded from the pores and pass directly through the column. Consequently, the largest molecules elute first and the smallest last.[15] These two techniques were used to analyze the oxidative modification of lignin exerted by tyrosinases. To limit the production of reactive quinone responsible of the enzyme inactivation, reactions were carried out in reducing conditions in the presence of ascorbic acid, as previously reported (Figure 5.4 and Chapter 3). The effect of substrate solubility on lignin modification was also studied using both aqueous and organic/aqueous solvent (Chapter 4).[16] Tyrosinase was immobilized on Eupergit®C250L and further coated by the Layer-by-Layer technique as previously described (Chapter 3 and Chapter 4).[17]

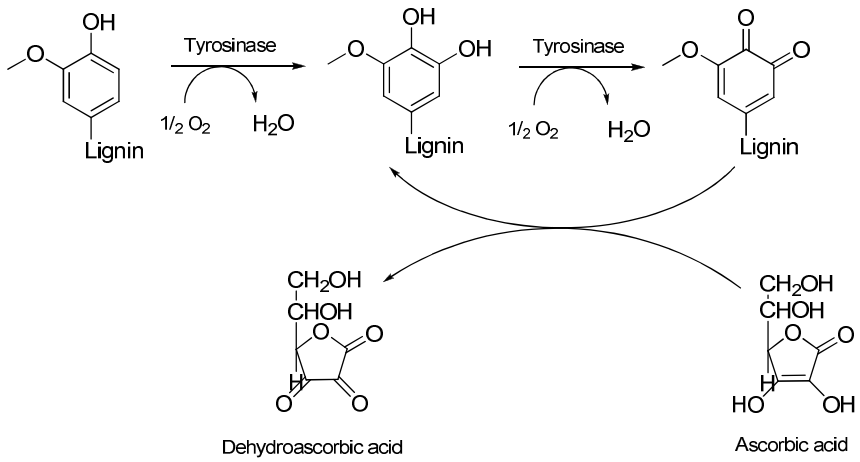

Figure 5.4 Role of ascorbic acid in the oxidation of lignin by tyrosinase.

5.2 Results and discussions

5.2.1 Treatment of lignin by tyrosinase

The effects of tyrosinase oxidation on lignin were studied to verify the possibility to introduce catechol moiety in the structure of the natural polymer. Such functionalized lignins could be very interesting for biotechnological applications thanks to their higher hydrophilic features and antioxidant properties. As previously reported, in fact, catechol derivatives are characterized by several biological activities related to the inhibition of the radical species.[18] The effect of tyrosinase in lignin functionalization was studied using three commercially available lignins: lignin alkali low sulphonate (LLS, softwood), lignin hydrolytic (LHY, Sugar cane bagasse) and lignin organosolv (LOR, hardwood). These lignins, as well as presenting significant structural differences, showed different solubility properties: LLS was mostly soluble in water, while LHY and LOR was better soluble in organic solvents. The oxidations were first performed under homogeneous conditions and later under heterogeneous conditions with immobilized tyrosinase on Eupergit®C250L and coating the system by the Layer-by-Layer technique. Early homogeneous reactions were carried out as follow: lignin (100.0 mg), tyrosinase (3000 U) and ascorbic acid were suspended in Na-phosphate buffer pH 7.0 (5.0 mL) at 25°C under vigorous stirring. The presence of ascorbic acid ensured the reduction of eventually-produced quinones to catechols (Figure 5.4). After 24 h, the mixture was acidified at pH 3.0 and centrifuged with Vivaspin® tubes equipped with 3.0 kDa MWCO membranes to separate the oligomeric component by the polymers (these latter retained by the membrane). The recovered lignin was washed with water three times and then freeze-dried and analyzed by ^{31}PNMR and GPC with the aim to evaluate any changes on the structure of the polymer. Specifically, ^{31}PNMR analysis was conducted to elucidate the possible effect of tyrosinase on lignin side-chain modification; in fact,

after the enzymatic treatment, a decrease in phenolic OH groups with contemporaneous increase in condensed OH group was expected in accordance with the catalytic cycle of the enzyme. The contemporary GPC analysis on lignin chain allows the study of the molecular weight distribution of lignin. On the other hand, the filtrate obtained after centrifugation, containing the oligomeric component, was extracted twice with EtOAc, dried over anhydrous Na_2SO_4 and concentrated under vacuum to yield coloured crude analyzed by GC-MS.

5.2.2 ^{31}PNMR characterization of lignin

The ^{31}PNMR is an advanced heteronuclear NMR technique allows the contemporary characterization and quantification of all labile OH groups present in lignins such as the aliphatic OH groups, the different phenolic OH and carboxylic acids. In particular, the samples of residual lignins were phosphitylated in quantitative yield with 2-chloro-4,4',5,5'-tetramethyl-1,3,2-dioxaphospholane in pyridine/deuterated chloroform mixture (Py:$CDCl_3$ 1.6:1.0, v/v) and then subjected to quantitative ^{31}PNMR analysis in the presence of cholesterol as internal standard. The assignment of the different OH signals was carried out on the basis of the comparison with the chemical shift of selected models as reported in previous works.[19] Table 5.2 shows the amount of the different OH groups analyzed by ^{31}PNMR expressed as mmol *per* gram of residual lignin (mmol g^{-1}). The oxidation performed on LHY as substrate did not show notable changes on amount of various OH groups that are slightly lower in the reaction than in the control (Table 5.2, entry 2 versus 1).

Table 5.2 ^{31}PNMR analysis of lignins and before and after tyrosinase oxidations.[a]

Entry	Lignin	Catalyst	Aliphatic OH (mmol g^{-1})	Condensed OH (mmol g^{-1})	Guaiacyl OH (mmol g^{-1})	Phenolic OH (mmol g^{-1})	COOH (mmol g^{-1})
1	LHY	None	1.78	1.11	0.78	0.97	0.81
2	LHY	Tyro	1.73	1.09	0.73	0.91	0.81
3	LOR	None	1.18	2.14	0.80	0.44	0.42
4	LOR	Tyro	1.17	1.99	0.79	0.37	0.39
5	LLS	None	1.08	0.73	0.40	0.08	0.50
6	LLS	Tyro	0.99	0.96	0.46	0.08	0.44
7	LOR[b]	None	0.58	0.51	0.11	0.05	0.08
8	LOR[b]	Tyro	0.50	0.41	0.10	0.01	0.02
9	LLS	Tyro/E	0.94	0.95	0.42	0.07	0.42
10	LLS	Tyro/E-LbL	0.98	0.88	0.41	0.08	0.41
11	LOR[b]	Tyro/E	0.40	0.36	0.07	0.03	0.02
12	LOR[b]	Tyro/E-LbL	0.55	0.45	0.08	0.01	0.01

[a] Reaction conditions: lignin (100.0 mg), tyrosinase (3000 U) and ascorbic acid were suspended in Na-phosphate buffer pH 7.0 (5.0 mL) at 25°C under vigorous stirring for 24h. Amount was expressed as mmol *per* gram of residual lignin (mmol g^{-1}). Data reported was the means of three different experiments with a standard deviation of $2x10^{-2}$ mmol g^{-1}; [b] Reactions performed in CH_2Cl_2/buffer.

Similar results were observed for lignin LOR (Table 5.2, entry 4 versus 3). Instead, in the case of LLS, a slight decrease in phenolic OH was observed with a significant simultaneous growing on condensed OH group (Table 5.2, entry 6 versus 5). This rising in condensed OH is indicative of the formation of catechol moieties as consequence of expected tyrosinase oxidation. The different reactivity of reported polymeric substrates could depend on the different lignin solubility: changes in condensed OH was in fact observed only in the case of LLS that was completely soluble in aqueous medium respect to LHY and LOR that exhibit a more hydrophobic properties. In order to assess the influence of the solubilization on lignin functionalization, the oxidation of LOR was also performed in biphasic medium, using dichloromethane as organic solvent, as described in Chapter 4 for the oxidation of phenols. Results showed no significant effect respect to aqueous reactions: as general trend, a slight decrease in the amount of all OH groups was detected after tyrosinase treatment (Table 5.2, entry 7,8 versus 3,4). This reduction can be ascribable to a partial degradation of the polymeric structure. The oxidation of LLS and LOR was also performed in heterogeneous condition, using two tyrosinase-based systems: one based on the immobilization of tyrosinase on Eupergit®C250L (Tyro/E) and the other based on a first immobilization of tyrosinase on Eupergit®C250L and its subsequent coating by the Layer-by-Layer technique (Tyro/E-LbL) as widely described in Chapter 3 and Chapter 4. About LLS oxidation, immobilized tyrosinase preserve its reactivity confirming the partial rise in condensed OH groups previously described (Table 5.2, entries 9,10 versus 5,6). Any specific reactivity was observed in the case of LOR. It is interesting to note that in the oxidation of LSS, Tyro/E and Tyro/E-LbL afforded the same results as the free enzyme, indicating that the immobilization procedure did not interfere with the catalytic cycle of tyrosinase (Table 5.2, entries 11,12 versus 7,8).

5.2.3 GPC analysis of lignin after tyrosinase treatment

Lignins isolated after treatments with free and immobilized tyrosinase were also submitted to acetobromination according to a previously reported procedure[20] and successively analyzed by Gel Permeation Chromatography (GPC) in order to investigate the effect of the oxidative treatments on lignin molecular weight distribution. GPC was carried out using a system of columns connected in series calibrated against monodisperse polystyrene standards, monomeric and dimeric lignin model compounds. More specifically 4-(1-hydroxyethyl)-2-methoxyphenol and (3-methoxy-4-ethoxy-2-phenyl)-2-oxoacetaldehyde were used as monomeric and dimeric lignin standard, respectively. Table 5.3 and Figure 5.5 show the GPC analyses before and after the enzymatic treatments. It is evident that, as expected by previous ^{31}PNMR analysis, the M_n (number average molecular weight) and M_W (number average indicative of the molar mass distribution) values of the treated LHY and LOR were similar to reference reactions, confirming the negligible effect of tyrosinase on lignin functionalization (Table 5.3 entries 1-7).

Table 5.3 Weight average (M_w) and number average (M_n) molecular weights and polydispersity (M_w/M_n) of lignin samples before and after the enzymatic treatments.[a]

Entry	Sample	M_w	M_n	M_w/M_n
1	LHY	223,547	19,925	11.2
2	LHY + Tyro	212,001	18,934	11.2
3	LOR	154,670	15,104	10.2
4	LOR + Tyro	202,828	18,803	10.8
5	LOR + Tyro[b]	199,288	18,625	10.7
6	LOR + Tyro/E[b]	204,408	18,753	10.9
7	LOR + Tyro/E-LbL[b]	203,504	18,843	10.8
8	LLS	175,139	7,309	24.0
9	LLS + Tyro	232,034	9,627	24.1
10	LLS + Tyro/E	231,125	9,435	24.4
11	LLS + Tyro/E-LbL	230,254	9,524	24.2

[a] Reaction conditions: lignin (100 mg), tyrosinase (3000 U) and ascorbic acid were suspended in Na-phosphate buffer pH 7 (5.0 mL) at 25°C under vigorous stirring for 24h. Data reported was the means of three different experiments. [b] Reactions performed in CH_2Cl_2/buffer

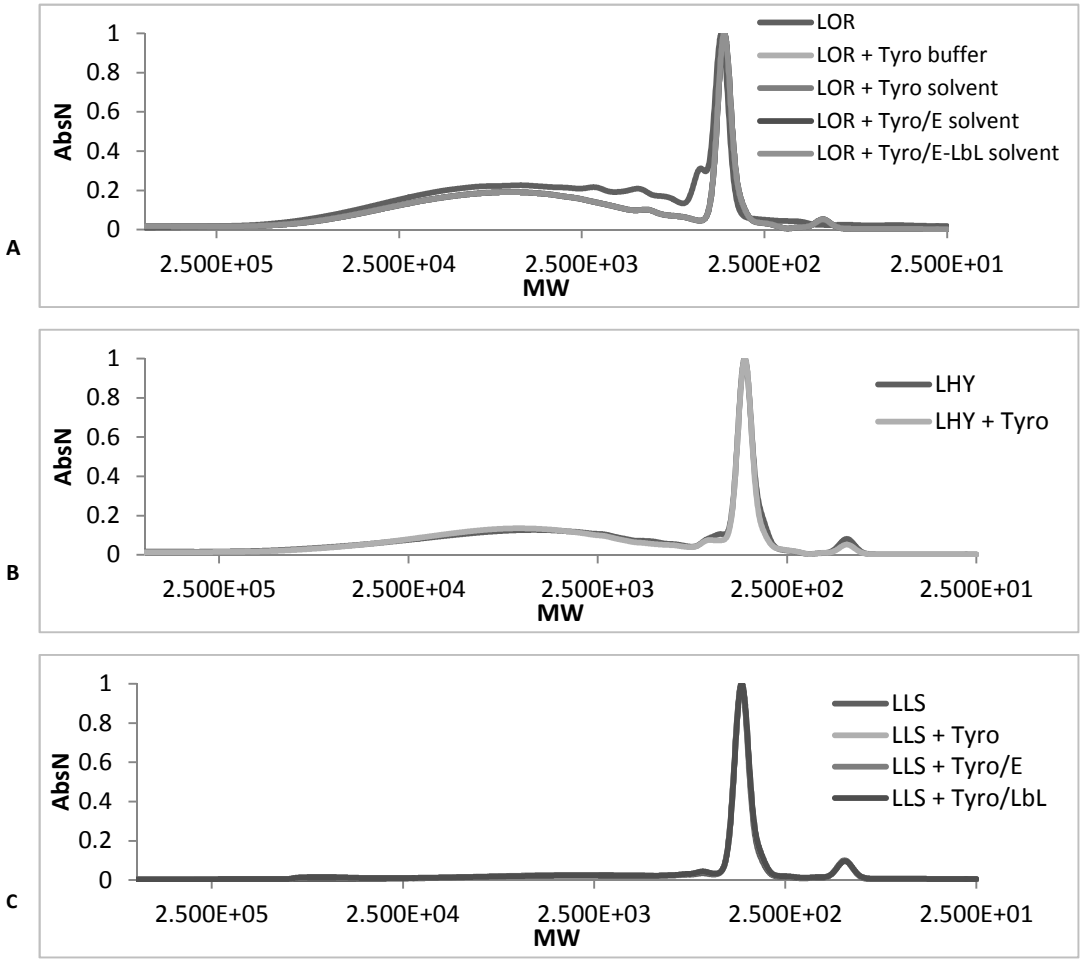

Figure 5.5 Gel permeation chromatography of (A) lignin organosolv, (B) lignin hydrolytic and (C) lignin alkali low sulphonate before and after the treatment with free and immobilized tyrosinase.

Similar results were observed in the case of LLS even if, in this latter case, a partial modification in the side-chain structure of lignin was observed by ^{31}PNMR. This data can be explained assuming that the addition of some OH groups on the polymeric structure of substrate does not alter significantly the Mw and Mn values of the sample (Table 5.3 entries 8-11). The lower influence of tyrosinase on lignin polymerization respect to other oxidase, such as laccase and peroxidase, can be attributing to its different reaction pathways that not involve phenoxy-radical intermediate.[8]

5.2.4 GC-MS analysis of lignin after tyrosinase treatment

The organic extracts containing the low molecular weight component of lignin obtained after centrifugation with Vivaspin® were analyzed by GC-MS using dodecane as internal standard. For all three lignin samples, the formation of novel compounds was observed after tyrosinase treatment. The yield of more significant recovered molecules where reported in , Table 5.5 and Table 5.6 for LHY, LOR and LLS, respectively. Data reported concern oxidations performed with immobilized tyrosinase (Tyro/E and Tyro/E-LbL); similar results were obtained under homogeneous conditions (data not shown).

Table 5.4 GC-MS analysis of extracted filtrate recovered after LHY lignin oxidation.

Compound	Tr (min)	Yield %[a]	
		Reaction	Control
Acetophenone, 3'-(trimethylsiloxy)-	10,40	20.60	9.80
1,2-Benzenedicarboxylic acid	14,90	1.13	-
Hexadecanoic acid, trimethylsilyl ester	16,53	2.50	1.80
Octadecanoic acid, trimethylsilyl ester	18,33	4.00	2.90

[a] Yield (%) was calculated using dodecane as internal standard and it was expressed as percentage respect to the total amount of product recovered.

As general rule, after tyrosinase treatment, alcohols, carboxylic acid, furan and aromatic derivatives compounds were isolated in significant yield respect to reference reaction, where they were in traces or completely absent. As examples, in LHY and LLS oxidations, the yield of acetophenone derivatives increased to 20.60 % and to 9.60 %, respectively, in reference to 9.8 % and 2.57 % of control reactions (Table 5.4 and Table 5.6); instead, in LOR oxidation, benzoic acid derivative rose from 0.02 % to 17.04 % of total isolated compounds (Table 5.5). Furan derivatives compounds recovered in the organic extract of LOR lignin (2-Furancarboxylic acid and 2,5-Furandicarboxylic acid) can be produced by oxidative degradation of aromatic ring (Table 5.5). Noteworthy, as reported in Figure 5.6, for all three lignins analyzed, aromatic compounds represent the main family of molecules isolated after tyrosinase oxidation, being recovered with an overall yield higher than non-aromatic ones. Aromatic derivatives probably arose by oxidation of side-chain in lignin.

Table 5.5 GC-MS analysis of extracted filtrate recovered after LOR lignin oxidation.

Compound	Tr (min)	Yield %[a]	
		Reaction	Control
Silane, (2-furanylmethoxy)trimethyl-	3.88	1.53	-
2-Ketoisocaproic acid, trimethylsilyl ester	5.25	1.15	-
Ethanedioic acid, bis(trimethylsilyl) ester	5.40	17.34	0.08
2-Furancarboxylic acid, trimethylsilyl ester	5.60	12.23	0.04
Propanoic acid, 2-methyl-3-[(trimethylsilyl)oxy]-, trimethylsilyl ester	5.79	1.59	-
2-Methoxyphenol-TMS	6.93	0.19	0.01
Propanoic acid, 2,3-bis[(trimethylsilyl)oxy]-, trimethylsilyl ester	8.12	1.34	-
2-Propenoic acid, 3-(2-furanyl)-, trimethylsilyl ester	9.07	0.67	-
Pentanedioic acid, bis(trimethylsilyl) ester	9.24	1.71	0.04
Butylated Hydroxytoluene	10.75	0.28	0.04
2-Furancarboxylic acid, 5-[[(trimethylsilyl)oxy]methyl]-, trimethylsilyl ester	11.14	1.52	-
Benzoic acid, 4-[(trimethylsilyl)oxy]-, trimethylsilyl ester	11.35	3.49	0.08
2-Ethyl-3-ketovalerate, bis(trimethylsilyl)	11.78	0.25	-
2,5-Furandicarboxylic acid, bis(trimethylsilyl) ester	12.31	0.37	-
Benzaldehyde, 3,5-dimethoxy-4-[(trimethylsilyl)oxy]-	13.12	0.86	0.26
4-Hydroxy-3-methoxyphenethylene glycol triTMS	14.25	0.15	-
Trimethylsilyl 3,5-dimethoxy-4-(trimethylsilyloxy)benzoate	15.05	17.04	0.02
2-Methyl-2(p-methoxy)mandelate, bis(trimethylsilyl)-	15.41	0.77	-
Octadecanoic acid, trimethylsilyl ester	18.32	5.17	0.17

[a] Yield (%) was calculated using dodecane as internal standard and it was expressed as percentage respect to the total amount of product recovered.

Table 5.6 GC-MS analysis of extracted filtrate recovered after LLS lignin oxidation.

Compound	Tr (min)	Yield %[a]	
		Reaction	Control
Ethanedioic acid, bis(trimethylsilyl) ester	5.35	10.40	-
Butanoic acid	6.34	0.39	1.24
Butanedioic acid, methyl-, bis(trimethylsilyl) ester	8.15	1.87	-
Acetophenone	12.21	9.60	2.57
1,2-Benzenedicarboxylic acid, bis(2-methylpropyl) ester	14.90	0.93	8.10
Hexadecanoic acid, trimethylsilyl ester	16.55	3.09	1.72
Octadecanoic acid, trimethylsilyl ester	18.36	4.37	2.38

[a] Yield (%) was calculated using dodecane as internal standard and it was expressed as percentage respect to the total amount of product recovered.

Accordingly with GC-MS data, tyrosinase was more reactive toward oligomeric component of lignin than polymeric chain, where it exerted a negligible effect as revealed by ^{31}PNMR and GPC analysis.

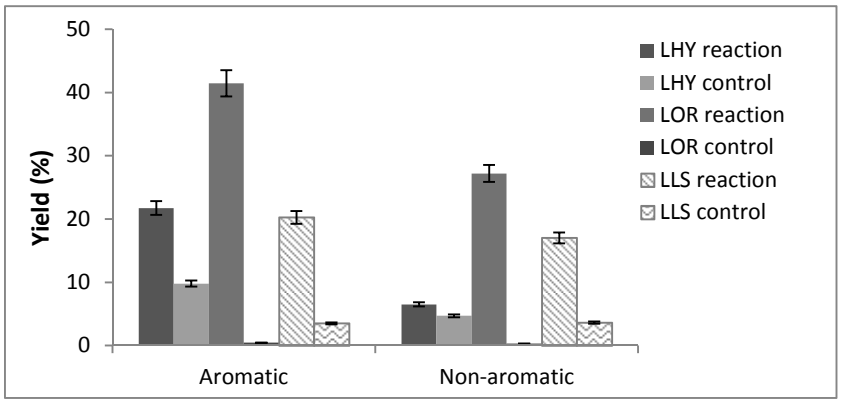

Figure 5.6 Yield percentage of aromatic and non-aromatic compounds recovered from oligomeric constituent of lignin after tyrosinase oxidation.

5.3 Conclusions

As a general trend tyrosinase showed a low reactivity toward lignin samples, with the only exception of LLS, where ^{31}PNMR analysis revealed a significant increase in condensed OH after enzymatic treatment. Since tyrosinase is efficient in the oxidation of lignin model compound as widely described in Chapter 3 and 4, the low reactivity toward the polymeric structure of lignin may be due to (i) the inhibitory effect exerted by lignin or (ii) to the low solubility of substrate that does not interact efficiently with the catalytic site of tyrosinase. The influence of solubility seems to be confirmed by the reactivity of LLS (that is the most soluble sample in buffer) and by the analysis of organic extracts by GC-MS. This suggest that tyrosinase might perform better in condition in which lignin is highly soluble, as in the case of ionic liquids.

5.4 Experimental Section

Tyrosinase extracted from *Agaricus bisporus,* Eupergit®C250L, poly(sodiuum 4-styrenesulfonate) (PSS, MW 70000), poly(allylamine hydrochloride) (PAH, MW 56000), L-tyrosine (L-Tyr), ascorbic acid, 2,2'-azino-bis(3-ethylbenzothiazoline-6-sulphonic acid) (ABTS), bovine serum albumin (BSA), dodecane, pyridine, hesamethyldisilazane (HMDS), trimethylchlorosilane (TMCS), 2-chloro-4,40,5,50-tetramethyl-1,3,2-dioxaphospholane, lignin alkali low sulphonate (LLS, softwood), lignin hydrolytic (LHY, Sugar cane bagasse) and lignin organosolv (LOR, hardwood) were purchased from Sigma-Aldrich. All experiments were carried out in triplicate.

5.4.1 Tyrosinase extraction

The mushroom tyrosinase was partially purified from commercial *Agaricus bisporus* as previously described (for detail see Chapter 4, paragraph 4.4.1).[21] Briefly, frozen sporocarps were first extracted twice with acetone and then subjected to solvent (acetone) and salt precipitations [35-70% with $(NH_4)_2SO_4$]. The resulting enzyme solution was dialyzed against water, concentrated by means of Vivaflow®50 equipped with a polyethersulfone (PES) membrane (10000 MWCO), lyophilized and stored at -20°C.

5.4.2 Lignin oxidation

Oxidations were performed in homogeneous and in heterogeneous conditions, in buffer and CH_2Cl_2/buffer medium. About oxidations carried out in aqueous solution, lignin (100.0 mg), tyrosinase (3000 U) and ascorbic acid were suspended in Na-phosphate buffer pH 7.0 (5.0 mL) at 25°C under vigorous stirring. The presence of ascorbic acid ensures the reduction of eventually-produced quinones to catechols (Figure 5.4). About biphasic oxidations, lignin (100.0 mg), tyrosinase (3000 U) and Na-phosphate buffer pH 7.0 (100.0 µL) were placed in 5.0 mL of CH_2Cl_2 at 25°C, in vigorous stirring. The work up was the same for both reactions: after 24 h, the mixture was acidified at pH 3.0 and centrifuged with Vivaspin® tubes equipped with 3.0 kDa MWCO membranes. Retained lignin was washed with water three times to eliminate solubilized lignin oligomers and then freeze-dried; lyophilized lignin was analyzed by ^{31}P NMR and GPC. The filtrate were extracted twice with EtOAc, dried over anhydrous Na_2SO_4 and concentrated under vacuum to yield coloured crude analyzed then by GC-MS.

5.4.3 Quantitative ^{31}PNMR

Derivatization of the sample with 2-chloro-4,4',5,5'-tetramethyl-1,3,2-dioxaphospholane was performed as previously described.[19] Samples of lignin (30.0 mg) were dissolved in a solvent mixture composed of pyridine and deuterated chloroform, [Py:$CDCl_3$ 1.6:1.0 (v/v)] (0.4 mL). Tetramethylphospholane (0.1 ml) was then added, followed by solution (0.1 ml) containing the internal standard (cholesterol) and the relaxation reagent (Chromiuum(III) acetylacetonate). The NMR spectra were recorded on a NMR Bruker 400 MHz spectrometer using reported methods.[19]

Data reported are the means of three phosphitylation experiments with a standard deviation of $2x10^{-2}$ mmol g^{-1}.

5.4.4 GPC analysis of lignin

Acetobromination of lignin samples for GPC analysis was carried out following the procedure described previously.[20] Briefly, 10.0 mg of lignin is suspended in acetic acid glacial/acetyl bromide mixture (2.5 ml of 92:8 v/v) and stirred at room temperature. After 2 h the solvent is evaporated under vacuum and then the residue is dissolved in 5.0 ml THF. The GPC analyses were performed using a Shimadzu LC 20AT liquid chromatograph with a SPD M20A ultraviolet diode array (UV) detector set at 280 nm. The sample (20.0 µl) is injected into a system of columns connected in series (Varian PL gel MIXED-D 5 µm, 1-40 K and PL gel MIXED-D 5 µm, MW 500-20 K) and the analysis is carried out using THF as eluent at a flow rate of 0.50 ml/min.

5.4.5 GC-MS analysis

The coloured crude obtained after EtOAc extraction was silanized using reported conditions.[22] The residue was treated with pyridine, hexamethyldisilazane (HMDS) and trimethylchlorosilane (TMCS) (HMDS:TMCS, 2:1 v/v) under vigorous stirring at room temperature. After 1 h solution was centrifuged and the surnatant (1.0 µl) was analysed by a GCMS-QP5050 Shimadzu apparatus using a SPB column (25 m × 0.25 mm and 0.25 mm film thickness) and an isothermal temperature profile of 100°C for 2 min, followed by a 10 °C/min temperature gradient to 280°C for 30 min. The injector temperature was 280°C. Chromatography-grade helium was used as the carrier gas with a flow of 1.0 mL/min. Mass spectra were recorded with an electron beam of 70 eV. Quantitative analyses were performed using dodecane as internal standard.

5.4.6 Tyrosinase immobilization

Tyrosinase was immobilized as previously described (i) on Eupergit®C250L (Tyro/E) and (ii) on Eupergit®C250L coated by Layer-by-Layer method (Tyro/E-LbL) using PAH and PSS as polyelectrolytes (for detail see Chapter 4, paragraphs 4.4.2 and 4.4.3). The amount in milligrams and the units of coupled tyrosinase (Tyro/E and Tyro/E-LbL) were calculated by the difference between the amount/units loaded and that recovered in the washings by conventional Bradford and activity assay (Chapter 4, paragraphs 4.4.4 and 4.4.5).

References

[1] Lewis, N.G.; Davin, L.B.; Sarkanen, S. In *Lignin and Lignan Biosynthesis* (Lewis, N.G.; Sarkanen, S. eds.), *ACS SymposUm series N. 697,* **1996,** Washington DC.

[2] Pearl, I. W. In *The Chemistry of Lignin*, (Marcel Dekker ed.), **1967,** New York.

[3] a) Alen, R. In: Forest product chemistry (StenUs, P. ed). **2000,** 12-58, Fapet Oy, Jyväskylä; b) Sjöström, E. in *Wood chemistry, fundamentals and applications* (Sjöström, E. ed), **1993,** Academic press, San Diego.

[4] Herman, F.M. In *Encyclopedia of Polymer Science and Technology,* **2004,** 100-109, Wiley-Interscience

[5] Eriksson, K.-E.L.; Blanchette, R.A.; Ander, P. In *Microbial and enzymatic degradation of wood components*, **1990,** Springer-Verlag, Berlin.

[6] Blanchette, R.A. *Annu Rev Phytophatol,* **1991**, *29*, 381-398.

[7] Grönqvist, S.; Suurnäkki, A.; Niku-Paavola, M-L.; Kruus, K.; Buchert, J.; Viikari, L. In *Applications of enzymes to lignocellulosics* (Mansfield, S.D.; Saddler, J.N. eds), **2003,** 46–65, ACS, Washington, DC.

[8] a) Perazzini, R.; Saladino, R.; Guazzaroni, M.; Crestini, C. *Bioorg Med Chem* ***2011,*** *19,* 440-447; b) Crestini, C.; Melone, F.; Saladino, R. *Bioorg Med Chem* ***2011,*** *19(16),* 5071-5078; c) Crestini, C.; Perazzini, R.; Saladino, R. *Appl Catal A* ***2010****, 372,* 115-123; d) Hong, F.; Joensson, L.J.; Lundquist, K.; Wei, Y. *Appl Biochem Biotechnol* **2006**, *129-132*, 303-319.

[9] Sánches-Ferrer, A.; Rodriguez-López, J.N.; Garcia-Cánovas, F.; Garcia-Carmonia, F. *Biochim Biophys Acta* ***1995,*** *1247*, 1-11

[10] a) Grönqvist, S.; Viikari, L.; Niku-Paavola, M.-L.; Orlandi, M.; Canevali, C.; Buchert, J. *Appl Microbiol Biotechnol* **2005**, *67*, 489-494; b) Kaplan, D.L. *Photochemistry* **1979,** *18*, 1917-1919.

[11] a) Nakano, J.; Mechitsuka, G. In *Methods in Lignin Chemistry* (Lin, S.Y.; Dence, C.W. eds.), **1992**, 23-32, Berlin Heideberg, Springer-Verlag; b) Obst, J.R.; Kirk, T.K. *Method Enzymol* **1981**, *161*, 3-12.

[12] a) Granata, A.; Argyropoulos, D.S. *J Agric Food Chem*, **1995**, *43*, 1538-1544; b) Dence, C.W. In *Methods in Lignin Chemistry*, (Lin, S.Y.; Dence, C.W. eds.), **1992**, 33-61, Berlin Heideberg, Springer-Verlag.

[13] Argyropoulos, D.S. *Res Chem Intermed* **1995**, *21*, 373-395.

[14] Ashcroft, A.E. In *Ionization Methods in Organic Mass Spectrometry* (Barnett, N.W. ed.), **1997,** Cambridge, The Royal Society of Chemistry.

[15] Gellerstedt, G. In *Methods in Lignin Chemistry* (Lin, S.Y.; Dence, C.W. eds.), **1992**, 487-497, Berlin Heideberg, Springer-Verlag.

[16] a) Ramsden, C.A.; Stratford, M.R.L.; Riley, P.A. *Org. Biomol. Chem.,* **2009**, *7*, 3388-3390; b) Muñoz-Muñoz, J.L.; García-Molina, F.; García-Ruiz, P.A.; Molina-Alarcón, M.; Tudela, J.; García-Canovas, F.; Rodriguez-Lopez, J.N. *Biochem. J.* **2008** *416,* 431-440; c) Espín, J.C.; Soler-Rivas, C.; Cantos, E.; Tomás-Barberán, F.A.; Wichers, H.J. *J. Agric. Food Chem.,* **2001**, *49 (3)*, 1187–1193. d) Brown, R.S.; Male, K. B.; Luong, J.H.T. *Anal. Biochem.* **1994**, *222*, 131-139.

[17] Decher, G. *Science* **1997**, *277*, 1232-1237.

[18] a) Perron, N. R.; García, C. R.; Pinzón, J. R.; Chaur, M. N.; Brumaghim, J. L. *J. Inorg. Biochem.* **2011,** *105,* 745-753; b) Perron, N. R.; Brumaghim, J. L. *Cell Biochem Biophys* **2009,** *53*, 75-100; c) Ginja Teixeira, J.; Barrocas Dias, C.; Martins Teixeira, D. *Electroanalysis* **2009**, *21*, 2345-2353.

[19] a) Peyratout, C.S.; Dähne, L. *Angew Chem Int Ed* **2004**, *43*, 3762-3783; b) Argyropoulos, D.S. *Res Chem Intermed* **1995**, *21,* 373-395; c) Granata, A.; Argyropoulos, D.S. *J Agric Food Chem* **1995**, *33*, 375-382.

[20] Lu, F.; Ralph, J. *J Agric Food Chem* **1998**, *46*, 547-552.

[21] a) MarongU, B.; Piras, A.; Porcedda, S.; Tuveri, E.; Sanjust, E.; Meli, M.; Sollai, F.; Zucca, P.; Rescigno, A. *J Agric Food Chem* **2007**, *55,* 10022-10027; b) Bouchilloux, S.; McMahill, P.; Mason, H.S. *J Biol Chem* **1963**, *238*, 1699-1707.

[22] a) Rodríguez-López, J.N.; Gómez-Fenoll, L.; Penalver, M.J.; García-Ruíz, P.A.; Varón, V.; Martínez-Ortíz, F.; García-Cánovas, F.; Tudela, J. *Biochim Biophys Acta* **2001**, *1548*, 238-256; b) Sweely, C.C.; Bentlry, R.; Makita, M.; Wells, W.W. *J Am Chem Soc* **1963**, *85,* 2497-2507.

Chapter 6

Immobilized laccase in chemical biotransformation: synthesis of aldehyde by laccase mediator system

6.1 Introduction

Laccases (EC 1.10.3.2, *p*-diphenol: dioxygen oxidoreductase) are multicopper oxidative enzymes that catalyze the oxidation of four molecules of substrate through the reduction of a dioxygen (O_2) to two water molecules.[1] The industrial interest in the application of these enzymes lies in the low substrate selectivity, high value of catalytic constants, use of air oxygen as primary oxidant and high thermal resistance.[2] However, laccases possess relative low redox potential [E^0= 0.5 to 0.8 V versus NHE (normal hydrogen electrode)] compared to other oxidases. [3] The redox potential is an essential factor in determining the feasibility of redox reactions. Enzymes can only oxidize substrates that have lower redox potentials than their own; thus, the action of laccase would be restricted to the oxidation of a small number of compounds, as the phenolic lignin moiety, whereas non-phenolic substrates, having high redox potential, cannot be oxidized directly.[4] Nevertheless, this limitation has been overcome by using redox mediators in the so-called laccase-mediator systems (LMS). Mediators are small molecules that act as electrons shuttles, providing the oxidation of complex substrates. Once oxidized by the enzyme and stabilized in more or less stable radicals, mediators diffuse far away from the enzymatic active site and, by mechanisms different from the enzymatic one, enable the oxidation of target compounds that in principle are not suitable for laccase, because of their encumbering size or high redox potential. In this way, laccases can oxidize "unnatural" compounds increasing their biotechnological applications in fine organic synthesis.[5] A general rise in laccase reactivity has been shown using mediators, such as ABTS [2,2'-azinobis-(3-ethylbenzothiazoline-6-sulphonic acid); E^0= 0.5 V[6]], HBT (1-hydroxybenzotriazole; E^0= 1.13 V[7]), VLA (violuric acid; E^0= 0.97 V[90]) and TEMPO (2,2,6,6-tetramethyl-1-piperidinyloxy free radical, E^0= 0.75 V[8]). It has been demonstrated that, depending on their chemical structure, mediators follow three different mechanisms of oxidation. Compounds as ABTS follow the electron-transfer (ET) mechanism (Figure 6.1a);[9] N–OH compounds, such as HBT and VLA prefer the radical H-abstraction (HAT) pathway (Figure 6.1b);[10] and TEMPO undergoes in one-electron transfer mechanisms to form the oxoammonium ion (Figure 6.1c).[11]

Recently laccase received particular attention for the oxidation of primary alcohols to corresponding aldehydes as alternative to traditional chemical synthesis, based on transition metal catalysis (palladium,[12] platinum[13] and ruthenium[14]) and inorganic oxidant as chromium (VI) salt.[15] In homogeneous condition, different kind of mediators (including TEMPO, HBT, ABTS and VLA) were used and compared for the oxidation of benzyl alcohol derivatives, based-TEMPO LMS resultant the best.[16] The mechanism of benzyl alcohol oxidation mediated by TEMPO was described by Tromp et al. in 2010.[17]

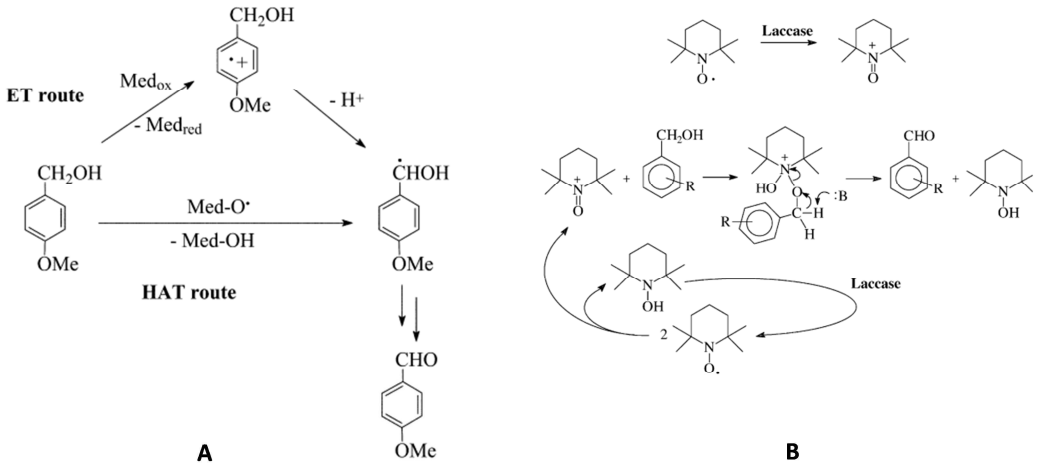

Figure 6.1 Reaction mechanism of primary alcohol oxidation by (A) the ET and HAT route; (B) the TEMPO mechanism. (adapted from Baiocco et al.[11a] and Fabbrini et al.[16b])

Although studies on the synthesis of aldehydes mediated by laccases has increased in recent years, the industrial application of the enzyme is still limited since the stability and catalytic activity of laccases are considerably affected by a wide variety of environmental conditions.[18] One approach to overcome these constraints is the use of immobilized laccases. In fact immobilized enzymes allow easy recovery of products, multiple reuses of the biocatalyst, plug flow processes, rapid termination of reactions and a greater variety of bioreactor designs. Immobilized laccases have been extensively reported in the scientific literature.[19] In this Chapter the oxidation of some primary alcohols by three immobilized laccase systems will be describe. The first heterogeneous biocatalists was based on the chemical immobilization of laccase on the epoxy-resin Eupergit®C250L (Lac/E); the second one was based on the coating of the Lac/E system by the Layer-by-Layer (LbL) method (Lac/E-LbL) and the third one was based on the chemical immobilization of laccase on alumina particles and its covering by LbL (Lac/Al). The Layer-by-Layer technique, based on the consecutive deposition of alternatively charged polyelectrolytes onto a surface, have the ability (i) to protect encapsulated protein from high-molecular-weight denaturing agents and (ii) to allow regulation of the permeability towards small substrates, which can enter the multilayer and react with the catalytic site of the enzyme.[20] Alcohol oxidations were performed in heterogeneous conditions in the presence of TEMPO, ABTS, HBT and

VLA as mediators. Lac/E, Lac/E-LbL and Lac/Al biocatalysts were also studied and compared for their kinetic properties, pH optimum, storage and thermal stability assay.

6.2 Results and discussions

6.2.1 Laccase immobilization

Laccase immobilization was first performed on the epoxy-activated acrylic beads of Eupergit®C250L, using a modification of previously reported procedures.[34] Briefly, laccase (Lac, 1.5 mg, 230 U mg^{-1}) was suspended in binding buffer (8.0 ml, Na-phosphate buffer 0.1 M, pH 7.0) in the presence of Eupergit®C250L (1.0 g) for 24 h at room temperature. The immobilized tyrosinases (Lac/E) were washed with water to remove excess of protein and treated with ethanolamine to block residual epoxy-groups (Figure 6.2).

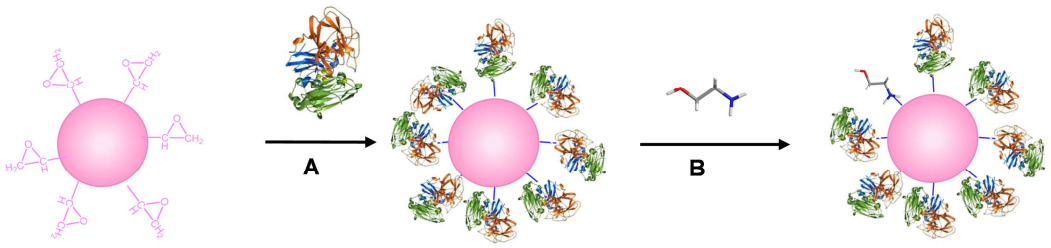

Figure 6.2 Scheme of laccase immobilization on Eupergit®C250L: (A) laccase cross-linking with the support; (B) treatment with glycine to block residual epoxy-groups.

The effectiveness of the immobilization procedure was investigated in terms of Immobilization Yield and Activity Yield (Eq. 3.1 and Eq. 3.2, Chapter 3) by the analysis of the residual enzymatic activity in the waste waters after the reaction with the support. Under these experimental conditions 200 U (58%) of laccase were immobilized, retaining about 66% of its native activity (132 U g^{-1}). With the aim to further increase the stability of Lac/E, the LbL technique was applied by coating the particles by a sequential deposition of alternatively charged polyelectrolytes. Briefly, biocatalysts were suspended in positively charged polyallylamine hydrochloride (PAH) (2.0 mg mL^{-1} in 0.5 M NaCl), filtrated and then treated with negatively charged polystyrene sulphonate (PSS) (2.0 mg mL^{-1} in 0.5 M NaCl) (Figure 6.3). This procedure was repeated until the formation of three layers. The deposition procedure started with PAH to ensure electrostatic interaction with the negatively charged laccase (laccase Isoelectric Point = 3.5[21]). The immobilized LbL enzyme (Lac/E-LbL) showed an activity of 123 U g^{-1} corresponding to about 93% of activity with reference to Lac/E. Laccase was also immobilized using a third method based on a first chemical binding of enzyme on alumina particle and its covering with LbL method as reported.[22] Briefly, alumina particles (Al_2O_3, 50.0 g) were first functionalized with

γ-aminopropyltriethoxysilane and glutaraldehyde and then suspended for 24 h in 100.0 mL of laccase solution (20 U ml^{-1}) in 0.1 M acetate buffer pH 5.0. After immobilization, the system was covered with PAH and PSS to obtain the formation of three layers (PAH^{+}-PSS^{-}-PAH^{+}). Even in this case, deposition started with positively charged PAH (Figure 6.4).

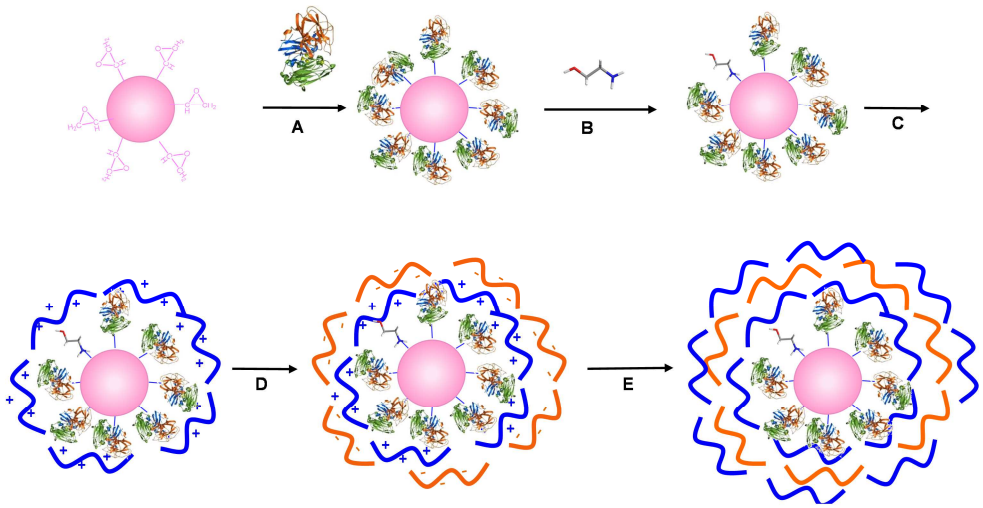

Figure 6.3 Scheme of preparation of PAH/PSS-coated laccase/Eupergit®C250L: (A) laccase cross-linking with the support; (B) treatment with glycine to block residual epoxy-groups; (C) PAH layer deposition; (D) PSS layer deposition; (E) LbL coating of supported laccase.

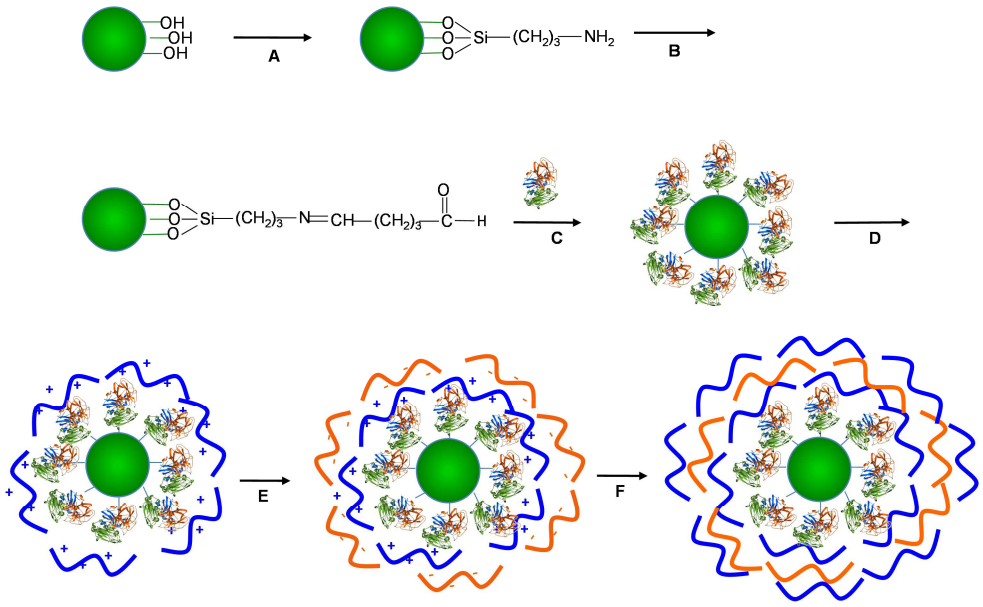

Figure 6.4 Scheme of preparation of PSS/PAH-coated laccase/alumina particles: (A) support silanization; (B) coupling with the cross-linker; (C) laccase cross-linking with the support; (D) PAH layer deposition; (E) PSS layer deposition; (F) further PAH layer deposition to complete the LbL coating of supported laccase.

Under these experimental conditions 1400 U (70%) of laccase were immobilized. Lac/Al retained about 50% of its native activity (28 U g^{-1}). Figure 6.5 shows the Scanning Electron Microscopy (SEM)

photographs of the immobilised enzyme before and after PSS/PAH coating on Eupergit® C250L beads (Figure 6.5a and Figure 6.5b) and on alumina particles (Figure 6.5c and Figure 6.5d).

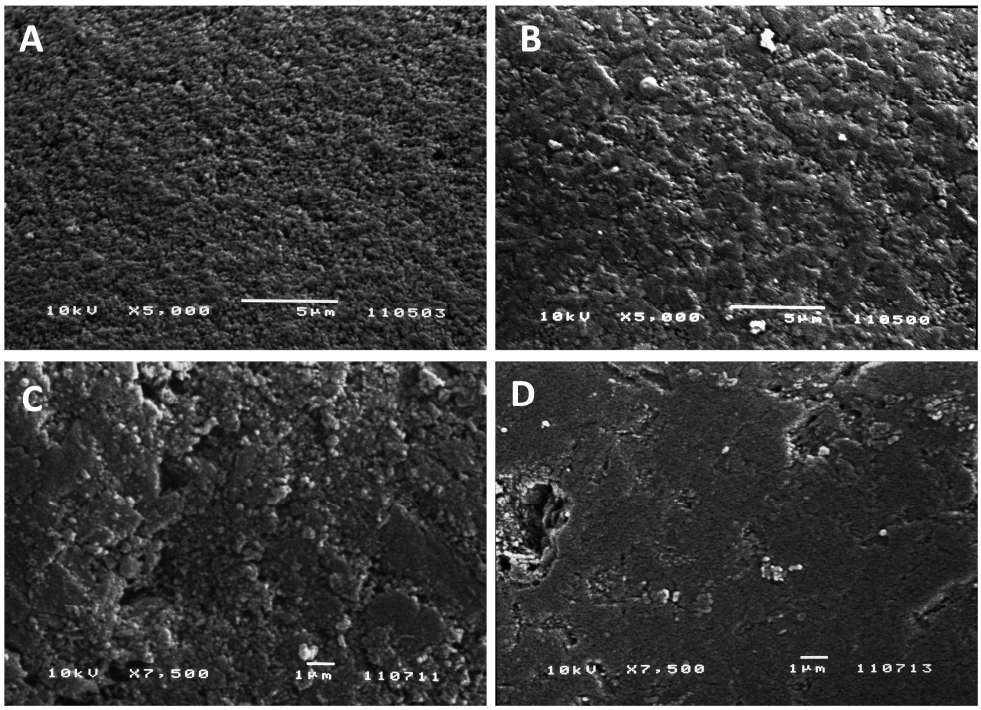

Figure 6.5 SEM images of the immobilised laccase before and after PSS/PAH coating on Eupergit® C250L beads (A and B, respectively) and on alumina particles (C and D, respectively).

The polyelectrolyte deposition was further confirmed by the Transmission Electron Microscopy (TEM) analysis of Lac/E-LbL where the PSS/PAH coating was highlighted by thickening of the surface of the capsules (Figure 6.6).

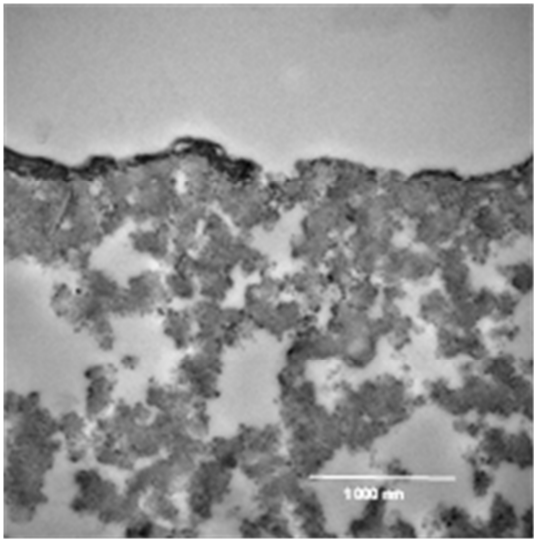

Figure 6.6 TEM images of Lac/E-LbL.

6.2.2 Kinetic parameters of immobilized laccases

Immobilized laccase systems were characterized for their kinetic properties using ABTS (4.0-13.0 mM) as substrate and plotting data to a double reciprocal plot Lineweaver-Burk plot (Table 6.1, Figure 6.7).

Table 6.1 Kinetic parameters of free (Lac) and immobilized laccase (Lac/E, Lac/E-LbL, Lac/Al).

Entry	Enzyme	K_m (mM)	V_{max} [a] ($x10^{-3}$)	V_{max}/K_m [b] ($x10^{-3}$)
1	Lac	1.6	1381.6	875.2
2	Lac/E	2.1	779.1	360.8
3	Lac/E-LbL	2.4	619.0	262.7
4	Lac/Al	2.4	596.3	252.1

[a] V_{max} was defined as ΔAbs (min μg_{enzyme})$^{-1}$. [b] V_{max}/K_m was defined as ΔAbs (min μg_{enzyme} mM)$^{-1}$. Each experiment was conducted in triplicate. Average errors in kinetic parameters were ± 2-4% for K_m and ±1-3% for V_{max}.

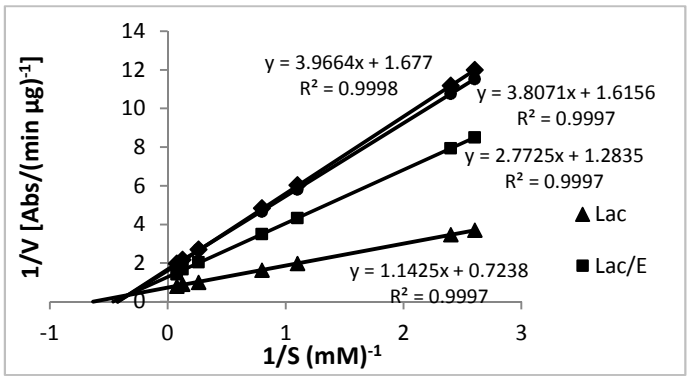

Figure 6.7 Lineweaver-Burk plots of free (Lac) and immobilized laccase (Lac/E, Lac/E-LbL, Lac/Al) activity determined at different concentrations of ABTS (4.0-13.0 mM). Data are the mean values of three experiments with standard deviation less than 1%.

Irrespective to procedures used for the immobilization, V_{max} decreased and K_m increased for supported tyrosinases, leading to a reduction of the catalytic efficiency with respect to free enzyme. Similar trends in K_m values were reported for laccase immobilized on Eupergit® and other support and are attributed to a possible mass transfer limitations.[23]

6.2.3 Effect of pH on laccase activity

The pH/activity curves related to free (Lac) and immobilized laccase (Lac/E, Lac/E-LbL and Lac/Al) at 25°C are shown in Figure 6.8. Immobilization of enzymes on charged supports often leads to displacements of the pH-activity profile to either alkaline or acidic regions.[24] In the present study, the pH-activity profile of immobilized laccase was similar to that of the free counterpart (optimum pH 5.0). At low pH value (2.0-4.0) Lac/Al and Lac/E-LbL retained more activity than Lac/E, confirming

the beneficial effect exerted by the polyelectrolyte coating on the maintenance of the active enzyme conformation.

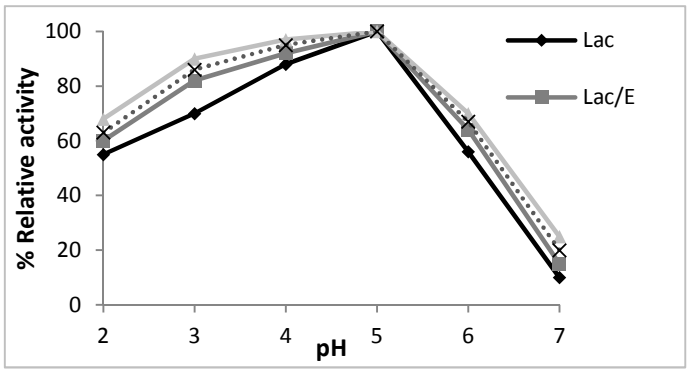

Figure 6.8 Optimal pH of free (Lac) and immobilized laccase (Lac/E , Lac/E-LbL, Lac/Al). Laccase activity was determined using ABTS as substrate in the range of pH 2.0–7.0. Results are the mean of triplicate assays.

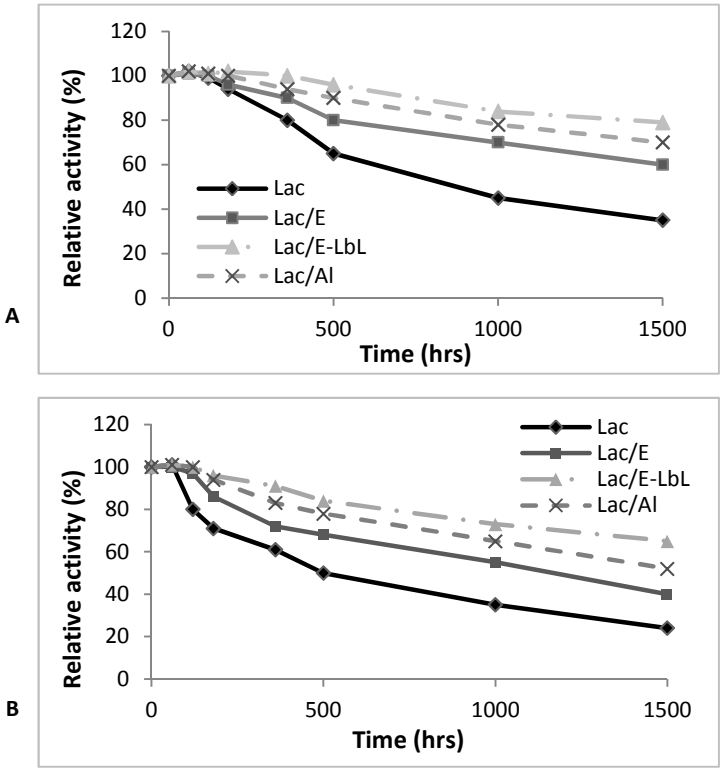

Figure 6.9 pH stability of free (Lac) and immobilized laccase (Lac/E, Lac/E-LbL and Lac/Al) incubated for 24 h at 25°C in acetate buffer 0.1 M pH 4 (A) and pH 3 (B). Data are the means of three experiments. Standard deviations of data were less than 6%.

The stability of laccase incubated for 24 h at 25°C in various pH buffers (pH 3.0-4.0) was reported in Figure 6.9. At pH 3.0 and 4.0 laccase showed a quick decreased in enzyme activity respect to storage at optimal pH 5.0, where after 48 h the enzyme maintain more than 95% of activity (see below, Figure 6.10). Specifically laccase was inactivated more rapidly at pH 3.0 than pH 4.0 (Figure 6.9a and Figure

6.9b, respectively). For each of the case reported, immobilized laccase maintained higher activity respect to free enzyme; LbL being the best immobilization procedure.

6.2.4 Storage and thermal stability

The stability of free and immobilized laccase was evaluated by storing the enzyme in Na-acetate buffer 0.1 M, pH 5.0 at 4°C for 30 days. At specific times, the activity was measured by the ABTS assay after the warming of the solution at room temperature. In Figure 6.10 laccase activity was expressed as relative percentage activity with respect to that at time zero. At each of the temperature studied, immobilized laccases were more stable than free enzyme, being the Lac/E-LbL the most stable biocatalyst retaining after 30 days more than 80% of native activity.

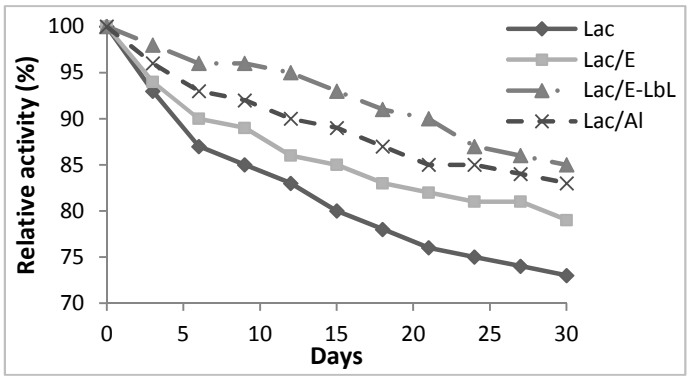

Figure 6.10 Storage stability of free (Lac) and immobilized laccase (Lac/E, Lac/E-LbL, Lac/Al) at 4°C in Na-acetate buffer 0.1 M, pH 5.0. Data are the means of three experiments. Standard deviations of data were less than 6%.

The thermal stability of laccase was also evaluated by storing the enzyme in Na-acetate buffer at 40 and 50°C and measuring the residual enzyme activity by the ABTS assay at specific time, after the solution was cooled to room temperature (Figure 6.11). Even in these assays, Lac/E-LbL was the most stable biocatalyst retaining more than 80% of activity after 200 h at 40°C and more than 60% after 20 h at 50°C. The major stability of immobilized laccase has been explained by hypothesis that the multipoint attachment of enzymes to solid supports could increase thermal and pH stability by stiffening of the protein structure.[25] Moreover, the presence of the polyelectrolyte coating further increases the stability of the enzyme preventing its denaturation.

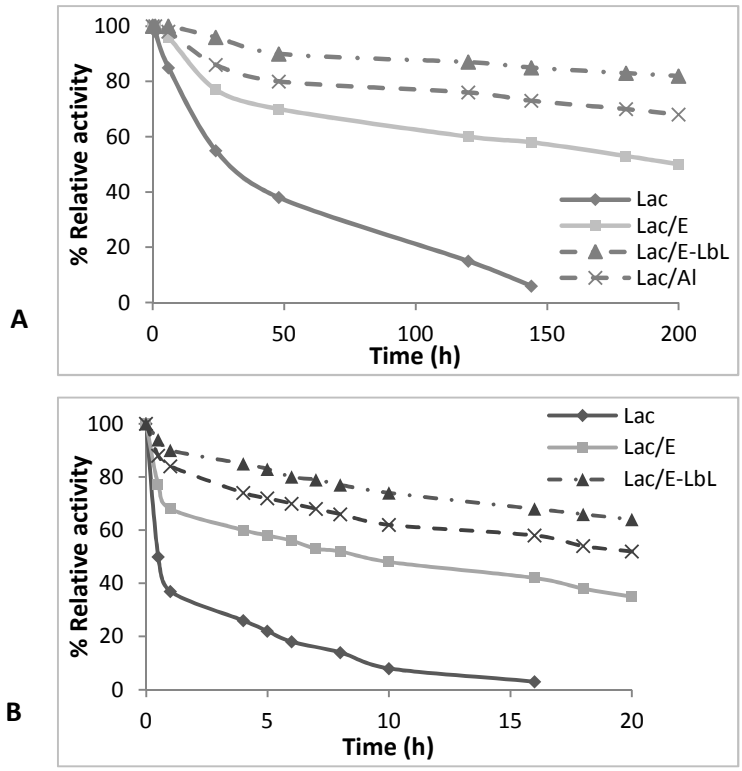

Figure 6.11 Storage stability of free (Lac) and immobilized laccase (Lac/E, Lac/E-LbL, Lac/Al) at (A) 40°C and (B) at 50°C in Na-acetate buffer 0.1 M, pH 5.0. Data are the means of three experiments. Standard deviations of data were less than 6%.

6.2.5 Alcohol oxidations

With the aim to evaluate and compare the catalytic relevance of immobilized laccases, a panel of alcohols (Figure 6.12) were oxidized, including benzyl alcohol **1**, 4-methoxybenzyl alcohol **2**, 3-methoxybenzyl alcohol **3**, 3,4-dimethoxybenzyl alcohol **4**, 3,4,5-trimethoxybenzyl alcohol **5**, cinnamyl alcohol **6**, geraniol **7**, 2-chlorobenzyl alcohol **8**, 4-chlorobenzyl alcohol **9** and 3-chlorobenzyl alcohol **10.** For selected substrates a comparison between mediators TEMPO, HBT, ABTS and VLA were conducted to evaluate the influence of immobilization on the LMS. Reactions were performed using a modified procedure based on previously reported conditions in homogeneous processes.[16] Briefly, alcohol (20 mM), appropriate laccase (10 U) and mediator (6 mM) were placed in 0.1 M Na-acetate buffer pH 5.0 (3.0 mL) in vigorous stirring at room temperature. The yields of reactions were determined by GC-MS using acetophenone as internal standard. As expected, no oxidations were observed in the absence of mediator since these compounds are a non-phenolic substrate and, as such, are not a natural target of the enzyme.[26] Moreover, the lack of reactivity in the absence of enzyme confirms that laccase first oxidised mediators, and then the oxidised mediator converts alcohol to aldehyde.

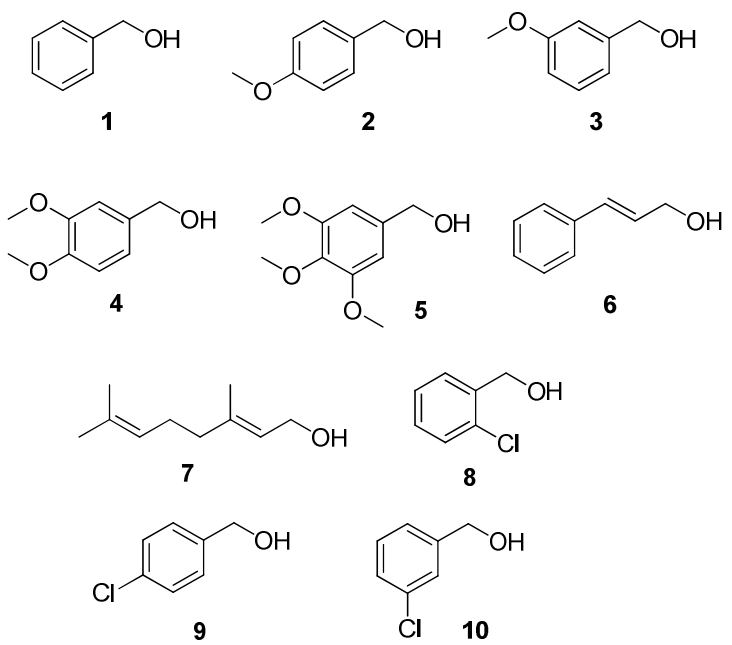

Figure 6.12 Alcohols oxidized by free and immobilized laccase mediator systems.

Irrespective to the mediator used in the transformation, the oxidation of **1** by immobilized laccase afforded aldehyde **11** as the only recovered product, the coated laccase being the most efficient heterogeneous system (Scheme 6.1, Table 6.2, entries 2-4 versus 1).

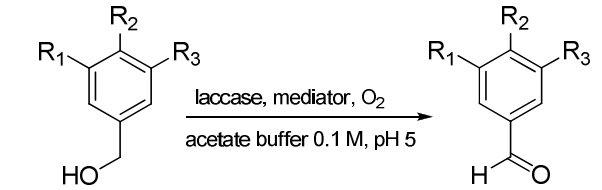

1,2,3,4,5 **11,12,13,14,15**

1,11: R_1=R_2=R_3=H;
2,12: R_1=R_3=H; R_2=OMe;
3,13: R_1=R_2=H; R_3=OMe;
4,14: R_1=H; R_2=R_3=OMe;
5,15: R_1=R_2=R_3=OMe;

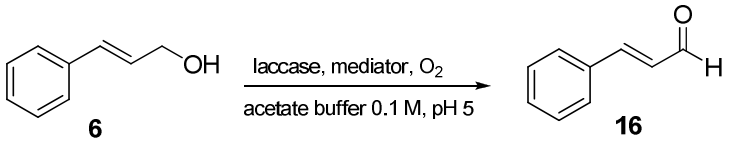

Scheme 6.1 Oxidation of alcohols 1-6.

Among mediators, TEMPO was the best system affording **11** in high yield and conversion of substrate (Table 6.2). The other mediators showed a yield lower than TEMPO: 43-48% with HBT, 4-10% with ABTS and 31-35% with VLA (Table 6.2, entries 2-4 versus 1). Similar results were obtained for the

oxidation of compounds **2-5** where the order of reactivity was TEMPO > HBT > VLA > ABTS. In particular TEMPO afforded a quantitative conversion of all substrates to corresponding aldehydes (Scheme 6.1, Table 6.2, entries 5-20). A different selectivity was observed for the other mediators. In particular, HBT showed the highest reactivity toward **4** (91-95% conversion, Scheme 6.1, Table 6.2, entries 13-16) and **5** (88-93% conversion, Scheme 6.1, Table 6.2, entries 17-20) respect to **2** (75-82% conversion, Scheme 6.1, Table 6.2, entries 5-8) and **3** (67-73% conversion, Scheme 6.1, Table 6.2, entries 9-13). Similarly, VLA showed the highest reactivity for compound **4** (65-72% conversion, Table 6.2, entries 13-16) and **5** (77-85% conversion, Table 6.2, entries 17-20) with respect to **2** (62-69% conversion, Table 6.2, entries 5-8) and **3** (45-50% conversion, Table 6.2, entries 9-12).

Table 6.2 Oxidation of alcohols 1-6.[a]

Entry	Substrate	Biocatalysts	Products	Yield (%)[b]			
				TEMPO	HBT[c]	ABTS[c]	VLA[c]
1	**1**	Lac	**11**	96	43	4	31
2	**1**	Lac/E	**11**	96	45	6	32
3	**1**	Lac/E-LbL	**11**	96	48	10	35
4	**1**	Lac/Al	**11**	96	46	8	33
5	**2**	Lac	**12**	>99	75	18	62
6	**2**	Lac/E	**12**	>99	79	20	65
7	**2**	Lac/E-LbL	**12**	>99	82	23	69
8	**2**	Lac/Al	**12**	>99	81	21	66
9	**3**	Lac	**13**	>99	67	13	45
10	**3**	Lac/E	**13**	>99	69	15	48
11	**3**	Lac/E-LbL	**13**	>99	73	25	53
12	**3**	Lac/Al	**13**	>99	70	20	50
13	**4**	Lac	**14**	>99	91	38	65
14	**4**	Lac/E	**14**	>99	93	40	67
15	**4**	Lac/E-LbL	**14**	>99	95	45	72
16	**4**	Lac/Al	**14**	>99	91	42	69
17	**5**	Lac	**15**	>99	88	45	77
18	**5**	Lac/E	**15**	>99	90	46	80
19	**5**	Lac/E-LbL	**15**	>99	93	49	85
20	**5**	Lac/Al	**15**	>99	91	48	82
21	**6**	Lac	**16**	97	58	6	21
22	**6**	Lac/E	**16**	97	60	8	23
23	**6**	Lac/E-LbL	**16**	99	63	12	27
24	**6**	Lac/Al	**16**	98	62	10	25

[a] Reaction conditions: substrate (20 mM), mediator (6 mM) and laccase (10 U) were taken in 3.0 mL of acetate buffer pH 5.0 for 12 h. [b] Conversion and yield were calculated by GC-MS analysis using acetophenone as internal standard; [c] Reaction performed for 24h.

A different response was showed by ABTS that produced **14** in appreciable yield (38-45%, Table 6.2, entries 13-16) while aldehyde **12, 13** and **15** were obtained in low yield and conversion of substrates (13-25%, Table 6.2, entries 5-12 and 17-20). TEMPO proved the best mediator also for the oxidation

of **6**, affording **16** as the only recovered product in 97-99% yield (Table 6.2, entries 21-24); again the Lac/E-LbL was the most efficient catalyst. Even in this case ABTS resulted as the lower reactive mediator affording **16** in lower yield (6-12%) with respect to VLA (21-27%) and HBT (58-63%) (Table 6.2, entries 21-24). The different reactivity of LMS toward substrates **1-6** are in accordance with data reported by Fabbrini et al., [16b] and can be explained by the different action mechanism of mediators. Taking ABTS as an example, its oxidised state (Med_{ox}) form is found to oxidise 3,4,5-trimethoxybenzyl alcohol **5** much better than the structurally similar alcohol that differs only for an higher redox potential, as brought about by the different number of electron-donor methoxy substituents in the aromatic ring. This consistency between redox potential of the substrate and conversion to products supports the operation of an ET mechanism (Figure 6.1a). The initial monoelectronic oxidation of the benzylic alcohol by the oxidised mediator (being the faster with the precursor of lower redox potential) is followed by a fast C-H deprotonation of the intermediate radical cation of the alcohol,[27] that drives the conversion to aldehyde. The mediators HBT and VLA share the structural feature of being N-OH derivatives. These mediators, at variance with ABTS, are able to react even with the stable compounds **1** and **6**, the conversion gradually increasing with **2**-**5**. A radical H-abstraction route of oxidation can be inferred where the redox features of the substrate have marginal importance (Figure 6.1a).[16a] The initial step of the HAT process would be the conversion of the mediator into a radical cation by monoelectronic enzymatic oxidation. Deprotonation of the radical cation of the mediator then follows, to give the corresponding N-oxyl radical (Med_{ox}) that abstracts the benzylic hydrogen from the substrate, thereby giving rise to the aldehyde.[28] In the HAT radical route, the redox potential of the substrate has a negligible relevance on reactivity. However, effects arising from the polarity of the N-oxyl radical, an electrophilic radical, and from the electron-richness of the substrate, could provide a dipolar stabilisation to the radical transition state of H-abstraction, due to the important contribution from a charge-separated resonance structure.[29] Thereby explaining the slightly higher oxidation yields obtained with methoxy-substituted substrates, bearing electron-donor groups. However Baiocco et al.[11a] demonstrated that this polar effects are small, compared with ABTS, as it can be seen by the appreciable yield of compounds **1** and **6**. In contrast, with TEMPO, the conversion of all substrates occurred in very high yields, thereby suggesting the presence of an oxidation mechanism that does not respond to the redox features of the substrate (Figure 6.1b). In the literature was reported that the active form of TEMPO is the oxoammonium ion formed by the oxidation of the N-oxyl radical by laccase. The oxoammonium ion was responsible for the oxidation of the alcohol to aldehyde producing the hydroxylamine. The N-oxyl species was then regenerated by a comproportionation with the oxoammonium cations.[17] These comparative oxidations demonstrate that the polylectrolyte layers used in immobilization procedure did not alter the catalytic mechanism of the laccase mediator system; indeed, since Lac/E-LbL and Lac/Al afforded aldehyde in higher yield

respect to Lac and Lac/E, the coating process seems to have a beneficial stabilizing effect on the oxidized mediator form. An enhanced activity of LMS in the presence of polyelectrolyte coating was also reported in literature.[22]

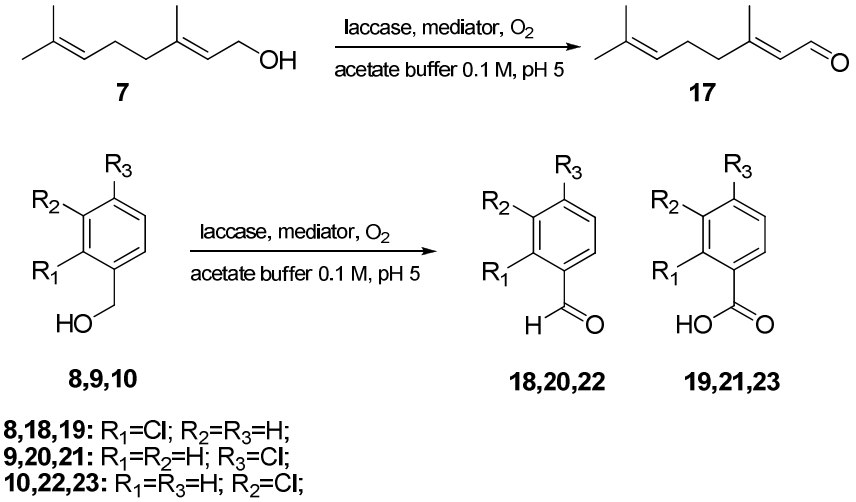

Scheme 6.2 Oxidation of alcohols 7-10.

The study proceeded with the analysis of the efficiency of LMS system using an aliphatic alcohol as substrate. The oxidation of geraniol **7** gave the best results using TEMPO as mediator and afforded aldehyde **17** as the only recovered product in high yield and conversion of substrate (93-95%). On the contrary, with HBT and VLA the yield was low (31-48%), while with ABTS the effect was negligible (4-6%, Scheme 6.2, Table 6.3, entries 1-3). Even in these cases, coated-immobilized biocatalysts were the most efficient systems (Table 6.3, entries 3-4 versus 1-2). The oxidation of three chlorobenzyl alcohols, 2-chlorobenzyl alcohol **8**, 4-chlorobenzyl alcohol **9** and 3-chlorobenzyl alcohol **10** was also studied. For these substrates, reaction conditions were first optimized in homogeneous condition in the presence of TEMPO as mediator, to enhance the synthesis of the corresponding aldehydes. Specifically, the oxidation of **8** performed for 3 h afforded aldehyde **18** and carboxylic acid **19** in ratio 1:1 and 50% conversion of substrate (Scheme 6.2, Table 6.3, entry 5). For decreasing reaction time, **18** was obtained in higher yield respect to **19** (ratio 1.7:1.0 mol/mol), even if with a low conversion of substrate (Table 6.3, entry 6). As expected, for long time, compound **19** became the major reaction product (Table 6.3, entry 7). This trend suggests the formation of **19** as by-product of further oxidation of the aldehyde. Similar behaviour was observed in heterogeneous conditions where it was not possible to obtain **18** as the only recovered product (Table 6.3, entry 8-10). Reactions performed with HBT and VLA produced **18** as the only recovered product (Table 6.3, entries 8-10), while in the presence of ABTS compound **8** did not react (Table 6.3, entries 8-10). These data are in accordance with previously reported data where the laccase/ABTS system was found to be unreactive towards

benzylic alcohols lacking at least one aromatic hydrogen atom at the *ortho*-positions of the substrate.[16c]

Table 6.3 Oxidation of alcohols 7-10.[a]

Entry	Substrate	Biocatalysts	Products	Yield (%)[b]			
				TEMPO	HBT[c]	ABTS[c]	VLA[c]
1	**7**	Lac	**17**	93	41	4	31
2	**7**	Lac/E	**17**	93	43	6	32
3	**7**	Lac/E-LbL	**17**	95	48	8	34
4	**7**	Lac/Al	**17**	94	46	8	33
5	**8**	Lac	**18(19)**	25(25)	-	-	-
6	**8**	Lac	**18(19)**[c]	19(11)	-	-	-
7	**8**	Lac	**18(19)**[d]	14(56)	-	-	-
8	**8**	Lac/E	**18(19)**	23(21)	13	-	10
9	**8**	Lac/E-LbL	**18(19)**	24(23)	15	-	12
10	**8**	Lac/Al	**18(19)**	24(23)	14	-	12
11	**9**	Lac	**20(21)**	66(33)	-	-	-
12	**9**	Lac	**20(21)**[c]	68(22)	-	-	-
13	**9**	Lac	**20(21)**[d]	52(48)	-	-	-
14	**9**	Lac/E	**20(21)**[c]	68(21)	38	-	36
15	**9**	Lac/E-LbL	**20(21)**[c]	69(21)	41	-	38
16	**9**	Lac/Al	**20(21)**[c]	68(22)	42	-	40
17	**10**	Lac	**22(23)**[e]	35(55)	-	-	-
18	**10**	Lac	**22(23)**[c]	20(74)	-	-	-
19	**10**	Lac	**22(23)**	13(85)	-	-	-
20	**10**	Lac	**22(23)**[d]	8(90)	-	-	-
21	**10**	Lac/E	**22(23)**[e]	34(53)	25	-	21
22	**10**	Lac/E-LbL	**22(23)**[e]	36(54)	28	-	25
23	**10**	Lac/Al	**22(23)**[e]	35(53)	28	-	23

[a] Reaction conditions: substrate (20 mM), mediator (6 mM) and laccase (10 U) were taken in 3.0 mL of acetate buffer pH 5.0 for 3 h; [b] Conversion and yield were calculated by GC-MS analysis using acetophenone as internal standard; [c] Oxidation performed for 2 h; [d] Oxidation performed for 3.30 h. [e] Oxidation performed for 1.30 h.

As described for compound **8**, even in the case of oxidation of **9** and **10** in TEMPO/laccase system, varying the reaction time it was possible modify the ratio between aldehyde and carboxylic acid, confirming the further oxidation of compounds **20** and **22** to **21** and **23**, respectively (Scheme 6.2, Table 6.3, entries 11-13 and 17-20). As shown for the other chlorobenzyl alcohols, immobilized laccases exhibited a similar reaction pathway to free enzyme. Oxidation of **9** with HBT and VLA led to corresponding aldehyde in appreciable yield (36-42%, Table 6.3, entries 14-16). As expected, no oxidation was found for laccase/ABTS where the electron-withdrawing substituent in *para*- position negatively influenced the ET mechanism of mediator.[16a] Similar results were recorded for the oxidation of **10** performed with HBT, VLA and ABTS (Table 6.3, entries 14-16) as mediators. With the aim to evaluate the reusability of immobilized laccase we selected 4-methoxybenzyl alcohol **2** as representative alcohol derivative. Compound **2** (20 mM) was oxidized with immobilized laccase (10 U)

and TEMPO (6 mM) under previously reported experimental conditions. After 10 h, the immobilized biocatalyst was recovered, washed and reused with fresh added substrate and TEMPO. As shown in Figure 6.13 the immobilized laccase retained high activity, mainly for polyelectrolyte covered-systems (Lac/E-LbL ad Lac/Al) that showed more than 80% of conversion after 10 runs.

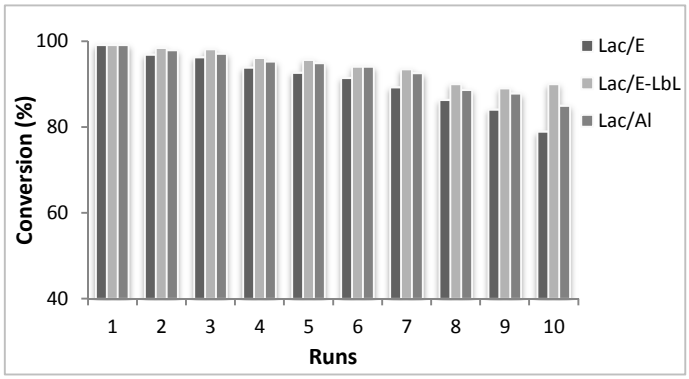

Figure 6.13 Conversion (%) of 2 after 10 runs. Each oxidation run was performed for 10 h. Results are the mean of three different experiments.

These results confirm reported data concerning the ability of microcapsules to create an internal microenvironment that protects the enzyme from denaturing agents.[30] Moreover, the restrictions imposed by immobilization might also be potentially beneficial for the retention of laccase activity in mediated reactions, due to the protective effect exerted by the support itself.[23b] In fact, radical species generated by mediator compounds can undergo chemical reactions with aromatic side-chains of laccase, thereby inactivating the enzyme.[31] From previous studies, the stability of the aminoxyl radical from VLA is known to be higher than that of the aminoxyl radical from HBT, this feature possibly enabling the reactive species to diffuse and cause stronger damage to the enzyme during the incubation time.[32] Alternatively, reaction of the oxidised mediator with the polymeric support employed could lead to undesired side processes; for example, oxidation of the alcoholic groups in alginates by TEMPO cannot be ruled out.[33]

6.3 Conclusions

Efficient heterogeneous biocatalysts were synthesized by immobilization of laccase on Eupergit®C250L, on Eupergit®C250L coated with polyelectrolytes, and on alumina particles covered by LbL method. In all systems laccase retained its catalytic activity even if LbL-based biocatalysts were more stable than other, in accordance with data reported in Chapter 3 and Chapter 4 for tyrosinase, confirming again the significant stabilizing and protective role exerted by the polyelectrolyte coating. Among LbL systems, Lac/E-LbL was more efficient than Lac/Al, suggesting that the chemical

immobilization through epoxy groups maintain more the conformational structure of enzyme respect to glutaraldehyde mediated binding. Moreover, immobilized laccase were stable enough to perform at least ten recycling experiments with a conversion higher than 80%. The stability of laccase at different pH and temperatures was also found to be increased in the presence of the support; Lac/E-LbL being again the most stable catalyst. The comparison between the catalytic efficiency of different LMS was made using TEMPO, HBT, VLA and ABTS as mediator of benzylic and aliphatic alcohols. With few exceptions, TEMPO provided the corresponding aldehyde in quantitative yield and conversion of substrates, while the efficiency of ABTS was strictly dependent on the redox potential of substrates. HBT and VLA exerted oxidations with high yields, although not comparable with those obtained with TEMPO. These data were in agreement with previously reported studies where the efficiency of LMS was correlated with the different action mechanism of mediators: electron transfer (ET) route for ABTS, radical H-abstraction (HAT) pathway for HBT and VLA and one-electron transfer mechanisms for TEMPO.

6.4 Experimental Section

Trametes versicolor laccase (Lac), Eupergit®C250L, alumina (Al_2O_3) spherical pellets (3 mm diameter), γ-aminopropyltriethoxysilane, glutaraldehyde poly(sodium 4 styrenesulfonate) (PSS, MW 70000), poly(allylamine hydrochloride) (PAH, MW 56000), bovine serum albumin (BSA), 2,2'-azino-bis(3-ethylbenzthiazoline-6-sulphonic acid) (ABTS), 1-hydroxybenzotriazole (HBT), violuric acid (VLA), 2,2,6,6-tetramethyl-1-piperidinyloxy free radical (TEMPO) and alcohols were purchased from Sigma-Aldrich. All spectrophotometric measurements were made with a Varian Cary50 UV-Vis spectrophotometer equipped with a single cell peltier thermostatted cell holder. Spectrophotometric data were analysed with Cary WinUV software. All experiments were carried out in acetate buffer pH 5.0, 0.1 M. All experiments were carried out in triplicate using free and immobilized tyrosinase.

6.4.1 Laccase immobilization on Eupergit® C250L

The enzyme immobilization was performed according to literature procedures.[23a,34] Dry Eupergit®C250L (1.0 g) was added to 8.0 mL of binding buffer (sodium phosphate buffer 1.0 M, pH 7.0) containing laccase (Lac, 1.5 mg, 230 U mg^{-1}). The mixture was incubated for 24 h at room temperature with orbital shaking. At the end of the coupling period, the resin beads were filtered and washed (3 x 8 mL) with Na-phosphate buffer 0.1 M, pH 7.0, until no activity was detected in the washing. The obtained beads were incubated with ethanolamine in Na-phosphate buffer 1.0 M, pH 7.0 (8.0 mL, 0.3 M) for 2 h to block residual epoxy groups, then washed with buffer and finally

air-dried and stored at 4°C. The amount in milligrams and the units of coupled laccase were calculated by the difference between the amount/units loaded and that recovered in the washings by conventional Bradford and activity ABTS assay. Immobilized laccase (Lac/E) was characterized for its kinetic properties.

6.4.2 Laccase immobilization on Eupergit®C250L covered with Layer-by-Layer method

Laccase-Eupergit®C250L system described above (Lac/E) was then coated with the Layer-by-Layer method (LbL) as reported.[22,35] Briefly the resins beads were suspended for 20 min at room temperature in a polyelectrolyte solutions (PAH or PSS, 2.0 mg mL^{-1} in 0.5 M NaCl, pH 6.5).[36] Since at operative pH laccase was negatively charged (Isoelectric Point, IP = 3.5[21]), deposition started with positively charged PAH to ensure the physical adsorption process.[37] PSS was then coated followed by the third layer of PAH to obtain the formation of three layers (PAH^+-PSS^--PAH^+). Immobilized laccase (Lac/E-LbL) was air-dried and characterized for its kinetic properties.

6.4.3 Laccase immobilization on alumina particles covered with Layer-by-Layer method

Alumina pellets (3 mm diameter) were functionalized by treatment first with silane, a coupling agents providing amino function on the particles surface, and then with glutaraldehyde that allows enzyme immobilization through a crosslink between the aldehyde group and NH_2 moiety of protein.[35] Briefly, alumina pellets were silanized with 2% (v/v) γ-aminopropyltriethoxysilane in acetone at 45°C for 20 h. The supports were washed once with acetone and silanized again for 24 h and the washed with deionised water. Silanized particles were then suspended in 2% (v/v) aqueous glutaraldehyde (50% v/v) for 2 h at room temperature, washed again with deionised water and dried through air. Thereafter, 150.0 g of support was immersed in 200.0 mL of laccase solution (10 U ml^{-1}) in 0.1 M acetate buffer pH 5.0. The particles were then washed several times with acetate buffer until no enzymatic activity was found in the washing solution. The amount in milligrams and the units of coupled laccase were calculated by the difference between the amount/units loaded and that recovered in the washings by conventional Bradford and activity assay. In the last stage, the pellets were first washed three times with 0.1 M NaCl and then the sequential deposition of polyelectrolyte (PAH^+, PSS^-) layers onto the alumina particles was performed to obtain a coating of three layers (PAH^+-PSS^--PAH^+), as described above. Immobilized laccase (Lac/Al) was air-dried and characterized for its kinetic properties.

6.4.4 Determination of protein concentration

Protein concentration was determined spectrophotometrically at 595 nm according to Bradford using BSA as standard.[38]

6.4.5 Activity assay

Free and immobilized laccase activity assay was determined spectrophotometrically using ABTS as substrate. Briefly, ABTS (300.0 µl, 5 mM), Na-acetate buffer 0.1 M, pH 5.0 (2.6 mL) was incubated under vigorous stirring at 25°C for 10 min. Then, an appropriate amount of free or immobilized enzyme in Na-acetate buffer (100.0 µl) was added to the mixture and the initial rate was immediately measured as increase in optical density at 420 nm.[39] One activity unit was defined as the amount of enzyme that oxidised 1 µmol ABTS/min. The immobilisation yield was calculated as the difference between the laccase unit (U) in the started enzyme solution and that recovered at the end of the immobilization procedure.

6.4.6 Kinetic assay

Kinetic parameters, K_m and V_{max} and V_{max}/K_m, were determined by measuring enzyme activity at different concentrations of ABTS (4.0-13.0 mM) and plotting data to a double reciprocal plot Lineweaver-Burk plot).[40] Reactions were carried out by means of the same procedure as for activity assay, using Lac (0.2 µg), Lac/E (0.6 µg), Lac/E-LbL (0.6 µg) and Lac/Al (0.6 µg), measuring absorbance at 420 nm as described above.

6.4.7 Storage stability assay

Laccase (0.2 µg for Lac and 0.6 µg for Lac/E, Lac/E-LbL and Lac/Al) was incubated in Na-acetate buffer 0.1 M, pH 5.0 at +4°C. At different times (0 - 30 days), aliquots were taken and the activity was determined by the ABTS method described. For each sample, laccase activity was expressed as relative percentage activity respect to that at time zero.

6.4.8 Enzyme recycling

Immobilized enzyme (Lac/E, Lac/E-LbL and Lac/Al) was recycled as follow: 3,4-dimethoxybenzyl alcohol (20 mM), immobilized laccases (10 U) and TEMPO (6 mM) were placed in Na-acetate buffer 0.1 M, pH 5.0 (3.0 mL). After 10 h, laccases were recovered by filtration, washed and reused with fresh TEMPO (6 mM) and substrate (20 mM). For each run, the reaction mixture was extracted with EtOAc and analysed by GCMS with acetophenone as internal standard.

6.4.9 Alcohol oxidation

A panel of alcohols (Figure 6.12) were oxidized, including benzyl alcohol **1**, 4-methoxybenzyl alcohol **2**, 3-methoxybenzyl alcohol **3**, 3,4-methoxybenzyl alcohol **4**, 3,4,5-methoxybenzyl alcohol **5**, cinnamyl alcohol **6**, geraniol **7,** 2-chlorobenzyl alcohol **8**, 4- chlorobenzyl alcohol **9**, 3-chlorobenzyl alcohol **10**. The reactions were performed under both homogeneous and heterogeneous systems. Oxidations were carried out using reported conditions:[16b] alcohol (20 mM), laccase (10 U) and mediator (6 mM) were placed in 0.1 M Na-acetate buffer pH 5.0 (3.0 mL) in vigorous stirring at room temperature. Reactions were monitored by thin layer chromatography (TLC). After the disappearance of the substrate, the reaction mixture was extracted twice with EtOAc. The organic extracts were treated with a saturated solution of NaCl and dried over anhydrous Na_2SO_4, then filtered and concentrated under vacuum to yield coloured crude. In the case of immobilized enzyme, biocatalysts were first recovered by filtration and the solutions were subjected to the same work up described above.

6.4.10 Identification and characterization of oxidative products

All products were identified by ^{1}H NMR, ^{13}C NMR and GC-MS. ^{1}H NMR and ^{13}C NMR were recorded on a Bruker 200 MHz spectrometer using $CDCl_3$ as solvent. All chemical shift are expressed in parts per million (δ scale). GC-MS analysis were performed on a Varian 450GC-320MS apparatus using a SPB column (25 m×0.25 mm and 0.25 mm film thickness) and an isothermal temperature profile of 70°C for 2 min, followed by a 10°C min^{-1} temperature gradient to 280°C for 25 min. The injector temperature was 280°C. Chromatography-grade hellum was used as the carrier gas with a flow of 1 mL min^{-1}. Mass spectra were recorded by a Varian 300 MS/MS with an electron beam of 70 eV. Selected products were also analysed by two-dimensional (2D) NMR, COSY NMR and HSQC NMR.
2D NMR spectra of 4-Methoxybenzaldehyde **12,** 3,4,5-Trimethoxybenzaldehyde **15** and 3,4-Dimethoxybenzaldehyde **14** are available in Appendix.

Benzaldehyde (11): Oil. ^{1}H NMR[41] (400 MHz, DMSO-d_6) δ_H (ppm) 7.47-7.83 (5H, m, Ph-H), 9.96 (1H, s, CHO). ^{13}C NMR (101 MHz, $CDCl_3$) δ_C (ppm) 125.6 (2xCH), 126.2 (2xCH), 131.0 (CH), 132.9 (C), 188.9 (C). *MS*, m/z (%): 106 (100, M^+), 105 (88), 77 (87), 51 (65), 50 (32).
4-Methoxybenzaldehyde (12): Oil. ^{1}H NMR[42] (400 MHz, $CDCl_3$) δ_H (ppm) 3.79 (3H, s, CH_3), 6.89 - 7.78 (4H, m, Ph-H), 9.80 (1H, s, CHO). ^{13}C NMR[42] (101 MHz, $CDCl_3$) δ_C (ppm) 55.4 (CH_3), 114.1 (2xCH), 129.7 (C), 131.8 (2xCH), 164.4 (C), 190.6 (C). *MS*, m/z (%): 136 (77, M^+), 135 (100), 107 (21), 92 (18), 77 (37).
3-Methoxybenzaldehyde (13): Oil. ^{1}H NMR (400 MHz, $CDCl_3$) δ_H (ppm) 3.78 (3H, s, CH_3), 7.00-7.48 (4H, m, Ph-H), 9.97 (1H, s, CHO). ^{13}C NMR (101 MHz, $CDCl_3$) δ_C (ppm) 55.7 (CH_3), 112.3 (CH), 121.2 (CH), 123.5 (CH), 130.1(CH), 137.6 (C), 160.2 (C), 192.4 (C). *MS*, m/z (%): 136 (100, M^+), 135 (93), 107 (41), 77 (43), 65 (23).

3,4-Dimethoxybenzaldehyde (14): Oil. ^{1}H NMR[43] (400 MHz, $CDCl_3$) δ_H (ppm) 3.93 (3H, s, CH_3), 3.90 (3H, s, CH_3), 6.94 - 7.40 (3H, m, Ph-H), 9.81 (1H, s, CHO) . ^{13}C NMR (101 MHz, $CDCl_3$) δ_C (ppm) 55.8 (CH_3), 56.0 (CH_3), 108.8 (CH), 110.2 (CH), 126.7 (CH), 130.0 (C), 149.4 (C), 154.3 (C), 190.7 (C). *MS*, m/z (%): 166 (100, M^+), 165 (62), 95 (44), 77 (41), 51 (38).

3,4,5-Trimethoxybenzaldehyde (15): Oil. ^{1}H NMR (400 MHz, $CDCl_3$) δ_H (ppm) 3.80 (6H, s, CH_3), 3.94 (3H, s, CH_3), 7.10 (2H, s, Ph-H), 9.85 (1H, s, CHO). ^{13}C NMR[41] (101 MHz, $CDCl_3$) δ_C (ppm) 55.7 (2xCH_3), 60.4 (CH_3), 106.1 (2xCH), 131.1 (C), 143.0 (C), 153.1 (2xC), 190.5 (C). *MS*, m/z (%): 196 (100, M^+), 181 (54), 124 (30), 109 (25), 92 (20).

Cinnamaldehyde (16): Oil. ^{1}H NMR[42] (400 MHz, $CDCl_3$) δ_H (ppm) 6.67-6.73 (1H, m, H), 7.44-7.59 (6H, m, Ph-H, H), 9.72-9.78(1H, m, CHO). ^{13}C NMR[42] (101 MHz, $CDCl_3$) δ_C (ppm) 128.4 (2xCH), 128.7 (2xCH), 129.0 (CH), 131.2 (CH), 133.9 (C), 152.7 (CH), 193.6 (C). *MS*, m/z (%): 132 (68, M^+), 130 (100), 103 (60.3), 77 (50), 51 (42).

Geranaldehyde (17): Oil. ^{1}H NMR[42] (400 MHz, $CDCl_3$) δ_H (ppm) 1.00 (3H, s, CH_3), 1.60 (3H, s, CH_3), 1.65 (3H, s, CH_3) 1.90-2.20 (4H, m, CH_2), 5.0-5.10(2H, m, CH), 9.75 (1H, m, CHO). ^{13}C NMR (101 MHz, $CDCl_3$) δ_C (ppm) 16.9 (CH_3), 17.5 (CH_3), 25.1 (CH_3), 26.7 (CH_2), 40.4 (CH_2), 123.2 (CH), 127.6 (CH), 132.3 (C), 165.4 (C), 190.6 (C). *MS*, m/z (%): 152 (6, M^+), 94 (19), 84 (30), 82 (11), 69 (100).

2-Chlorobenzaldehyde (18): Oil. ^{1}H NMR[44] (400 MHz, CDCl 3) δ_H (ppm) 7.52 – 7.86 (4H, m, Ph-H). 10.43 (1H, s, CHO). ^{13}C NMR[44] (101 MHz, $CDCl_3$) δ_C ppm 127.3 (CH), 129.5 (CH), 130.3 (CH), 132.2 (C), 135.2 (CH), 137.7 (C), 189.8 (C) *MS*, m/z (%): 138 (100), 140 (71, M^+), 110 (47), 142 (33), 113 (15).

2-Chlorobenzoic acid (19): Oil. *MS*, m/z (%): 139 (100), 156 (58,M^+), 110 (45), 141 (35). Oil. ^{1}H NMR (400 MHz, CDCl 3) δ_H (ppm) 7.42- 7.86 (4H, m, Ph-H), 11.5 (1H, s, COOH). ^{13}C NMR (101 MHz, $CDCl_3$) δ_C ppm 126.3 (CH), 126.7 (CH), 129.3 (CH), 129.7 (CH), 131.1 (C), 132.3 (CH), 163.2 (C).

4-Chlorobenzaldehyde (20): Oil. ^{1}H NMR[41] (400 MHz, $CDCl_3$) δ_H (ppm) 7.50 - 7.55 (2H, m, Ph-H), 7.81 - 7.85 (2H, m, Ph-H), 9.95 - 10.04 (1H, m, CHO). ^{13}C NMR[41] (101 MHz, CDCl 3) δ_C (ppm) 131.4 (2xCH), 132.0 (2xCH), 135.1 (C), 141.4 (C), 191.3 (C). *MS*, m/z (%): 142 (42), 140 (68, M^+), 138 (100), 111 (65), 75 (52).

4-Chlorobenzoic acid (21): Oil. ^{1}H NMR[45] (400 MHz, $CDCl_3$) δ_H (ppm) δ=10.18 (s, 1H, COOH), 7.58–7.56 (2H, m, Ph–H); 7.96–7.94 (2H, m, Ph–H), ^{13}C NMR (101 MHz, DMSO-d_6) δ_C (ppm) 128.7 (2xCH), 129.5 (C), 131.1 (2xCH), 137.7 (C), 166.3 (C). *MS*, m/z (%): 156 (5, M^+), 155 (75), 138 (100), 110 (48), 75 (35).

3-Chlorobenzaldehyde (22): Oil. ^{1}H NMR[42] (400 MHz, $CDCl_3$) δ_H (ppm) 7.46-7.81 (4H, m, Ph–H), 9.95 (1H, CHO); ^{13}C NMR[42] (100MHz, $CDCl_3$) δ (ppm) 127.9 (CH), 129.1 (CH), 130.3 (CH), 134.2 (CH), 135.3 (C), 137.7 (C), 190.7 (C). *MS*, m/z (%): 138 (100), 140 (81, M^+), 111 (57), 142 (27), 75 (24).

3-Chlorobenzoic acid (23): ^{1}H NMR[42] (400MHz, CDCl3) δ_H (ppm) 7.44-7.86 (4H, m Ph–H), 13.2 (1H, s, COOH); ^{13}C NMR (100MHz, $CDCl_3$) δ_H (ppm) 128.1 (CH), 129.2 (C), 130.7 (CH), 132.8 (CH), 133.2(CH), 133.7 (C), 166.4 (C). *MS*, m/z (%): 139 (100), 156 (76, M^+), 112 (62), 140 (29).

References

[1] Yaropolov, A.I.; Skorobogatko, O.V.; Vartanov, S.S.; Varfolomeyev, S.D. *Appl Biochem Biotechnol* **1994,** *49,* 257-280.

[2] a) Xu F. *Industrial Biotechnol* **2005**, *1*, 38-50; b) Riva, S. *Trends Biotechnol* **2006**, *24*, 219-226.

[3] a) Messerschmidt, A. in *Multi-Copper Oxidases* (Messerschmidt, A., ed.), **1997,** 23-80, World Scientific, Singapore; b) Reinhammar, B. in *Multi-Copper Oxidases* (Messerschmidt, A., ed.), **1997,** 167-200, World Scientific, Singapore; c) Jonnsson, L.; Sjonstronm, K.; Hanggstronm, I.; Nyman, P.O. *Biochim Biophys Acta* **1995,** *1251*, 210-215.

[4] Burton, S.G. *TRENDS in Biotechnol* **2003,** *21(12)*, 543-549.

[5] a) Babot, E.D.; Rico, A.; Rencoret, J.; Kalum, L.; Lund, H.; Romero, J.; del Río, J.C.; Martínez, Á.T.; Gutiérrez, A. *Bioresour Technol* **2011,** *102,* 6717-6722; b) Andreu, G.; Vidal, T. *Bioresour Technol* **2011**, *102(10),* 5932-5937; c) Crestini, C.; Melone, F.; Saladino, R. *Bioorg Med Chem* **2011**, *19(16),* 5071-50788; e) Strong, P. J.; Claus, H. *Crit Rev in Environ Sci Technol* **2011**, *41(4),* 373-434; Martinez-Ortiz, J.; Flores, R.; Vazquez-Duhalt, R. *Biosens Bioelectron* **2011,** *26*, 2626-2631; f) Barilli, A.; Belinghieri, F.; Passarella, D.; Lesma, G.; Riva, S.; Silvani, A.; Danieli, B. *Tetrahedron Asym* **2004**, *15*:2921-2925.

[6] a) Abalyaeva, V.V.; Efimov, O.N. *Russ J Electrochem* **2002**, *38*, 1212-1215; b) Bourbonnais, R.; Leech, D.; Paice, M.G. *Biochim Biophys Acta* **1998**, *1379*, 381-390.

[7] Li, K.; Xu, F.; Eriksson, K.-E.L. *Appl Environ Microbiol*, **1999**, *65*, 2654-2660.

[8] Golibev, V.A.; Kozlov, Y.N.; Petrov, A.N.; Purmal, A.P. In *Bioactive spin labels* (Zhdanov, R.I., ed.) **1992,** 119-140, Springer.

[9] a) Bourbonnais, R.; Paice, M.G.; Freiermuth, B.; Bodie, E.; Borneman, S. *Appl Environ Microbiol* **1997**, *63*, 4627-4632; b) Muheim, A.; Fiechter, A.; Harvey, P. J.; Schoemaker, H. E. *Holzforschung* **1992**, *46*, 121-126; c) Potthast, A.; Rosenau, T.; Fischer, K. *Holzforschung* **2001**, *55*, 47-56; d) Marjasvaara, A.; Janis, J.; Vainiotalo, P. *J Mass Spectrom* **2008**; *43*: 470–477; d) Branchi, B.; Galli, C.; Gentili, P. *Org Biomol Chem*, **2005**, *3*, 2604-2614.

[10] a) Crestini, C.; Argyropoulos, D.S. *Bioorg Med Chem* **1998**, *6*, 2161-2169.

[11] a) Baiocco, P.; Barreca, A.N.; Fabbrini, M.; Galli, C; Gentili, P. *Org Biomol Chem* **2003,** *1*, 191-197; b) Galli, G.; Gentili, P. *J Phys Org Chem* **2004**, *17*, 973–977

[12] a) Muzart, J. *Tetrahedron* **2003**, *59*, 5789-5816; b) Stahl, S. S. *Angew Chem, Int. Ed.* **2004**, *43*, 3400-3420.

[13] a) Anderson, R.; Griffin, K.; Johnston, P.; Alsters, P. L. *Adv Synth Catal* **2003**, *345*, 517-523; b) Besson, M.; Gallezot, P. *Catal Today* **2000**, *57*, 127-141.

[14] Yamaguchi, K.; Mizuno, N. *Chem Eur J* **2003**, *9*, 4353-4361.

[15] Sheldon, R.A.; Arends, I.W.C.E.; Ten Brink, G.J.; Dijksman. A. *Acc Chem Res* **2002**, *35*, 774-781.

[16] a) Fabbrini, M.; Galli, C.; Gentili, P. *J Mol Catal B: Enzym* **2002**, *16*, 231-240; b) Fabbrini, M.; Galli, C.; Gentili, P.; Macchitella D. *Tetrahedron Lett* **2001**, 42, 7551-7553; c) Potthast, A.; Rosenau, T.; Chen, C. L.; Gratzl, J. S. *J Mol Catal A: Chem* **1996**, *108*, 5-9; d) Arends, I.W.C.E.; Li, Y.-X.; Ausan, R.; Sheldon, R.A. *Tetrahedron* **2006,** *62,* 6659-6665.

[17] Tromp, S.A.; Matijošyté, I.; Sheldon, R.A.; Arend, I.W.C.E.; Mul, G.; Kreutzer, M.T.; Moulijn, J.A.; de Vries, S. *ChemCatChem* **2010**, *2*, 827-833.

[18] Rodríguez-Couto, S.; Osma, J.F.; Saravia, V.; Gübitz, G.M.; Toca-Herrera, J.L. *Appl Catal A: Gen* **2007,** *329*, 156-160.

[19] a) Krajewska, B. *Enzyme Microb Technol* **2004**, *35*, 126-139; b) Abadulla, E.; Tzanov, T.; Costa, S.; Robra, K.-H.; Cavaco-Paulo, A.; Gübitz, G. M. *Appl Environ Microb* **2000**, *66*, 3357-3362; c) Ryan, S.; Schnitzhofer, W.; Tzanov, T.; Cavaco-Paulo, A.; Gübitz, G. M. *Enzyme Microb Technol* **2003**, *33*, 766-774; d) Kandelbauer, A.; Maute, O.; Erlacher, A.; Cavaco-Paulo, A.; Gübitz, G.M. *Biotechnol Bioeng* **2004**, *87*, 552-563.

[20] a) Ariga, K.; Lvov, Y.M.; Kawakami, K.; Ji, Q.; Hill, J.P. *Adv Drug Deliv Rev.* **2011**, *63*, 762-71; b) Decher, G. *Nachr Chem Tech Lab* **1993**, *41*, 793; c) Decher, G.; Schmitt, J. *Prog Colloid Polym Sci* **1992**, *89*, 160; d) Held, C.; Kandelbauer, A.; Schroeder, M.; Cavaco-Paulo, A.; Gubitz, G.M. *Environ Chem Lett* **2005,** *3*, 74–77.

[21] Piontek, K.; Antorini M.; Choinowski, T. *J Biol Chem* **2002,** *277,* 37663-37669.

[22] Crestini, C.; Perazzini, R.; Saladino, R. *App Catal A: Gen* **2010,** *372,* 115-123.

[23] A) D'Annibale, A.; Stazi, S.R.; Vinciguerra, V.; Giovannozzi Sermanni, G. *J Biotechnol* **2000,** *77,* 265-273; b) Brandi, P.; D'Annibale, A.; Galli, C.; Gentili, P.; Nunes Pontes, A. S. *J Mol Catal B: Enzym* **2006,** *41,* 61-69.

[24] a) Leontievsky, A.A.; Myasoedova, N.M.; Baskunov, B.P.; Golovleva, L.A.; Bucke, C.; Evans, C.S. *Appl Microbiol Biotechnol* **2001**, *57*, 85-91; b) D'Annibale, A.; Stazi, S.R.; Vinciguerra, V.; Mattia, D.E.; Sermanni, G.G. *Process Biochem* **1999**, *34*, 697-706.

[25] Klibanov, A.M. *Anal Biochem* **1979,** *93*, 1-25.
[26] Eggert, C.; Temp; J.F.D. Dean, Eggert, C.; Eriksson, K.-E.L. *FEBS Lett* **1996,** *391,* 144-148.
[27] Baciocchi, E.; Bietti M.; Lanzalunga, O. *Acc Chem Res* 2000, *33*, 243-251.
[28] a) Iwahama, T.; Yoshino, Y.; Keitoku, T.; Sakaguchi S.; Ishii, Y. *J Org Chem* **2000**, *65*, 6502-6507; b) Minisci, F.; Punta, C.; Recupero, F.; Fontana, F.; Pedulli, G. F. *J Org Chem* **2002**, *67*, 2671-2676; c) d'Acunzo, F.; Baiocco, P.; Fabbrini, M.; Galli C.; Gentili, P. *New J Chem* **2002**, *26*, 1791-1794.
[29] Walling, C.; Rieger, A.L.; Tanner, D.D. *J Am Chem Soc* **1963**, *85*, 3129-3134; b) Baciocchi, E.; Lanzalunga, O. *Tetrahedron* **1993**, *49*, 7267-7276.
[30] Sukhorukov, G.; Fery, A.; Möhwald, H. *Prog Polym Sci* **2005**, *30,* 885-897.
[31] a) Li, K.; Xu, F.; Eriksson, K.-E.L. *Appl Environ Microbiol* **1999**, *65*, 2654-2660; b) Soares, G.M.B.; Pessoa de Amorim, M.T.; Costa-Ferreira, M. *J Biotechnol* **2001,** *89,* 123-129.
[32] Astolfi, P.; Brandi, P.; Galli, C.; Gentili, P.; Gerini, M.F.; Greci, L.; Lanzalunga, O. *New J Chem* **2005,** *29,* 1308-1317.
[33] de Nooy, A.E.J.; Rori, V.; Masci, G.; Dentini, M.; Crescenzi, V. *Carbohydr Res* **2000***, 324,* 116-126.
[34] Baratto, L.; Candido, A.; Marzorati, M.; Sagui, F.; Riva, S.; Danieli, B. *J Mol Catal B: Enzym* **2006,** *39,* 3-8.
[35] Ryan, S.; Schnitzhofer, W.; Tzanov, T.; Cavaco-Paulo, A.; Gübitz, G.M. *Enzym Microb Technol* **2003,** *33,* 766-774.
[36] Djugnat, C.; Sukhorukov, G.B. *Langmuir*, **2004***, 20 (17),* 7265-7269.
[37] Wang, F.; Guo, C.; Yang, L.-R.; LU, C.-Z. *Bioresour Technol* **2010,** *101*, 8931-8935.
[38] a) Sedmak, J.J.; Grossberg, S.E. *Anal Biochem* **1977**, *79*, 544-552; b) Bradford, M.M. *Anal Biochem* **1976**, *72*, 248-254.
[39] Wolfender, B.S.; Willson, R.L. *J Chem Soc, Perkin Trans 2* **1982**, 805–810.
[40] Lineweaver, H.; Burk, D. JACS 1934, 56, 658–661.
[41] Wang, X.; LU, R.; Jin, Y.; Liang, X. *Chem Eur J* **2008**, *14*, 2679 -2685.
[42] Jiang, N.; Ragauskas, A.J. *J Org Chem* **2007,** *72(18),* 7030-7033.
[43] Sedelmeier, J.; Ley, S.V.; Baxendale I.R.; Baumann M. *Org Lett*, **2010**, *12* (16), pp 3618–3621
[44] Lin, C.-K.; Lu T.-J. *Tetrahedron* **2010,** *66*, 9688-9693.
[45] Wu, S.; Ma, H.; Lei, Z. *Tetrahedron* **2010,** *66,* 8641- 8647.

APPENDIX

2D ^{1}H - ^{1}H COSY 4-Methoxybenzaldehyde **12**

2D HSQC 4-Methoxybenzaldehyde **12**

2D ^{1}H - ^{1}H COSY 3,4-Dimethoxybenzaldehyde **14**

2D HSQC 3,4-Dimethoxybenzaldehyde **14**

2D ^{1}H - ^{1}H COSY 3,4,5-Trimethoxybenzaldehyde **15**

2D HSQC 3,4,5-Trimethoxybenzaldehyde **15**

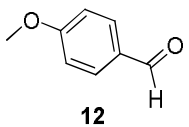

12

BRUKER

```
Current Data Parameters
NAME                  Melissa
EXPNO                       5
PROCNO                      1

F2 - Acquisition Parameters
Date_              20110701
Time                   13.01
INSTRUM                spect
PROBHD    5 mm PABBO BB-
PULPROG          cosygpmfqf
TD                       2048
SOLVENT                 CDCl3
NS                          4
DS                          8
SWH                5341.880 Hz
FIDRES             2.608340 Hz
AQ                 0.1917428 sec
RG                     88.81
DW                    93.600 usec
DE                     6.50 usec
TE                    299.8 K
D0                 0.00000300 sec
D1                 4.00000000 sec
D13                0.00000400 sec
D16                0.00020000 sec
IN0                0.00018720 sec

======== CHANNEL f1 ========
NUC1                       1H
P1                      12.50 usec
PLW1              15.00000000 W
SFO1              400.1324057 MHz

====== GRADIENT CHANNEL =====
GPNAM1             SMSQ10.100
GPNAM2             SMSQ10.100
GPNAM3             SMSQ10.100
GPZ1                    16.00 %
GPZ2                    12.00 %
GPZ3                    40.00 %
P16                   1000.00 usec

F1 - Acquisition parameters
TD                       128
SFO1                400.1324 MHz
FIDRES             41.733440 Hz
SW                     13.350 ppm
FnMODE                    QF

F2 - Processing parameters
SI                       2048
SF                400.1300000 MHz
WDW                      SINE
SSB       0
LB        0 Hz
GB        0
PC                        1.00

F1 - Processing parameters
SI                       2048
MC2                       QF
SF                400.1300000 MHz
WDW                    States
SSB       0
LB        0 Hz
GB        0
```

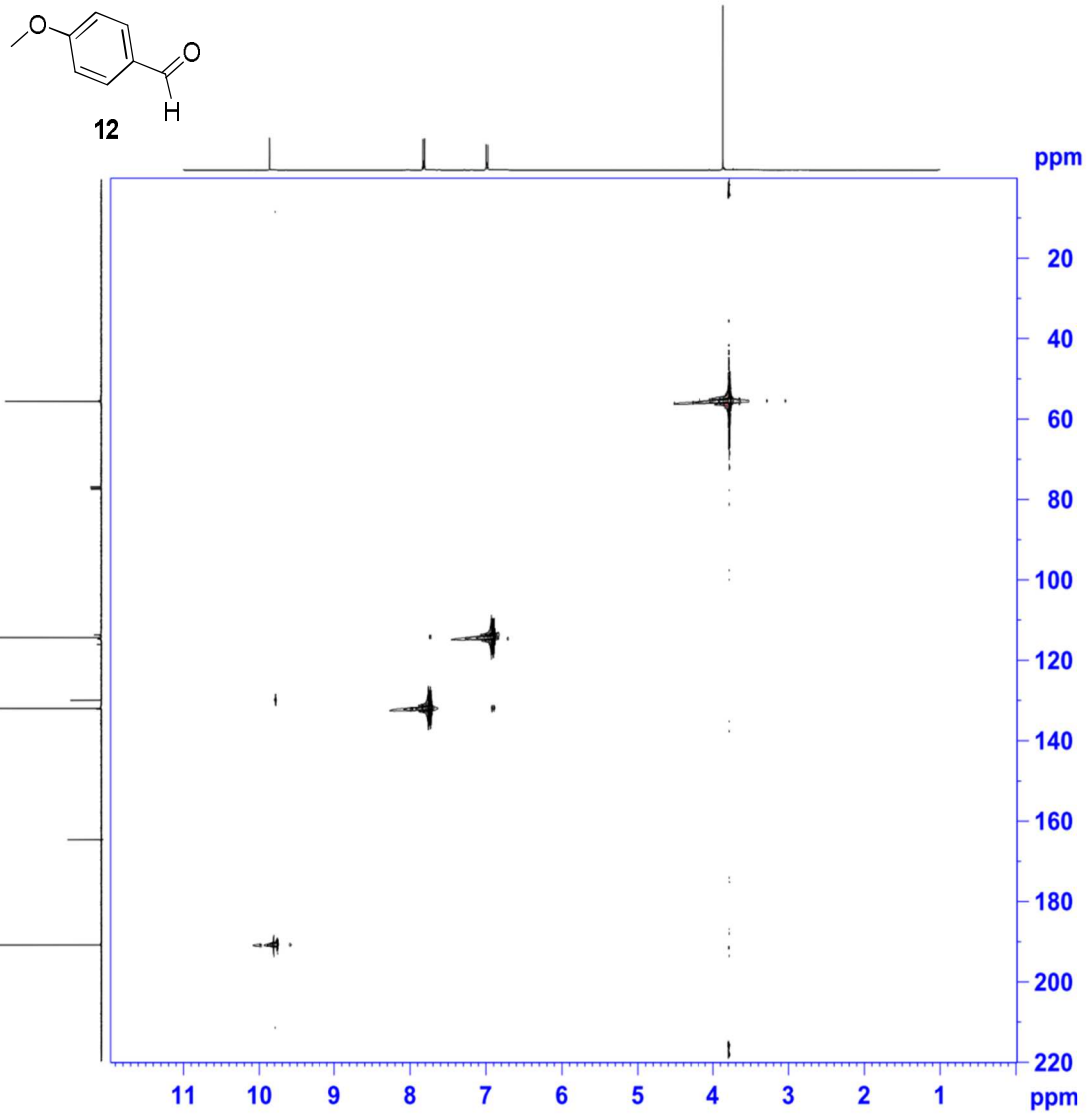

BRUKER

```
Current Data Parameters
NAME                  Melissa
EXPNO                      25
PROCNO                      1

F2 - Acquisition Parameters
Date_              20110715
Time                  14.52
INSTRUM                spect
PROBHD   5 mm PABBO BB-
PULPROG             hsqcetgp
TD                      4096
SOLVENT                 CDCl3
NS                         75
DS                         16
SWH                 4795.396 Hz
FIDRES              1.170751 Hz
AQ                  0.4271263 sec
RG                      88.81
DW                    104.267 usec
DE                      6.50 usec
TE                     301.0 K
CNST2              145.0000000
D0                  0.00000300 sec
D1                  4.00000000 sec
D4                  0.00172414 sec
D11                 0.03000000 sec
D13                 0.00000400 sec
D16                 0.00020000 sec
IN0                 0.00002260 sec
ZGOPTNS

======== CHANNEL f1 ========
NUC1                       1H
P1                      12.50 usec
P2                      25.00 usec
P28                   1000.00 usec
PLW1               15.00000000 W
SFO1              400.1324008 MHz

======== CHANNEL f2 ========
CPDPRG2                 garp
NUC2                     13C
P3                       9.00 usec
P4                      18.00 usec
PCPD2                   80.00 usec
PLW2               75.00000000 W
PLW12               0.94922000 W
SFO2              100.6238364 MHz

====== GRADIENT CHANNEL =====
GPNAM1             SMSQ10.100
GPNAM2             SMSQ10.100
GPZ1                    80.00 %
GPZ2                    20.10 %
P16                   1000.00 usec

F1 - Acquisition parameters
TD                         256
SFO1              100.6238 MHz
FIDRES             86.470551 Hz
SW                   219.992 ppm
FnMODE     Echo-Antiecho

F2 - Processing parameters
SI                        2048
SF                400.1300000 MHz
WDW                       SINE
SSB                          2
LB          0 Hz
GB          0
PC                        1.40

F1 - Processing parameters
SI                        2048
MC2            echo-antiecho
SF                100.6127690 MHz
WDW                     States
SSB                          2
LB          0 Hz
GB          0
```

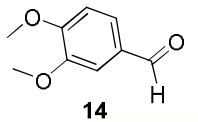

14

BRUKER

```
Current Data Parameters
NAME                  Melissa
EXPNO                      15
PROCNO                      1

F2 - Acquisition Parameters
Date_                20110707
Time                    15.12
INSTRUM                 spect
PROBHD    5 mm PABBO BB-
PULPROG          cosygpmfqf
TD                       4096
SOLVENT                 CDCl3
NS                         18
DS                          8
SWH                  5341.880 Hz
FIDRES               1.304170 Hz
AQ                  0.3834356 sec
RG                      99.67
DW                     93.600 usec
DE                      6.50 usec
TE                     300.0 K
D0                  0.00000300 sec
D1                  4.00000000 sec
D13                 0.00000400 sec
D16                 0.00020000 sec
IN0                 0.00018720 sec

======== CHANNEL f1 ========
NUC1                       1H
P1                      12.50 usec
PLW1               15.00000000 W
SFO1              400.1324057 MHz

====== GRADIENT CHANNEL =====
GPNAM1           SMSQ10.100
GPNAM2           SMSQ10.100
GPNAM3           SMSQ10.100
GPZ1                    16.00 %
GPZ2                    12.00 %
GPZ3                    40.00 %
P16                   1000.00 usec

F1 - Acquisition parameters
TD                         256
SFO1                400.1324 MHz
FIDRES             20.866720 Hz
SW                     13.350 ppm
FnMODE                     QF

F2 - Processing parameters
SI                       4096
SF                400.1300000 MHz
WDW                      SINE
SSB          0
LB           0 Hz
GB           0
PC                       1.00

F1 - Processing parameters
SI                       2048
MC2                        QF
SF                400.1300000 MHz
WDW                    States
SSB          0
LB           0 Hz
GB           0
```

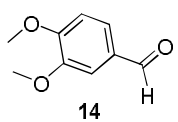

14

BRUKER

```
Current Data Parameters
NAME                  Melissa
EXPNO                      16
PROCNO                      1

F2 - Acquisition Parameters
Date_               20110707
Time                   20.51
INSTRUM                spect
PROBHD    5 mm PABBO BB-
PULPROG             hsqcetgp
TD                      4096
SOLVENT                CDCl3
NS                        26
DS                         8
SWH                5341.880 Hz
FIDRES             1.304170 Hz
AQ                 0.3834356 sec
RG                     99.67
DW                    93.600 usec
DE                     6.50 usec
TE                    300.1 K
CNST2             145.0000000
D0                 0.00000300 sec
D1                 1.50000000 sec
D4                 0.00172414 sec
D11                0.03000000 sec
D13                0.00000400 sec
D16                0.00020000 sec
IN0                0.00002260 sec
ZGOPTNS

======== CHANNEL f1 ========
NUC1                       1H
P1                      12.50 usec
P2                      25.00 usec
P28                   1000.00 usec
PLW1              15.00000000 W
SFO1             400.1324057 MHz

======== CHANNEL f2 ========
CPDPRG2                 garp
NUC2                      13C
P3                       9.00 usec
P4                      18.00 usec
PCPD2                   80.00 usec
PLW2              75.00000000 W
PLW12              0.94922000 W
SFO2             100.6238364 MHz

====== GRADIENT CHANNEL =====
GPNAM1          SMSQ10.100
GPNAM2          SMSQ10.100
GPZ1                    80.00 %
GPZ2                    20.10 %
P16                   1000.00 usec

F1 - Acquisition parameters
TD                        256
SFO1             100.6238 MHz
FIDRES           86.473610 Hz
SW                  220.000 ppm
FnMODE      Echo-Antiecho

F2 - Processing parameters
SI                       1024
SF               400.1300000 MHz
WDW                     QSINE
SSB                        2
LB          0 Hz
GB          0
PC                      1.00

F1 - Processing parameters
SI                       1024
MC2           echo-antiecho
SF               100.6127690 MHz
WDW             States-TPPI
SSB                        2
LB          0 Hz
GB          0
```

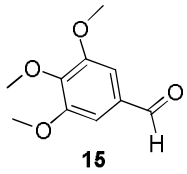

15


```
Current Data Parameters
NAME                 Melissa
EXPNO                     22
PROCNO                     1

F2 - Acquisition Parameters
Date_              20110709
Time                   8.12
INSTRUM               spect
PROBHD    5 mm PABBO BB-
PULPROG        cosygpmfqf
TD                      4096
SOLVENT              CDC13
NS                        50
DS                        16
SWH                4807.692 Hz
FIDRES             1.173753 Hz
AQ                 0.4260340 sec
RG                    88.81
DW                  104.000 usec
DE                    6.50 usec
TE                   300.0 K
D0                 0.00000300 sec
D1                 4.00000000 sec
D13                0.00000400 sec
D16                0.00020000 sec
IN0                0.00020825 sec

======== CHANNEL f1 ========
NUC1                      1H
P1                     12.50 usec
PLW1           15.00000000 W
SFO1           400.1324057 MHz

====== GRADIENT CHANNEL =====
GPNAM1          SMSQ10.100
GPNAM2          SMSQ10.100
GPNAM3          SMSQ10.100
GPZ1                  16.00 %
GPZ2                  12.00 %
GPZ3                  40.00 %
P16                 1000.00 usec

F1 - Acquisition parameters
TD                       256
SFO1             400.1324 MHz
FIDRES          18.756207 Hz
SW                    12.000 ppm
FnMODE                   QF

F2 - Processing parameters
SI                      4096
SF             400.1300000 MHz
WDW                    SINE
SSB       0
LB        0 Hz
GB        0
PC                     1.40

F1 - Processing parameters
SI                      2048
MC2                      QF
SF             400.1300000 MHz
WDW                  States
SSB       0
LB        0 Hz
GB        0
```

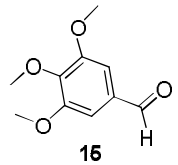

15

BRUKER

```
Current Data Parameters
NAME                  Melissa
EXPNO                      21
PROCNO                      1

F2 - Acquisition Parameters
Date_              20110708
Time                  16.22
INSTRUM                spect
PROBHD   5 mm PABBO BB-
PULPROG             hsqcetgp
TD                      4096
SOLVENT                 CDCl3
NS                        50
DS                        16
SWH                 4795.396 Hz
FIDRES              1.170751 Hz
AQ                  0.4271263 sec
RG                     88.81
DW                   104.267 usec
DE                     6.50 usec
TE                    300.0 K
CNST2              145.0000000
D0                  0.00000300 sec
D1                  4.00000000 sec
D4                  0.00172414 sec
D11                 0.03000000 sec
D13                 0.00000400 sec
D16                 0.00020000 sec
IN0                 0.00002260 sec
ZGOPTNS

======== CHANNEL f1 ========
NUC1                       1H
P1                      12.50 usec
P2                      25.00 usec
P28                   1000.00 usec
PLW1               15.00000000 W
SFO1              400.1320007 MHz

======== CHANNEL f2 ========
CPDPRG2                 garp
NUC2                      13C
P3                       9.00 usec
P4                      18.00 usec
PCPD2                   80.00 usec
PLW2               75.00000000 W
PLW12               0.94922000 W
SFO2              100.6228303 MHz

====== GRADIENT CHANNEL =====
GPNAM1             SMSQ10.100
GPNAM2             SMSQ10.100
GPZ1                    80.00 %
GPZ2                    20.10 %
P16                   1000.00 usec

F1 - Acquisition parameters
TD                         256
SFO1               100.6228 MHz
FIDRES              86.470551 Hz
SW                    219.994 ppm
FnMODE     Echo-Antiecho

F2 - Processing parameters
SI                        2048
SF                 400.1300000 MHz
WDW                       SINE
SSB                          2
LB          0 Hz
GB          0
PC                        1.40

F1 - Processing parameters
SI                        2048
MC2            echo-antiecho
SF                 100.6127690 MHz
WDW                     States
SSB                          2
LB          0 Hz
GB          0
```

Ringrazio il Prof. Saladino, che mi ha ospitato nel suo laboratorio, e la Prof.ssa Masci, coordinatrice del corso di dottorato.

Un ringraziamento speciale e un abbraccio caloroso vanno alle mie compagne di pranzo: Francesca, Tiziana, Maria Cristina e Marina. Grazie per tutte le volte che avete sopportato le mie lune storte e per tutte le risate che mi avete regalato durante i nostri "filosofici" pranzi! A voi sono legati i ricordi più belli e spensierati di questi tre anni!

Troppo dovrei dire a Maurizio e Fernanda. Tornassi indietro rifarei le stesse scelte solo perché gli errori scaturiti da questi sbagli mi hanno fatto conoscere voi. E sapete bene a quali errori mi riferisco! Ma pensateci bene, se non fosse stato per la Tuscia non ci saremmo mai conosciuti… certo per voi sarebbe stata una vera disgrazia! Chi avrebbe giocato con voi a Cluedo? E a Taboo? Chi vi avrebbe fatto vincere tanto a burraco? Vogliamo parlare di Cirano? Per non dire poi dei film, della fantastica pizza carbonizzata… potrei continuare per ore!! Vi voglio bene…ehm sì! Anche a quel musone di Maurizio!

Per non parlare di Arianna. Lontana, ma vicinissima nel cuore!! Sei sempre stata un'amica sincera per me, ma soprattutto ci sei sempre stata, nei momenti buoni e in quelli cattivi! Sei un punto di riferimento! Ti auguro un futuro radioso, sereno e pieno di felicità…

Ringrazio soprattutto la mia famiglia che sono anni ormai che mi sopporta!! Avete sempre creduto in me e avete appoggiato ogni mia decisione, anche quando pensavate che non fosse quella giusta! Grazie!

Infine Daniele. Non serve scrivere quello che hai rappresentato per me in questi anni, avrò tutta una vita per ringraziarti di tutte le volte che mi sei vicino!